

**Three-Dimensional Dynamic  
Modelling  
of the Human Cervical Spine  
in Whiplash Situations**

---

**Waldemar Z. Golinski**

A thesis submitted in partial fulfilment of the requirements of the  
Nottingham Trent University for the degree of  
Doctor of Philosophy

This research programme was carried out in the  
Department of Mechanical & Manufacturing Engineering,  
Faculty of Engineering and Computing,  
The Nottingham Trent University, Burton Street, Nottingham NG1 4BU, UK

November 2000

ProQuest Number: 10183459

All rights reserved

INFORMATION TO ALL USERS

The quality of this reproduction is dependent upon the quality of the copy submitted.

In the unlikely event that the author did not send a complete manuscript and there are missing pages, these will be noted. Also, if material had to be removed, a note will indicate the deletion.



ProQuest 10183459

Published by ProQuest LLC (2017). Copyright of the Dissertation is held by the Author.

All rights reserved.

This work is protected against unauthorized copying under Title 17, United States Code  
Microform Edition © ProQuest LLC.

ProQuest LLC.  
789 East Eisenhower Parkway  
P.O. Box 1346  
Ann Arbor, MI 48106 – 1346

# ABSTRACT

Despite many previous studies into the “whiplash” phenomenon, including sled tests on volunteers, animals and post mortem test objects as well as *in vitro* clinical studies, many questions remain unanswered.

The purpose of the work described here is to answer some of the questions by developing a biomechanical 3 – dimensional Finite Element (FE) model of the human cervical spine, capable of simulating the whiplash accident situation, and hence making recommendations for improving car safety as well as defining the Mechanism of Injury (MoI).

A 3-dimensional biomechanical model of the head-neck complex has been developed, including the intervertebral discs, the neck ligaments and the muscle structure in addition to the vertebrae themselves. The model has been evaluated against experimental data from volunteer sled tests, successfully predicting the kinematics of the head and cervical spine. The model behaviour confirms the MoI of whiplash as being hypertranslation of the head, in agreement with recent experimental results. It has been clearly shown that biomechanical FE modelling has significant advantages over other kinds of research, as it can indicate the actual injury risk in individual soft tissues.

Furthermore, the final model has been used to investigate not only the sagittal plane whiplash scenario, but also, for the first time, the situation where the car occupant is initially looking to one side. The model is the first research tool capable of investigating this scenario, since other computational investigations, as well as experimental approaches, have been restricted to the facing forward position.

Finally a new approach to car safety research has been indicated by implementing the biomechanical head-neck model onto a Hybrid III dummy model, producing what has been shown to be an original and powerful design tool. This combined model has been successfully used to investigate different factors affecting whiplash injury as well as to design an anti-whiplash protection device.

# ACKNOWLEDGEMENTS

I would like to extend my sincerest thanks to my director of studies, Professor Richard Gentle, for his enthusiasm and help throughout this study, and to Dr. Martin Lacey for his supervision.

I also thank the many fellow students who were involved with the Biomechanical Research Group during this project. I would like to express my particular thanks to Dr. Frank Heitplatz, for help and advice during our collaboration.

My final and greatest thanks go to my wife Dorota and to my parents and my brother for continues support they gave me during my study.

## LIST OF PUBLICATIONS

Heitplatz F., Golinski W.Z., Gentle C.R., *Guidelines for Car Seat Design based on FE Analysis of Whiplash Injuries*, Proc. of Mechanics in Design (MID'98), Nottingham, UK, 6-9 July, 1998,

Heitplatz F., Golinski W.Z., Gentle C.R., *Development of a Biomechanical FE Model to investigate "Whiplash"*, Proc. of the LS-Dyna User Conference, Williams Grand Prix Engineering, UK, 1-2 July, 1998, (Award for the best conference paper)

Gentle C.R., Golinski W.Z., Heitplatz F., *Experimental and Computational Studies of "Whiplash" Injuries.*, Proc. of the 18th Symposium on Experimental Mechanics of Solid Jachranka, Poland, 14-16 October, 1998,

Nagy G.T., Golinski W.Z., Heitplatz F., Gentle C.R., *Investigation into the range of motion of the cervical spine based on a non-linear finite element model*, Proceedings of Osteology, vol 1, pp 27-30, 1999,

Golinski W.Z., Gentle C.R., *Assessment of a Whiplash Prevention Device with a Dynamic Biomechanical Finite Element Model*, Proc. of the 2<sup>nd</sup> European LS-DYNA Users Conference, Gothenburg, Sweden, 14-15 June, 1999,

Sobczak P., Golinski W.Z., Gentle C.R., *Biomechanical Evaluation of Anterior Cervical Spine Stabilisation Using the Finite Element Approach*, Acta of Bioengineering and Biomechanics, vol 1, No 1.pp 95-101, 1999,

Nagy G. T., Golinski W. Z., Gentle C. R., *Three-dimensional Non-linear Finite Element Analysis of the Human Lumbar Intervertebral Disc*, Proc. of the BUDAMED '99 Conference on Biomedical and Clinical Engineering, Budapest, Hungary, 1999,

Nagy G. T., Golinski W. Z., Gentle C. R., *Analysis of the Human Lumbar Intervertebral Disc Based on a Three-dimensional Non-linear Finite Element Model*, Journal of Technology in Engineering and Medicine, 1, February, 2000.

Golinski W.Z., Gentle C.R., *Finite Element Modelling of Biomechanical Dummies – the Ultimate Tool in Anti-whiplash safety design?* , Proc. of the 6<sup>th</sup> International LS-DYNA Users Conference, Dearborn, USA, 9-11 April, 2000,

Golinski W.Z., Gentle C.R., *Design of an Anti-Whiplash Safety Device Based on Biomechanical Finite Element Modelling*, Proc. of Mechanics and Materials in Design 2000, Orlando, Florida, USA, 29-31 May, 2000,

Golinski W.Z., Gentle C.R., *An Investigation of Whiplash Using Finite Modeling of Biomechanical Dummies*, To be presented at the ICRASH2000 – International Crashworthiness Conference, London, UK, September, 2000,

## LIST OF ABBREVIATIONS AND SYMBOLS

|               |                            |
|---------------|----------------------------|
| v             | Poisson's Ratio            |
| CAD           | Computer Aided Design      |
| CT            | Computerised Tomography    |
| DOF           | Degree of Freedom          |
| E             | Young's Modulus            |
| FE            | Finite Element             |
| FEA           | Finite Element Analysis    |
| FEM           | Finite Element Method      |
| G             | Shear Modulus              |
| Ixx, Iyy, Izz | Moment of Inertia          |
| k             | Contact Stiffness          |
| LCM           | Tearing Force of Ligament  |
| M             | Mass                       |
| MoI           | Mechanism of Injury        |
| MRI           | Magnetic Resonance Imaging |
| NIC           | Neck Injury Criterion      |
| PMTO          | Post Mortem Test Object    |
| SD            | Standard Deviation         |
| t             | Uniform thickness          |
| VHP           | Visible Human Project      |

# TABLE OF CONTENTS

|   |     |
|---|-----|
| ABSTRACT.....   | i   |
| ACKNOWLEDGEMENTS .....  | ii  |
| LIST OF PUBLICATIONS .....  | iii |
| LIST OF ABBREVIATIONS AND SYMBOLS .....                           | vi  |
| TABLE OF CONTENTS.....  | vii |
| CHAPTER 1 INTRODUCTION .....                                      | 1   |
| 1.1 The Whiplash Injury .....                                     | 2   |
| 1.1.1 Radiological research .....                                 | 3   |
| 1.1.2 Statistical research.....                                   | 4   |
| 1.1.3 Animal testing .....  | 5   |
| 1.1.4 Dummy sled testing.....                                     | 6   |
| 1.1.5 Pathological investigations and Post Mortal sled tests..... | 9   |
| 1.1.6 Volunteer sled testing.....                                 | 10  |
| 1.1.7 Testing <i>in vitro</i> on harvested cervical spines .....  | 12  |
| 1.1.8 Numerical models .....                                      | 13  |
| 1.2 The Anatomy Of The Spine.....                                 | 16  |
| 1.2.1 Anatomy of cervical spine from C3 to C7 .....               | 18  |
| 1.2.1.1 Vertebrae.....  | 18  |

|   |    |
|---|----|
| 1.2.1.2 Intervertebral disc .....   | 19 |
| 1.2.1.3 Ligaments.....  | 19 |
| 1.2.2 Anatomy of occipital-atlanto-axial complex (C0-C1-C2) .....   | 20 |
| 1.2.2.1 Occipital condyle and C1, C2 vertebrae. ....  | 21 |
| 1.2.2.2 The ligaments of the CO-C2 complex. ....  | 23 |
| 1.3 The Objectives Of The Project .....   | 27 |
| CHAPTER 2 2.5 DIMENSIONAL FEM MODEL TO INVESTIGATE<br>“WHIPLASH” .....                                      | 30 |
| 2.1 Introduction .....  | 31 |
| 2.2 Model Geometry.....   | 31 |
| 2.3 Material Properties .....   | 35 |
| 2.4 Loading Conditions .....  | 37 |
| 2.5 Results .....   | 38 |
| CHAPTER 3 3-DIMENSIONAL FEM MODEL.....  | 42 |
| 3.1 Introduction .....  | 43 |
| 3.2 Model Geometry.....   | 44 |
| 3.3 Material Properties .....   | 46 |
| 3.4 Loading Conditions .....  | 48 |
| 3.5 Results .....   | 50 |
| CHAPTER 4 3-DIMENSIONAL FEM MODEL OF THE HEAD-NECK<br>COMPLEX ON A SIMPLIFIED MODEL OF THE HUMAN BODY. .... | 55 |
| 4.1 Introduction .....  | 56 |

|  |        |
|--|--------|
| 4.2 Model Geometry.....  | 56     |
| 4.3 Whiplash Protection Device.....  | 58     |
| 4.4 Material Properties.....   | 60     |
| 4.5 Loading Conditions.....  | 61     |
| 4.6 Results.....   | 63     |
| <br>CHAPTER 5 ADVANCED FE MODEL OF THE HEAD-NECK COMPLEX ON<br>A FE MODEL OF THE HYBRID III DUMMY.....                                   | <br>66 |
| 5.1 Introduction.....  | 67     |
| 5.2 Model Geometry.....  | 67     |
| 5.3 Model Properties.....  | 69     |
| 5.4 Loading Conditions.....  | 70     |
| 5.5 Results.....   | 72     |
| <br>CHAPTER 6 ANTI-WHIPLASH DEVICE INVESTIGATION USING THE<br>BIO-HYBRID-DUMMY MODEL.....  | <br>76 |
| 6.1 Introduction.....  | 77     |
| 6.2 Model.....   | 77     |
| 6.3 Loading Conditions.....  | 78     |
| 6.4 Results.....   | 79     |
| <br>CHAPTER 7 THE INFLUENCE OF THE DYNAMICALLY INCREASING<br>GAP BETWEEN HEAD AND HEAD RESTRAINT ON THE WHIPLASH<br>INJURY SEVERITY..... | <br>82 |
| 7.1 Introduction.....  | 83     |
| 7.2 Seat Model.....  | 83     |

|   |     |
|---|-----|
| 7.3 Results .....   | 84  |
| CHAPTER 8 CRASH PULSE INFLUENCE ON THE WHIPLASH INJURY SEVERITY .....   | 88  |
| 8.1 Introduction .....  | 89  |
| 8.2 Loading Conditions .....  | 90  |
| 8.3 Results .....   | 91  |
| CHAPTER 9 THE INFLUENCE OF INITIAL HEAD ROTATION (NON SAGITTAL PLANE POSITIONING) ON WHIPLASH INJURY .....        | 95  |
| 9.1 Introduction .....  | 96  |
| 9.2 Model .....   | 96  |
| 9.3 Loading Conditions .....  | 97  |
| 9.4 Results .....   | 98  |
| CHAPTER 10 SEAT RAKING IN WHIPLASH ACCIDENT SITUATIONS WITH INITIAL VERTICAL ROTATION OF THE HEAD. ....           | 104 |
| 10.1 Introduction .....   | 105 |
| 10.2 Results .....  | 105 |
| CHAPTER 11 LOAD IMPULSE VARIATION IN WHIPLASH ACCIDENT SITUATIONS WITH INITIAL VERTICAL ROTATION OF THE HEAD..... | 112 |
| 11.1 Introduction .....   | 113 |
| 11.2 Results .....  | 113 |
| CHAPTER 12 CONCLUSION AND FURTHER WORK .....  | 121 |
| REFERENCES .....  | 126 |
| APPENDIX A .....  | I   |

|                  |     |
|------------------|-----|
| APPENDIX B ..... | II  |
| APPENDIX C ..... | III |
| APPENDIX D ..... | IV  |
| APPENDIX E ..... | V   |

**CHAPTER 1**  
**INTRODUCTION**

## 1.1 The Whiplash Injury

The term **whiplash** was first used by Crowe (1928) while describing patients with neck injuries. It is used to describe **whip-like** movement of the head and neck relative to the torso. Whiplash injury is associated with a wide range of symptoms with the most common being neck pain. However other symptoms such as blurred vision, tinnitus, dizziness, nausea, paresthesias, numbness and even back pain are often reported (Foreman and Croft, 1997).

Even though the term whiplash has been used for over seventy years, the injury associated with it became a point of world-wide interest with the growing popularity and speed of automobiles. The term whiplash was initially used to describe injuries to the neck caused by the head being forced backwards during a rear end collision in cars without head restraints. Research indicated that head restraints could prevent whiplash injuries, as early as the 1960's (Insurance Institute for Highway Safety, 1999). In 1969, head restraints became mandatory standard equipment in all new cars sold in the USA (Croft, 1997). Even though they were intended primarily as safety devices, they became known almost universally as headrests. This was partly the fault of the manufacturers who were worried about being sued by occupants who suffered a whiplash injury in spite of their presence. In fact if these early head restraints were adjusted to a low position to provide a comfortable resting point, they could even make the injury worse than without the head restraint. The restraint will actually act as a fulcrum over which the cervical spine pivots. This is especially likely with tall drivers (Severy et al. 1968). Most head restraints are adjustable and they are left in the low position. They are therefore nowhere near high enough or close enough to the back of many people's heads for effective protection in rear end crashes. As a result, the introduction of the head restraint did not solve the problem, and the whiplash injury still constitutes a big problem worldwide. In 93.5% of rear-end accidents with personal injuries at least one of the occupants claims a neck injury (VdS, 1994), while other injuries are comparatively rare (Muenker et. al, 1994).

Being the most common injury in car accidents makes whiplash very significant from both the economical and medical points of view.

From the early 1960's the engineering, as well as the medical, community became involved in research to understand the whiplash injury phenomenon and prevent its appearance. Different means have been employed to achieve this goal, producing numerous hypotheses of the mechanism of injury (MoI) and leading to new designs of car seats which were hoped to prevent the occurrence of whiplash injury. As a result of this effort, numerous scientific publications have been presented including two full books (Forman and Croft, 1997; Gunzburg and Szpalski, 1998) in recent years. The following overview of research into whiplash, divided into 8 logical groups, has been provided to show the present state of knowledge. This review will identify the gaps that exist in current knowledge about whiplash injuries and the contribution that computational biomechanical modelling can make.

#### 1.1.1 Radiological research

Radiology has been used widely by the medical community to assess whiplash injuries sustained by car occupants. However, the use of radiology to detect the signs of whiplash can be summed up by McNab's (1990) statement that the results of this approach are inconclusive. Nevertheless, radiology has been lately used by the engineering community to record the behaviour of the spine during sled tests with volunteers.

Griffith et al. (1995) compared the X-rays of clinically proven whiplash injuries with those from a control group of "healthy" subjects. He states in the introduction to the paper, that on many occasions little or no bony damage is present, whereas ligament injury is common.

Penning, in a series of articles (1992a, 1992b, 1994), presented a new MoI of whiplash. Based on a literature review and his own radiological data, Penning proposed the primary whiplash MoI as being backwards hypertranslation of the head relative to the torso and not the commonly thought hyperextension. This

suggested over-stretching of the posterior ligaments of the C0-C2 spinal complex, leading to instability of the complex and even possible rupture of the ligaments.

In a series of articles Matsushita (1994), and later Ono et al. (1997a, 1997b, 1998) employed radiology to study cervical spine kinematics during sled tests with volunteers. The X-ray cineradiography technique was used to analyse the motion of individual vertebrae during frontal and rear accident scenarios as well as to analyse the influence of seat stiffness on that motion. Ono et al. (1997a) recorded the formation of an S-shape in the cervical spine during the rear-end accident scenario, with flexion in the upper part and extension in the lower part of the cervical spine. Furthermore they found the extension motion in the lower vertebral segments (C6, C5 and C4) as being beyond the normal physiological range of motion.

#### 1.1.2 Statistical research

In recent years there have been several epidemiological studies of whiplash associated injuries, resulting in certain statistics regarding injury risk based on sex, age, accident conditions and so on, in many cases producing contradictory conclusions. However a few of them are worthy of mention due to their interesting concluding factors which, according to the authors, affect whiplash injury.

Olsson et al. (1990), after studying the occupants of Volvo cars and following their progress over twelve months, observed a significant difference between duration of symptoms and whether the distance between the head and the head restraint was greater or smaller than 10 cm. Distances greater than 10 cm produced symptoms lasting at least one year, as opposed to less than a year for gaps below 10cm.

Koch et al. (1995) found that the injury risk is higher where there is a significant difference in the masses of the striking and struck cars. Bostrom et al. (1997), in their combined study of accident data and simulations, concluded that the mass ratio between the struck and striking car correlated with the injury risk. The higher the difference in mass between striking and struck car, the higher the injury risk.

This implies that the risk of injury in the struck car increases due to the increasing change of velocity following impact.

Krafft (1998) compared the characteristics of rear impacts causing short- and long-term disability neck injuries. She found a strong influence of mass ratio between the struck and the striking car in terms of initial disability, while the crash pulse influenced long-term disability.

Worth (1985) investigated the kinematics of the cervical spine in his study of patients with neck pain following car accidents. He reported decreased mobility in the C0-C1, despite the post-accidents X-rays being reported as normal in 90% of cases.

Skovron (1998) in her "Epidemiology of Whiplash" presents neck pain as the common symptom of whiplash (88-100%) followed by headache (54-66%) and shoulder pain (40-42%). Furthermore she shows the economic aspect of the injury, as only 47% of the victims are able to return to work after 4 weeks, with 2% not being able to do so even after 1 year.

### 1.1.3 Animal testing

Even though animal experiments are not fully comparable with the humans' behaviour in crashes, due to the similar anatomy of specific regions of the body they continue to be used in safety testing. Especially under severe crash conditions which could lead to permanent damage, animal tests are used to obtain data not available from volunteers or PMTO's (Post Mortem Test Object). In the field of whiplash the following two studies have brought valuable information.

Unterharnscheidt et al. (1986) subjected rhesus monkeys to deadly accelerations (Figure 1). For both positive and negative accelerations, the autopsy showed a dislocation of C1 with destruction of transverse and alar ligaments as well as the spinal cord. They concluded, based on the pictures from the experiment, that the injury had occurred before the translation of the head was completed.

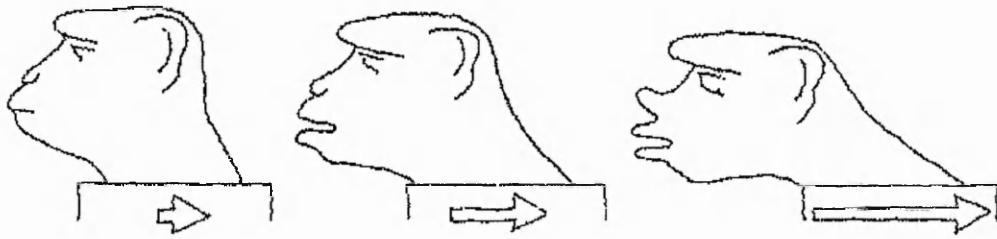


Figure 1 Rhesus monkey under rapid acceleration of the trunk backwards.

Bostrom et al. (1996), following on from the earlier work of his group (Svensson et al., 1993; Ortengren et al., 1996) exposed pigs to swift extension-flexion motions (whiplash) of the cervical spine, measuring pressure changes in the spinal canal. They found signs of spinal ganglia injuries and indicated the pressure change in the spinal canal as being responsible for it. Furthermore their preliminary results showed that the ganglion injuries, as well as pressure changes in the spinal canal, seemed to correlate to the phase when, during the rearward motion of the head, the neck forms an S-shape. Moreover, they proposed a possible candidate for the Neck Injury Criterion (NIC), based on the relative acceleration between the top and the bottom of the cervical spine.

#### 1.1.4 Dummy sled testing

Development of cars involves intensive testing, including full-scale car crashes as well as sled tests of selected parts (seat, restraint systems), to meet legislative occupant safety requirements. Even though it has been used for over 20 years (Foster et al., 1977), the Hybrid III Dummy (Figure 2) is still the main biomechanical surrogate for the human body in those tests. The neck of the Hybrid III Dummy (Figure 3) is a flexible vertical component consisting of three rigid aluminium vertebral elements in butyl elastomer, with two aluminium end plates for attachment purposes, and a single tensioned steel cable running through the centre of it to provide axial strength. A special transducer is used to measure the axial and shear loads and the moment about the occipital condyle (C0). It is attached to the neck through a “nodding” joint.



Figure 2 Hybrid III dummy

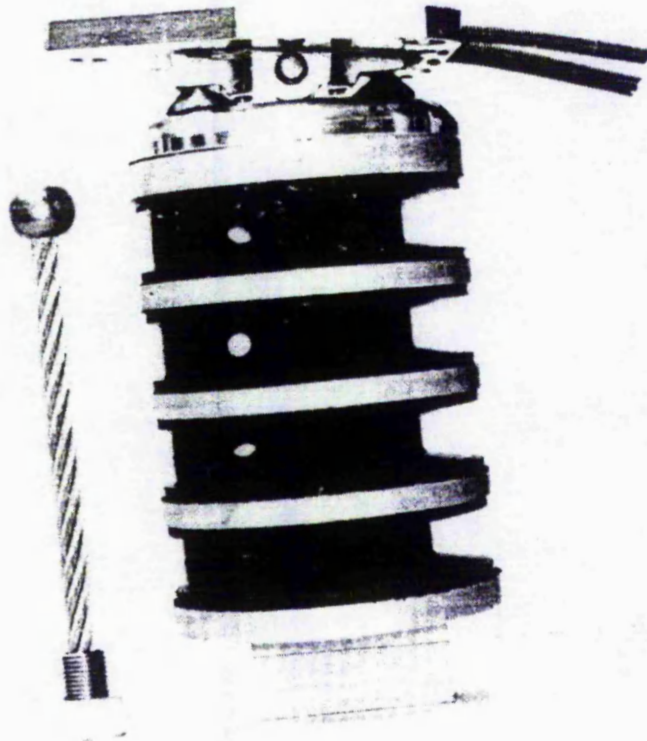


Figure 3 The standard neck of Hybrid III dummy.

Due to a growing awareness of whiplash injuries, two new neck designs for the Hybrid III Dummy have been proposed. The Rear Impact Dummy – neck (RID – neck; Figure 4) by Svensson and Lovsund (1992) and the TRID – neck (TNO Rear Impact Dummy – neck; Figure 5) by Thunnissen et al. (1996) were designed to be better than the Hybrid III neck by more closely replicating the behaviour of the human neck in rear end collisions. They both were validated against volunteer experiments based on angular displacement of the head relative to the torso. The dynamic response of the two necks appears to be very similar.

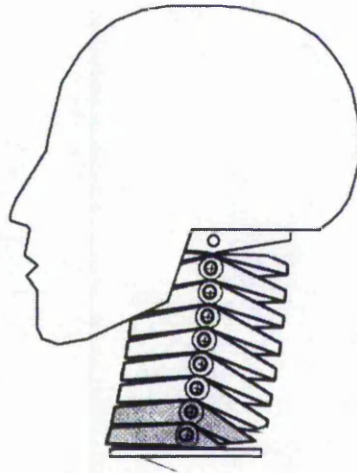


Figure 4 RID neck.



Figure 5 TRID neck.

However, Geigl et al. (1995), in a comparative sled study between volunteers, PMTO's and a Hybrid III Dummy with standard and RID necks, has shown strong deficiency in biofidelity of the dummy neck. He concluded that both necks did not show the significant degree of flexion between the head and the upper cervical spine observed in PMTO tests. Furthermore neither had sufficient modelling of the initial lordosis of the cervical spine.

Lately a new dummy prototype for low speed rear –end collisions was developed and validated (Davidsson et al., 1998a). The BioRID (Biofidelic Rear Impact Dummy) was developed mainly as a research tool, consisting of a flexible human-like spine, soft torso and new pelvis (Figure 6). Preliminary sled-tests showed that BioRID behaved better than Hybrid III, and can be seen as representing significant progress. However, there is still long way ahead to achieve sufficient biofidelity of dummies in rear end accidents.

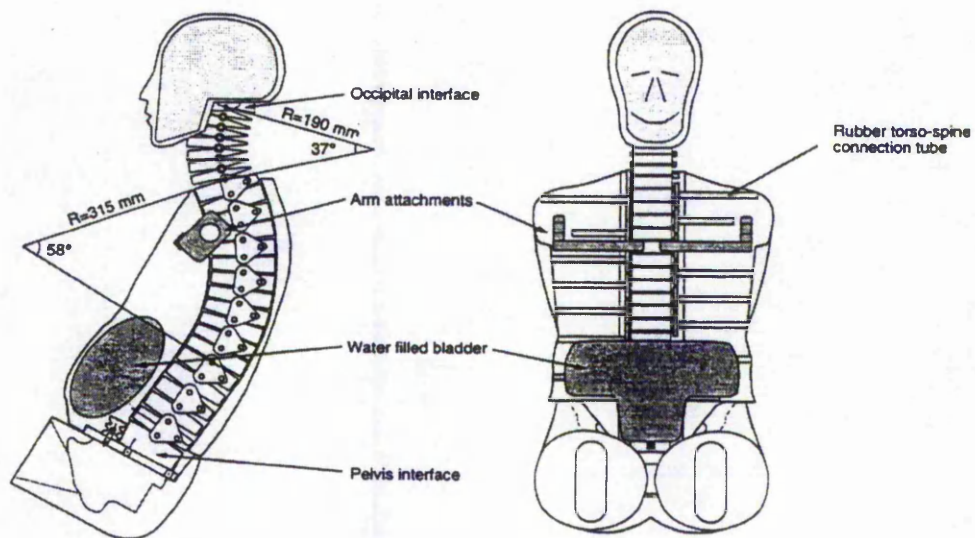


Figure 6 BioRID dummy.

### 1.1.5 Pathological investigations and Post Mortal sled tests

Pathological investigations in fatal car accidents have revealed several cases of cervical dislocations as a result of acceleration of the head. Davis et al. (1971) described dislocation of the C1-C2 segment with complete destruction of the alar

ligaments and spinal cord, but intact transverse ligament. Alker et al. (1978) has reported dislocation of the C0-C1 element in the posterior direction.

To investigate such extreme human body response under severe loading, sled tests with PMTO's have been conducted. Geigl et al. (1994) have subjected 6 PMTO's during sled test to a speed difference of up to 15 km/h. The whole event was documented by high speed video camera, with two vertebrae body being mounted with extra targets to better understand the relative rotation between different segments of the cervical spine. Based on this study, the authors noted that in the first phase of the event, up to 50 to 80 ms, there was no relative rotation between vertebrae bodies. Afterwards they noted a relative flexion in the upper cervical spine. Autopsy was not performed after the experiments, therefore no data on internal neck damage is available.

Later on, a series of experiments with PMTO's at the University of Heidelberg (Germany) led to a discussion, involving the public media, on the moral implications of such experiments. As a result of this, PMTO tests have been put under strict control and even stopped in some countries.

#### 1.1.6 Volunteer sled testing

During recent years many tests with volunteers have been performed. They were used mainly as a comparison base to assess the biofidelity of existing car crash dummies (Geigl et al., 1995), or as a base for new dummy development (Davidsson et al., 1998b), as well as to assess different seats designs with regard to human head-neck kinematics (Eichberger et al., 1996). All volunteer tests, regardless of their purpose, are useful in understanding the natural human neck behaviour, and help the engineering and medical community to understand the kinematics behind whiplash injury, even though they are performed at safe levels under strict safety protocols.

Geigl et al. (1994) performed 37 experiments with 25 volunteers using a mini-sled (Figure 7). The sled was first accelerated to a certain speed by electric motor and then was decelerated using special longitudinal friction-brake elements. Measurements from real accidents were used in order to achieve realistic

deceleration of the sled. No injuries were reported and the relative rotation of the head was extracted from analysing the video recordings. Regardless of the initial seating position, they noted no head rotation during the first 60 to 100 ms. Afterwards, the head started to rotate backwards with shoulders already reflected forward and the head still keeping a low translatory movement backwards. Moreover they did not note any relative rotation between vertebrae up to 50 to 80 ms, after which period the motion started resulting in relative flexion of the upper part of the cervical spine. They also indicated the possibility of the inclination of the seat back being responsible for dynamic enlargement of the initial gap between the head and the head restraint.

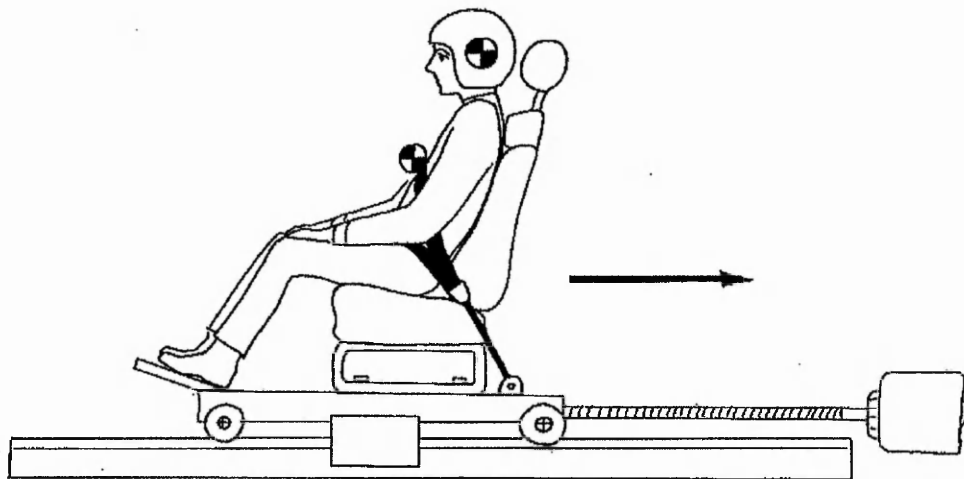


Figure 7 Schematic diagram of the sled test setup.

Tests with volunteers have been used to calculate new NIC (Bostrom et al., 1996) for human subjects, but with mixed success. Wheeler et al. (1998) performed experiments at 4 km/h and 8 km/h rear-end speed. The subjects' clinical data revealed injury symptoms in 33% of the tests and in 52% of the subjects despite the NIC not exceeding the proposed injury threshold. Furthermore, reported post-impact examination suggested no nerve-based symptoms, against the proposed NIC based on nerve injuries. On the other hand, Eichberger et al. (1998) concluded that their NIC predicts dangerous impact conditions with acceptable accuracy. They also pointed out an extensive relative motion between head and

neck associated with a high NIC, suggesting for the future design of seats the use of NIC in conjunction with neck loads and displacement.

### 1.1.7 Testing *in vitro* on harvested cervical spines

Dvorak et al. (1988) provided extensive *in vitro* investigation into the biomechanics of the upper cervical spine. He suggested that the role of the alar ligament with respect to the stability of the C0-C2 complex and that the whiplash injury mechanism might have been long underestimated, especially when the transverse ligament remained intact. They pointed out the stabilisation role of the musculature of the suboccipital region in view of the relatively low strength of the alar ligament compared with the weight of the head, suggesting a partial or complete rupture of the alar ligaments in the case of unexpected trauma, when the muscles are relaxed. However, this was a static investigation into the biomechanics of the craniocervical region and did not include the dynamic response of the spine.

In a series of articles, Panjabi and his group (Grauer et al., 1997; Panjabi et al., 1998a, 1998b, 1998c) published results from an extensive *in vitro* test series. Fresh human cadaveric specimens (C0-T1), with preserved osteoligamentous structure, were subjected to whiplash trauma on a specially constructed sled (Figure 8). Due to the long term use of the specimen, they had to remove quickly decaying brain. Therefore, the whole head was removed and substituted with a steel surrogate, what resulted in altering the mass and rotational inertia properties of the head. Furthermore, the specimens used lacked the associated muscular structures. During the simulations the following parameters were monitored: sled and head surrogate accelerations, head surrogate displacements, relative motions of all intervertebral joints, loading at C0 and T1 vertebrae, and elongations of the vertebral artery and capsular ligaments. They concluded that the mechanism of the whiplash injury is the formation of the S-shape curvature of the spine in the initial stage of the trauma, with extension at the lower levels and flexion at the upper levels of the spine. They proposed that the lower cervical spine is injured by extreme hyperextension during the S-shape formation and noted the tendency for injuries to occur also at the upper levels of the cervical spine at higher trauma accelerations. Analysing capsular ligament stretching they found only moderate

values of the strain. However, they hypothesised that the capsular ligament stretching will be significantly larger when, during the whiplash trauma, the head of the subject is turned to one side, based on physiological loading results. During these tests, they recorded the maximum elongation of the capsular ligaments in axial rotation and lateral bending, when the head-turn scenario under whiplash loading will produce axial rotation, lateral bending and extension of the neck.

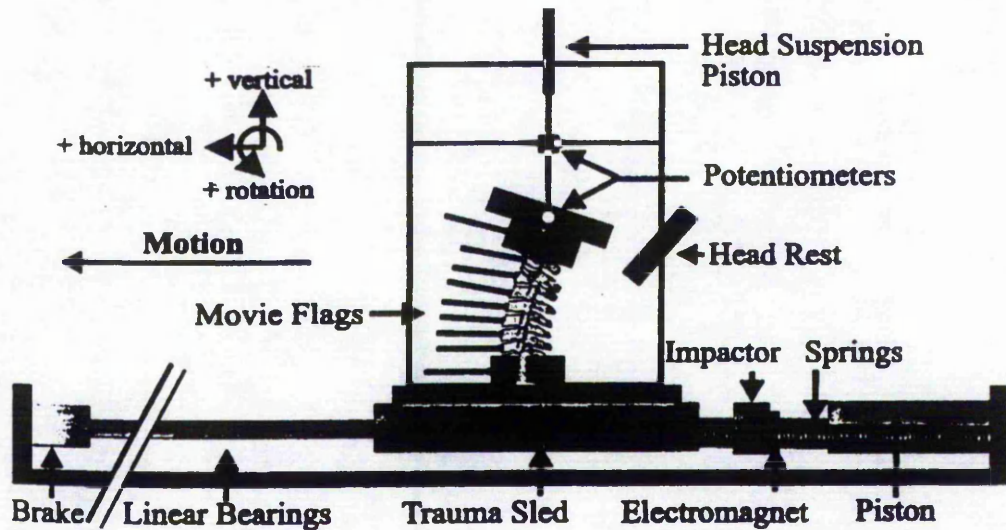


Figure 8 Schematic diagram of the whiplash trauma apparatus.

### 1.1.8 Numerical models

Different numerical methods have been employed to investigate neck behaviour. In early studies continuum and lumped parameters models were used to describe head neck motion (Liu and Murray, 1966; McKenzie and Williams, 1971; Merrill et al., 1984; Wismans et al., 1986, 1987; Deng and Goldsmith, 1987). However, they tended to oversimplify the cervical spine. In more recent years two methods: Multibody and Finite Elements seem to dominate the field of neck modelling.

De Jager et al. (1994) adapted and implemented the head-neck model of Deng and Goldsmith (1987) into the multibody code MADYMO and later proposed a global and detailed model of the cervical spine (de Jager et al., 1996). The model comprised a rigid body head and vertebrae connected through linear viscoelastic discs, nonlinear viscoelastic ligaments, facet joints and muscles and was validated against volunteer experiments in lateral and frontal impact. Van der Horst et al.

(1997) improved de Jager's (1996) model by representing the muscles in more detail. Camacho et al. (1997; 1999) presented a lumped mass model to investigate the near vertex head impact. Most recently Nightingale et al. (2000) formulated and implemented a 2-dimensional multibody model of the neck to investigate the buckling modes of the cervical spine. Rigid body dynamics models are computationally highly efficient and they represent the kinematics quite well. Recently the MADYMO code has even integrated finite element components.

However, Finite Element modelling is the most suitable numerical method for analysing complex geometrical structures with complex loading conditions and multiple material compositions, such as the cervical spine. In recent years there have been several finite element models of the human neck. Saito et al. (1991) used a 2-dimensional cervical spine model to study laminectomy deformity. Kleinberger (1993) developed a 3-dimensional model of the C0-T1 part of the spine and subjected it to transient loading. The model topology was highly simplified, especially in the C0-C2 region, with no differences between the facet joints and was not related to any specimens. Linear elastic properties were applied to the intervertebral discs and ligaments, with no representation of the complex ligamentous structure of the C0-C2 complex and muscles. Simulations were run for axial compression and frontal flexion. Dauvilliers et al. (1994) proposed a model of the human cervical spine (C1-T1) with rigid vertebrae and head. Once again the topology of the model was highly simplified with the interfaces between C0-C1 and C1-C2 represented by joints with no ligamentous representation. Elastic bricks and spring elements were used to model the discs and the ligaments, with the passive muscle response included in the characteristics of the ligaments. The simulations were conducted in the frontal and lateral directions. Nitsche et al. (1996) created a C1-C7 cervical spine model with deformable vertebrae, intervertebral discs and ligaments modelled by brick and membrane elements. As in the previous models, the geometry was highly simplified and muscles were not present. The model was tested against experimental results in frontal and lateral flexion and compression. Finally Yang et al. (1998) presented a model of the head-neck complex based on a detailed geometrical description of the C1-T1 vertebrae. Vertebrae and intervertebral discs were modelled using brick elements, with the first using linear elastic-plastic materials, whereas the latter used linear

viscoelastic formulation. The ligaments present in the model were represented by non-linear bar elements or as tension-only membranes. The model incorporated a previously developed head and brain model and passive muscle response. Simulations included a head drop test, rear-end impacts, and, after integrating with a skeleton torso model, interaction with a pre-deployed airbag.

## 1.2 The Anatomy Of The Spine

The human spine consists of thirty three vertebrae, separated by inter-vertebral discs, and stiffened by muscles and ligaments.

The spine is divided into five logical subsections, numbered from the top to the bottom (Figure 9):

- **Cervical Spine** - seven vertebrae from the skull to the top of the thoracic spine (C1-C7)
- **Thoracic Spine** - twelve vertebrae to which the ribs are attached (T1-T12)
- **Lumbar Spine** - five vertebrae (L1-L5)
- **Sacral Spine** - five fused vertebrae
- **Coccygeal Spine** - three to four fused segments

In the frontal plane the spine is generally straight and symmetrical. In the lateral plane there are four normal anatomic curves (Figure 9) which are convex anteriorly in the cervical and lumbar regions (lordosis) and convex posteriorly in the thoracic and sacral regions (kyphosis).

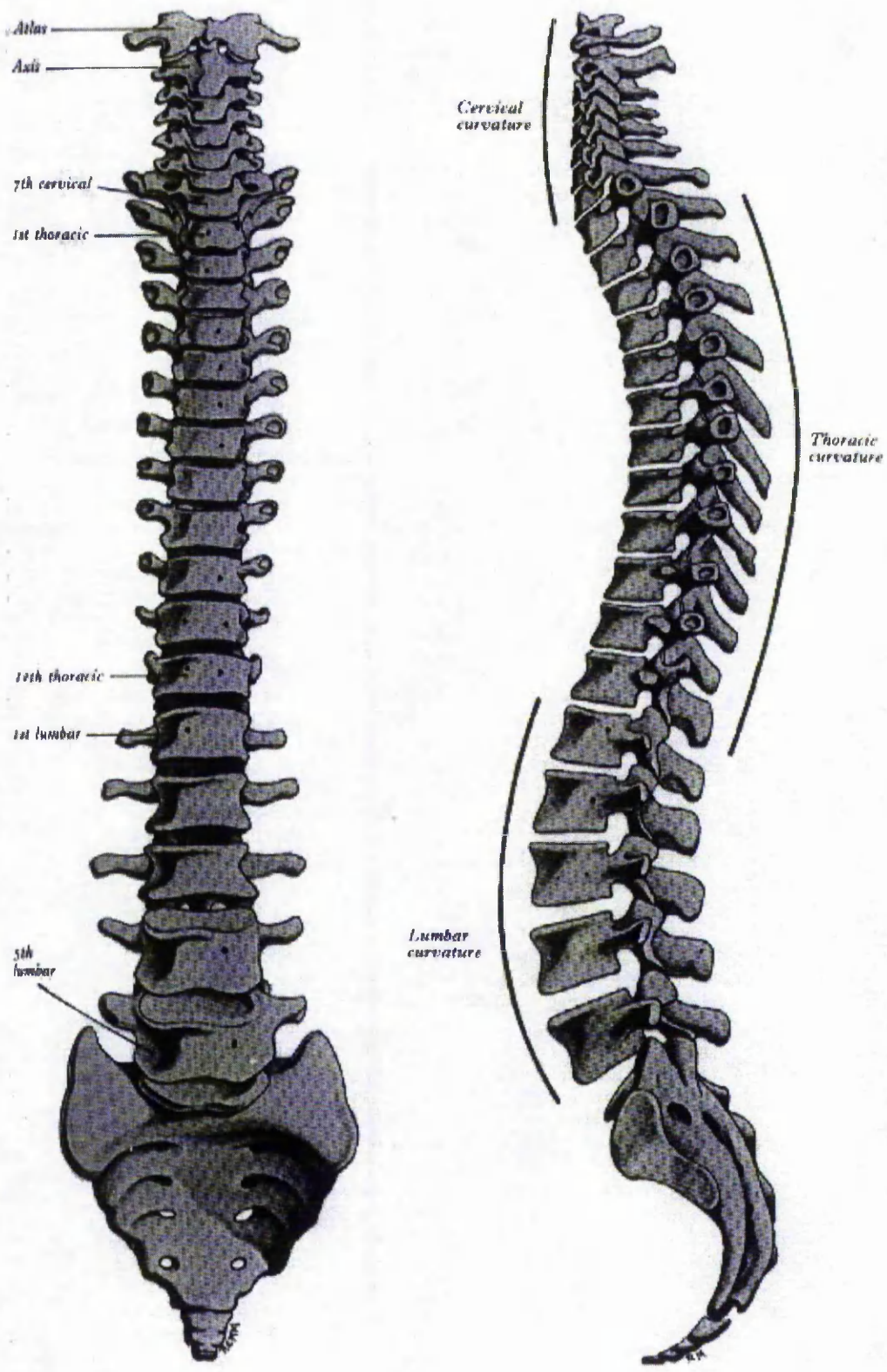


Figure 9 Human Spine.

The cervical spine is the main area of interest with regard to the whiplash injury problem since it is the part of the spine located in the human neck.

From an anatomical point of view the cervical spine can be divided into two main parts:

- **C0 - C2 complex.** Upper cervical spine is responsible for the movement of the head upon neck. The C0-C1 joint is used when the head nods forwards and backwards, or rocks from side to side. The C1-C2 joint allows the head to turn from side to side. Therefore the upper cervical vertebrae, atlas (C1) and axis (C2) differ from other human vertebrae and this part of the spine is lacking intervertebral disc
- **C3 – C7.** Middle and lower cervical spine allow the neck to bend forwards, backwards or to the side and to be rotated from side to side. The C3-C7 vertebrae have a typical structure and are connected by intervertebral discs.

### 1.2.1 Anatomy of cervical spine from C3 to C7

#### 1.2.1.1 Vertebrae.

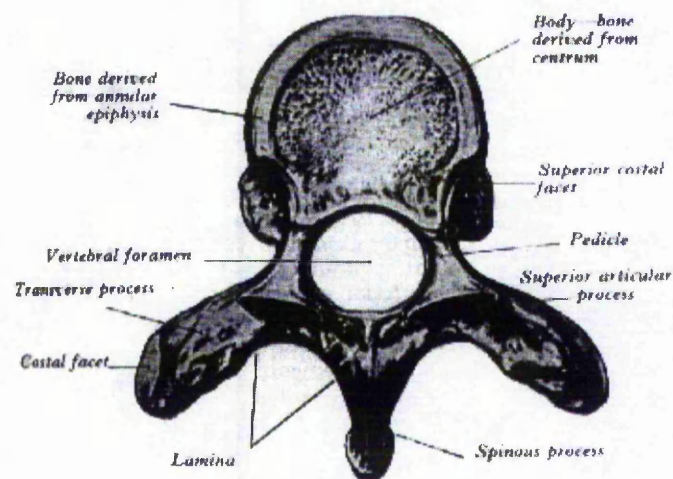


Figure 10 Typical human vertebra

The design of the vertebrae in the cervical spine from C3 -C7 is approximately the same (Figure 10). The vertebrae consist of the vertebral body and posterior bony

ring - the neural arch containing two pedicles, from which arise seven processes: articular, transverse, and spinous. The neural arch and vertebral body form a spinal canal for the spinal cord.

#### 1.2.1.2 Intervertebral disc.

Between vertebrae are the intervertebral discs (Figure 11), which contain three parts:

- **Nucleus Pulposus** - centrally located area composed of loose fibres in a mucous gel.
- **Annulus Fibrosus** - outer boundary of the disc composed of fibrous tissue in concentric laminated bands. In each bands fibres run in the same direction, but fibres in any two adjacent bands run in opposite direction.
- **Cartilaginous End-Plate** - form of hyaline cartilage that separates the other two components of the disc from the vertebral body.

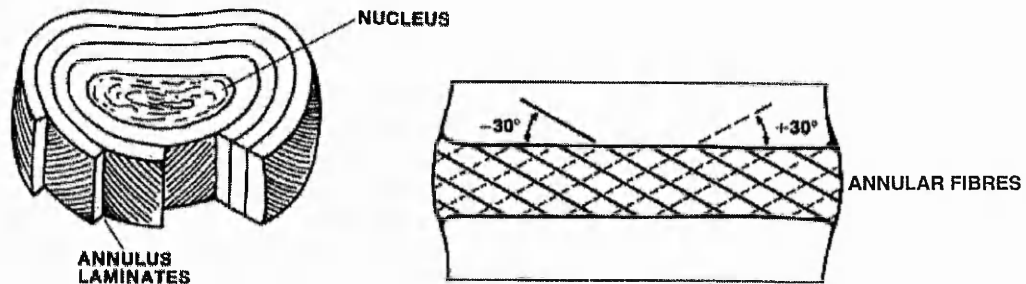


Figure 11 Intervertebral disc

#### 1.2.1.3 Ligaments.

Between C2 and C7 are seven ligaments of the spine, which are common for the whole spine from C2 to the sacrum (Figure 12). They vary in size, orientation and attachment point:

- **Anterior Longitudinal Ligament** - attached to the atlas and anterior surfaces of all vertebrae, including a part of the sacrum

- **Posterior Longitudinal Ligament** - runs over the posterior surfaces of all the vertebral bodies to the coccyx
- **Intertransverse ligament** - between the transverse processes in the thoracic region
- **Capsular Ligaments** - attached just beyond the margins of the adjacent articular process
- **Interspinous Ligaments** - connect the spinous processes, attached from the root to the apex of each process
- **Superspinous Ligament** - connect the apices of the spinous processes

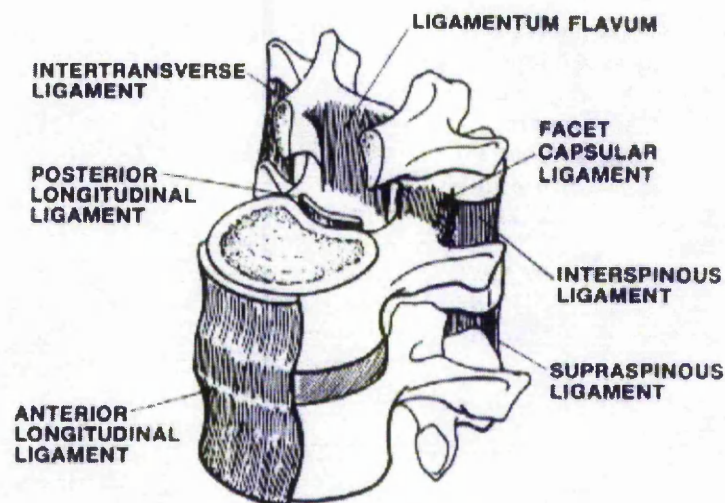


Figure 12 Ligaments of the spine.

### 1.2.2 Anatomy of occipital-atlanto-axial complex (C0-C1-C2)

The C0-C2 complex is the most complicated and untypical part of the spine, due to its unique vertebral anatomy and lack of intervertebral discs. This complex consists of two joints:

- **Occipital-Atlantal Joint** - which is a joint between the skull ( occipital condyle ) and C1 vertebra ( atlas )
- **Atlanto-Axial Joint** - C1 vertebra (atlas ) and C2 ( axis )

1.2.2.1 Occipital condyle and C1, C2 vertebrae.

Going from the top of the complex to the bottom there are three parts:

- **C0 - Occipital Condyle** (Figure 13) - the surfaces on the bottom part of the skull, which create the C0-C1 joint with the atlas.

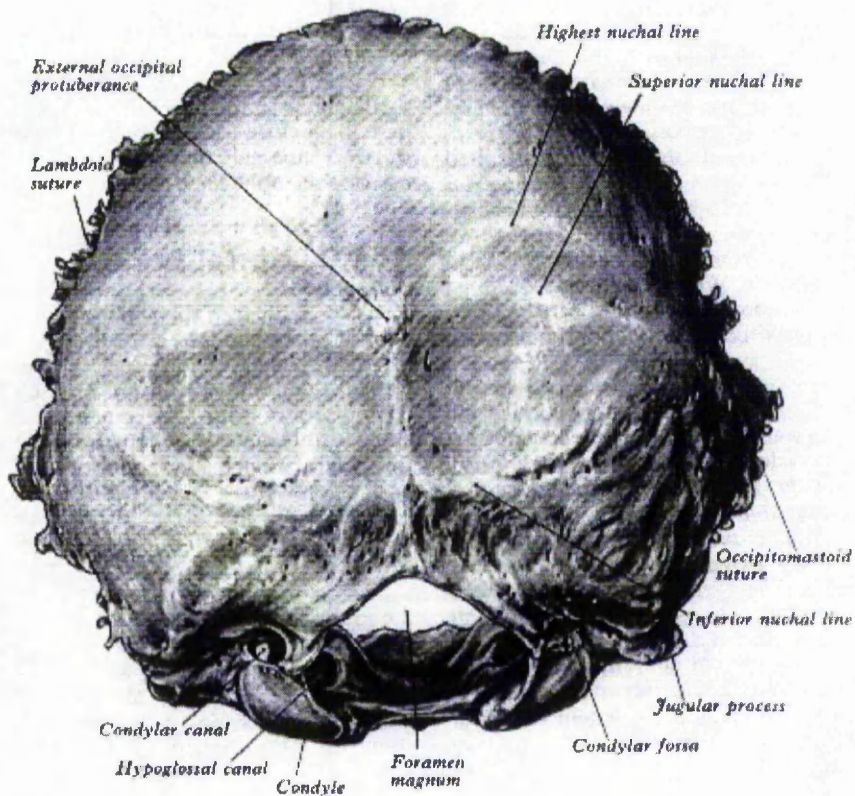


Figure 13 Bottom of the skull.

- **C1 - Atlas** (Figure 14) - the first cervical vertebra. It differs from all other vertebrae in lacking a body; its position is occupied by the dens of the axis. It consists of two lateral masses, connected in front by an anterior arch and posteriorly by a posterior arch. The anterior arch is slightly curved. It has on the inferior part the facet for the dens, and on the exterior part the anterior

tubercle. The lateral masses have on the upper surface facets for the corresponding occipital condyle, and on the bottom part facets for the axis. The posterior arch accounts for about two-fifths of the ring of the atlas. It has on the posterior side the posterior tubercle, which represents a spinous process. The transverse process is unusually long.

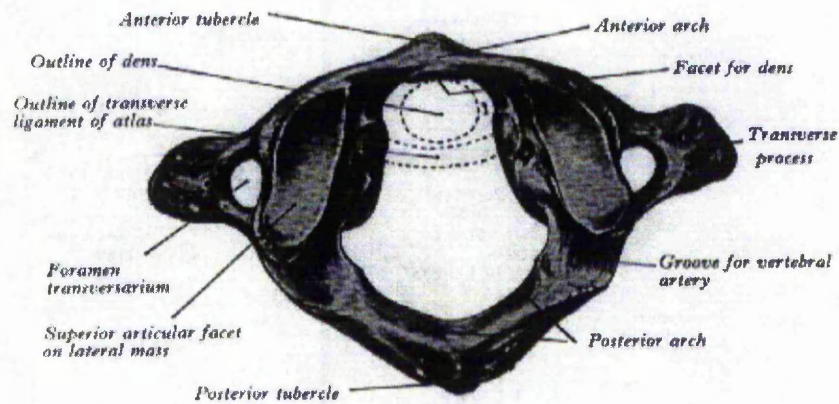


Figure 14 The first cervical vertebra - atlas (C1).

- **C2 - Axis** (Figure 15, Figure 16) - the second vertebra, is the pivot on which the atlas and the head rotate. It is located on the odontoid process - dens, which is a vertical extension of the body. On the front of the dens is a facet which forms a joint with the anterior arch of the atlas. The body is flanked by a pair of facets, which extend laterally from the body on the pedicles. These facets make a joint with the atlas. The laminae are thicker than in any other cervical vertebra. They fuse with a large and powerful spinous process. The transverse processes of the axis are small. The inferior articular facets are carried at the junction of pedicles and laminae and face as in a typical cervical vertebra.

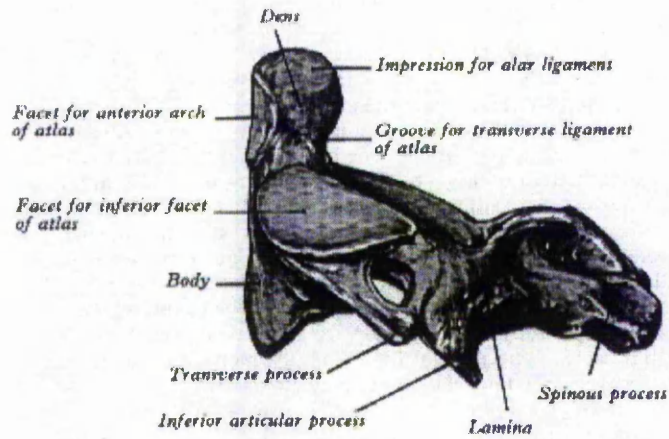


Figure 15 The second cervical vertebra - axis (C2) in left lateral view.

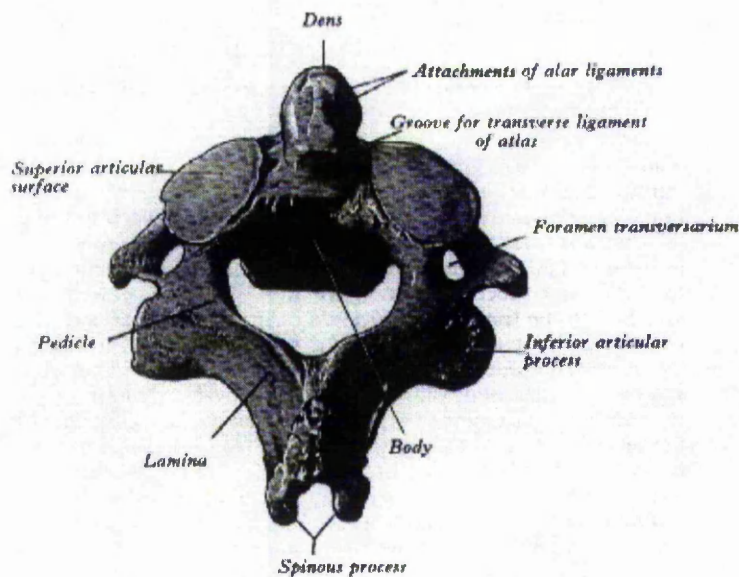


Figure 16 The second cervical vertebra - axis (C2) in posterosuperior view.

#### 1.2.2.2 The ligaments of the C0-C2 complex.

The structure of the ligaments is very complicated, because of the kinematics of this region. There are (Figure 17):

- **The Anterior Longitudinal Ligament** is a continuation of the ligament that runs the entire length of the spine. It begins at the anterior body of C2, attaches to the anterior ring of C1, and courses to the tubercle of C0.

- **The Anterior Atlanto-Dental Ligament** runs between the anterior part of the dens and the bottom portion of the anterior ring of C1.
- **The Anterior Atlanto-occipital Membrane** runs between the anterior ring of C1 and the anterior margin of the foramen magnum. This is thought to be a continuation of the anterior longitudinal ligament.
- **The Alar Ligaments** are a pair of structures attached to the tip of the dens and run to the medial surfaces of the occipital condyles.
- **The Posterior Atlanto-occipital Membrane** is attached to the posterior ring of C1 and the posterior portion of the foramen magnum.

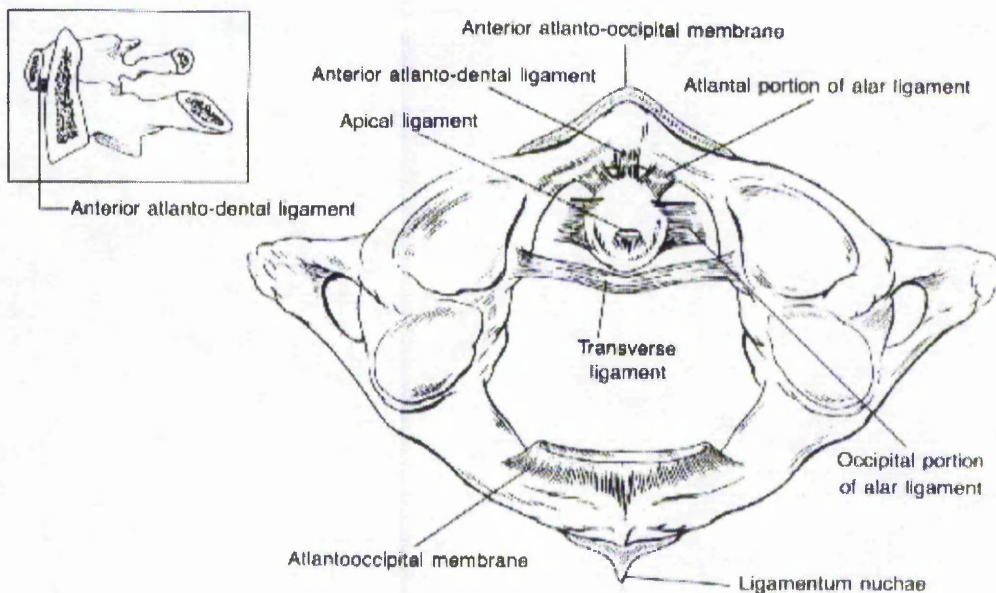


Figure 17 Ligaments of the upper cervical spine.

- **The Cruciate Ligament** (Figure 18) consists of **The Transverse Ligament** and an ascending and a descending band. The ascending band of this ligament is attached to the anterior edge of the foramen magnum. The descending band is attached to the body of C2.
- **The Transverse Ligament** is the most important ligament of the C0-C2 complex. It is attached to the two condyles of the atlas.

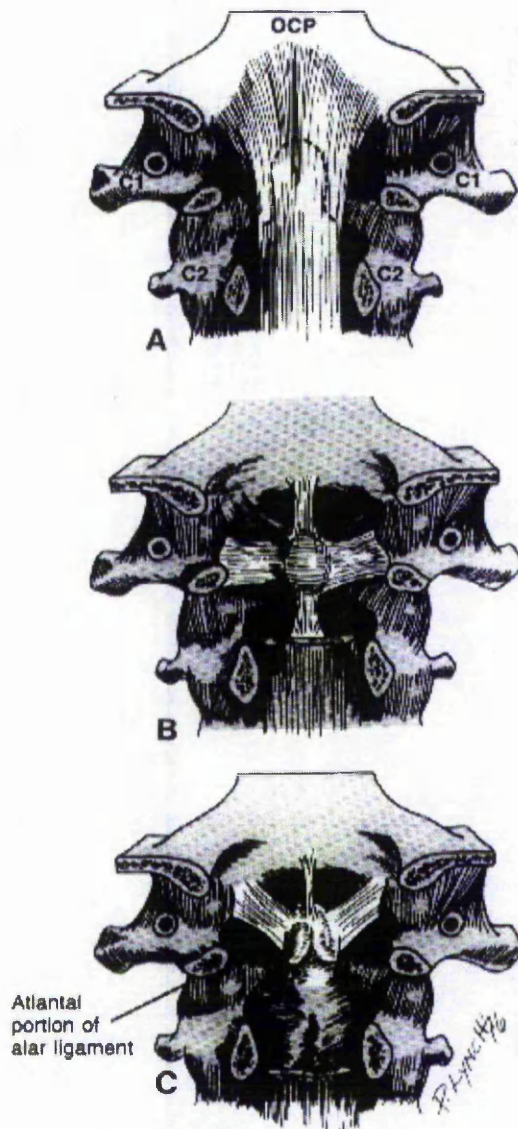


Figure 18 The major stabilising ligaments of the C0-C1-C2 complex: (A) The tectorial membrane. (B) The cruciate ligament. (C) Alar ligaments and the apical ligament.

- **The Tectorial Membrane**(Figure 18) is a continuation of the posterior longitudinal ligament. It runs from the body of C2 up over the dens, then makes a 45° angle in the anterior direction and is attached to the anterior edge of the foramen magnum.
- **The Nuchal Ligament**(Figure 19) consist of two parts. The funicular portion is a distinct band which runs from the posterior border of the occiput to the spine

of C7. The lamellar portion divides the posterior neck into right and left halves. Its superior border is attached to the posterior tubercle of the atlas, the spinous processes of the cervical vertebrae and the interspinous ligament.

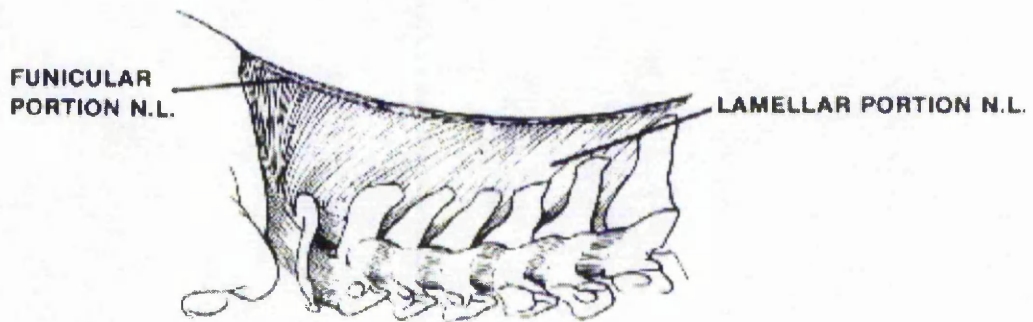


Figure 19 The nuchal ligament.

### **1.3 The Objectives Of The Project**

Based on the findings of the literature review reported in the previous section, it can be concluded that the MoI of whiplash can not be fully explained as a hyperextension/hyperflexion trauma. Experimental findings point to soft tissue trauma, with is most likely to be sustained by the ligaments of the C0-C2 complex. However lately, based on experiments with pigs, possible trauma to the neural system has been presented. Nevertheless, in both cases, the authors pointed to the formation of an S-shape by the spine, due to translation of the head in the initial stage of the event, as the cause of the injury. To summarise, the experimental approaches were not able to produce conclusive findings leading to full explanation of the whiplash phenomenon. In contrast numerical methods, with a leading role being played by the finite element approach, have been shown to be promising in simulating the cervical spine under transient loading, giving the unique possibility of monitoring in real time the deformations of selected spinal structures (Table 1).

Two preliminary objectives of this study have been therefore already achieved, as follows.

1. The limitations of experimental investigation of whiplash have been demonstrated.
2. The role that computational studies have in complementing existing experimental work has been demonstrated.

|                                  | Ethical | Injury Mechanism | Accurate anatomy | Spinal elements loads | High speed accidents | Impact response | Impact tolerance | Accessibility | Repeatability |
|----------------------------------|---------|------------------|------------------|-----------------------|----------------------|-----------------|------------------|---------------|---------------|
| <b>Radiological Research</b>     | ✓       | ×                | ✓                | ×                     | ✓                    | ×               | ×                | ✓             | ×             |
| <b>Statistical Research</b>      | ✓       | ×                | ✓                | ×                     | ✓                    | ×               | ×                | ✓             | ×             |
| <b>Animal Testing</b>            | ×       | ✓                | ×                | ×                     | ✓                    | ✓               | ✓                | ×             | ×             |
| <b>Dummy Testing</b>             | ✓       | ×                | ×                | ×                     | ✓                    | ×               | ×                | ✓             | ✓             |
| <b>PMTO Testing</b>              | ×       | ×                | ✓                | ×                     | ✓                    | ✓               | ✓                | ×             | ×             |
| <b>Volunteer Testing</b>         | ✓       | ×                | ✓                | ×                     | ×                    | ✓               | ×                | ✓             | ×             |
| <b><i>In Vitro</i> Specimens</b> | ×       | ✓                | ✓                | ✓                     | ✓                    | ✓               | ✓                | ×             | ×             |
| <b>Numerical Modelling</b>       | ✓       | ✓                | ✓                | ✓                     | ✓                    | ✓               | ✓                | ✓             | ✓             |

Table 1 Summary of advantages and disadvantages of available methods to investigate whiplash.

Therefore the purpose of this work described here is to use computational methods to study the behaviour of all the relevant parts of the cervical spine in a 3-dimensional, dynamic simulation of real rear end collisions, looking for evidence of ligamentous damage. A second aim is to investigate the engineering design criteria for reducing this damage.

The objectives to achieve these aims are as follows:

1. Produce a full 3-dimensional model of the head/neck complex based on the best anatomical data available.
2. Integrate this model onto a computer simulation of a whole body on a car seat.
3. Validate the combined model against existing volunteer data.
4. Extend the model to a high range of speeds.
5. Use the model to study whiplash with a sideways-facing head and a dynamically altering head restraint gap.
6. Study the amelioration of injuries as a result of incorporating a range of buffer devices.

**CHAPTER 2**

**2.5 DIMENSIONAL FEM MODEL TO**

**INVESTIGATE “WHIPLASH”**

## **2.1 Introduction**

The FE model described in this chapter was developed in collaboration with Dr F. Heitplatz who was at the time also a Research Student in the Biomechanics Research Group.

## **2.2 Model Geometry**

At this stage of the project, research into different techniques to generate FE model of spine was undertaken. Three techniques available to the author were investigated to establish the optimum final approach for modelling biomechanical structures used to create the spinal models for the purpose of this study.

Firstly it was considered to purchase a CAD model of the spine (Viewpoint Datashop, 1996) and mesh the structure using the automatic mesh generation procedure available in Pro/Engineer (PTC, 1997). This would lead to creation of a highly accurate model of the spine in a short time. However, after previewing a few available models, problems with this technique became apparent. These models, created solely for an optical representation of the spine, show surfaces discontinuities. Therefore no closed volume, required to create 3-D FE mesh, can be easily defined. Moreover, the use of automatic free mesh will lead to an excessive number of elements, exceeding the available computing power. These problems, in conjunction with the high price of CAD models (circa £500) led to the abandonment of this modelling technique.

Secondly, a new technique of generating FE models of bony structures through automated interpretation of CT data (Kullmer et al, 1997) was investigated. Research collaboration with research group at the University GH Paderborn was founded. They developed FEM-CT software that can isolate the bony structure from digital CT scan images by filtering the grey levels. This leads to creation of 2-D contour areas at a known position in the z-axis. Once this is done, following meshing algorithm is used to create the FE model:

- Several voxels of one plane are merged into a rectangular structure.
- 2-D rectangular meshes are connected to build full 3-D elements. At this stage only rectangular bricks are created leading to discontinuous surfaces.
- In order to create a smooth surface corner nodes are moved to the position of corresponding nodes in the upper and lower levels.

Several models of vertebrae were created using direct generation algorithm at The Nottingham Trent University in order to evaluate the suitability of this method. It was noted that the smoothing algorithm creates error elements with very small aspect ratios. In many cases this process effectively reduces the brick elements to wedge or tetrahedral elements with overlying nodes. This problem could be overcome if rigid material properties were applied to the bony structure. Moreover, close inspection of vertebrae interface surfaces revealed a high degree of discontinuity in the models with low resolution. This would create a high friction due to mechanical interlocking, not present in the human anatomy. This could be avoided by a high resolution for the mesh. However, this will create a large number of elements (circa 2800 for mid and lower cervical spine), making this method not suitable for the simulation of whiplash with the computing power on hand.

It was concluded that the cervical spine structure had to be simplified in order to accommodate meshing of the structure while keeping the number of degrees of freedom (DOF) as small as possible. However special focus has to be given to the contact interfaces between the vertebrae to allow a continuous surface to surface contact. Since the dimensions and relative location of the vertebrae are very important, the new and final modelling technique based on the actual anatomical sample from the Visible Human data set was developed.

The Visible Human Project (National Library of Medicine, 1994) currently consists of CT, MRI and full-colour pictures of male and female cadavers cross sections. The Nottingham Trent University has gained the right to use VHP data set for this research project. The data used in this work are male images taken from the body of a 39 year old convicted murderer who was sentenced to death by

lethal injection. The body was frozen after death, then sliced in 1mm intervals. The images were obtained by photographing each slice of the body (Figure 20).



Figure 20 Part of typical image from Human Visible Project.

The required geometry data was extracted using the image processing software Adobe Photoshop 4.0 (Adobe Systems Incorporated, 1997) and the characteristic datum points were manually extracted and saved in point-arrays. The pixel number gave the X-Y position and the image number the Z position. The CAD model was built using CAD-software Pro/Engineer (PTC, 1997) in the following stages. First, the point arrays were transferred to Pro/Engineer and used to create splines which then were used as boundaries to create surfaces. During modelling simplifications were made to the geometry to allow mapped meshing with hexagonal 8 noded FE-elements. However the topology of the contact facets was preserved to allow a realistic motion characteristic of the vertebrae. The CAD model was transferred to the FEM-software Ansys 5.3(Ansys, 1997) by creating IGES files consisting of the surfaces of the model. The imported IGES files were used to create volumes. Mapped meshing using brick elements was then performed on each individual volume.

For the purpose of this initial investigation, the 3-D model of the C0-C2 complex developed using the method described above, was integrated into a very simplified model of the full cervical spine, head and trunk. This model was developed in order to simulate whiplash with a minimum number of DOF while still maintaining a reasonable representation of the human body. The model represents posterior impact for an adult sitting in a normal seating position.

Symmetry conditions are assumed along the sagittal plane and, in order to reduce calculation times, the skull, the vertebra bodies (C3-C7), the nuchal ligament, the discs and the torso are modelled as linear elastic shells with appropriate wall thickness. The skull, torso and head restraint are projections of 2-D shapes. Particular attention is given to the vertebral facet joints as their shape is of importance for the motion characteristic of the spine. Therefore they are modelled as 3-D solids and sliding contacts are established between the interacting surfaces (Figure 21). Consequently the whole model is a mixture of 2-D and 3-D structures and therefore is referred to as a 2.5-D model.

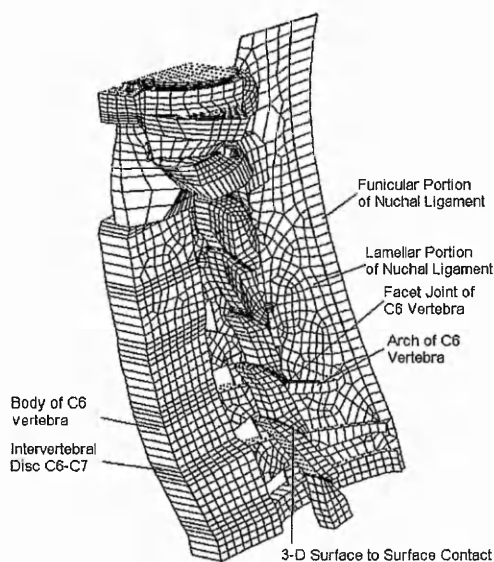


Figure 21: ISO-View of the C0-T1 part of the FEA Model

The alar and transverse ligaments were modelled as 3-D solid structures (Figure 22). The head restraint was modelled as a solid block with contact elements generated wherever it touched the posterior part of the skull (Figure 23). An algorithm was developed to modify easily the initial gap between the skull and the head restraint.

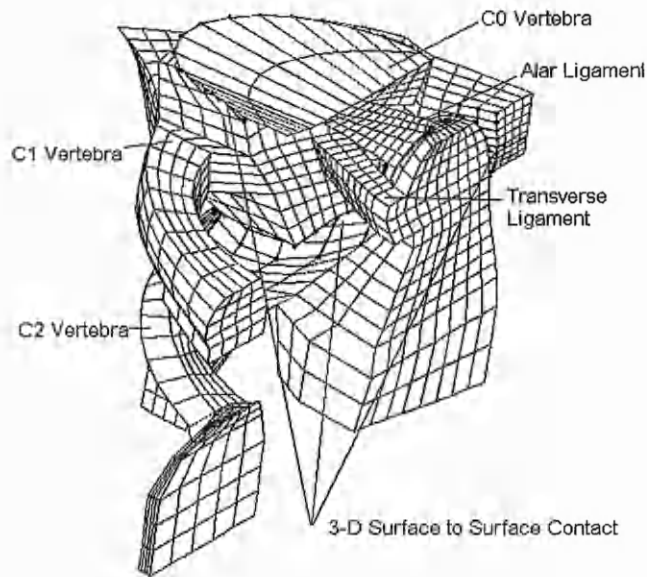


Figure 22: The C0-C2 Motion complex with ligamentous structure

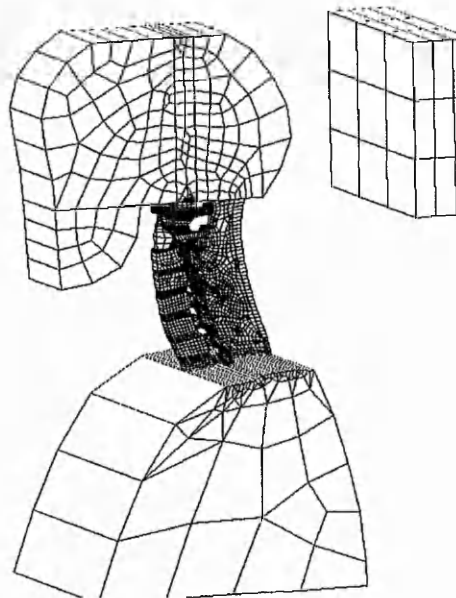


Figure 23: ISO-View of the FEA Model.

## 2.3 Material Properties

All materials in this model were defined as having linear elastic properties. The bony structures are seen as stiff compared to the spinal soft tissue. Material properties for the disc were applied as found in the literature (Lin et al., 1978).

The role of the nuchal ligament for the biomechanics of the neck region is generally unclear and no material properties could be found in the literature. Therefore their strength was estimated from data for the supraspinous ligament (Myklebust et al., 1988) of the lower spine. The topology of the transverse and alar ligaments and their ultimate strength has been previously reported by Dvorak et al. (1987a and 1988) and from these results a Young's modulus was calculated for both ligaments. Visual interpretation of the experimental video results reported by Dr Steffan Datentechnik GmbH (1996, CD-Crash Ver. 1.3) shows a small deformation of the torso. Therefore a low Young's modulus was applied, allowing the model torso to deform in a similar fashion. Details of the material properties are summarised in Table 2.

| <i>Structure</i>                               | <i>Material Properties</i> |            |        |
|--|----------------------------|------------|--------|
| <i>Skull</i>                                   | E=1200                     | $\nu=0.3$  | t=75   |
| <i>Bony structure of C0-C2 complex</i>         | E=1200                     | $\nu=0.3$  |        |
| <i>Vertebrae C3-T1 body</i>                    | E=1200                     | $\nu=0.3$  | t=11.5 |
| <i>Vertebrae C3-T1 arch</i>                    | E=1200                     | $\nu=0.3$  | t=5    |
| <i>Discs</i>                                   | E=4.3                      | $\nu=0.45$ | t=11.5 |
| <i>Alar ligament</i>                           | E=42.23                    | $\nu=0.3$  |        |
| <i>Transverse ligament</i>                     | E=74.34                    | $\nu=0.3$  |        |
| <i>Nuchal ligament-Lamellar Portion</i>        | E=10                       | $\nu=0.3$  | t=0.25 |
| <i>Nuchal ligament-Funicular Portion</i>       | E=10                       | $\nu=0.3$  | t=0.5  |
| <i>Contact between vertebrae</i>               | k=120                      |            |        |
| <i>Contact between head and head restraint</i> | k=240                      |            |        |
| <i>Torso</i>                                   | E=0.5                      | $\nu=0.3$  | t=200  |
| <i>Head restraint</i>                          | E=15                       | $\nu=0.3$  |        |

Table 2: Summary of material properties: E = Young's Modulus (MPa);  $\nu$  = Poisson's Ratio; k = Contact Stiffness (MPa), t = Uniform Thickness of Shell Element (mm)

## 2.4 Loading Conditions

Instead of uniform acceleration to load the model, real live acceleration of the torso from experiments conducted by Dr. Steffan Datentechnik GmbH (1996, CD-Crash Ver. 1.3) was used. In collaboration with Graz University of Technology, Dr. Steffan Datentechnik GmbH conducted sled tests with volunteers, PMTO's and Hybrid III dummies to gain better understanding of the head-neck kinematics in rear-end impact (Geigl et al., 1994; 1995). The sled was first accelerated to a certain speed by electric motor and then was decelerated using special longitudinal friction-brake elements. The brake force can be adjusted by setting a certain air-pressure on a compressed-air cylinder. Measurements from real accidents were used in order to achieve realistic deceleration of the sled. For this purpose, data was obtained from black boxes mounted on 3000 street vehicles recording accelerations in the event of an accident occurrence. The seats from used cars were mounted on the sled, with the whole seat mounting system to include all the deformation within seat mounting and the seat itself. The volunteers and PMTO's were equipped with 3-axis accelerometers and targets for the high-speed video analysis of the event. The relative rotation of the head was extracted from analysing the video recordings (Geigl et al., 1994).

To validate the model, one of the experiments (MERCEDES 200-300 W 124, 1987 [MB 190] test NR.2) was recreated by loading the torso with the acceleration history from the experiment and leaving the head-neck motion to be determined by the model.

Two parameters were chosen to evaluate the model performance against the experiments: acceleration of the head and torso, and rotation of the head, as shown in Figure 24. Due to employing implicit solving algorithm, Ansys could not converge the simulation beyond the point of head-head restraint impact, even if very small time steps were used. Therefore, the numerical simulation for this investigation was conducted only up to the point of impact between the head and the head restraint, which is why the simulation results are discontinued at 0.13 second.

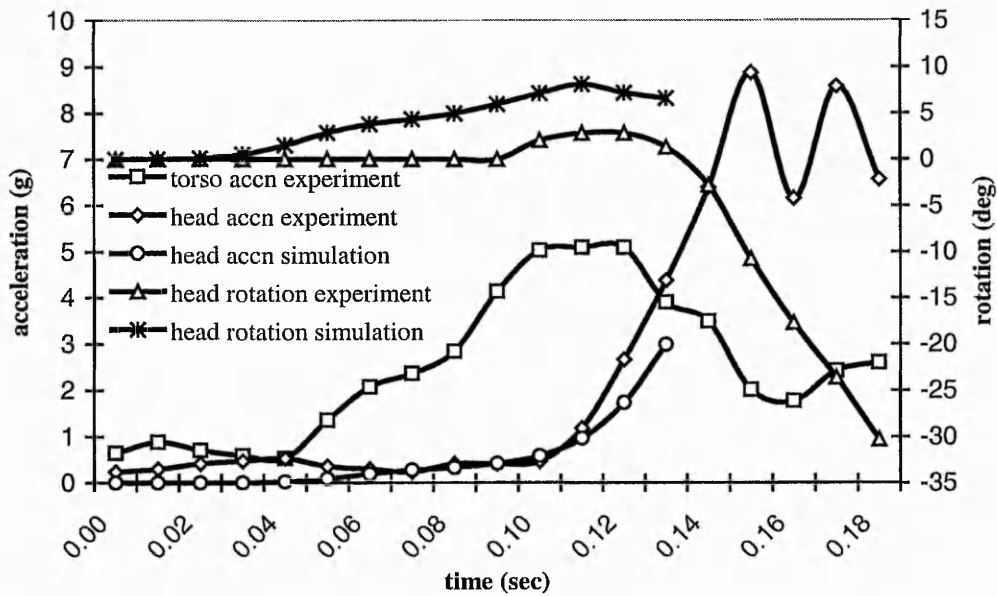


Figure 24: Acceleration and head rotation during a 10.5 km/h impact, comparing the experimental data of Geigl et al. with the numerical prediction.

The model performance may be assessed as good, particularly in terms of the acceleration history for the head. However, the relative rotation between the head and the C3 vertebra is somewhat stronger in the simulation than in the experiment. This may be caused by the linear elastic material properties applied to the soft tissue, particularly the nuchal ligament, when the literature suggests that non-linear properties would be more appropriate. Following successful evaluation, nine simulations were conducted in total, with variations of initial relative impact speed between 10.5 and 21 km/h and initial head/head restraint gap between 80 and 120 mm.

## 2.5 Results

Visual interpretation of the results shows the same S-shaped curvature of the neck as reported recently by Grauer et al. (1996) and also identified the same two main areas of traumatic strains. During impact there is hyperflexion of the C0-C2 Complex and hyperextension of the lower cervical spine (Figure 25).

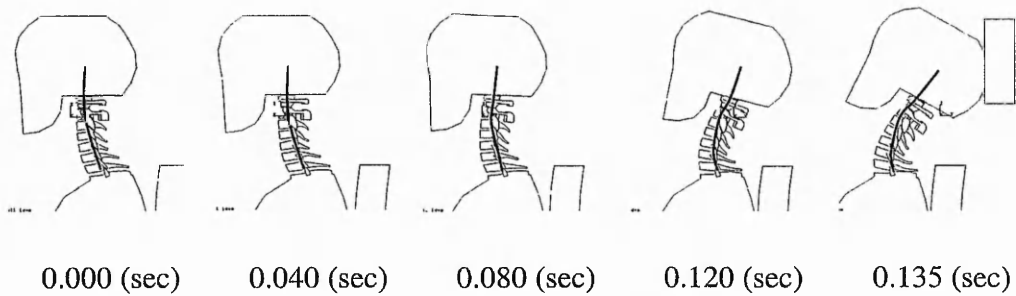


Figure 25: Deformation of the head/neck model during a 10.5 km/h rear end impact with an initial gap between head and head restraint of 120 mm. Notice the initial translation of the head leading to flexion of the upper spine and extension of the lower spine.

The current FE model concentrates on the ligaments located in the C0-C2 complex and to evaluate the injury risk for the different load cases the time/strain history of the alar ligament was recorded for all load steps. The von Mises strains at the middle cross-section of the ligament were chosen to represent the ligament load since this avoids possible peak strains at the attachment points and takes torsional effects into account. The time/strain history was then compared with experimental data showing the maximum tensile load of the alar ligament at the point of rupture, as recorded by Dvorak et al. (1988). To allow direct comparison with the simulation results, the experimentally reported maximum tensile forces were divided by the Young's modulus and the cross-section area of the ligament, as used for the model, to give strains. Figure 26 shows the von Mises strain/time relation for the alar ligament for all impact speeds. The average breaking strain and the standard deviation, as reported by Dvorak et al., are also shown.

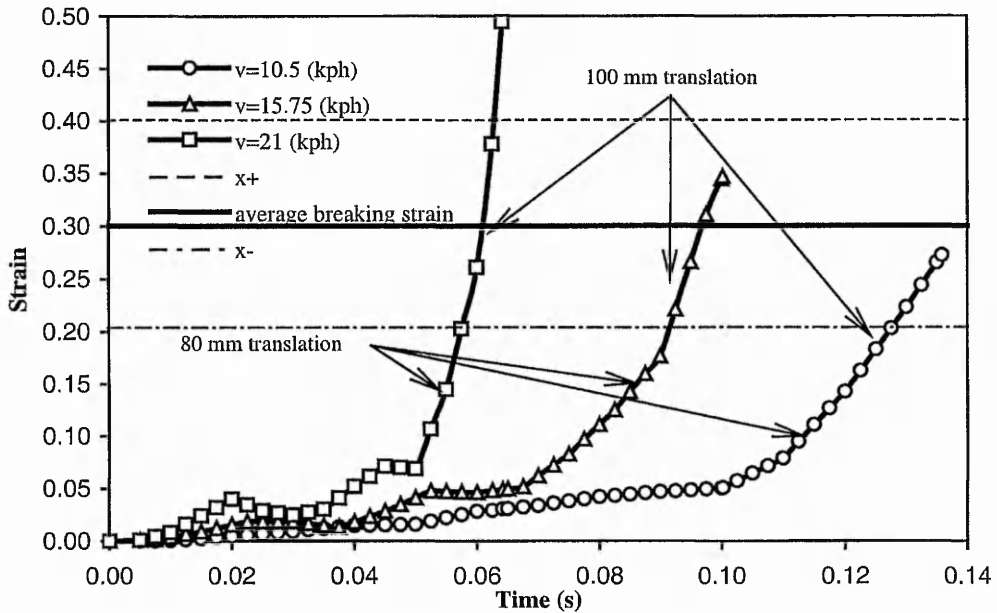


Figure 26 Von Mises strain of the alar ligament for an impact simulation with an initial head/head restraint gap of 120 mm. Strains are recorded up to the point of impact with the head restraint

The ligament strains increase exponentially for increasing speed and head restraint gap. There is a strong increase in strain when the neck forms the characteristic S-shaped deformation, a situation which is reached much faster for simulations with high speed. However, by noting the indicated translations of the head relative to the torso, it will be seen that a low initial head restraint gap of less than 80 mm would successfully prevent this MoI, even if the acceleration of the torso is high due to large speed differences.

This initial model, although showing promising results, has some fundamental limitations. First of all the simplified representation of the lower vertebrae did not fully resemble the real life geometry and kinematics of the cervical spine. Secondly, further representation of the ligamentous structure of the cervical spine in the model, especially in the vital C0-C2 complex will influence the kinematics of the spine and bring the model closer to the real life cervical spine behaviour. At the same time, the inclusion of the passive response of the muscle present in the neck could play an important role in achieving a realistic response of the model. Last but not least, in the future attempts of modelling the cervical spine attention

should be paid to the non-linear representation of the material properties. Therefore it was decided to create a full 3-D model of the cervical spine implementing the technique of vertebrae modelling used for the C0-C2 complex in the present model to the middle and lower cervical vertebrae. At the same time, fuller representation of the ligamentous structure as well as selected representation of muscles is planned.

**CHAPTER 3**  
**3-DIMENSIONAL FEM MODEL**

### 3.1 Introduction

The previous investigation (CHAPTER 2) was conducted using the FEM solver Ansys 5.3. The weak points of this solver for conducting dynamic solutions were quickly realised:

- First of all the performed calculations using the full transient large deformation option of the Ansys 5.3 solver required extensive computing power (up to 16 hours CPU time). Even though this time does not appear to be excessive, it has to be pointed out that the model used in previous investigation was very simplified and consisted of only 3704 structural elements.
- Secondly, the implicit solving algorithm used by Ansys 5.3 is difficult in contact situations. The implicit algorithm makes relatively large time steps, and then produces a linear approximation of the results for the time at the end of the time step as a starting point for the iterative process. Therefore, the algorithm has a problem in finding convergence if the physical state of the model has changed dramatically during one time step. This is often the case with contact problems. For the previously investigated model Ansys could not converge the simulations beyond the point of the head-head restraint impact even if very small time steps were used.

Therefore the new 3 dimensional model was developed using the explicit dynamic FEM solver LS-Dyna (LSTC, 1997). The explicit solver technology offers advantages for the calculation of impact problems. The model response is calculated in very small time steps and no equilibrium convergence criteria have to be satisfied, leading to much faster solution for every time interval. This enables the solution of problems with large deformation of the structure in rapidly changing physical circumstances. Explicit solvers are widely used at the present for car crash simulations and other rapid physics applications like projectile impact.

### 3.2 Model Geometry

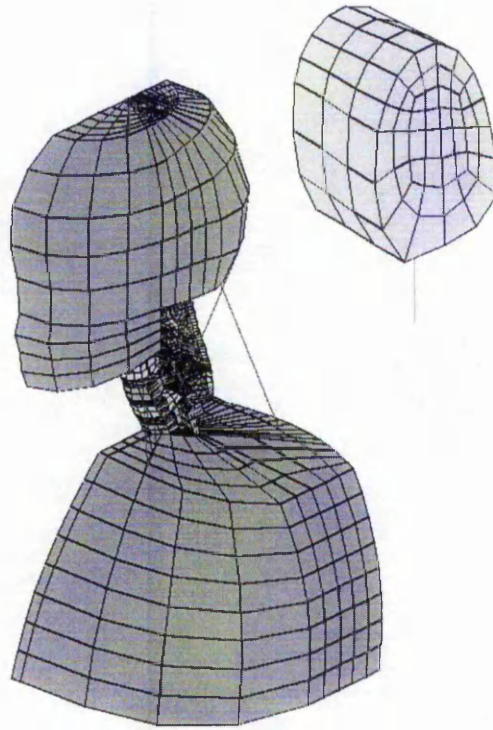


Figure 27: Isometric-View of the FEA Model

This study again investigates posterior impact for an adult, sitting in a normal seating position. Symmetry conditions are again assumed along the sagittal plane and topological information relating to the size and shape of the skull and the human cervical vertebrae was extracted from full colour pictures obtained by the Visible Human Project (National Library of Medicine, 1994). A 3-D parametric CAD model was created by interpreting the images of the male dataset. The FE-mesh was developed with respect to the hardware available. The number of elements was kept as small as feasible, still representing all major anatomical parts of the cervical spine. Therefore, the topology was simplified to accommodate 8-node brick meshing of the structure with special focus given to the joint surfaces in order to allow realistic motion characteristics, using surface to surface contact. The mesh structure and joint contact surfaces are illustrated in Figure 27 and Figure 28 which, when compared against Figure 23 and Figure 21, clearly show the full 3-D nature of this newer model.

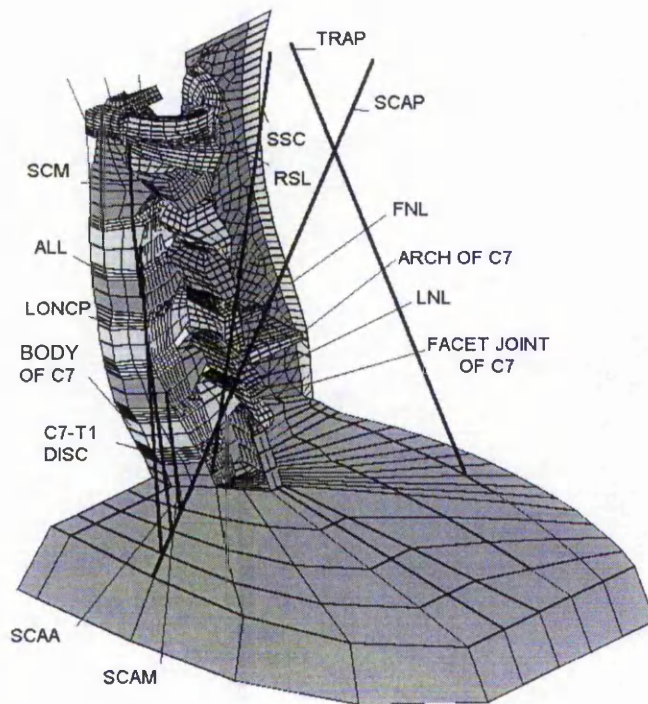


Figure 28 Isometric-View of the C1-T1 part of FEA Model. ALL: anterior longitudinal ligament; FNL: funicular portion of the nuchal ligament; LNL: lamellar portion of nuchal ligament; TRAP: trapezius; SSC: semispinalis capitis; LONCP: longus capitis; SCM: sternocleidomastoid; SCAA: scalenus anterior; SCAM: scalenus medius; SCAP: scalenus posterior; RSL: rectus capitis lateralis.

In order to achieve a realistic deformation pattern the model incorporates intervertebral discs and a wide range of ligaments, particularly in the C0-C2 complex (Figure 29). The two strongest ligaments of the complex, alar and transverse, are modelled as 3-D structures using solid elements, whilst the remaining ligaments are modeled with non-linear springs. The tectorial membrane and the vertical portion of the cruciate ligament were combined into one structure due to their close anatomical relationship. A mixed structure of non-linear spring and shell elements is used to simulate the bio-mechanics of the ligamentum flavum and the nuchal ligament, with the latter divided into lamellar and funicular portions. Furthermore, the muscular structure of the neck is represented by nine non-linear springs, with the location of the attachments based on anatomical description (Gray, 1980)

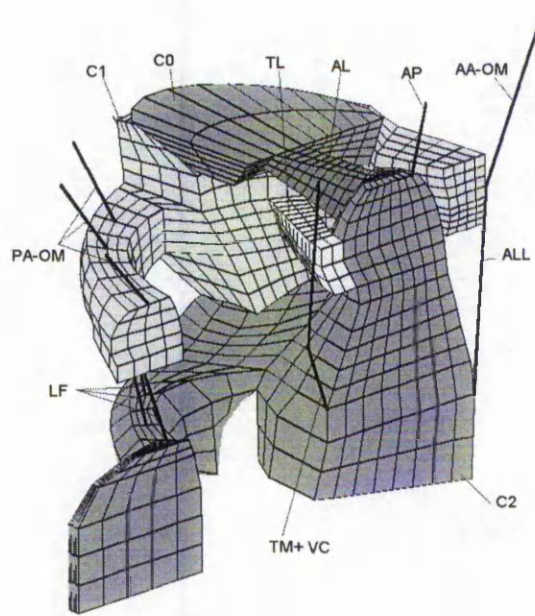


Figure 29: The C0-C2 motion complex with ligamentous structure. AL: alar ligament; TL: transvers ligament; AP: apical ligament; AA-OM: anterior atlanto-occipital membrane; ALL: anterior longitudinal ligament; TM+VC: tectorial membrane with vertical portion of cruciate ligament; LF: ligamentum flavum; PA-OM: posterior atlanto-occipital membrane

Figure 28 shows the C1-T1 spine unit with nomenclature of the muscular and ligamentous structure. The topology of the head restraint is a simplified representation of the Mercedes W124 head restraint modelled as a combination of soft foam and steel tubing. Surface to surface contact has been established between the facet joints as well as the head and headrest.

### 3.3 Material Properties

The main obstacle to be overcome in this study was to implement to the model the highly non-linear material properties found in human tissue. Due to hardware restrictions the model of the intervertebral disc in particular had to be a compromise. Therefore in the present model a simplified representation of the disc, using a hyperelastic material law (MAT\_BLATZ-KO\_RUBBER) was used, since this material allows large strain with nearly incompressible material properties (Poisson's ratio fixed at 0.463). The Shear Modulus (G) required by

this material formulation was calculated from experimental results (Shea et al., 1991) to be  $G=3.8 (\pm 1.02)$  MPa. Values from this range have been evaluated through simple tests, leading to  $G=4$ MPa being used in the model.

The Alar and Transverse ligaments are also modelled using the hyperelastic material law, applying material properties as found in the literature (Dvorak et al., 1988). Due to its large extension the nuchal ligament has been modelled using 4 node Belytschko-Tsay shell elements which have been reinforced by tension-only beams in the funicular part of the ligament, using a positive offset in order to model the non-linear progressive stiffness which is characteristic for all ligamentous structures (Figure 30). The remaining ligaments are modelled using non-linear discrete tension-only elements. Force/deformation load curves have been developed using *in vitro* test data (Myklebust et al., 1988).

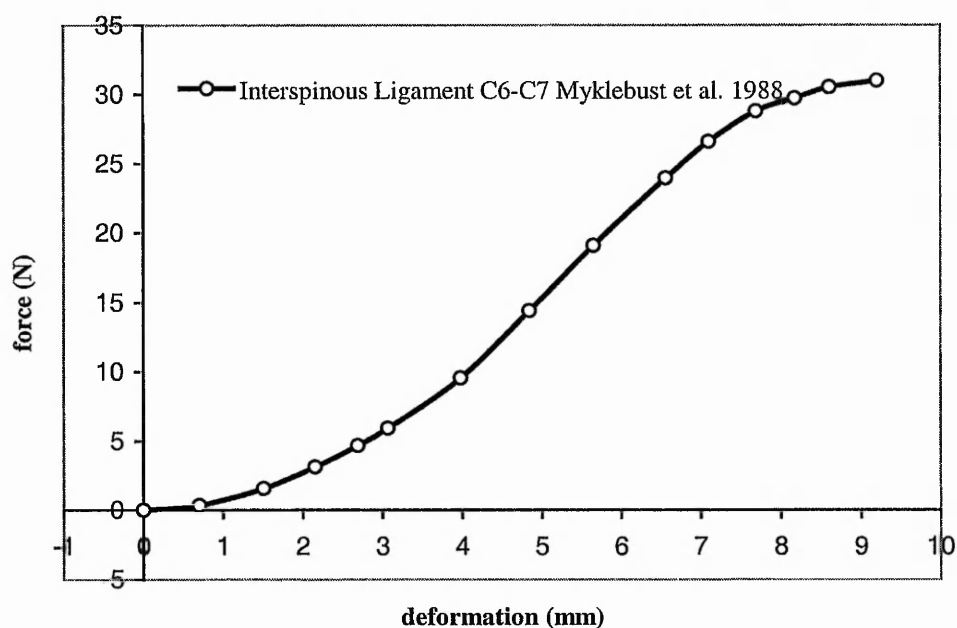


Figure 30 Force/deformation characteristic of typical spinal ligament.

The same technique has been applied to the muscular structure using *in vitro* test data of the sternocleidomastoid as a reference (Yamada, 1970). No active muscular response is expected, due to the short simulation period, which has been shown to be well below the human reaction time (Panjabi, 1998a). The bony structure of the spine can be assumed stiff in respect to the soft tissue.

Furthermore, according to accident statistics (VdS, 1994) no deformation of the bony structure is expected for the applied load cases. Therefore, all bony structures, as well as the head and torso, are modelled as rigid bodies, thereby reducing the calculation time. The acceleration/time profile of the head during rear-end impact is largely dependent on the stiffness and the energy absorbing characteristics of the head restraint. The present model uses the Blatz-Ko foam material law for the cushion material. Table 3 shows a summary of all material properties used for the model.

| <b>Structure</b>                         | <b>Material formulation used in LS-Dyna</b> | <b>Material Properties</b> |       |
|--|---|----------------------------|-------|
| <i>Skull</i>                             | *MAT_RIGID                                  | -                          | -     |
| <i>Cervical vertebrae</i>                | *MAT_RIGID                                  | -                          | -     |
| <i>Discs</i>                             | *MAT_BLATZ-KO_RUBBER                        | G=4                        |       |
| <i>Alar ligament</i>                     | *MAT_BLATZ-KO_RUBBER                        | G=14.12                    |       |
| <i>Transverse ligament</i>               | *MAT_BLATZ-KO_RUBBER                        | G=25.37                    |       |
| <i>Nuchal ligament-Lamellar Portion</i>  | *MAT_ELASTIC                                | E=4.42                     | v=0.3 |
| <i>Nuchal ligament-Funicular Portion</i> | *MAT_ELASTIC                                | E=4.42                     | v=0.3 |
| <i>Other Ligaments</i>                   | *MAT_CABEL_DISCRETE_BEAM                    | E=5                        |       |
| <i>Muscles</i>                           | *MAT_SPRING_NONLINEAR_ELASTIC               | Loadcurve                  | -     |
| <i>Torso</i>                             | *MAT_RIGID                                  | -                          | -     |
| <i>Head restraint Foam</i>               | *MAT_BLATZ-KO_FOAM                          | G=1.5                      |       |
| <i>Head restraint Mounting</i>           | *MAT_ELASTIC                                | E=210000                   | v=0.3 |

Table 3: Summary of material properties: E = Young's Modulus (MPa);  
v = Poisson's Ratio; G =Shear Modulus (MPa),

### 3.4 Loading Conditions

To achieve a realistic motion pattern during the whiplash simulation, the loading data from the experiments on volunteers was used (Dr. Steffan Datentechnik GmbH 1996, CD-Crash Ver. 1.3). For the investigation here, one of the experiments (MERCEDDES 200-300 W 124, 1987 [MB 190] test NR.2) was recreated using the original acceleration history of the torso as an input but

leaving the motion of the head and cervical spine to be determined by the model (Figure 31 and Figure 32).

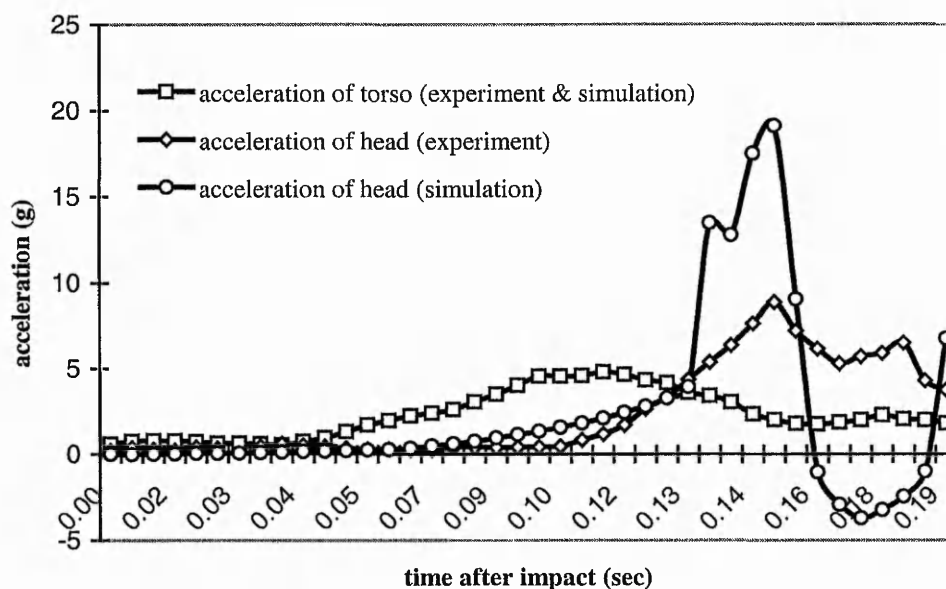


Figure 31: Acceleration of the head and torso during a 10.5 km/h rear-end impact, comparing the experimental data of Geigl et al. with the numerical prediction

Interpretation of the video data shows that the car seat back is bent backwards due to the acceleration force of the body, thereby continuously increasing the gap between head and head restraint from its starting value of 80 mm. This effect can not be simulated with the present FE-Model. Therefore, the simulation was conducted with a fixed horizontal gap of 110 mm. This produced a more accurate acceleration profile in terms of the time/acceleration relationship than a simulation with an 80 mm horizontal gap and generally the agreement is good both qualitatively and quantitatively up to the point of impact with the head restraint at 0.132 s. However, the magnitude of the acceleration peak is a factor of two higher in the numerical simulation than in the experiment after the head contacts the restraint. It is apparent that the ability to absorb energy is higher for the experimental head restraint, leading to a longer impact period and a reduced rebound.

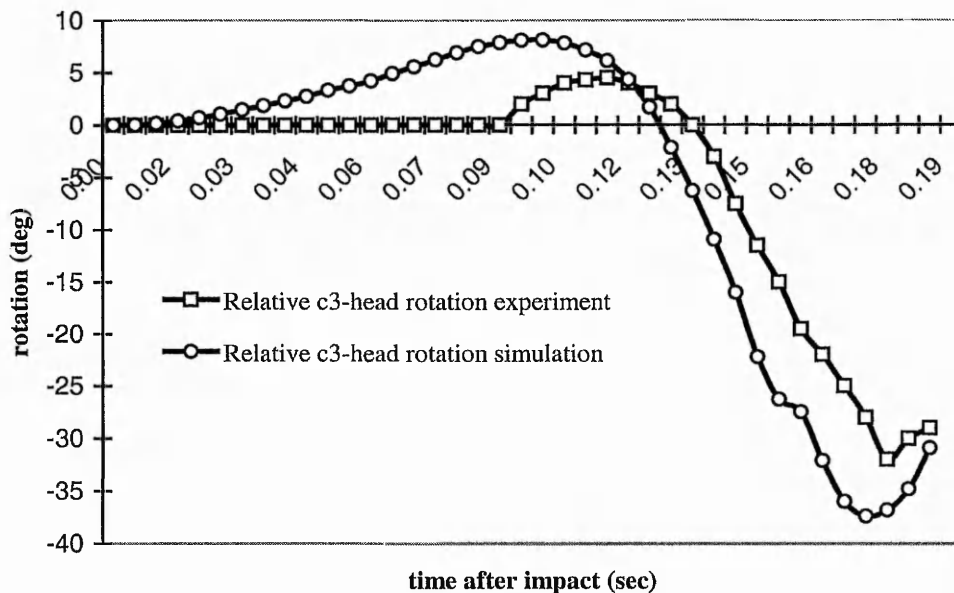


Figure 32: Relative rotation between head and C3 during a 10.5 km/h rear-end impact, comparing the experimental data of Geigl et al. with the numerical prediction.

Figure 32 shows the rotation of the head relative to the C3 vertebra adopting the convention of Geigl. With respect to the relative head rotation, a much better qualitative match was found between experiment and simulation, thereby showing that the model reproduced natural motion behaviour under dynamic loading.

### 3.5 Results

Following successful evaluation of the model, several simulations were conducted using twice the impact speed of the volunteer experiment. Visual interpretation of the results shows the same S-shaped curvature of the neck as reported recently by Grauer et al. (1997) who also identified the same two main areas of traumatic strains. During impact there is hyperflexion of the C0-C2 Complex and hyperextension of the lower cervical spine.

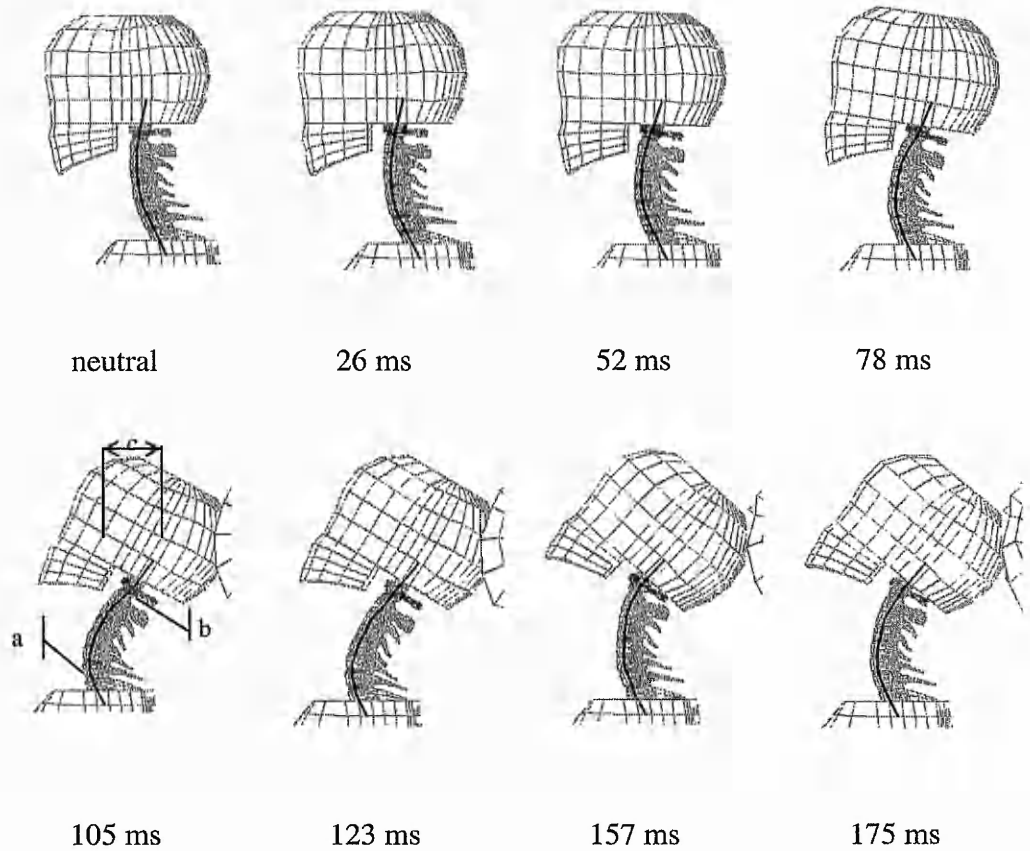


Figure 33: Deformation of the head/neck model during a 21 km/h rear end impact with an initial gap between head and head restraint of 80 mm. Notice the initial translation of the head c) leading to flexion of the upper spine b) and extension of the lower spine a).

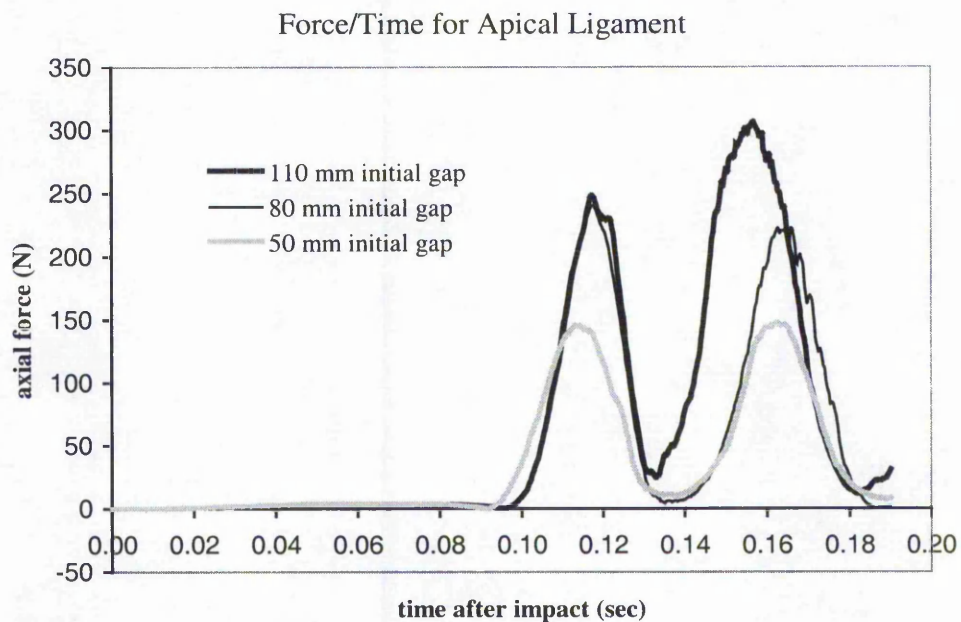


Figure 34 Force/time relationship of the apical ligament for a simulated 21 km/h impact and three different initial gaps between head and head restraint

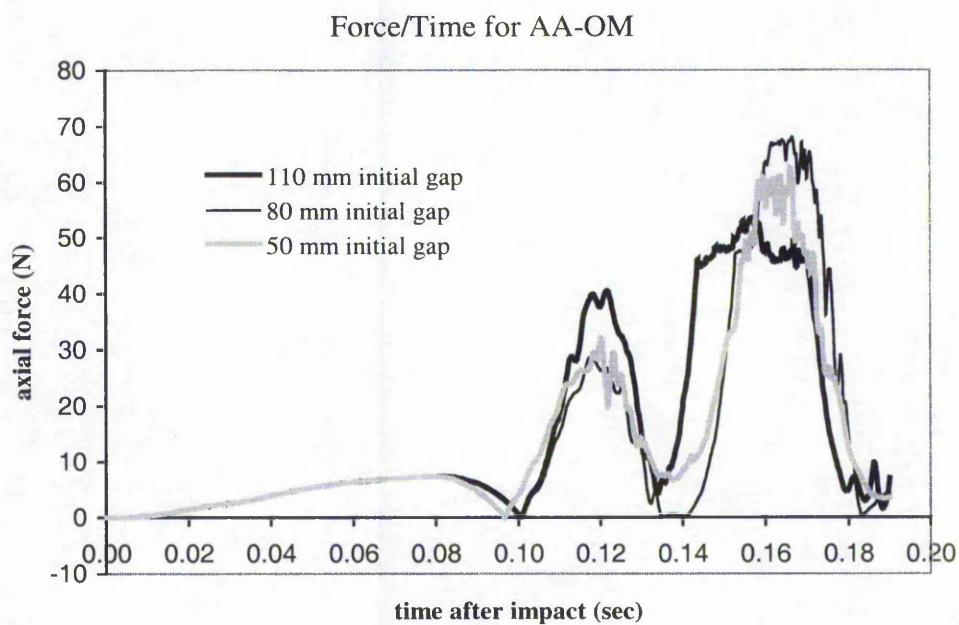


Figure 35 Force/time relationship of the anterior atlanto-occipital membrane for a simulated 21 km/h impact and three different initial gaps between head and head restraint

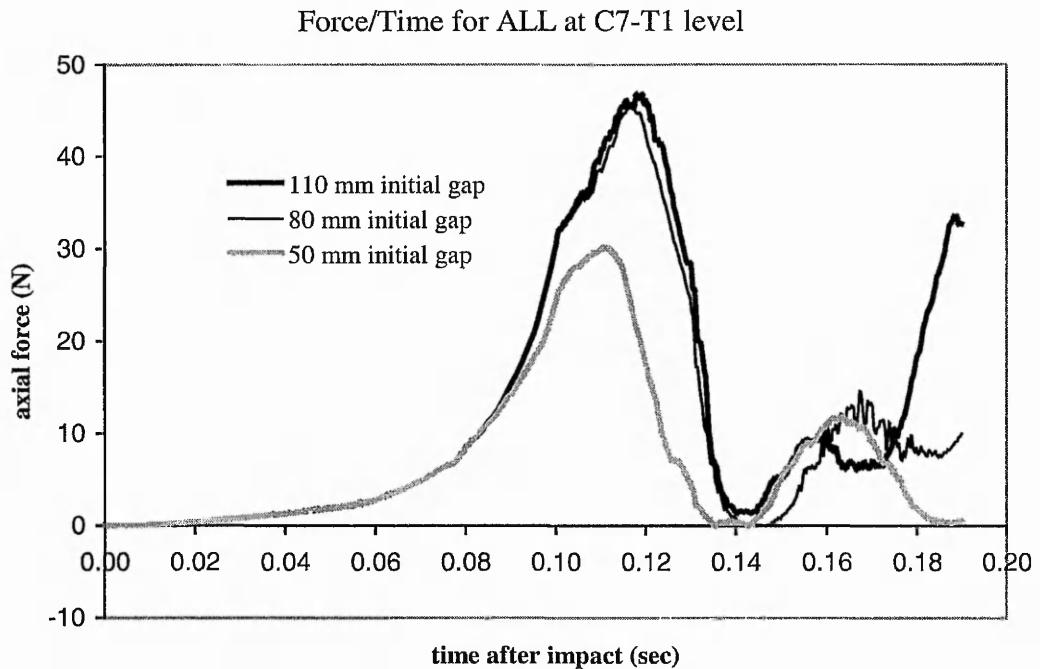


Figure 36 Force/time relationship of the anterior longitudinal ligament at C7-T1 level for a simulated 21 km/h impact and three different initial gaps between head and head restraint

Quantitative interpretation of the ligament axial forces in Figure 34 shows previously unreported high loads on the apical ligament situated within the C0-C2 complex. These are particularly high if the initial gap is large, reaching 310N. The average breaking load of the apical ligament is reported to be 214N ( $\pm 115$ ) (Myklebust et al. 1988). The forces in the anterior atlanto-occipital membrane in Figure 35 remain at a low level ( $< 70$ N) for all three load-cases. The average breaking force of this structure is reported to be 281N ( $\pm 136$ ). There is a strong increase in strain for the discs of the lower cervical spine when the neck forms the characteristic S-shaped deformation. By noting the indicated translations of the head relative to the torso, it has been shown that maintaining a small initial head restraint gap of less than 50 mm would successfully prevent this MoI, even if the acceleration of the torso is high due to large speed differences.

The present model, although valuable to the explanation of the whiplash MoI, does not include the response of the whole body during the accident. Therefore,

the model could not be used in full-scale crash simulation or to analyse existing or new anti-whiplash safety devices. It was decided to extend the present head-neck model to include the occupant body model, to be able to show a fuller picture of the whiplash injury and enable the model to be a real industry design tool, not only a research model. At the same time, the stabilising role of the capsular ligaments was realised, resulting in inclusion of this structure in the future model.

**CHAPTER 4**

**3-DIMENSIONAL FEM MODEL OF THE HEAD-  
NECK COMPLEX ON A SIMPLIFIED MODEL  
OF THE HUMAN BODY.**

## 4.1 Introduction

Work presented in this chapter was presented at the European LS-DYNA Users Conference 1999 and has been published in the proceedings of this conference (Appendix C).

## 4.2 Model Geometry

This investigation concentrates on developing a whiplash protection device. Therefore the model presented in CHAPTER 3 was extended to a whole 3-dimensional structure and implemented onto a simplified model of a vehicle occupant body (Figure 37).

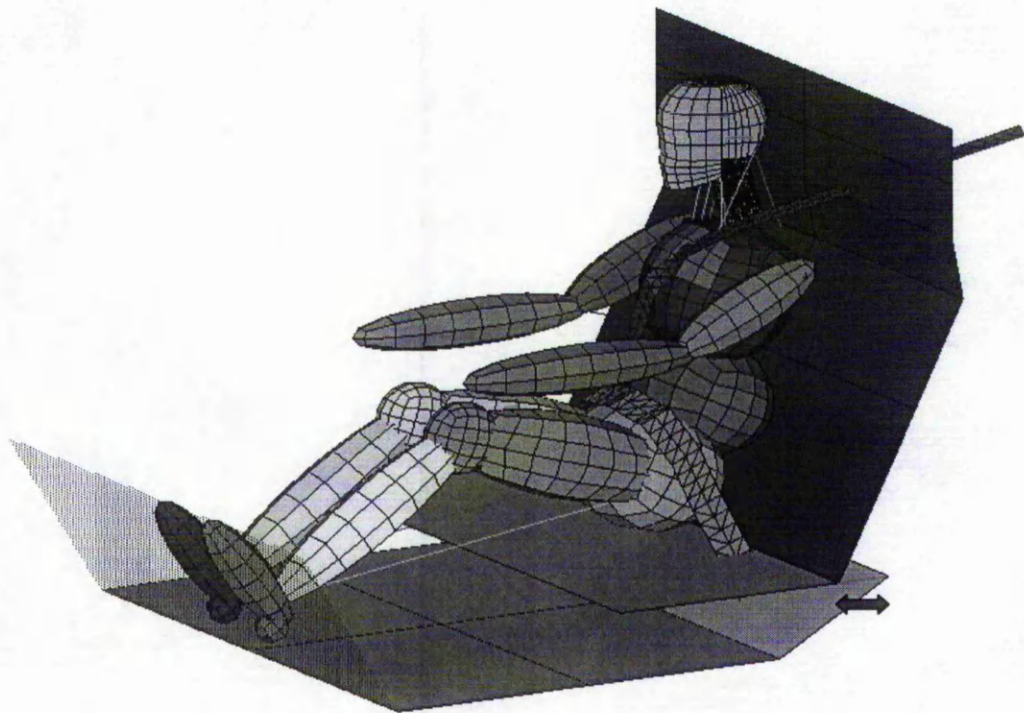


Figure 37: Isometric View of the FEA Model

The model of the neck was extended to include the Capsular Joints and the Posterior Longitudinal Ligament (Figure 38, Figure 39). To implement non-linear

material properties, the Transverse and Alar ligaments are here represented by non-linear spring elements (Figure 39).

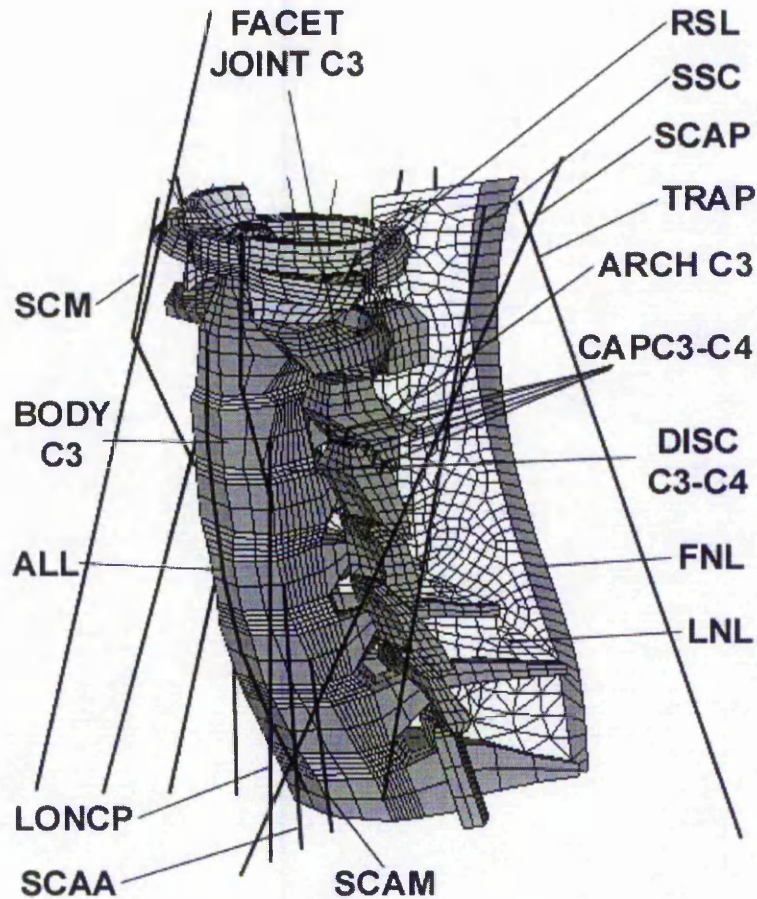


Figure 38 Isometric-View of the C1-T1 part of FEA Model. ALL: anterior longitudinal ligament; CAPC3-C4: joint capsules C3-C4; FNL: funicular portion of the nuchal ligament; LNL: lamellar portion of nuchal ligament; TRAP: trapezius; SSC: semispinalis capitis; LONCP: longus capitis; SCM: sternocleidomastoid; SCAA: scalenus anterior; SCAM: scalenus medius; SCAP: scalenus posterior; RSL: rectus capitis lateralis.

The dummy model used in this investigation was supplied with the LS-Dyna solver as a part of the example database (LSTC, 1994). It was used in frontal impact simulation to present the seat belt response. It consists of ellipsoidal rigid bodies connected through cylindrical joints, springs and dampers and includes a seating system consisting of seat and seat belts.

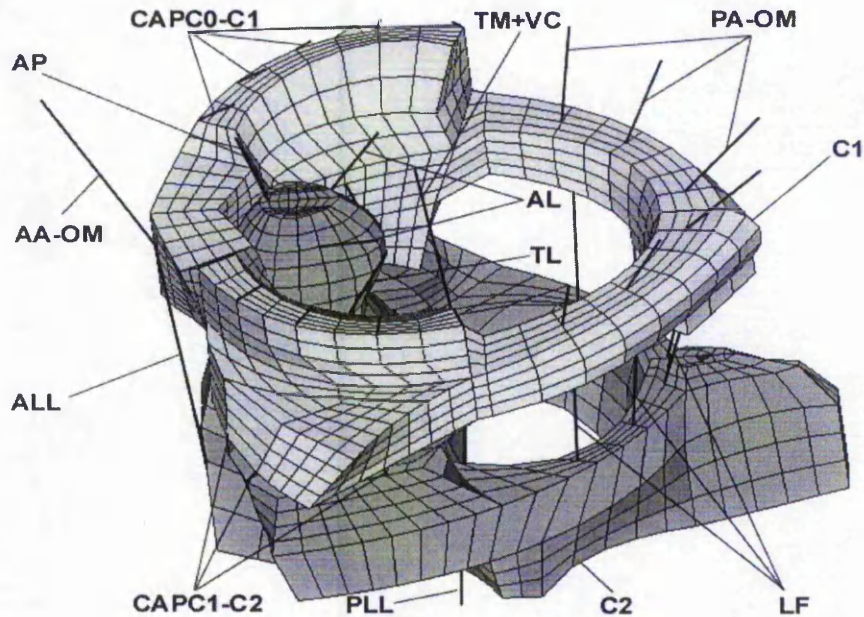


Figure 39: The C1-C2 motion complex with ligamentous structure. AL: alar ligament; TL: transvers ligament; AP: apical ligament; AA-OM: anterior atlanto-occipital membrane; ALL: anterior longitudinal ligament; PLL: posterior longitudinal ligament; TM+VC: tectorial membrane with vertical portion of cruciate ligament; LF: ligamentum flavum; PA-OM: posterior atlanto-occipital membrane; CAPC0-C1: joint capsules C0-C1; CAPC1-C2: joint capsules C1-C2

### 4.3 Whiplash Protection Device

The collapsing spring considered in this investigation as a whiplash prevention device could be mounted in existing seats designs, aligned along the main axis of the car. The physical design of the device can be seen in Figure 40. The proposed design consists of two conical tubes on a double conical mandrel. The effect of linear resistance during the compression of the device will be achieved by the elastic deformation of the tubes on the mandrel. One of the tubes will be fastened to the seat while the other will be mounted on the floor of the car. When the floor is loaded due to the accident, the loading acceleration will progress to the seat and will try to compress the device. The conical tubes will be pushed onto the cone and will deform elastically with the properties of a linear spring. However, friction between the cones and the central rod will prevent the device springing back and so the device is locked like a one-way spring.

The collapsing spring was represented in the model by a pair of simple springs located on both sides of the seat (Figure 37).

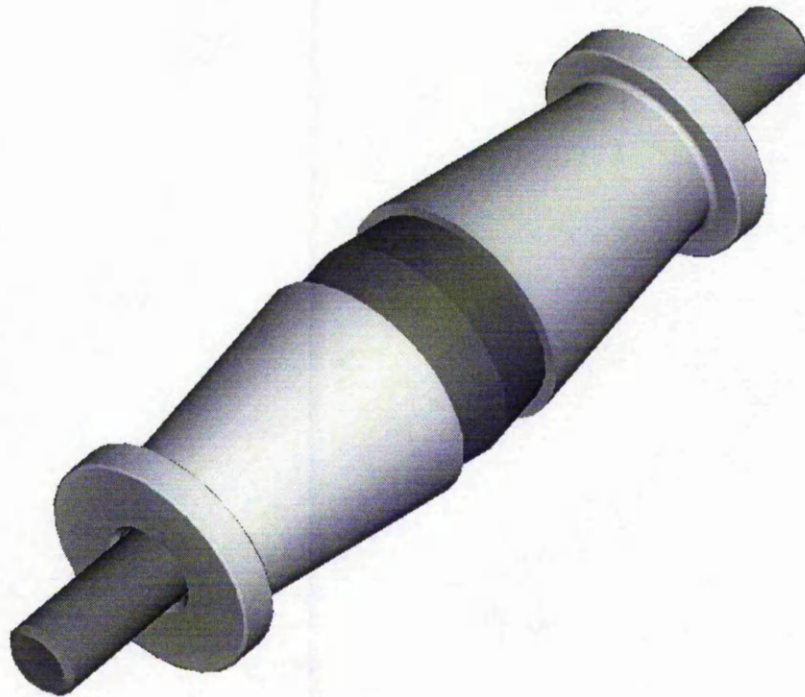


Figure 40 Whiplash protection device.

The material formulation for the device in the model is based on an inelastic spring. This material formulation gave the possibility of defining the element as being a one way spring with a tension or compression-only formulation. Furthermore the inelastic formulation in LS-Dyna allows the user to formulate the unloading stiffness.

In this study the spring elements were used in the compression-only mode with a maximum loading force of 3500 N and two different movement lengths – 50 and 100 mm. The length of the spring was based on consideration of the safety of back seat passengers. After investigating the average distance between the front seat and the back seat it was decided that a movement of the front seat of up to 100 mm during the accident should not lead to any injury of the back seat passengers. However, due to increasing emphasis on smaller car designs the 50 mm deformable spring has been included in the investigation as a more likely option. To achieve self-locking behaviour of the spring elements in LS-Dyna, the

unloading stiffness was set on a very high level (1E +12 N/m<sup>2</sup>) which successfully prevented the spring from unloading.

#### 4.4 Material Properties

The skull and vertebrae were assumed to be rigid since, according to the accident statistics (VdS, 1994), no damage to the bone structure is expected. All the ligaments, except the nuchal, were modelled as non-linear discrete tension-only elements. The force/deformation load curves were based on experimental results (Dvorak, 1988; Myklebust, 1988). The same technique was applied to the muscular structure using test data for the sternocleidomastoid as a reference (Yamada, 1970). The discs were modelled with a Blatz-Ko rubber model using a shear modulus of 4 MPa which has been shown to lead to a realistic deformation.

The dummy body parts are rigid bodies with discrete springs and dampers between them to provide relative stiffness and viscous damping.

Table 4 shows a summary of the material properties used for the model of the head-neck complex. For the properties of the body model refer to LSTC (1994).

| <i>Structure</i>          | <i>Material formulation used in LS-Dyna</i> | <i>Material Properties</i> |       |
|---------------------------|---|----------------------------|-------|
| <i>Skull</i>              | *MAT_RIGID                                  | -                          | -     |
| <i>Cervical vertebrae</i> | *MAT_RIGID                                  | -                          | -     |
| <i>Discs</i>              | *MAT_BLATZ-KO_RUBBER                        | G=4                        |       |
| <i>Nuchal Ligament</i>    | *MAT_ELASTIC                                | E=4.42                     | v=0.3 |
| <i>Other Ligaments</i>    | *MAT_SPRING_NONLINEAR_ELASTIC               | Loadcurve                  | -     |
| <i>Muscles</i>            | *MAT_SPRING_NONLINEAR_ELASTIC               | Loadcurve                  | -     |

Table 4: Summary of material properties of the head-neck complex.

E = Young's Modulus (MPa); v = Poisson's Ratio; G = Shear Modulus (MPa)

## 4.5 Loading Conditions

As in the previous investigation, the loading data for the present study was based on experiments conducted by Dr. Steffan Datentechnik GmbH (1996, CD-Crash Ver. 1.3). To evaluate the model, one of the experiments (MERCEDES 200-300 W 124, 1987 [MB 190] test NR.2) was reconstructed. Due to the extension of the model to include the occupant in the seating system, the recorded test sled acceleration history was used to load the floor of the simplified car environment, leaving the motion of the seating system with the occupant to be determined by the model. This is different from the previous investigations, where the cervical model was loaded with recorded acceleration history of the volunteer torso.

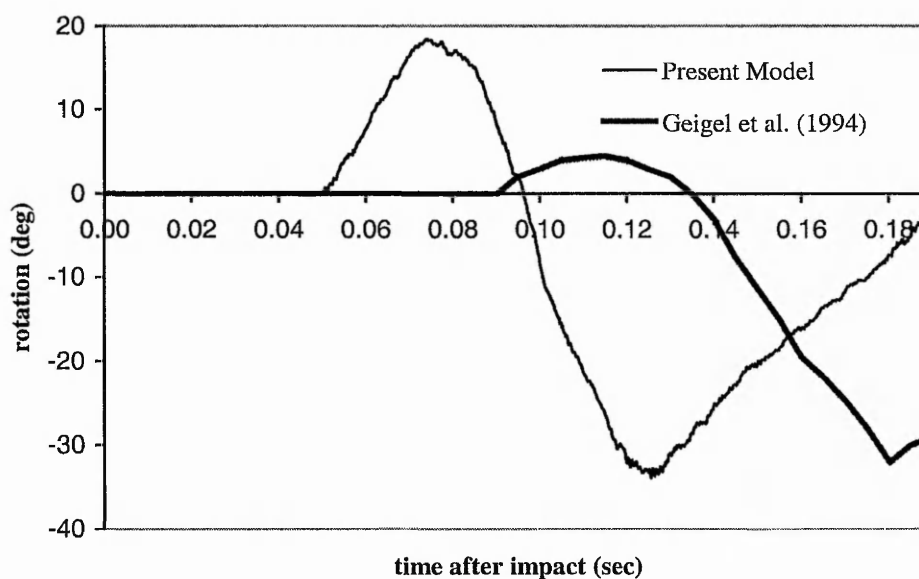


Figure 41: Relative rotation between head and C3 during a 10.5 km/h rear-end impact, comparing the experimental data of Geigl et al. with the numerical prediction

A real seat would deform under the impact with the torso, not only internally (seat back cushions and internal springs) but also the whole seat back construction will yield and rake. Since the movement of the head-neck starts once the raking of the seat back stops (full loading of the torso begins), the whiplash loading of the head-neck complex will not start from the beginning of the impact, resulting in the

response of the head being later in the event. At the same time, due to the raking of the seat, the real gap between the head and the head restraint will be wider than the initial distance, influencing the head-head restraint impact time and head kinematics. The use of a non-deformable symbolic seat system in the present model resulted in moving the impact of the head to an earlier stage in the event (Figure 41). Therefore, in the model under investigation, the rotation of the head starts earlier than in the volunteer experiment. However the translation of the head can be clearly seen. Looking at the difference in the peak values of the rotation a few issues must be borne in mind.

- First of all the experimental results are based on a movie recorded during the experiments and the points taken as data providers for these results (markers on the volunteer's head and neck) are different from the ones used in the simulation. For the simulations the results of the head and cervical vertebrae were computed from the exact locations of the centres of gravity, whereas the experiment markers were placed on the skin of volunteers in the anticipated centre of gravity of the head and the initial position of the C3 vertebrae. Since the marker of the C3 vertebra was located on the skin of the neck, the kinematics of this marker will differ from the C3 vertebra behaviour. This variation will lead to differing results between the volunteer experiment and the computational simulation.
- Secondly the simple model of the occupant body, as well as the simple model of the seat environment, used in the simulation did not satisfy energy conservation as well as the real deformations observed in the experiment.
- Lastly the volunteer would be likely to have tensed neck muscles in anticipation of the crash. This would reduce the initial neck flexion but would have little effect on the subsequent extension where the neck is subject to the full effect of the impact.

In that light the performance of the model can be assessed as quite good.

## 4.6 Results

Following the evaluation of the model several simulations with the same loading conditions were conducted to establish the optimum properties of the one-way spring buffer device as well as the gap between the head and the head restraint. Finally it was decided to test the device using an 80 mm gap between the head and the head restraint and springs of 50 mm and 100 mm movement length with linear characteristics and a maximum force of 3500 N.

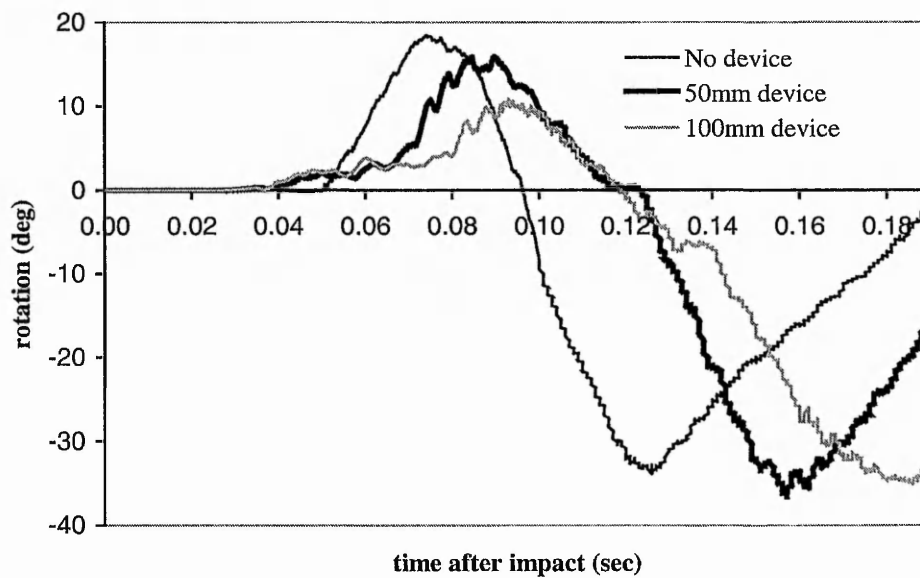


Figure 42: Head relative rotation for simulation with and without device.

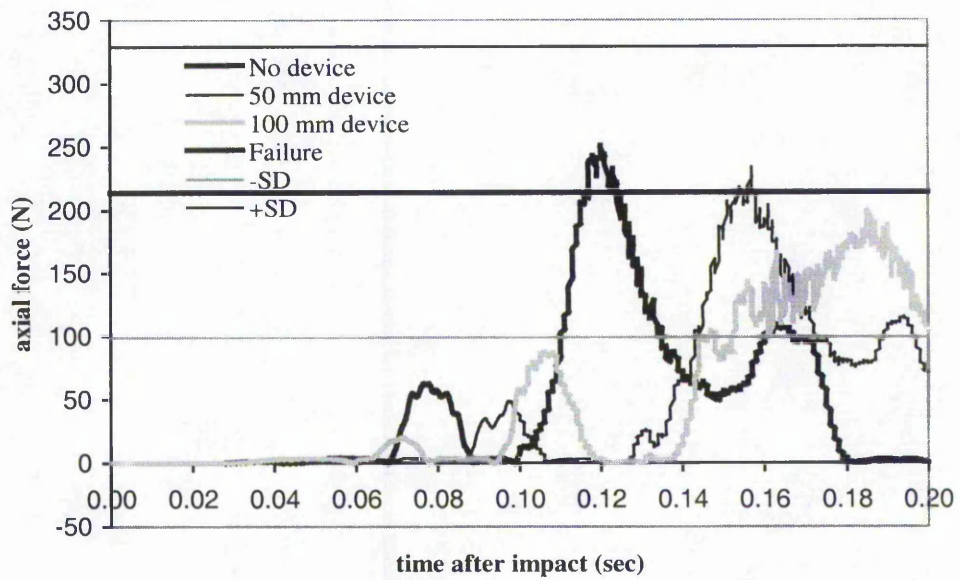


Figure 43: Force/time relationship of the apical ligament with and without the device. SD – standard deviation.

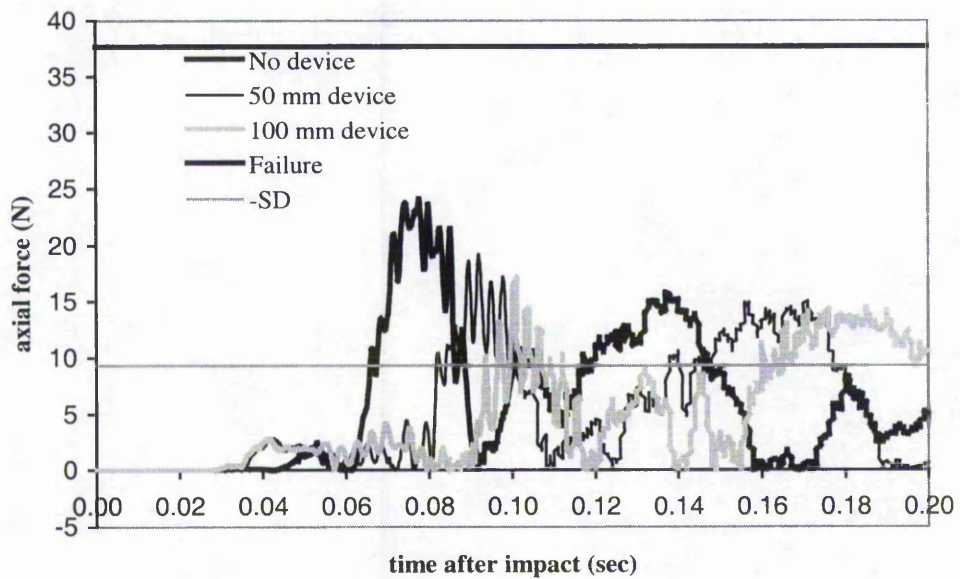


Figure 44: Force/time relationship of the ligamentum flavum with and without the device.

The use of this self-locking device reduced the acceleration of the head before impact with the head restraint by about 1.5g. Furthermore it reduced the peak rotation as well as the relative angular acceleration quite significantly (Figure 42).

The potential benefit of the device can be most clearly seen, however, on the individual ligaments' loading, particularly in the C0-C2 motion complex. The device reduced the maximum force in the apical ligament (Figure 43), enough to bring it under the average breaking force reported by Myklebust et al. (1988). The reduction in loading can be seen as well in the ligamentum flavum (Figure 44). Unlike the apical ligament, this was already under the average breaking force, but now it is close to the lowest value reported for injury ever to occur.

While information such as head rotation and acceleration can already be extracted from existing mechanical dummy models, this approach of using a hybrid model with a fully biomechanical head-neck complex is completely new and gives a unique opportunity to investigate the loading in individual ligaments. This investigation shows the present model to be a useful and original tool for studying various modifications to the seat in terms of their effect on the loads on all the ligaments of the neck.

**CHAPTER 5**

**ADVANCED FE MODEL OF THE HEAD-NECK  
COMPLEX ON A FE MODEL OF THE HYBRID  
III DUMMY.**

## 5.1 Introduction

Work presented in this chapter was presented at the International LS-DYNA Users Conference 2000 and has been published in the proceedings of this conference (Appendix D).

## 5.2 Model Geometry

The model of used in this stage of the investigation (Figure 45) consists again of an occupant in a simplified vehicle seat environment. The occupant model this time, however, is based on the Hybrid III dummy model but with the biomechanical head-neck complex. This occupant model will be addressed from now on as a Bio-Hybrid-Dummy.

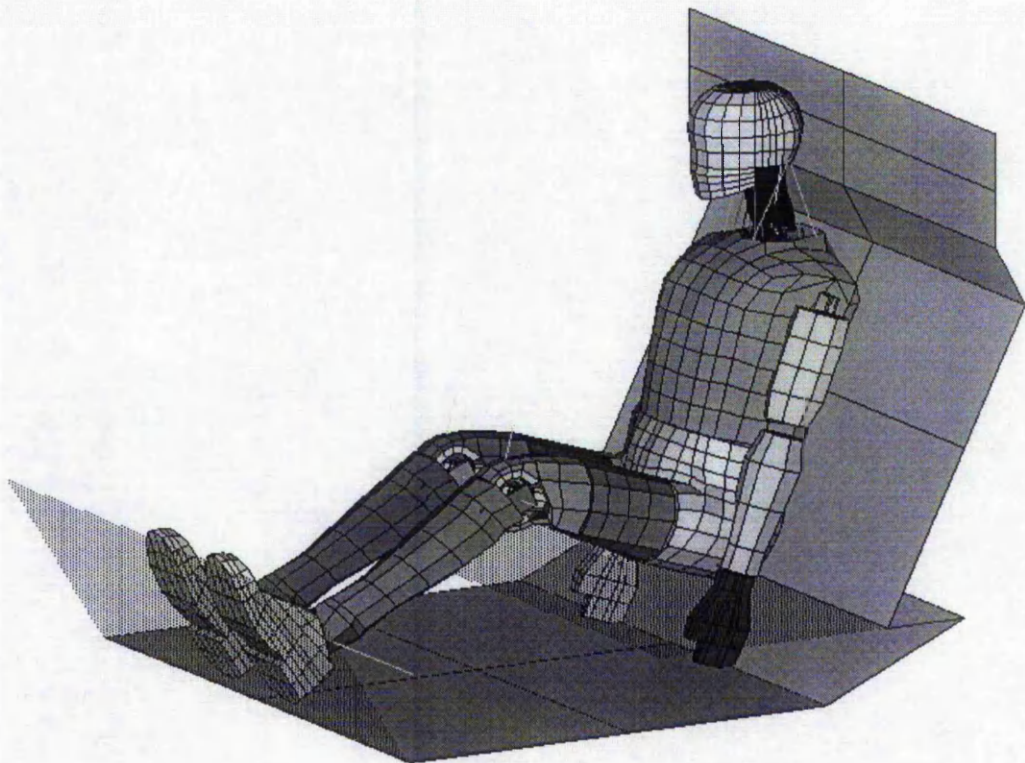


Figure 45: Isometric view of the FEA Model

The new head-neck model was developed using the preliminary model (Golinski et al., 1999; Heitplatz et al., 1998) as an overall geometrical reference. The bony structures are modelled using shell elements with the geometry modified to achieve better interaction with soft tissue. All the ligaments of the cervical spine are represented in the model using a mixed structure of shell and non-linear spring elements, except for the Nuchal Ligament, which is modelled with shell elements only. Due to this approach, interaction through the contact interfaces between ligaments and bones was made possible, preserving the non-linear properties of soft tissue. This was not possible in the previous model, where the rough brick element mesh of the vertebrae gave poor interaction between the bones of cervical spine and the ligaments modelled using single spring elements. Spring elements are used to model the nine muscles present in the model. The intervertebral discs are represented using solid elements. Symmetry conditions in the head-neck model were assumed along the sagittal plane. The details of the head-neck model can be seen in Figure 46.

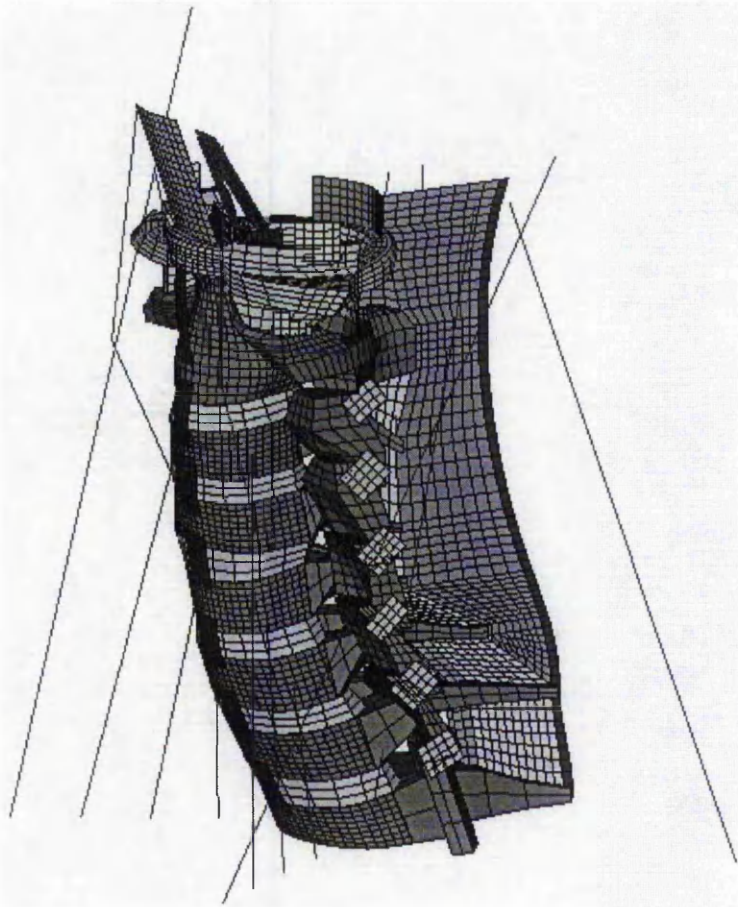


Figure 46 Isometric view of the C1-T1 part of the FEA Model.

The rigidised FE Hybrid III dummy model of a 50th percentile male, supplied with LS-DYNA (LSTC, 1999), has been used in this investigation as a representation of an industry standard for occupant safety engineering. The combined model of the Hybrid III dummy model with the biomechanical head-neck complex was placed in a simple model of a seat environment.

### 5.3 Model Properties

The skull and vertebrae were assumed rigid since, according to the accident statistics (VdS, 1994), no damage to the bone structure is expected. All the ligaments, except the Nuchal Ligament, were modelled as mixed structures of non-linear discrete tension-only elements and elastic shells. The force/deformation load curves for discrete elements were based on experimental results (Dvorak et al., 1988; Myklebust et al., 1988). The shell element stiffness properties were calculated from 1% of the breaking force and the corresponding deflection. The geometrical properties of the ligaments were based on available experimental results (Yoganandan et al., 1998; Dvorak et al., 1988; Panjabi et al., 1991a, 1991b; Przybylski et al. 1998), while properties of the muscular structure were established from test data for the sternocleidomastoid muscles (Yamada, 1970). The discs were modelled with a Blatz-Ko rubber model using a shear modulus of 4 MPa which has been shown to lead to a realistic deformation.

The inertia properties of the head-neck model were implemented using LS-Dyna's PART\_INERTIA card, giving the possibility to implement accurate real life values, and no longer relying on the solver calculation based on the mesh density.

The head mass and inertia characteristics were taken from a study by Dauvilliers et al. (1994):

$$M = 4.615 \text{ kg}; I_{xx} = 0.0159 \text{ kgm}^2; I_{yy} = 0.024 \text{ kgm}^2; I_{zz} = 0.0221 \text{ kgm}^2$$

The position of the head centre of gravity was based on the results of Ewing et al. (1973) and Beier et al. (1980).

The vertebrae inertia properties were calculated from the preliminary models (CHAPTER 3, CHAPTER 4).

Table 5 shows a summary of the material properties used for the model of the head-neck complex. For the properties of the Hybrid III body model please refer to LSTC (1999).

| <i>Structure</i>          | <i>Material formulation used in LS-Dyna</i> | <i>Material Properties</i> |       |
|---------------------------|---|----------------------------|-------|
| <i>Skull</i>              | *MAT_RIGID                                  | -                          | -     |
| <i>Cervical vertebrae</i> | *MAT_RIGID                                  | -                          | -     |
| <i>Discs</i>              | *MAT_BLATZ-KO_RUBBER                        | G=4                        |       |
| <i>Nuchal Ligament</i>    | *MAT_ELASTIC                                | E=4.42                     | v=0.3 |
| <i>Other Ligaments</i>    | *MAT_SPRING_NONLINEAR_ELASTIC               | Loadcurve                  | -     |
|                           | *MAT_ELASTIC                                | E~1%LCM                    | v=0.3 |
| <i>Muscles</i>            | *MAT_SPRING_NONLINEAR_ELASTIC               | Loadcurve                  | -     |

Table 5: Summary of material properties of the head-neck complex.

E = Young's Modulus (MPa); v = Poisson's Ratio; G = Shear Modulus (MPa);  
LCM = Tearing Force of Ligament

## 5.4 Loading Conditions

The loading data for the present study were based on sled experiments conducted by Dr. Steffan Datentechnik GmbH (1996, CD-Crash Ver. 1.3). To evaluate the model, one of the experiments (MERCEDES 200-300 W 124, 1987 [MB 190] test NR.2) was reconstructed. The recorded test sled acceleration history was used to load the floor of the car, leaving the motion of the seating system with the occupant to be determined by the model.

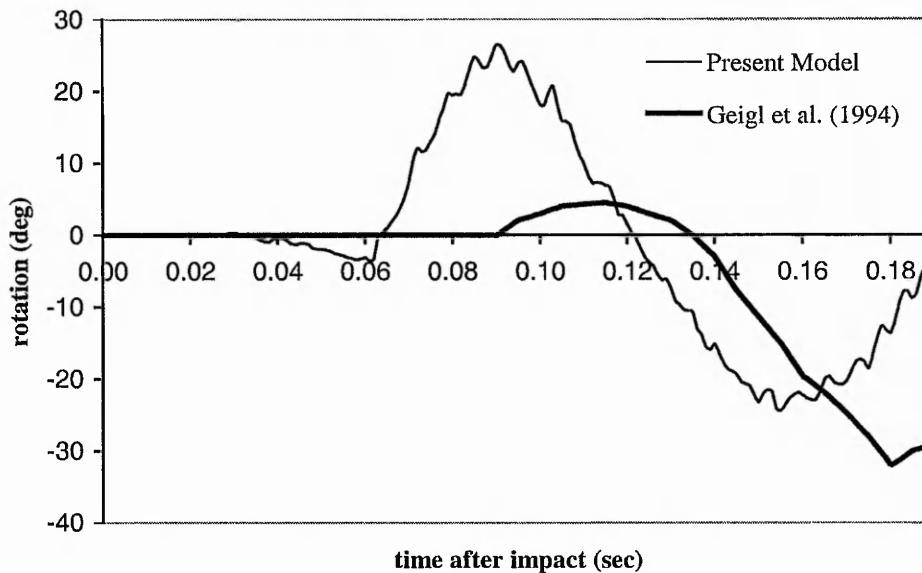


Figure 47: Relative rotation between head and C3 during a 10.5 km/h rear end impact, comparing the experimental data of Geigl et al. with the numerical prediction.

The performance of the model can be assessed as quite good bearing in mind the following issues:

- The symbolic seat system used in this investigation did not satisfy energy conservation as well as the real deformation.
- The Hybrid III body model, even though being the best representation of the human body on the commercial crash test market, does not resemble the full kinematics of the human thorax and lumbar spine. This issue has been addressed in a research project (Davidsson et al., 1998) where the flexible human-like spine was introduced with BioRid (Biofidelic Rear Impact Dummy)
- The results from the simulation are taken from the exact location of the centres of gravity, whereas the experiment relies on approximately located markers on the skin of volunteers using a video camera to record their behaviour. This will definitely lead to differences in results.

- Volunteer expecting the crash will definitely tense their neck muscles, thus influencing the head-neck kinematics.

## 5.5 Results

Since the Bio-Hybrid-Dummy uses the dummy body, the first natural comparison is made against the behaviour of the dummy itself. Due to the design of the Hybrid III neck, which consists of only three vertebral elements, it was not possible to extract the results relating to the C3 vertebra. Therefore it was decided to compare head kinematics relative to the base of the neck (Figure 48), this being the common part to both neck models. It can be clearly seen that the Hybrid III Dummy neck is very stiff and does not recreate the kinematics of the human neck, represented in this case by the advanced biomechanical model.

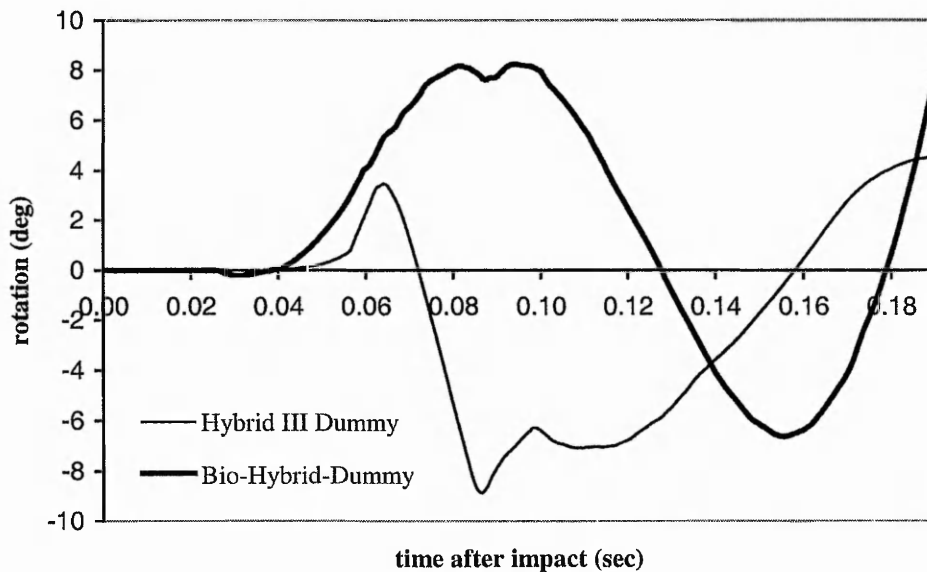


Figure 48: Head rotation relative to the base of the neck.

It has to be pointed out that the head restraint for the dummy simulation had to be moved backwards by 52 mm to achieve the same initial 80 mm gap between the head and the head restraint. The difference in the head location between the Hybrid III dummy and biomechanical model is due to the design of the dummy neck. The biomechanical cervical spine demonstrates the proper curvature of the

human neck, unlike the dummy neck which is designed as a vertical “tube” (Figure 49).

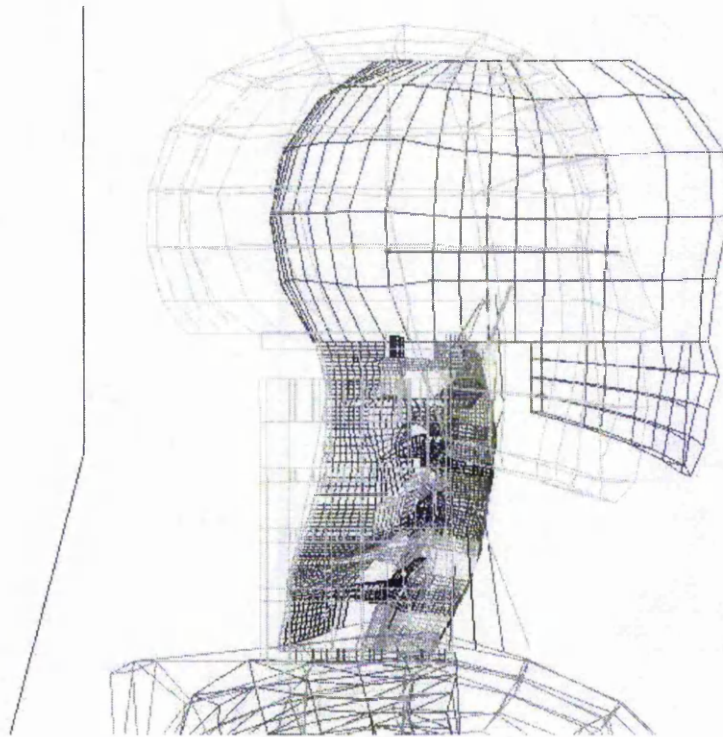


Figure 49 The difference in the location of the head between Hybrid III dummy and Bio-Hybrid-Dummy.

This result alone is a good recommendation for using the Bio-Hybrid-Dummy model for safety design. The dummy on its own is not capable of representing the behaviour of the real neck in rear accident situations, and will give misleading results to designers.

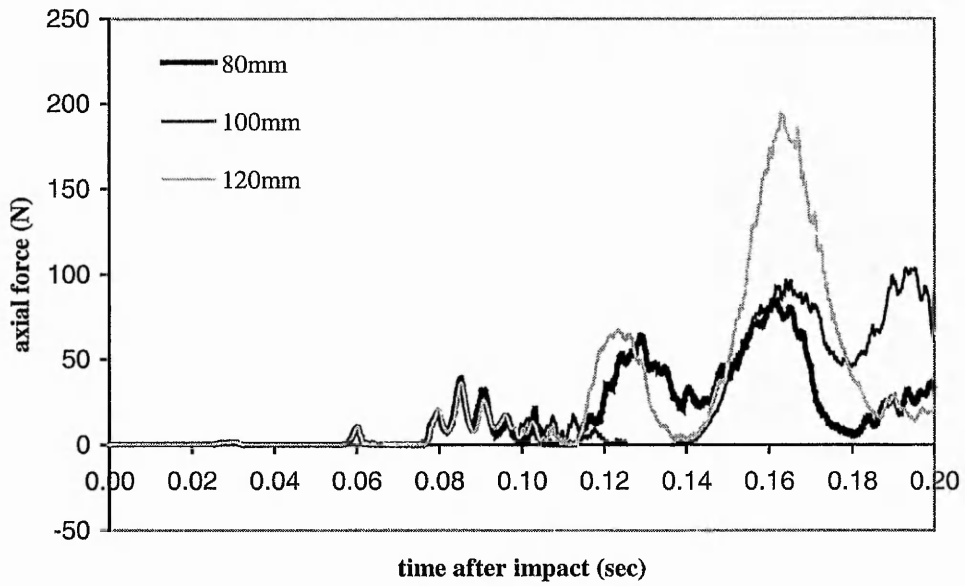


Figure 50 Force/time relationship of the apical ligament.

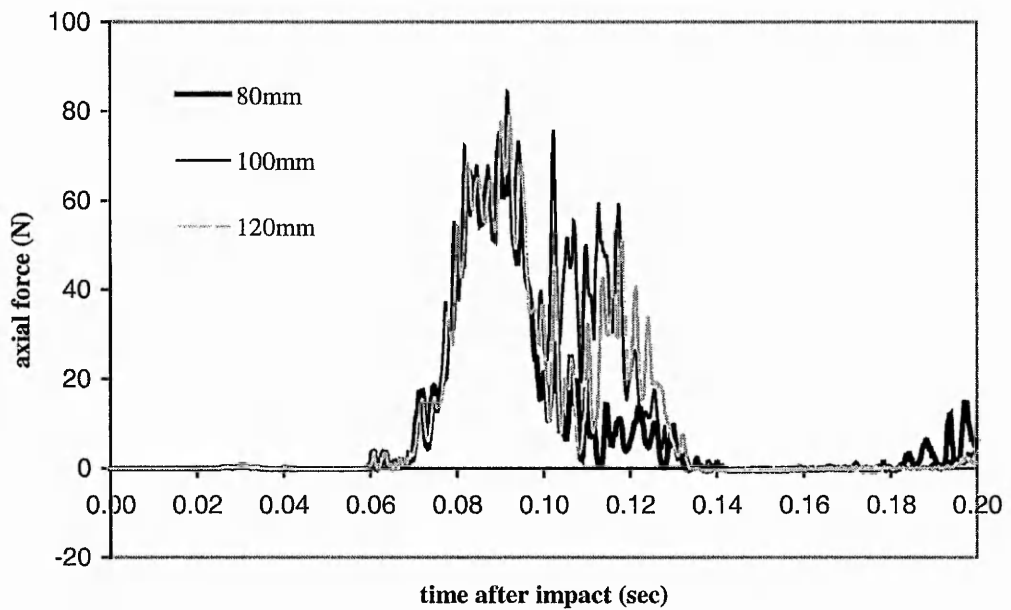


Figure 51 Force/time relationship of the ligamentum flavum.

To show the most important characteristic of the Bio-Hybrid-Dummy model, some more solutions with different initial gaps have been calculated. The biomechanical modelling advantage over the common dummy models can be

clearly see on the two following examples of loading on individual ligaments shown in Figure 50 and in Figure 51. For example the loading of the Apical ligament increases with the remoteness of the head restraint, implying the need to keep the head restraint as close as possible to the head.

This kind of data, which can be very valuable for safety design, is not available using crash test dummy models. Based on the results from individual ligaments, present seat designs can be assessed and new anti-whiplash designs can be developed.

**CHAPTER 6**

**ANTI-WHIPLASH DEVICE INVESTIGATION**

**USING THE BIO-HYBRID-DUMMY MODEL**

## 6.1 Introduction

Work presented in this chapter has been accepted for presentation at ICRASH2000 International Crashworthiness Conference to be held in September 2000 (Appendix E)

## 6.2 Model

The model used in the present investigation (Figure 52) consists of the Bio-Hybrid-Dummy model in a simplified vehicle seat environment.

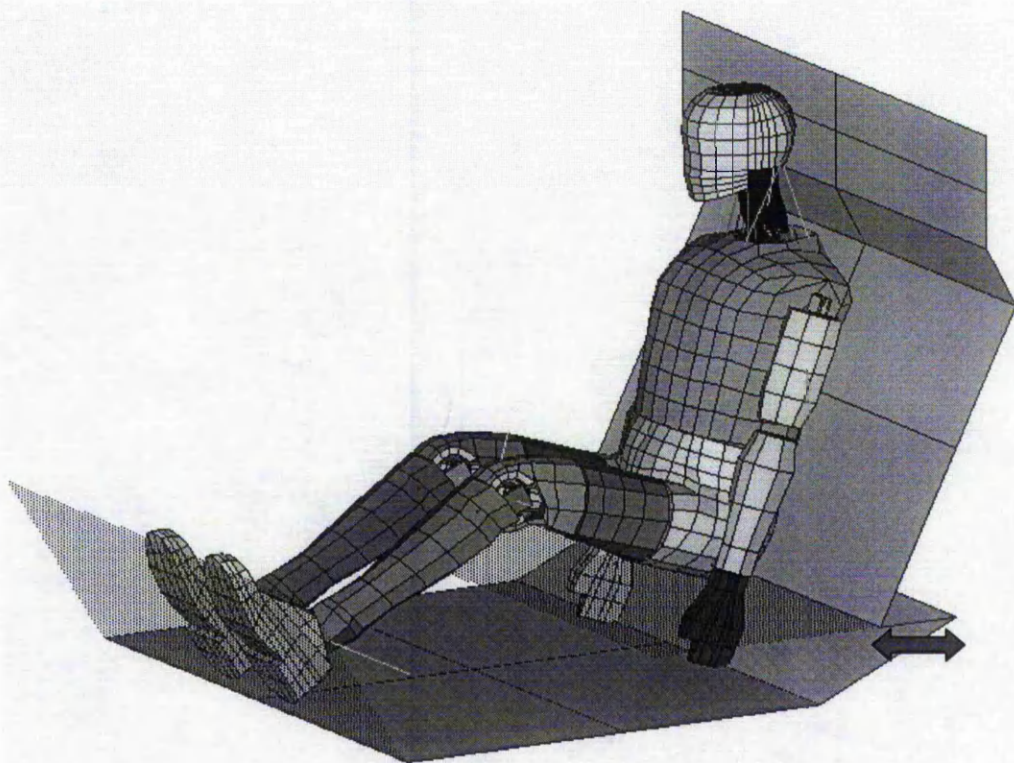


Figure 52: Isometric view of the FEA Model

The model used in this investigation is based on the model presented in the previous chapter, with modified representation of the contact between vertebrae and ligaments, and better positioning in a seat. Therefore, for detailed description of the model, please refer to CHAPTER 5. The anti-whiplash device under

investigation was introduced in one of the previous chapters, thus for more information please refer to CHAPTER 4.

### 6.3 Loading Conditions

The loading data for the present study were based on sled experiments conducted by Dr. Steffan Datentechnik GmbH (CD-Crash Ver 1.3, 1996). To evaluate the model, one of the experiments (MERCEDES 200-300 W 124, 1987 [MB 190] test NR.2) was reconstructed. The recorded test sled acceleration history was used to load the floor of the car, leaving the motion of the seating system with the occupant to be determined by the model.

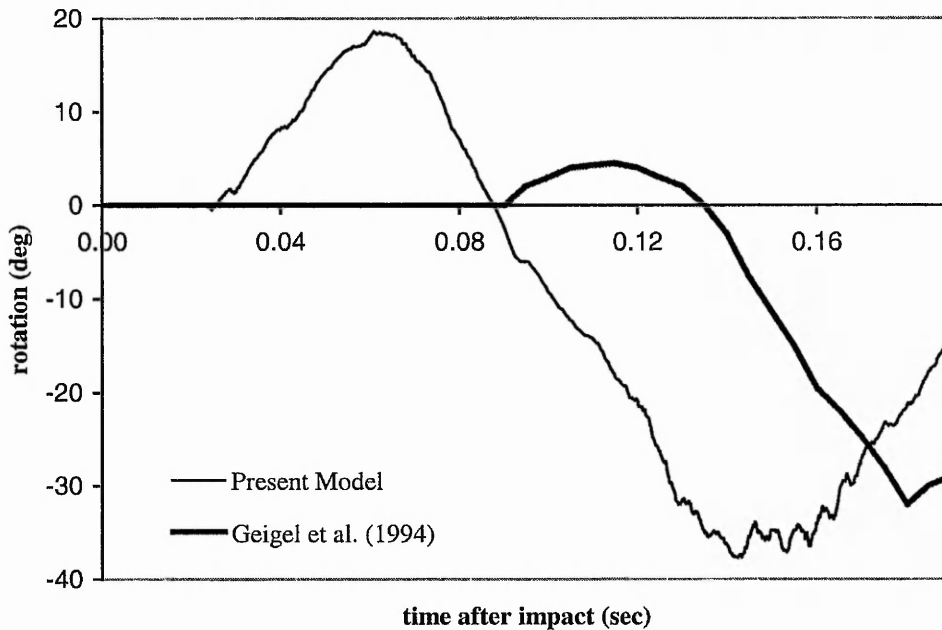


Figure 53: Relative rotation between head and C3 during a 10.5 km/h rear end impact, comparing the experimental data of Geigl et al. with the numerical prediction.

The fine tuning of the contact algorithms and better positioning of the Dummy in the seat resulted in a smoother response of the model compared to the preliminary model (Golinski et al., 2000). At the same time, due to the reducing initial distance between the torso and seat back, the response of the head has been moved even farther to the beginning of the event. In that light, and due to the use

of a symbolic seat system, the performance of the model can be assessed as quite good, in spite of the obvious discrepancies in Figure 53.

## 6.4 Results

Following the evaluation of the model several simulations were conducted, using the same crash conditions, to establish the optimum properties of the one-way spring buffer device as well as the most representative gap between the head and the head restraint. Finally, it was decided to test the device using an 80 mm gap between the head and the head restraint and springs of 50 mm and 100 mm length with linear characteristics and a maximum force of 3500N.

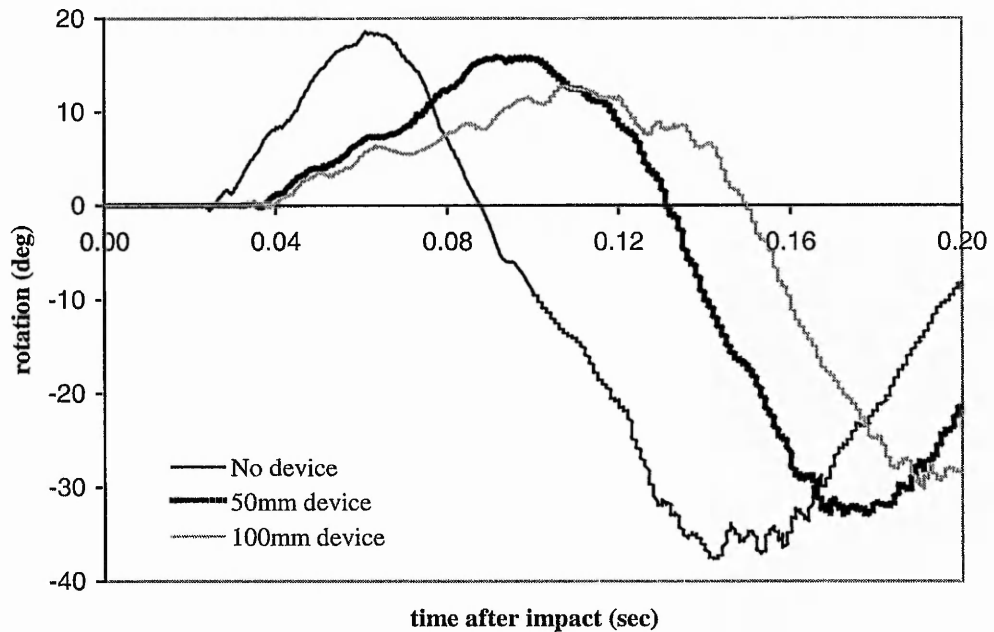


Figure 54: Relative rotation between head and C3.

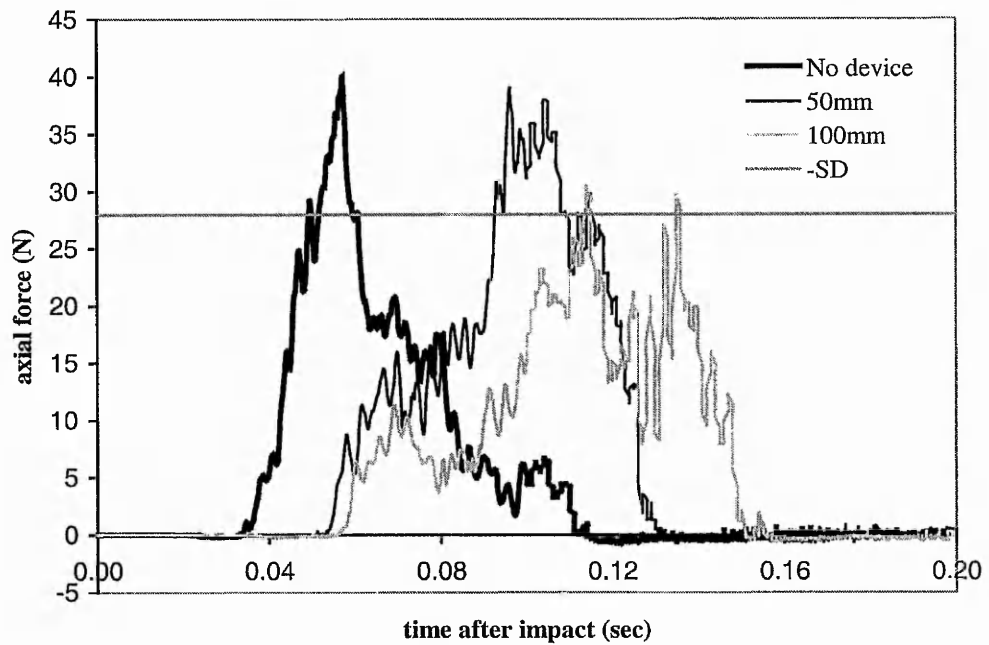


Figure 55 Force/time relationship of the ligamentum flavum with and without the device.

It was found that the anti-whiplash device significantly reduced the relative rotation between the head and C3 which produces hyperflexion in the C0-C2 complex and is thought to lead to whiplash injuries. As shown in Figure 54, the rotation also takes place over a longer time and so the angular accelerations are doubly reduced.

The potential benefit of the device can be most clearly seen, however, on the individual ligaments' loading, particularly in the C0-C2 motion complex. The 100 mm device reduced the maximum force in the ligamentum flavum (Figure 55), enough to bring it under the lowest breaking force of 28N reported by Myklebust et al. (1988). The reduction in loading can be seen as well in the posterior atlanto – occipital membrane (Figure 56). Unlike the ligamentum flavum, this already experienced less than the lowest breaking force, but it has to be seen in the context of the loading being deduced from tests on volunteers, implying they are harmless to test subjects.

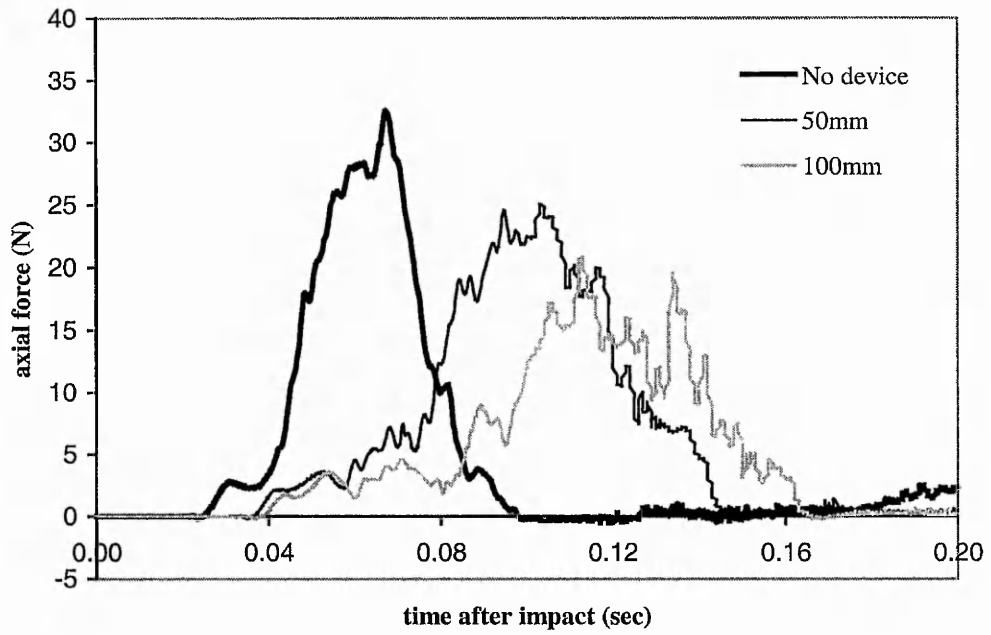


Figure 56 Force/time relationship of the posterior atlanto – occipital membrane with and without the device.

**CHAPTER 7**

**THE INFLUENCE OF THE DYNAMICALLY  
INCREASING GAP BETWEEN HEAD AND  
HEAD RESTRAINT ON THE WHIPLASH  
INJURY SEVERITY.**

## 7.1 Introduction

The Bio-Hybrid-Dummy model presented in the previous chapter has been used here to investigate the seat rake influence on the whiplash injury severity. Therefore, for the details of the occupant model, as well as loading conditions, please refer to CHAPTER 5 and CHAPTER 6.

## 7.2 Seat Model

The Bio-Hybrid-Dummy was placed in a simple model of a seat environment (Figure 57). The seating system used in the investigation, although rigid, is able to represent overall raking of the seat i.e. the inclination of the seat back to the vertical is allowed to alter dynamically as a result of the impact.

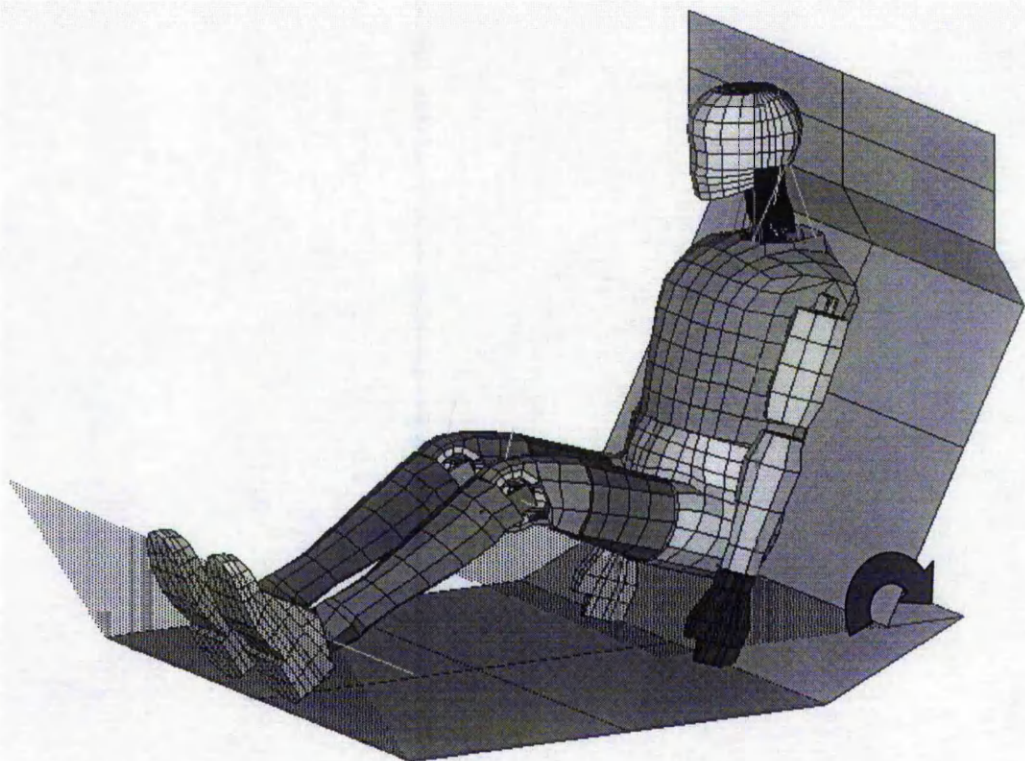


Figure 57: Isometric view of the FEA Model

To specify a relative movement LS-Dyna `CONSTRAINED_JOINT_REVOLUTE` has been used in conjunction with `CONSTRAINED_JOINT_STIFFNESS_GENERALIZED`, which enables the control of the rotational stiffness as well as the stop angles. The maximum strength of the seat back from the experiments was implemented into the model by defining a maximum value of the rake using “stop angle” function. The raking characteristics used in the present investigation were based on experimental results for production seats (Benson et al., 1996). The full listing of the raking stiffness of the seat backs as well as the stop angles implemented in the model can be found in Table 6.

| <i>Based on Seat</i>                 | <i>Raking Stiffness</i><br><i>(Nm/deg)</i> | <i>Stop angle</i><br><i>(deg)</i> |
|--------------------------------------|--|-----------------------------------|
| 1988 <b>Ford</b> Aerostar (modified) | 530.407                                    | 15.23                             |
| 1985 <b>Mercedes</b> 190E            | 97.912                                     | 25.99                             |
| 1989 <b>Toyota</b> Corolla (4-dr)    | 76.374                                     | 22.83                             |

Table 6 Properties of the seat rake.

### 7.3 Results

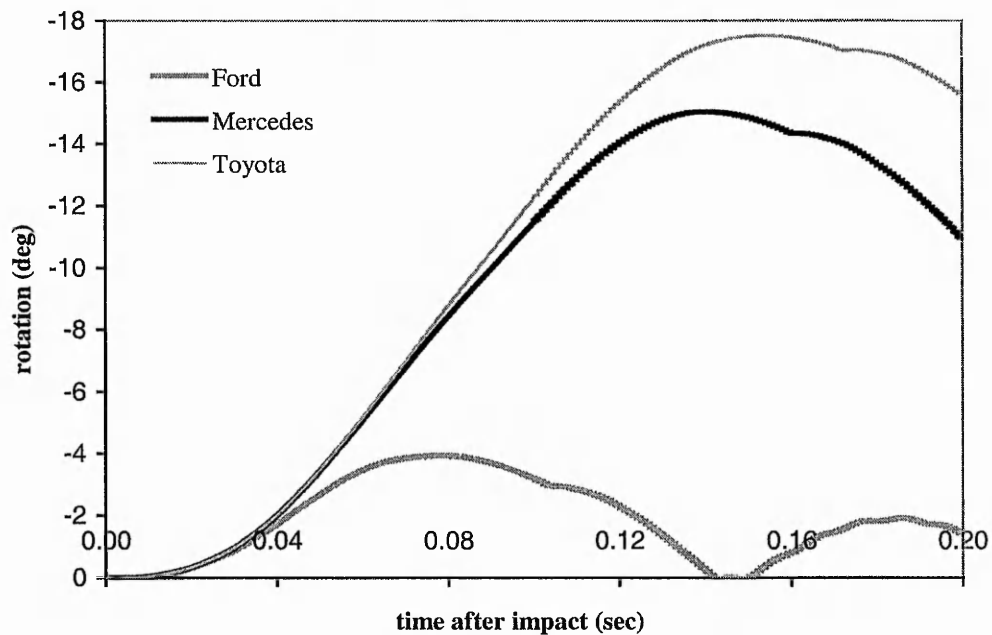


Figure 58: Raking angles for different seats

Three raking seats as well as the non-raking one have been tested, under the same loading conditions, to establish the influence of the dynamic gap between head and head restraint using an initial gap of 80 mm. The raking angles of the seat backs due to the applied loading, ranged from 3.94deg for the stiffest seat up to 17.5deg for the softest one, as can be seen in Figure 58.

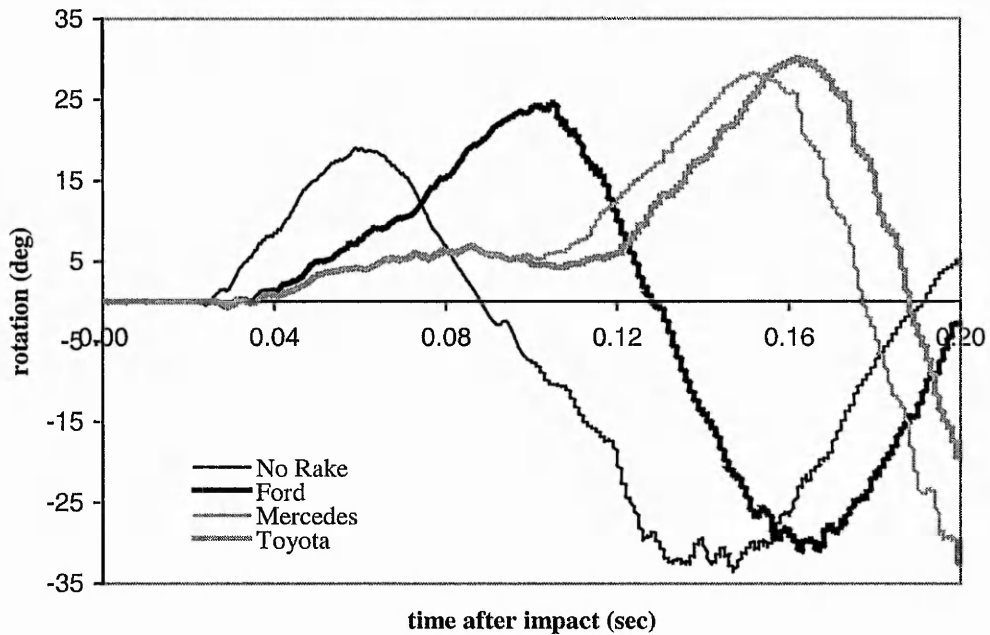


Figure 59: Relative rotation between head and C3.

It was found that the raking of the seat, resulting in a dynamically increasing gap between head and head restraint, increases the relative rotation between the head and C3 (Figure 59) which produces hyperflexion in the C0-C2 complex and is thought to lead to whiplash injuries.

The influence of the rake of the seat can be seen clearly on the loading over time characteristics of individual ligaments. The loading of the posterior atlanto – occipital membrane (Figure 60) due to the use of raking seats increases dramatically, reaching more than double the loading of the non-raking seat. This increased load is over the minimum breaking force reported by Myklebust et al. (1988). It is even more significant when it is noted how narrow is the breaking zone of this ligament, indicating the possibility of injury being quite high. In the case of the ligamentum flavum, the loading is over the minimum breaking force of 28N even for the non-raking seat (Figure 61). However, the results of the raking

seats show a significant increase of loading, almost doubling the loading received from the non-deforming seat, indicating the increase of whiplash injury for a wider population.

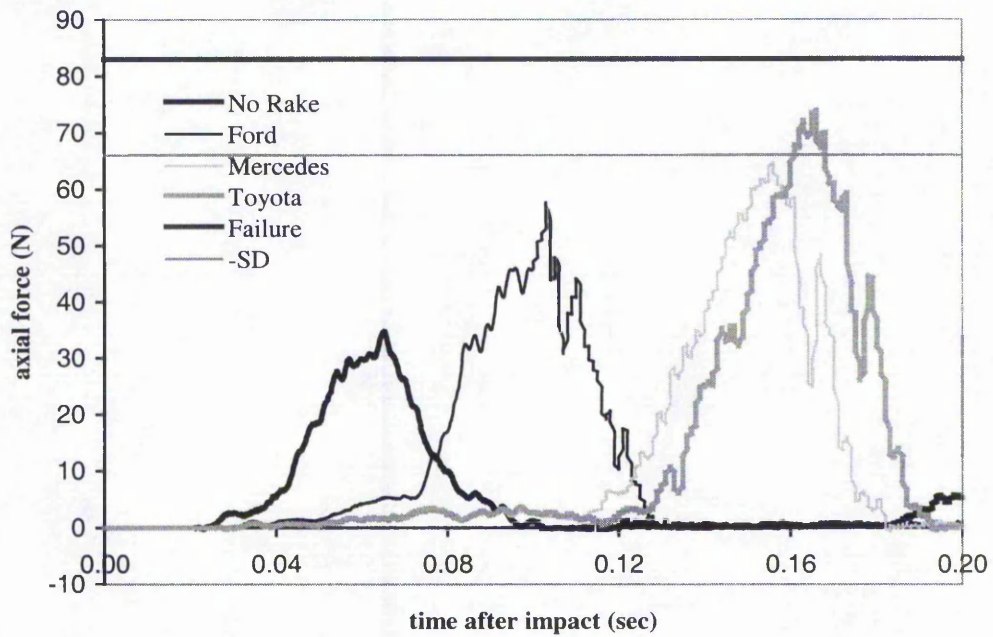


Figure 60 Force/time relationship of the posterior atlanto – occipital membrane.

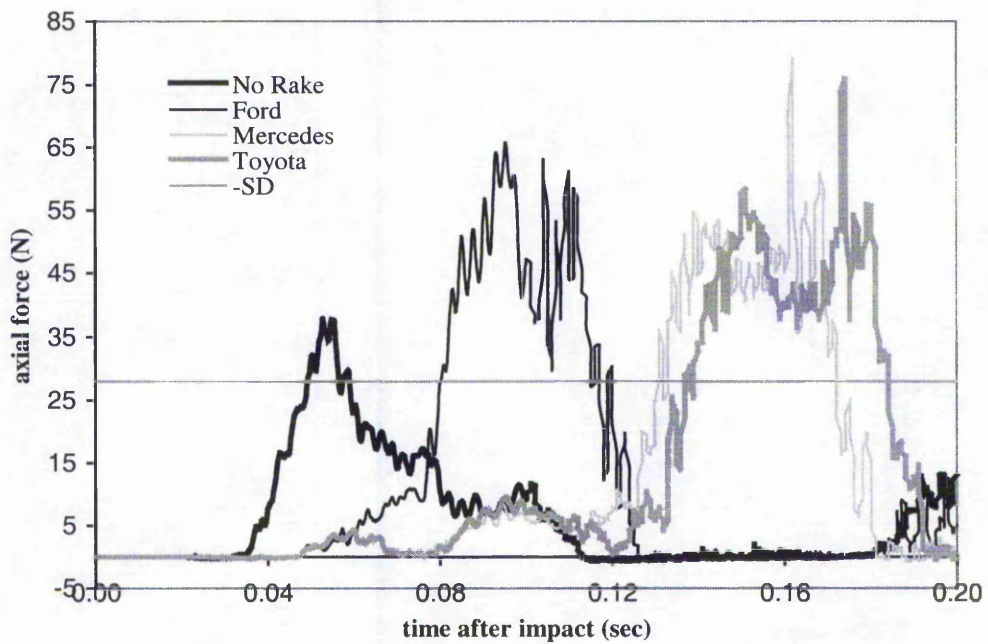


Figure 61 Force/time relationship of the ligamentum flavum.

It has to be pointed out, that the present model only represented the overall rake of the seat back being modelled as rigid, lacking any realistic deformation of the internal springs and padding. Nevertheless, these results are clearly showing the importance of not only the initial gap between the head and the head restraint, but also for the first time how the dynamic increase of the gap increases the injury risk. They are giving clear indications of the need for car seat designs which will not only decrease the loading transferred onto the occupant body, but also will prevent the dynamic increase of the initial head - head restraint gap.

**CHAPTER 8**

**CRASH PULSE INFLUENCE ON THE**

**WHIPLASH INJURY SEVERITY.**

## 8.1 Introduction

When describing accidents, there are various possibilities to describe the occurring forces. However, only the acceleration curve over time (crash pulse) and the change in velocity are useful. Description of the crash pulse gives more information, but it is abstract to common person who is not technically literate. Whereas the change of velocity is easier to imagine, but it does not take the impact's duration into account. For example, the long-lasting collision produces lower stresses due to longer impact duration in which the velocity change is produced, whereas the short duration impact produces velocity change very quickly (Meyer et al. 1998). In real life, there is a possibility of accidents with different crash pulses leading to similar changes of velocity, but with different time duration. To investigate the crash pulse influence on injury levels, the occupant model in the Mercedes-based model of the raking seat presented in the previous chapter has been used. Therefore, for the details of the Bio-Hybrid-Dummy, please refer to CHAPTER 5 and CHAPTER 6, whereas the raking seat description can be found in CHAPTER 7.

## 8.2 Loading Conditions

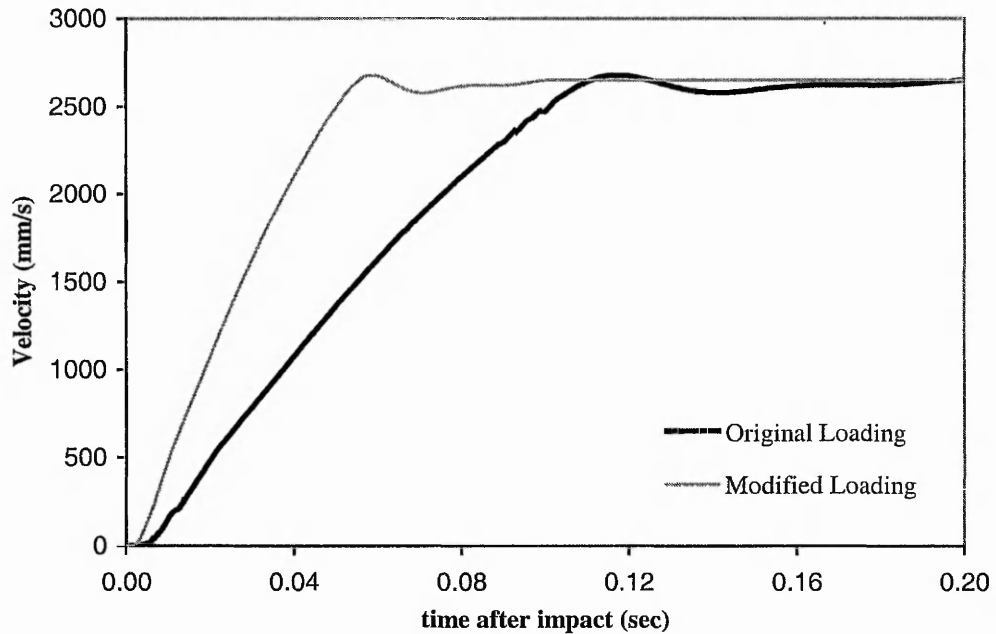


Figure 62: Velocity profiles of the seat base.

For the first simulation, the same loading as in previous investigations has been used. To achieve a different crash pulse for the second simulation, however, resulting in this same relative velocity, simple mathematical operation has been performed. The loading profile used in the previous investigations has been applied over half of the time. As a result of that operation two velocity profiles were created, being the same in terms of absolute value of the change of velocity (Figure 62), but with different crash pulses (velocity change duration).

### 8.3 Results

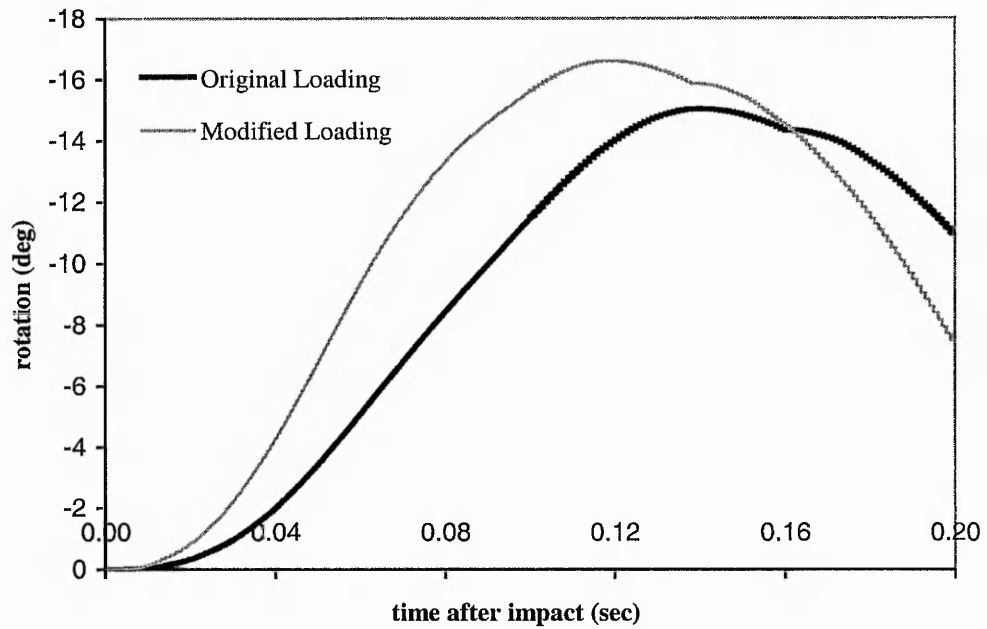


Figure 63: Raking angles of the seats for different loading conditions

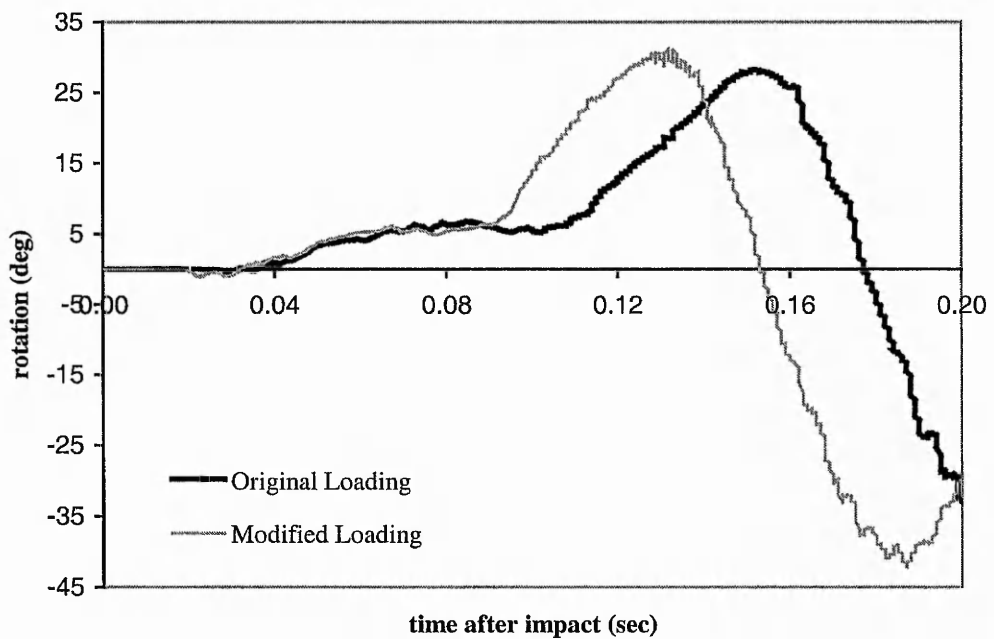


Figure 64: Relative rotation between head and C3.

As expected, an increase in the crash pulse resulted in a higher raking angle, achieving a maximum of 16.3deg, over 1.5deg more compared with the original

pulse raking. This effect in itself, as documented in CHAPTER 7, through creating a wider dynamic gap will lead to higher injury risk. However, combined with the higher angular acceleration and the higher deformation in the upper cervical spine (Figure 64) a situation with even higher injury risk is created.

Due to the unique features of the Bio-Hybrid-Dummy, instead of speculating on possible injury risk increases one can assess them quantitatively based on an individual ligament's loading. In the following graphs, force versus time characteristics from three individual ligament structures located in the upper cervical spine are presented, showing an increase of loading for all of them. In the case of the posterior atlanto – occipital membrane (Figure 65), due to the shorter duration of a change of velocity, the ligament loading was raised from a safe level to a level reported by Myklebust et al. (1988) as corresponding to failure for this structure. To make matters worse, this particular structure is characterised with a very narrow breaking zone, making the possibility of injury even greater for a wider part of the population.

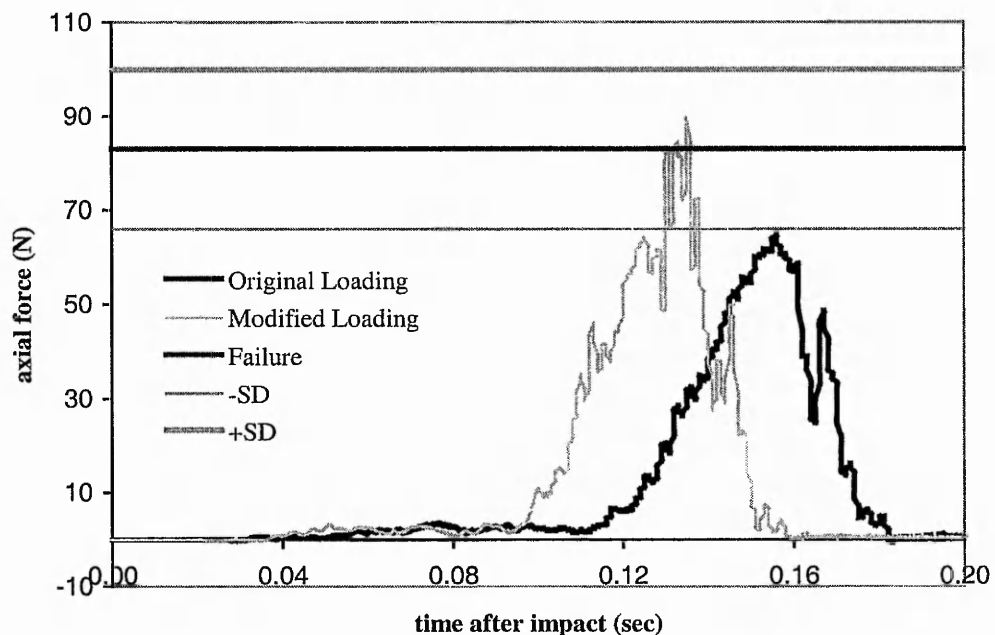


Figure 65 Force/time relationship of the posterior atlanto – occipital membrane.

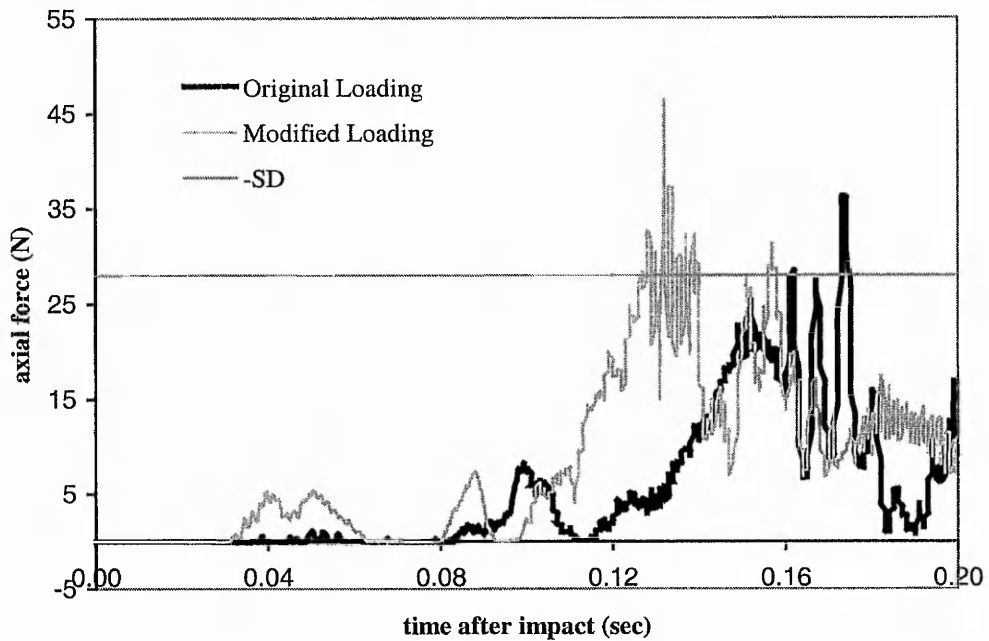


Figure 66 Force/time relationship of the tectorial membrane.

The tectorial membrane (Figure 66) and the alar ligament (Figure 67), located in the anterior aspect of the spinal cord, both noted an increased loading. For the first, already over the minimum recorded breaking level even for the original loading, the increase would result in more casualties, whereas in the case of the latter, the loading is getting too close to the breaking zone for the comfort of the safety designer. This confirms the observations presented by Dvorak et al. (1988) in their *in vitro* investigation into the biomechanics of the upper cervical spine, where a partial or even complete rupture of the alar ligament was suggested due to unexpected trauma. The over-stretching of these particular ligaments could be significant in terms of spinal cord trauma because of their proximity to the cord. So far, only the ligaments located posterior to the spinal cord were noted as being overloaded. Now, when even the anteriorly located structures are reaching dangerous loads, the possibility of injuring the spinal cord becomes clear.

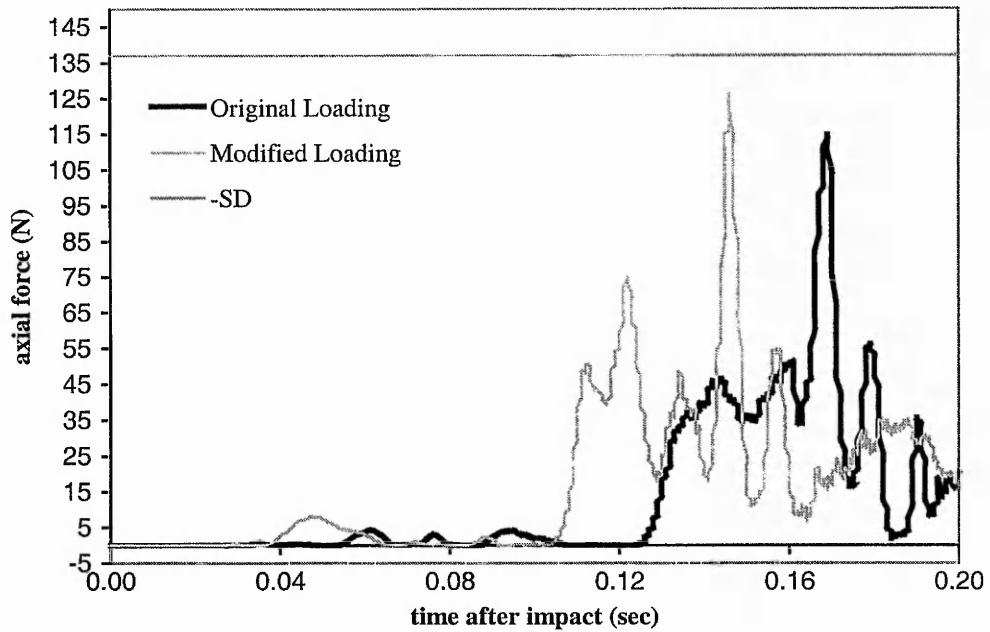


Figure 67 Force/time relationship of the alar ligament.

In real life, a difference in the stiffness of the structure between two struck cars, or a difference in the mass between the striking and struck cars, could result in loading with similar relative velocity but with very different crash pulses. (change of velocity duration). This study confirms the observation by Koch et al. (1995), who showed from a statistical study of accidents, that there is a higher risk of injury where there is significant difference in the mass of the striking and the struck car. Bostrom et al. (1997), in a combined study of accident data and simulations confirmed Koch's observation, found that there is an increase in the injury risk when the weight ratio between striking and struck car increases. Moreover, Bostrom stated that the injury risk increases due to increasing change of velocity of the struck car. This has been shown exactly in the present study, by applying two loadings with different velocity change duration, but with this same velocity change absolute value of the struck car.

**CHAPTER 9**

**THE INFLUENCE OF INITIAL HEAD ROTATION**  
**(NON SAGITTAL PLANE POSITIONING) ON**  
**WHIPLASH INJURY.**

## **9.1 Introduction**

Work presented in previous chapters has concentrated on the whiplash scenario where the occupant is looking straight ahead and there is no rotation of the head about a vertical axis involved. However, a new “worst case” scenario of a whiplash accident involving rotation has lately been described by Adams (1998). He describes the situation where the occupant is turning around to look back or is looking into the rear view mirror when the car is struck from behind. In that situation the inertial forces of the head will combine rotation with translation, leading to even more severe damage, especially in the C0-C2 complex. This is a common situation since many rear end impacts occur when the driver is anticipating a crash and is looking in to the mirror to see if it will happen. Therefore the work presented in this chapter focuses on investigating this newly proposed whiplash scenario involving rotation of the head about a vertical axis.

## **9.2 Model**

The model first presented in CHAPTER 5 was designed with vertical rotation in mind. Therefore, no changes to the structure of the model had to be made to use it in this new whiplash scenario, making the model very versatile and giving the user the possibility of comparing the results between the sagittal plane scenario and the vertical rotation scenario. To use the previously presented model in the vertical rotation scenario, only the sagittal plane constraints had to be taken out from the head and cervical vertebrae, leaving the whole model free to move in all directions.

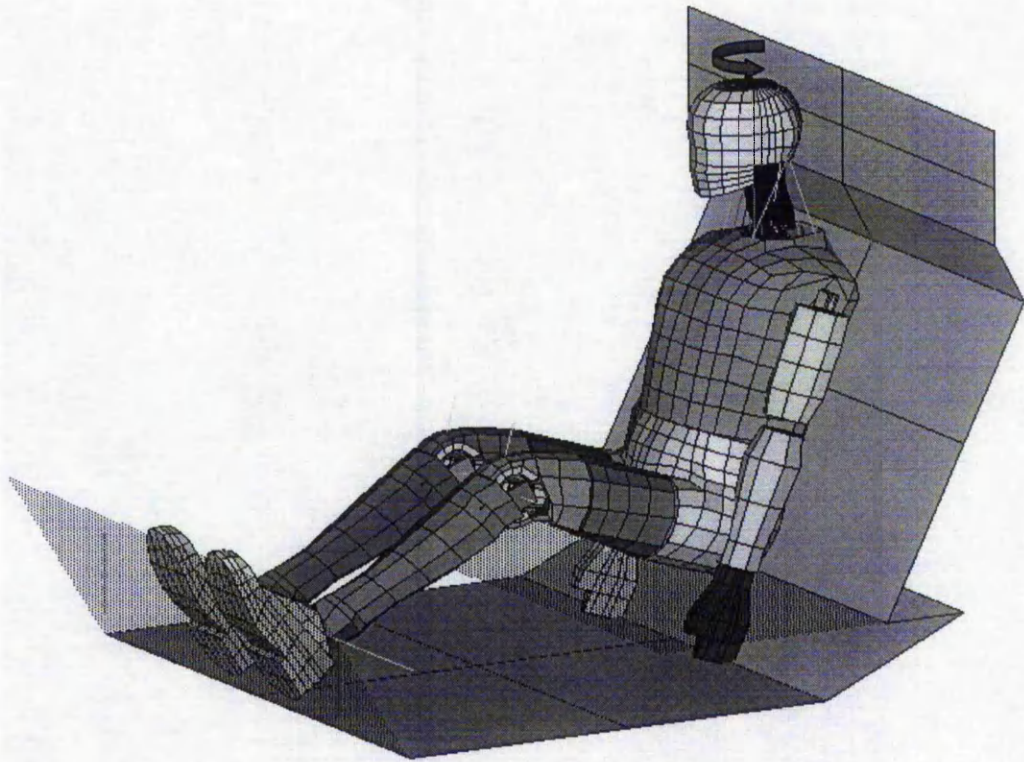


Figure 68 Isometric view of the FEA Model

### 9.3 Loading Conditions

To achieve realistic pre-loading from an initial vertical rotation in all the deforming structures of the model, the whole event has been simulated in one run, where the rotation of the head is followed by the rear end accident loading.

The rotational loading of the head has been applied as a pure moment of maximum value 1.5 Nm applied anticlockwise to the C0 (base of skull). This loading has been taken from an experimental investigation into the kinematics of the upper cervical spine presented by Panjabi et al. (1988). They found this loading to be sufficiently large to produce the physiological motions, but small enough to not injure spine specimens. The explicit nature of the LS-Dyna solver (time dependent) requires all loading to be applied over time including the initial rotation of the head. Therefore the moment was applied evenly in real time, reaching a level of 1.5Nm after 0.3s, when the whiplash loading of the seat begins (Figure 69). To make it realistic, the moment is kept at this level till the end of the whole event, reconstructing the situation when the driver is suddenly rotating his

head to check in the rear mirror what is going on and is hit by the car following him. The time of 0.3s was chosen as realistic for this sudden movement.

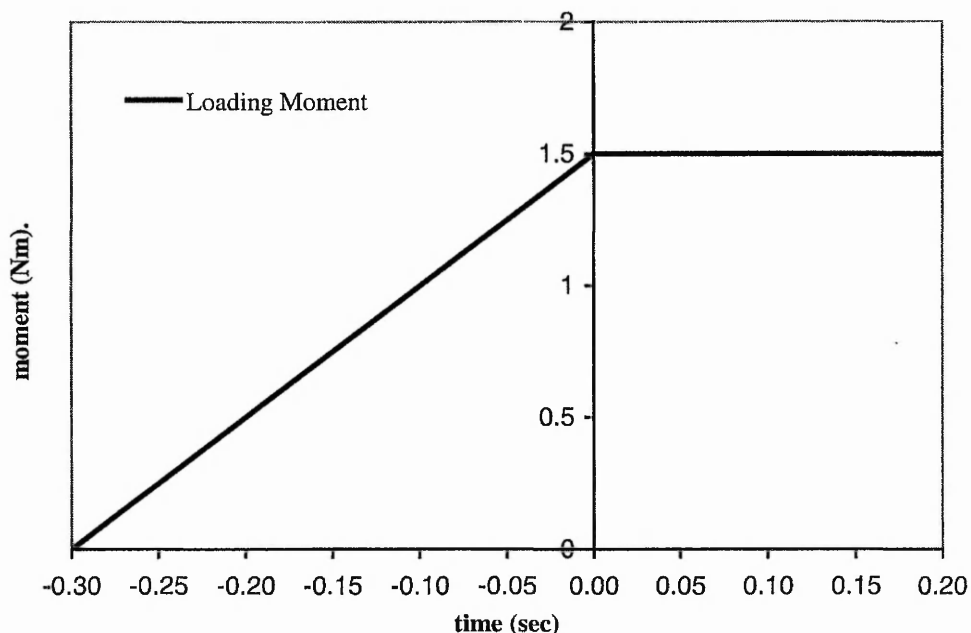


Figure 69 Head vertical rotation loading characteristics.

For the impact loading, once again the data from sled experiments conducted by Dr. Steffan Datentechnik GmbH (CD-Crash Ver 1.3, 1996) has been used. By reconstructing the same test as in previous investigations, comparison of results was made possible.

To make analysis of results clear, the time convention for the event has been set so that the beginning of the rear end impact is marked as time 0s. Therefore the results from the vertical rotation of the head will be presented from -0.3s till 0s, followed by the main impact event starting from 0s till the end of it at 0.2s.

## 9.4 Results

As a result of the initial uniform rotation, at the beginning of the impact the head was rotated through over 36deg, with relative rotations in joints C0-C1 and C1-C2 of 11.72deg and 14.21deg respectively (Figure 70). Due to the rate of axial rotation loading and the lack of restriction to the movement of the head, there is no possibility to compare the range of motion with experimental results from

static loading. However it is believed, based on the established trend of higher relative rotation in the C1-C2 joint than in the C0-C1 joint, that the kinematics of the upper cervical spine in the present model reflect the real life kinematics of humans.

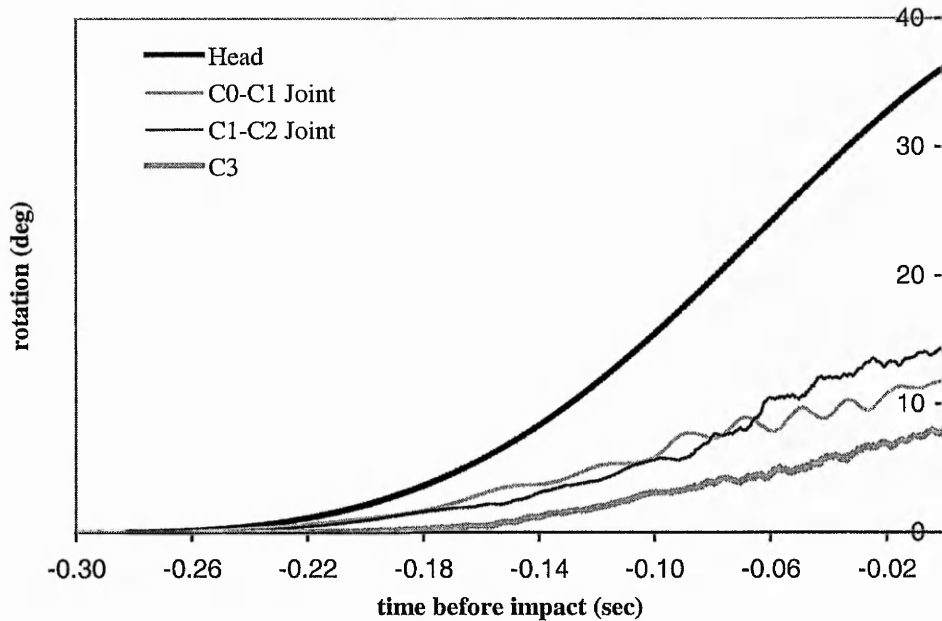


Figure 70 Vertical rotation due to initial loading of 1.5 Nm over 0.3s.

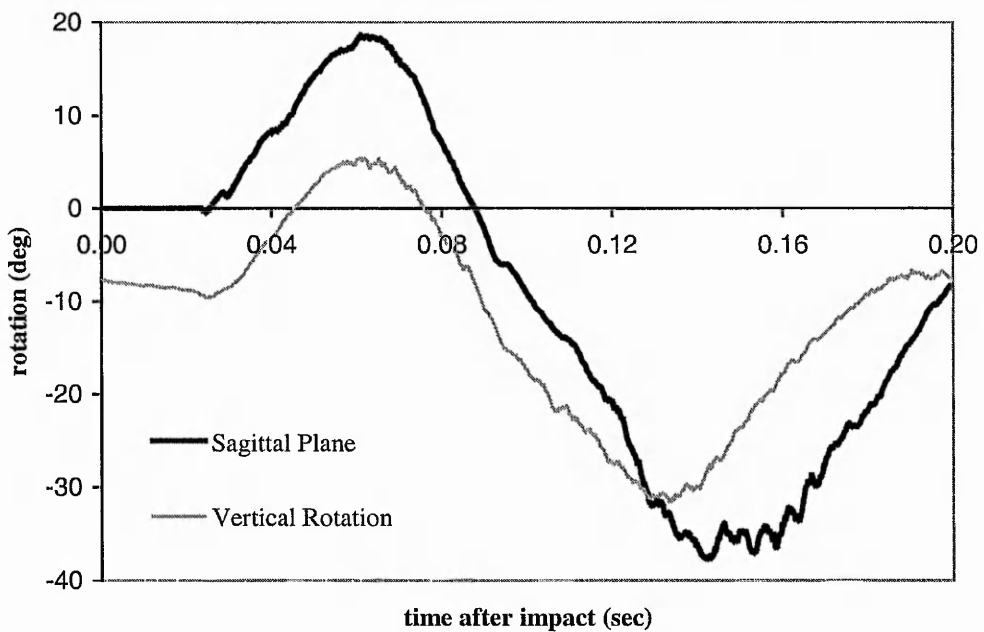


Figure 71 Relative rotation between head and C3 in sagittal plane.

So far, in the whiplash scenario restricted to one plane only, the relative rotation between the head and the C3 vertebrae in the sagittal plane was used as a simple way of assessing the motion trend characteristics in the upper cervical spine. Looking at Figure 71, the vertical rotation scenario might be thought to lead to lower loading on individual ligaments compared with the sagittal plane characteristics, since the maximum value of relative rotation in the upper cervical spine is lower than in the sagittal scenario. However, since now the movement of the cervical spine is no longer restricted to a 2D plane, but happens in 3D space, this specific indicator can not be used for comparison purposes against the sagittal plane case to establish injury intensity.

It can be seen on the following figures that despite lower relative rotation between the head and C3 in the sagittal plane, the rotation in 3-dimensional space is actually higher, leading to higher loading of individual ligamentous structures. For example, in the case of the interspinous ligament between the C1 and C2 vertebrae (Figure 72), inclusion of the initial vertical rotation leads to doubling of the maximum loading force compared with the sagittal plane case. Moreover, this particular ligament, which was under no danger in the sagittal plane scenario has been put almost in to the breaking zone in the rotational case. This must be seen in the light of how narrow is the breaking zone for the interspinous ligament. It becomes even more worrying; with a statistical spread of only 4N in the breaking load this ligament will be injured in a majority of the whiplash accident cases including initial rotation scenario. A similar situation can be noted for the ligamentum flavum at this same level (Figure 73). However this ligament was already in the breaking zone even for the sagittal plane case, and the inclusion of initial rotation resulted in a doubling of the loading. In simple words this means higher possibility of injury for a wider representation of the population.

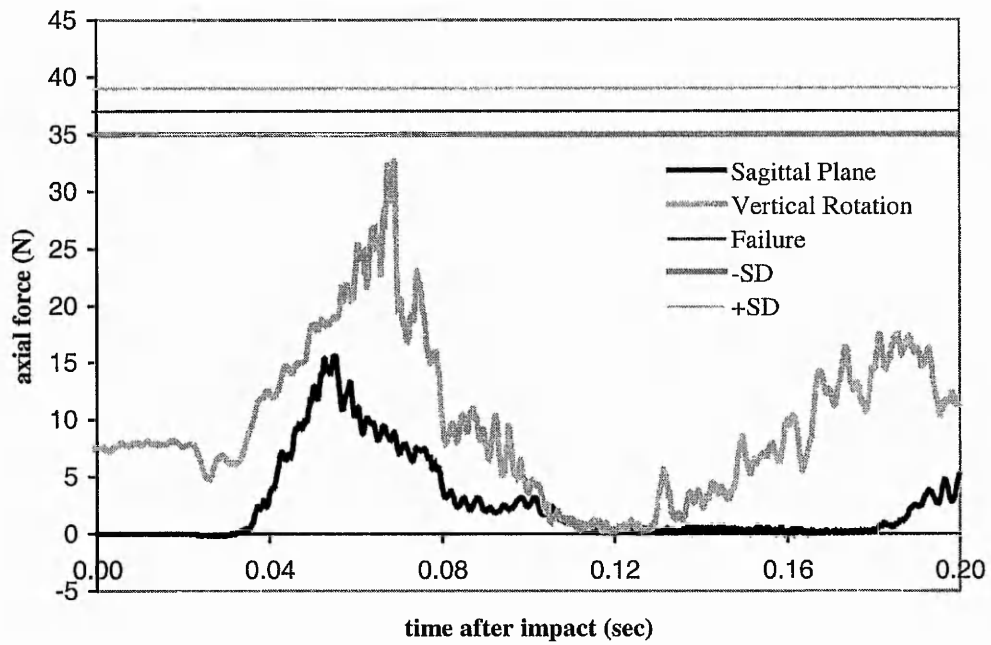


Figure 72 Force/time relationship of the interspinous ligament (C1-C2).

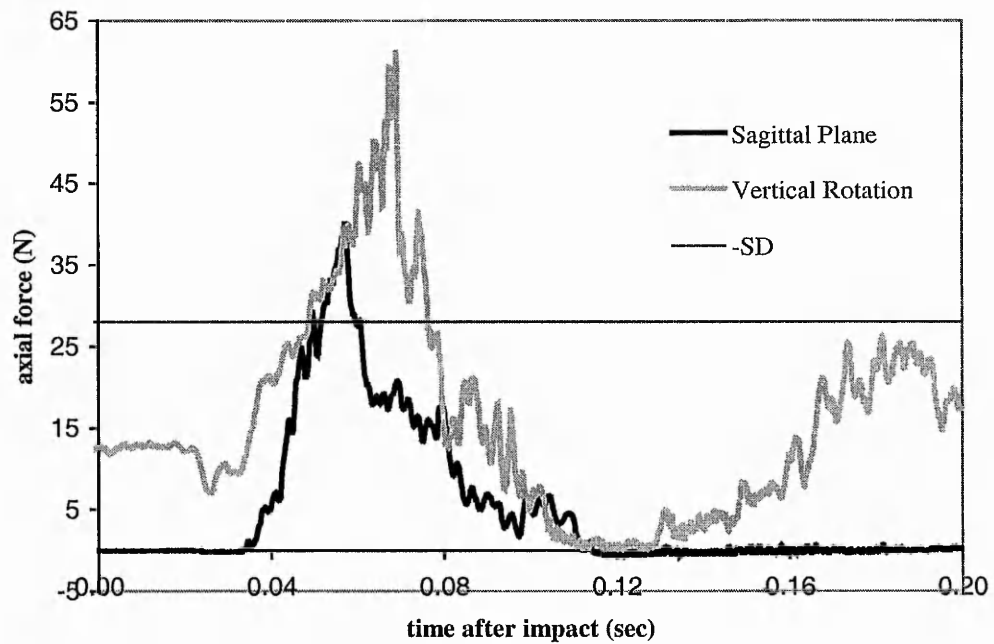


Figure 73 Force/time relationship of the ligamentum flavum (C1-C2).

Panjabi et al. (1998b) tested capsular ligament stretch during whiplash simulation using an *in vitro* model. They recorded a modest increase in capsular ligament strain over the maximum physiological values during sagittal plane trauma.

However they suggested significantly larger stretch of capsular ligaments during whiplash if the subject's head was turned to one side, based on results from physiological loading where the maximum elongations of capsular ligaments were recorded in axial rotation and lateral bending. The head-turn posture of the neck will produce, under whiplash loading, complex head and intervertebral motion including the suspected axial rotation and lateral bending on top of the extension of the neck. Figure 74 presents results from capsular ligaments to confirm Panjabi's statement. Although the loads are still underneath the minimum recorded breaking loading of 181N (Myklebust, 1988) the influence of axial rotation can be clearly seen. The recorded loading compared with the sagittal plane case is doubled for the left capsular ligament and tripled for the right capsular ligament.

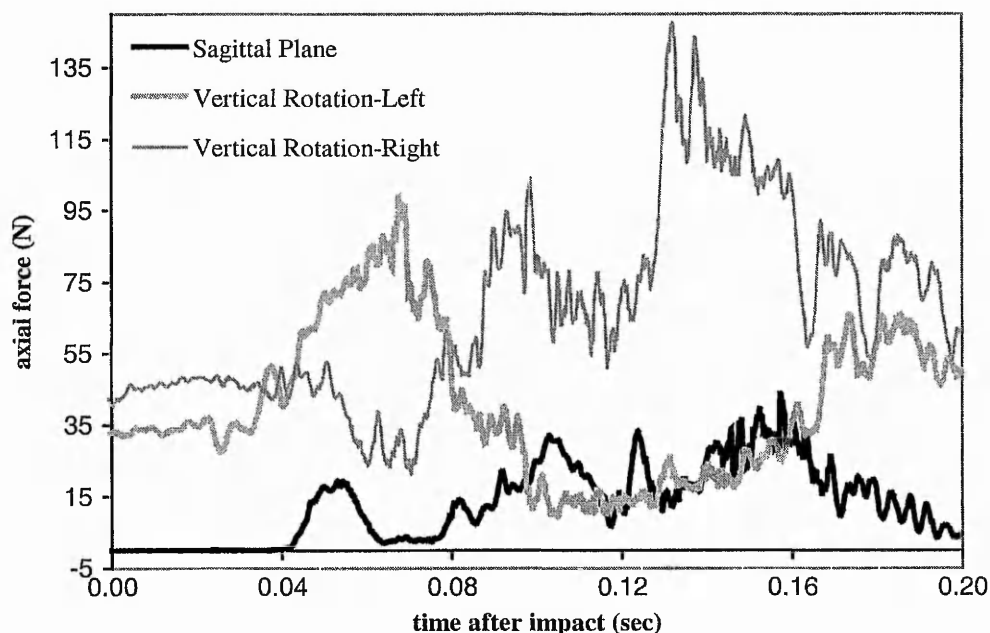


Figure 74 Force/time relationship of the capsular ligaments (C1-C2).

Goel et al. (1990) performed axial rotational loading on the C0-C2 complex until failure. In all cases subluxation of the C1-C2 facet joint with rupture of the C1-C2 joint capsular ligament and rupture of the posterior atlanto-axial ligament were identified. The danger loading in the case of the presented model has been recorded in ligaments located in the posterior aspect between the atlas (C1) and the axis (C2) as well as the capsular ligaments of the C1-C2 intervertebral joint.

Therefore the present model agrees with the results presented by Goel, indicating the same structures which failed in static rotational loading as being most sensitive to rupture under the whiplash scenario which includes axial rotation.

**CHAPTER 10**

**SEAT RAKING IN WHIPLASH ACCIDENT**

**SITUATIONS WITH INITIAL VERTICAL**

**ROTATION OF THE HEAD.**

## **10.1 Introduction**

The successful introduction of an initial axial rotation into the whiplash scenario (CHAPTER 9) showed the potential danger lying behind this new situation. To further investigate the whiplash scenario with initial rotation of the head, the model presented in the previous chapter has here been extended to include the raking seat model. The seat model firstly introduced in CHAPTER 7 has been included in the present study. Therefore for the raking properties of the seat back please refer to the above mentioned chapter, while the description of the occupant model and loading characteristics can be found in CHAPTER 9.

## **10.2 Results**

In similar fashion to the sagittal plane scenario, the raking of the seat resulted in a dynamic extension of the gap between the head and the head restraint, postponing the transmission of the loading onto the neck further into the event (Figure 75). Moreover the extension of the gap between the head and the head restraint resulted in an increase in the maximum relative angle between the head and the C3 vertebra. So far, at least for the sagittal plane whiplash scenario, an increase of flexion in the upper cervical spine has indicated a possible increase in ligamentous trauma. However as shown in the previous chapter, straight comparison of ligamentous injury between the sagittal and vertical rotation scenarios based on relative rotation in the C0-C3 complex is not possible. Therefore, the raking seat results will be compared only to the non-raking seat results from the vertical rotation scenario presented partly in CHAPTER 9.

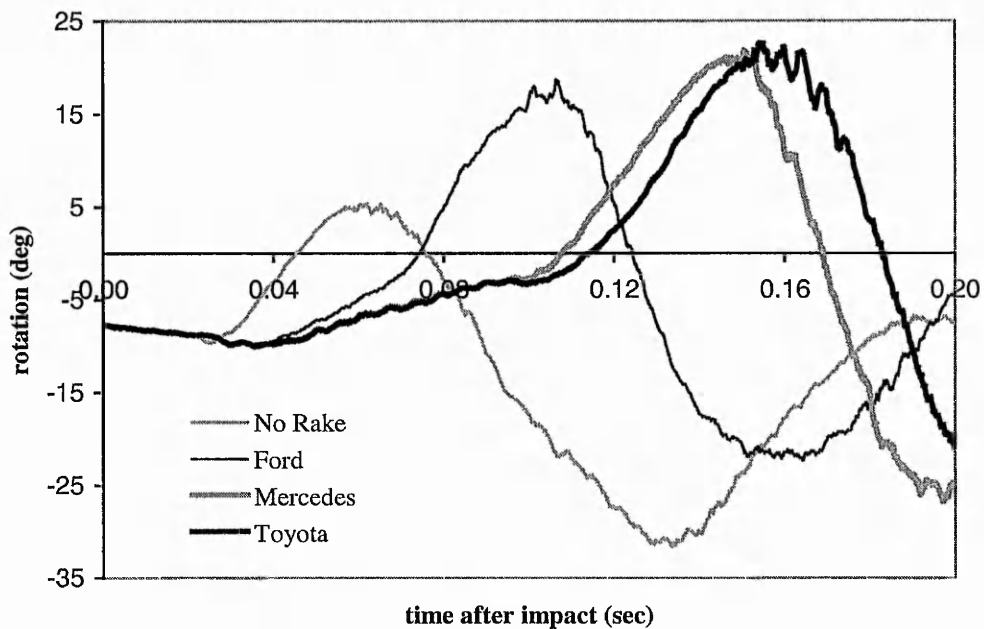


Figure 75 Relative rotation between head and C3 in the sagittal plane.

As expected, the introduction of a raking seat resulted in an increase of loading in the posterior located ligaments of the upper cervical spine. The interspinous ligament (Figure 76) and ligamentum flavum (Figure 77), both located between the atlas and the axis, recorded increases in loading due to the dynamic extension of the head-head restraint gap, with the first even going over the breaking zone for the Ford and Toyota seats. However, unlike the sagittal plane case, a steady increase of loading with a decrease of seat stiffness can not be established for these particular structures. Due to the steady axial rotational loading throughout the whiplash event, the position of the head and vertebrae at the time of loading transmission to the neck will be different between the tests. This, combined with the free movement of the model in 3-dimensional space, could explain the fluctuation in results.

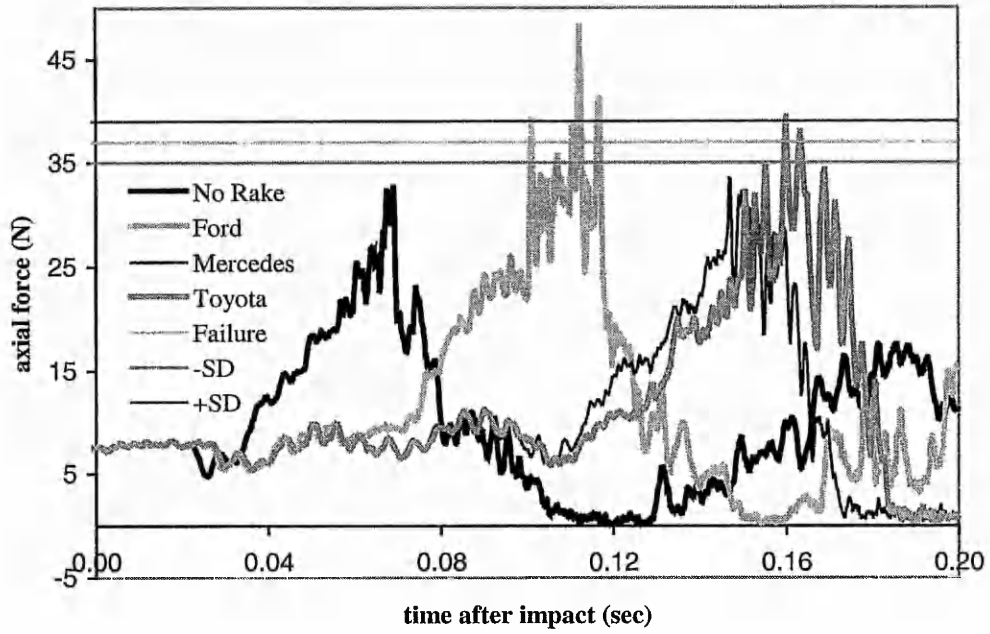


Figure 76 Force/time relationship of interspinous ligament (C1-C2).

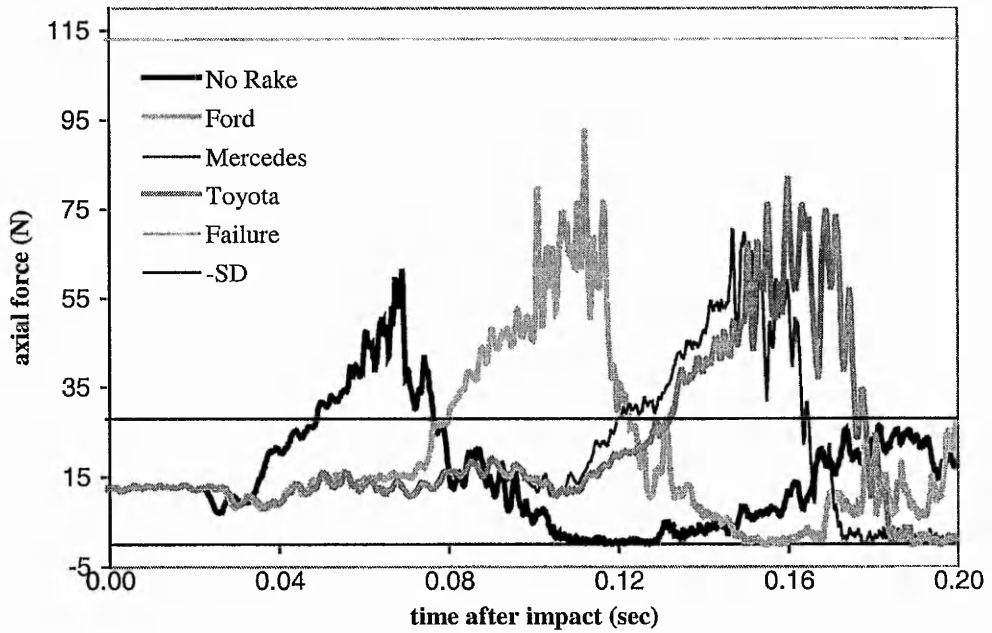


Figure 77 Force/time relationship of ligamentum flavum (C1-C2).

Similar fluctuation in results can be noted for the capsular ligaments of the C1-C2 intervertebral joints (Figure 78 and Figure 79). For both sides, the highest value of loading was recorded for the stiffest rake seat (Ford type) with the following two

seat types falling even below the non-raking seat results. As in the case of the posterior ligaments of the C1-C2 motion complex, it can be explained by the positions of the head and vertebrae relative to the whiplash loading direction, resulting in different kinematics of the head/neck complex due to inertia loading. Nevertheless, in the case of the right capsular ligament, the maximum value is dangerously approaching the breaking zone, suggesting more than likely injury of this structure due to the combination of axial rotation and lateral bending as a result of out of sagittal plane positioning of the head.

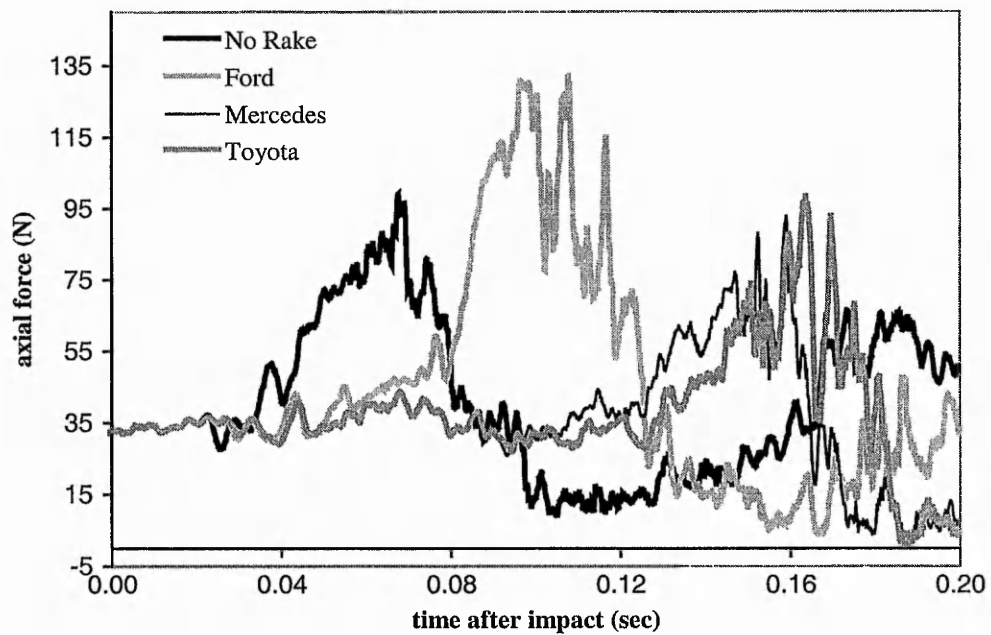


Figure 78 Force/time relationship of left capsular ligament (C1-C2).

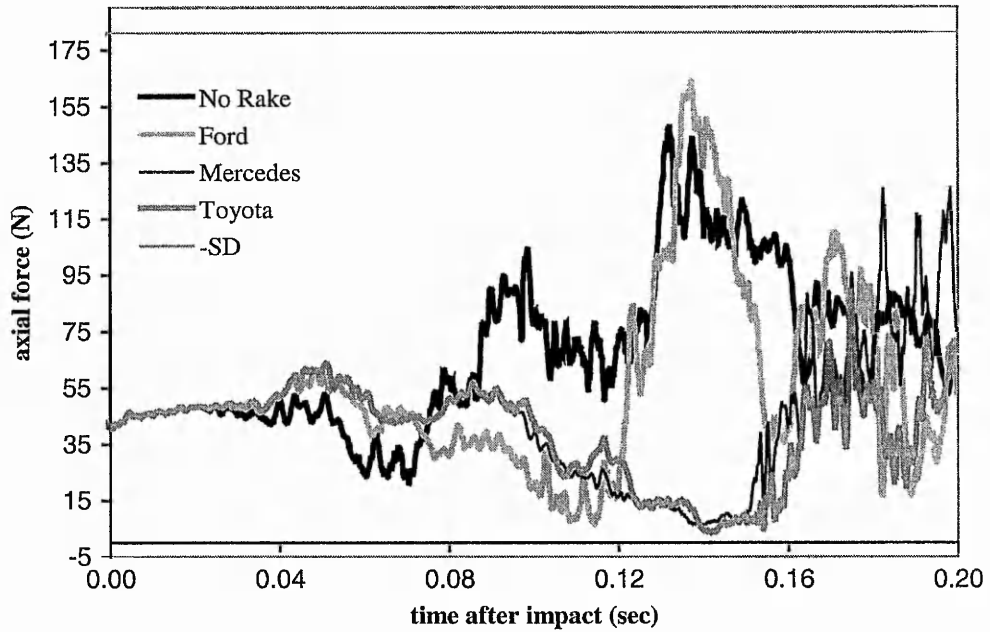


Figure 79 Force/time relationship of right capsular ligament (C1-C2).

In the case of the posterior atlanto – occipital membrane (Figure 80) a similar progressive trend as in the sagittal plane loading can be noted. The decrease of seat raking stiffness resulted in a steady increase in the recorded loading for this particular structure. Comparing each seat case separately to the same case from the sagittal plane scenario, it can be noted that the recorded loadings are lower for the vertical rotation cases. Nevertheless, they are approaching the breaking zone for the softest seat, indicating injury for this ligament.

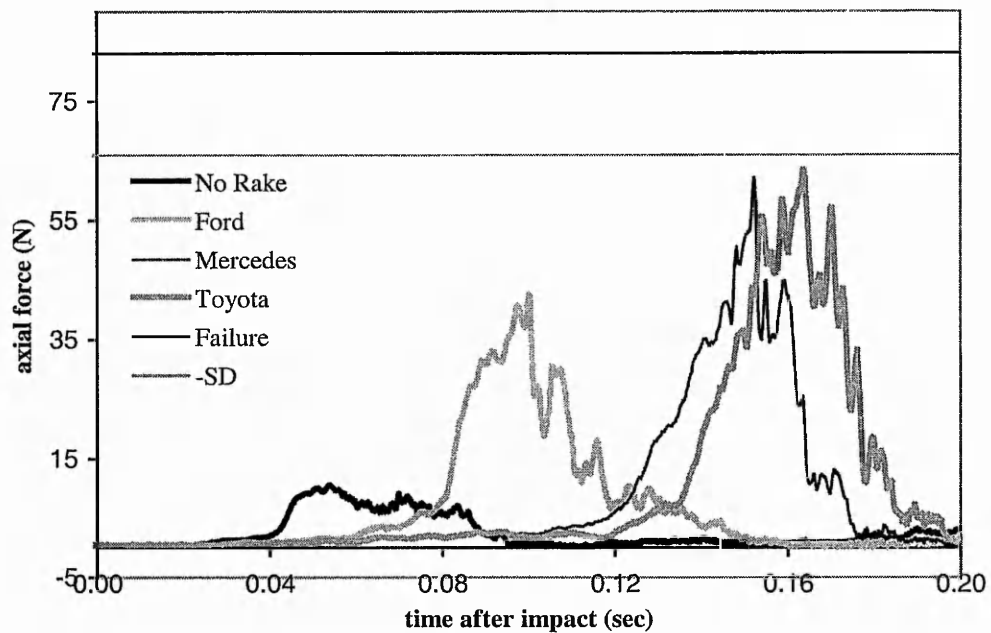


Figure 80 Force/time relationship of posterior atlanto – occipital membrane.

It has been suggested in a number of publications (Dvorak et al., 1987a, 1987b, 1988; Saldinger et al., 1990) that the alar ligament could be under the threat of injury during the whiplash scenario including axial rotation of the head. They showed the alar ligament as being the main structure controlling the rotation in the occipito- atlanto-axial complex (C0-C2). Moreover, they pointed out that when the head is rotated and additionally flexed, the alar ligaments are stretched the most, and are therefore, most vulnerable to injury. This combination of rotation and flexion, seldom induced physiologically, is characteristic to the whiplash scenario with the head initially rotated. They suggest that this kind of trauma could easily overstretch the alar ligament leaving the transverse ligament undamaged. The present study confirms these observations. The results from both alar ligaments (Figure 81 and Figure 82) show loading reaching the breaking zone in the case of the left alar ligament and even passing the lower recorded breaking force limit in the case of the test with the Mercedes seat. Notable fluctuations of the results can be explained once again by different positioning of the head and cervical vertebrae at the time of seat locking, being the beginning of the impact loading progression onto the occupant neck.

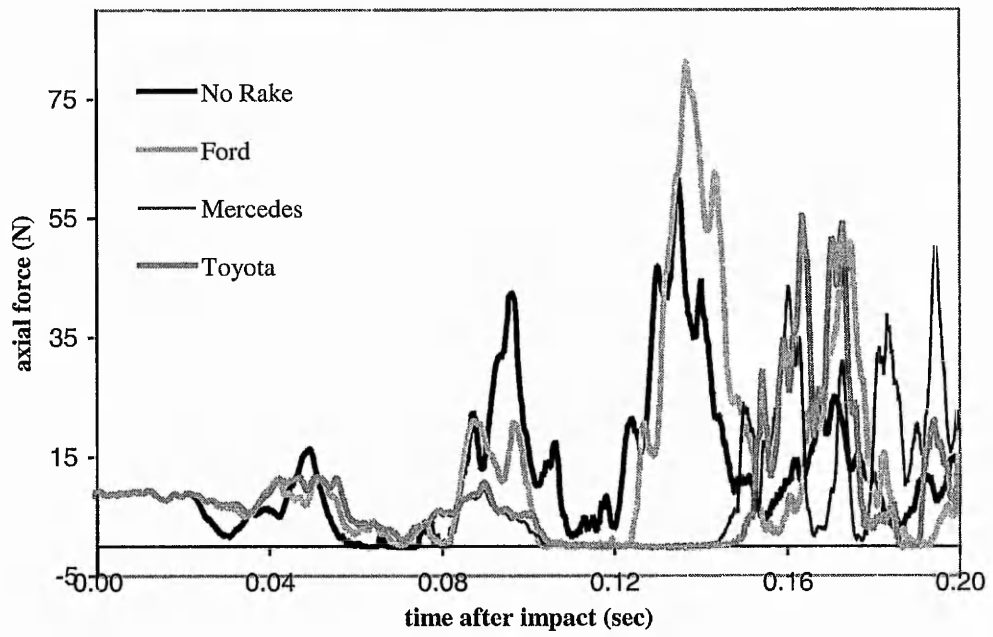


Figure 81 Force/time relationship of right alar ligament.

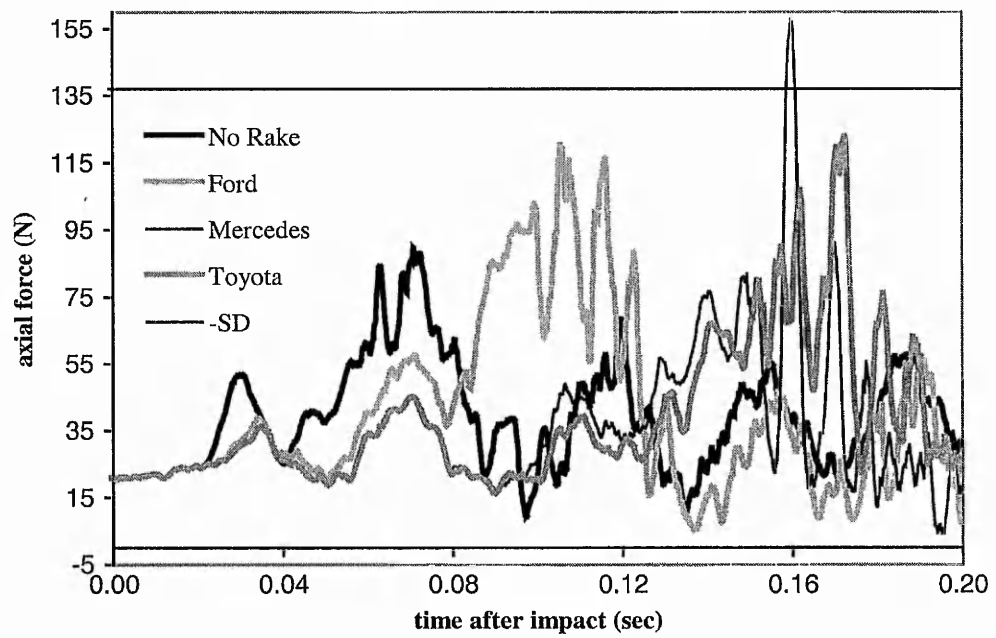


Figure 82 Force/time relationship of left alar ligament.

**CHAPTER 11**

**LOAD IMPULSE VARIATION IN WHIPLASH**

**ACCIDENT SITUATIONS WITH INITIAL**

**VERTICAL ROTATION OF THE HEAD.**

## **11.1 Introduction**

The newly proposed whiplash scenario with initial vertical rotation of the head has been successfully investigated in the two previous chapters (CHAPTER 9 and CHAPTER 10). Due to the use of the same model of the occupant as well as the same seating system and impact loading, the results could be directly compared to the similar case in the sagittal plane whiplash scenario. To fully explore this possibility, the study investigating the influence of the crash pulse in the whiplash accident situation (CHAPTER 8) has been repeated with the non-sagittal whiplash scenario. Therefore, for the characteristics of the raking seat (Mercedes type) used in the present study, please refer to CHAPTER 7, while detailed descriptions of the impact pulses can be found in CHAPTER 8.

## **11.2 Results**

In similar fashion to the sagittal plane scenario, the use of modified loading resulted in a higher raking angle of the seat (Figure 83) transferred into an earlier stage of the event than for the original loading. This alone will lead to higher injury risk through the creation of a wider dynamic gap between the head and the head restraint. However, it has been shown in CHAPTER 10 that this statement, even though true for the sagittal plane whiplash scenario, is not so obvious in the rotational whiplash scenario. As has been explained in the previous chapter (CHAPTER 10), due to the continuing rotation of the head applied throughout the impact loading, the position of the head and vertebrae will vary between the two impact pulses. Nevertheless, this is still a valid case, very likely to happen in a real life accident, and therefore worth investigating.

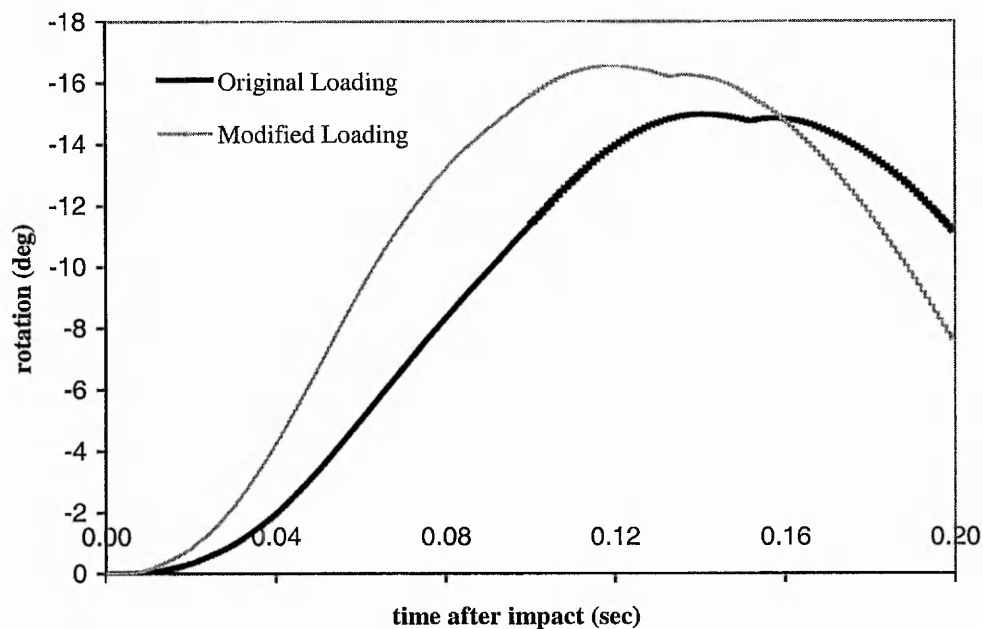


Figure 83 Raking of the seat back.

The use of a more severe crash impulse resulted in an actually lower flexion in the upper cervical spine (Figure 84). This is a different response from the one gained in the sagittal plane scenario under the same loading conditions, where the higher acceleration impulse leads to higher flexion in the occipito-atlanto-axial complex, thus indicating higher loading in the posterior located ligamentous structures. Therefore, once again it can be clearly seen that the sagittal plane flexion in the C0-C3 complex, despite being a simple indicator of whiplash injury severity in the sagittal plane scenario, does not work in this same manner for the scenario involving vertical rotation of the head.

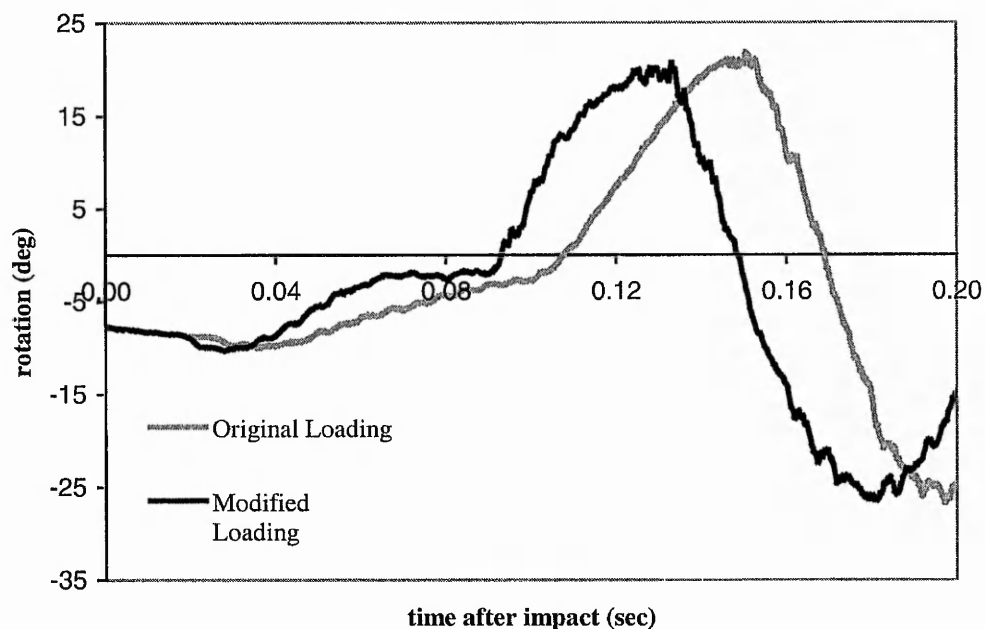


Figure 84 Relative rotation between head and C3 in sagittal plane.

However, the present model, due to its unique capabilities of recording loading in individual ligaments in real time, does not have to rely on such indicators as flexion angle to assess whiplash injury severity under different loading conditions and scenarios. Therefore, even with contradictory indicators as in the present study, when a raking seat indicates an increase of injury, even though flexion angle is actually lower, the detailed analysis of individual tissue structure will give an indisputable answer.

The following figures show the loading in the ligamentous structures located in the posterior aspect between the C1-C2 vertebrae. The interspinous ligament (Figure 85) has been elevated from the safe level of loading to a level over the breaking zone, giving clear indication of this structure being definitely injured during the increase of velocity ratio. At the same time, it can be seen that although the ligamentum flavum (Figure 86) was already in the breaking zone, the velocity ratio increase leads to an even higher deformation of this structure. This will lead statistically to a higher group of occupants being under the injury threat.

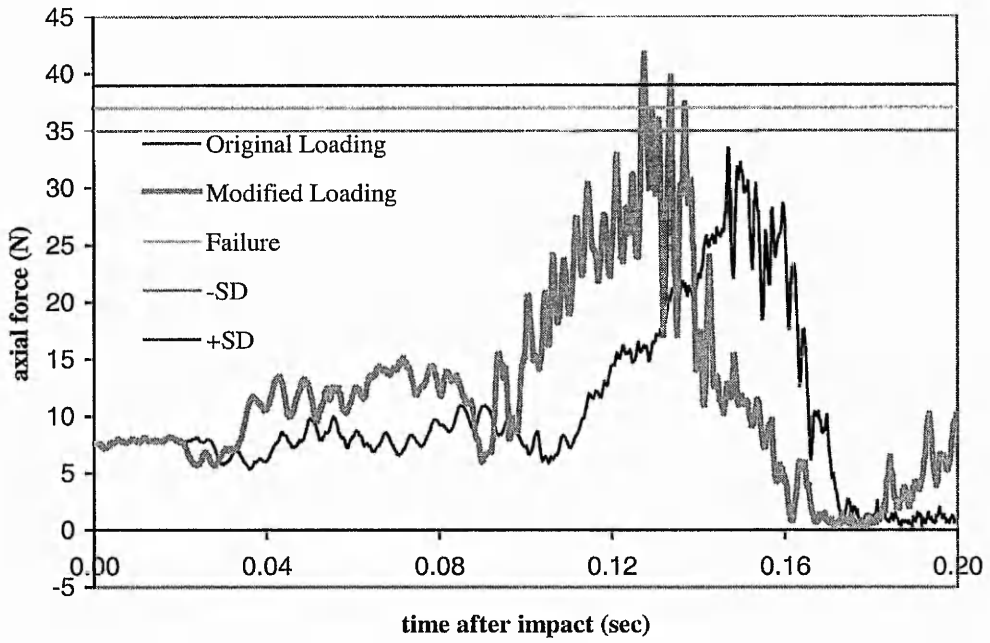


Figure 85 Force/time relationship of interspinous ligament (C1-C2).

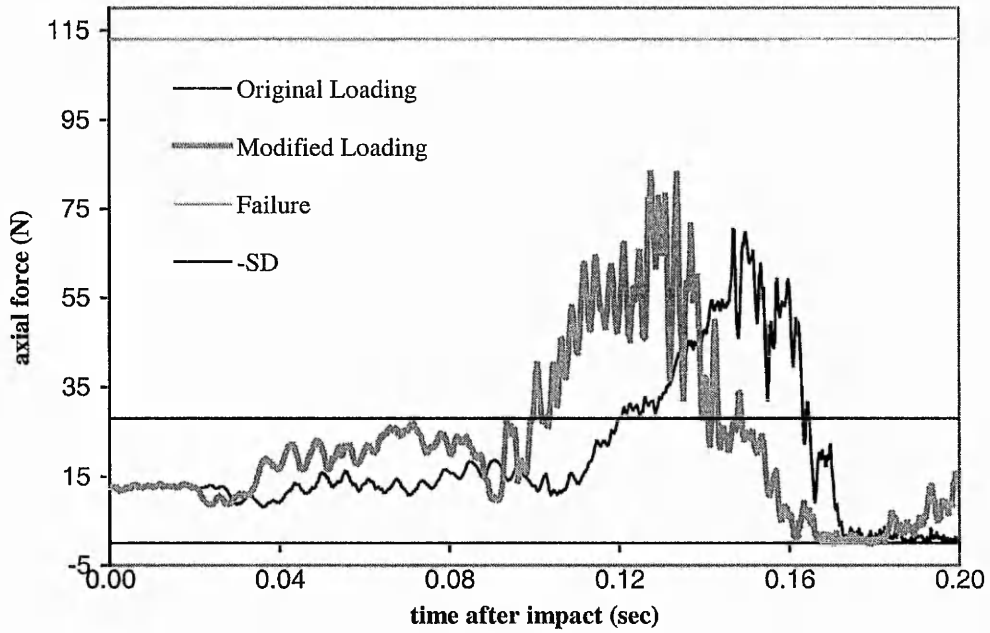


Figure 86 Force/time relationship of ligamentum flavum (C1-C2).

Furthermore, the capsular ligament loadings (Figure 87 and Figure 88) show that the new loading characteristic will also lead to higher stretching of these particular

ligaments. Even though they remain underneath the breaking loading, it indicates a possible injury zone if the crash pulse or relative velocity became higher.

These results prove the main injury zone due to axial rotation, firstly indicated in the experimental work by Goel (1990) and confirmed already in the previous two chapters, as being located between the atlas and the axis. At the same time they show an increase of injury risk when there is a higher velocity increase ratio, which could be a result of difference in stiffness or mass between the two colliding automobiles as suggested by Bostrom et al. (1997) and Koch et al. (1995).

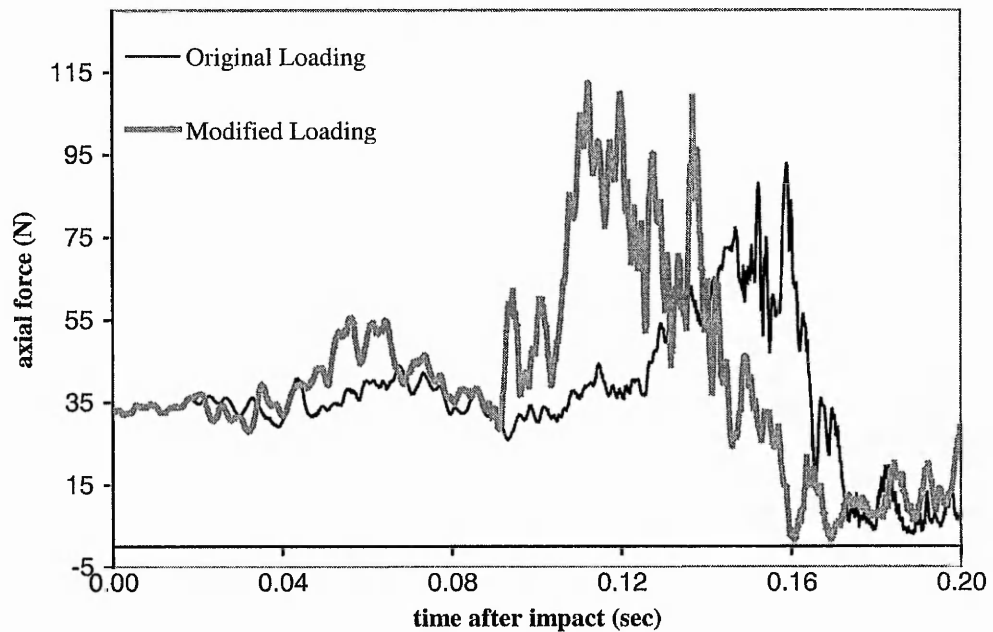


Figure 87 Force/time relationship of the left capsular ligament (C1-C2).

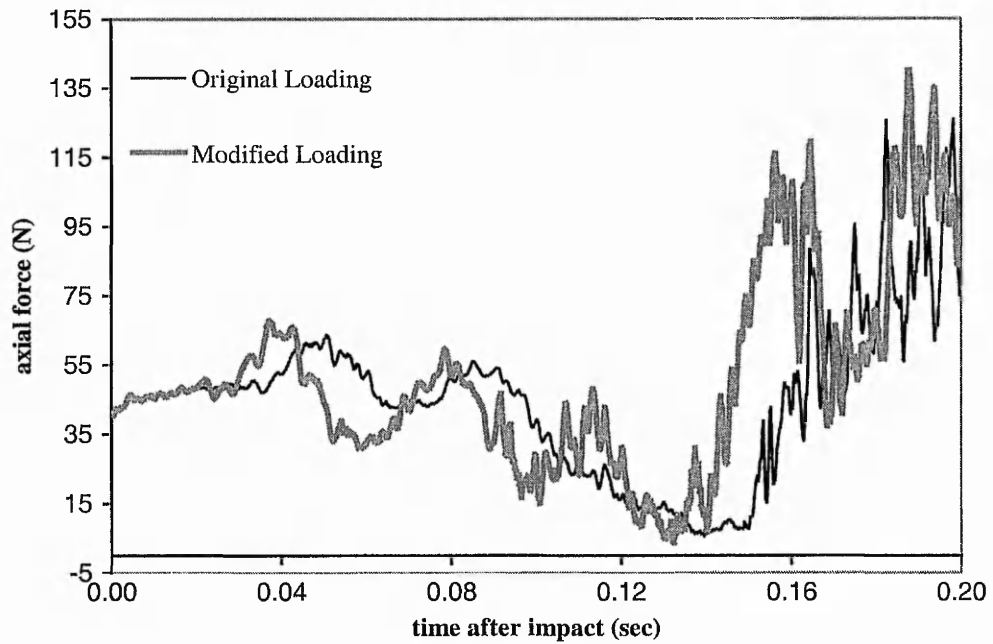


Figure 88 Force/time relationship of the right capsular ligament (C1-C2).

It has to be said that since there is no restriction in movement of the cervical spine structures, and possible different locations of the head and vertebrae due to the continued rotational loading of the head, there is no straightforward trend in injury level when dealing with the whiplash scenario that includes initial rotation. This can be clearly seen in the loading recorded for the alar ligament. While the higher impact impulse leads to doubled loading in the right alar ligament (Figure 89), the left portion of it (Figure 90) actually noted a decrease in the maximum force, nevertheless still remaining on the edge of the breaking zone. Furthermore, the posterior atlanto – occipital membrane (Figure 91) shows a decrease in loading for the higher impact pulse, suggesting a lower influence of it at this particular spinal level.

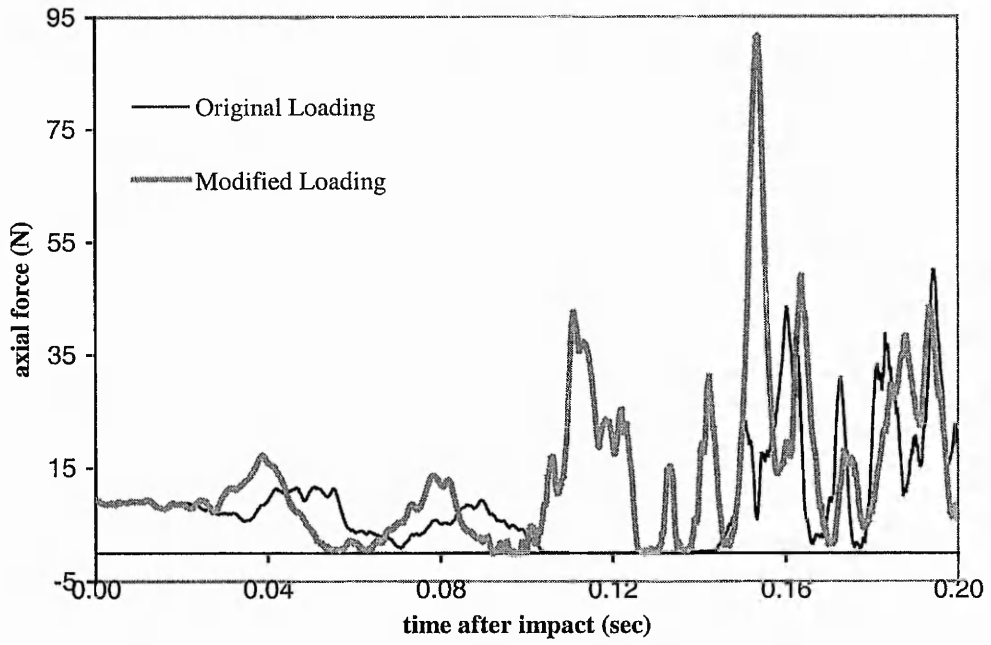


Figure 89 Force/time relationship of the right alar ligament.

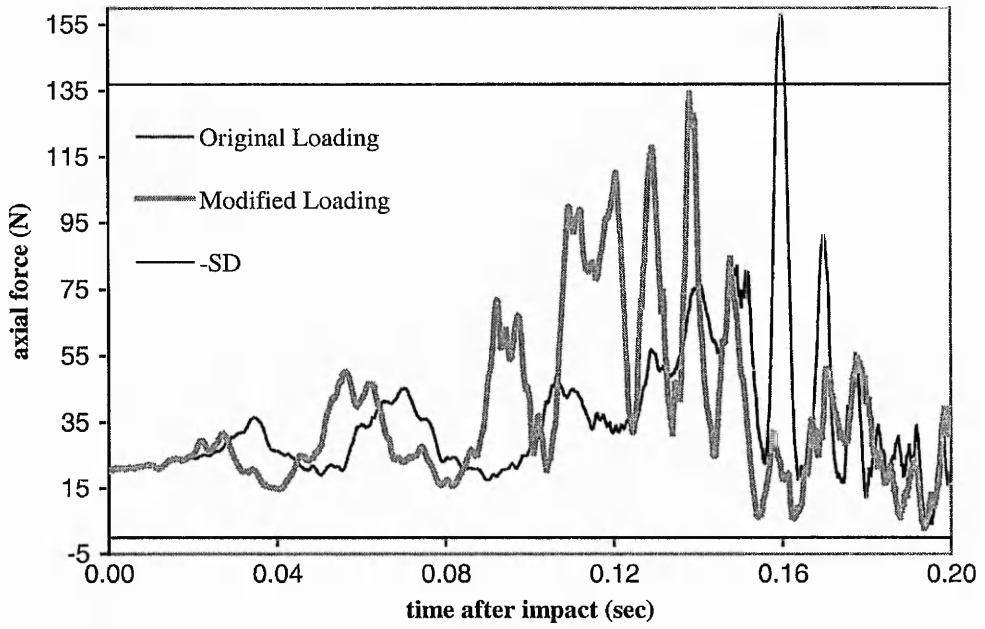


Figure 90 Force/time relationship of the left alar ligament.

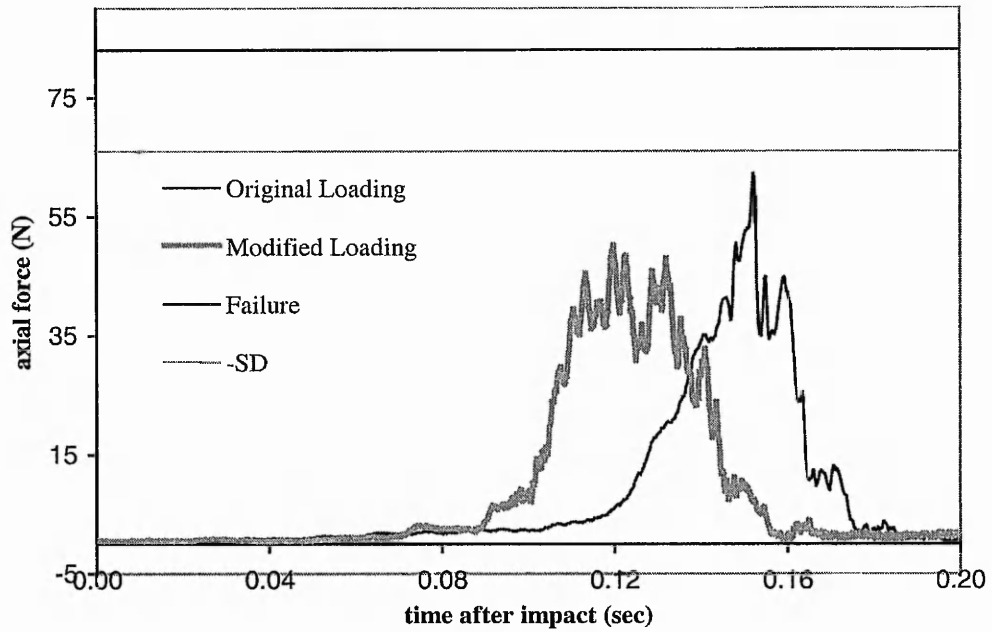


Figure 91 Force/time relationship of posterior atlanto – occipital membrane.

Although possibly seen as controversial, these mixed loading results from different ligaments actually are the best recommendation for use of the present model to study different whiplash scenarios. It can be clearly seen that, while for the sagittal plane scenario there was the possibility to establish injury trends based on the kinematics of the model, such as the flexion angle, this is not possible with the rotational scenario of whiplash. In this new scenario, the only way to establish injury risk is to monitor the real life deformation/loading of individual ligamentous structures, which is a unique capability of the present model.

**CHAPTER 12**

**CONCLUSION AND FURTHER WORK**

Throughout this project several FE models of the cervical spine were created, showing a logical progression which follows a clear path of research and development.

First of all, a 2.5 dimensional model was created to establish the feasibility of using FEA to investigate Whiplash accidents and injuries. Even though the geometry was very simplified and there was only a limited representation of soft tissue, the model showed promising results from the point of biofidelity when compared against volunteer data and it gave insight into ligamentous damage.

In the next step, a 3 dimensional model was created to overcome what were perceived as the main shortcomings of its predecessor. More accurate geometry was created with the intention of providing anatomically correct articulation of the contacts between the vertebrae as well as correct location of all the ligament anchorage points. Soft tissue representation was enhanced by including muscles and by implementing non-linear material properties. As a result of those changes, even better biofidelity was achieved and access was given to real-time loading data from more ligaments. This enabled a more comprehensive picture to be obtained of the ligamentous damage in the head/neck structure.

Up to this point all the models were self-contained and consisted of a head, a neck and a torso only; there was no mention of the fact that the torso is part of the larger body and that the body is located on a seat within a car. Acceleration loadings were applied to the torso directly rather than via the floor pan of a car, the car seat and the whole body of the car occupant. At that stage it was realised that the main impediment to full and successful whiplash modelling lay in the lack of occupant body/seat interaction. Therefore, in the next stage of the project, an attempt was made to extend the existing model to a full occupant body in a seating system.

The model created included the previously developed head-neck complex, now with capsular ligaments, joined onto a simplified FE model of the human body in a generic representation of a seating system. This model showed further improvement in head-neck biofidelity as a result of the inclusion of the whole body response and the stabilising role of the capsular ligaments. At the same time,

it was now possible to investigate an anti-whiplash device, showing the capabilities of the biomechanical modelling in the design field.

However, there was still room for improvement. Therefore, the final product of this research - the most advanced biomechanical FE model of cervical spine so far used to study whiplash - was created. First a new representation of the vertebrae and ligaments was included to give better interaction between those structures. Second, to achieve better kinematics, the head's inertia properties were reformulated based on experimental results. Lastly the simple FE model of the human body was replaced by an FE model of the Hybrid III dummy, which is the industry standard. These final changes resulted in the model achieving better biofidelity than all the previous models, and it can be characterised as very accurate from the point of view of ligamentous damage predictions.

The final model has been successfully used to confirm the mechanism of injury as hypertranslation, in full agreement with the latest experimental results. Not only is the model capable of replicating the kinematics of the human cervical spine but also, due to its unique capabilities, the model gives for the first time the possibility of investigating real time loading in individual ligaments.

The fact that the biomechanical model of the cervical spine was successfully grafted onto the body of the Hybrid III dummy model has created an original and powerful design tool since the combination could be immediately used by professional car safety designers. The combined model has so far been successfully used to analyse the influence of several different factors on whiplash injury severity, including the initial head – head restraint gap, the change in the gap due to raking of the seat under the dynamic load, and different loading conditions, confirming the experimental hypothesis. This would not be possible using just a self-contained cervical spine model, since the occupant body interaction is necessary to understand and explore the whiplash injury phenomenon fully.

Moreover, the model has been used to design an anti-whiplash device. In its proposed form, the device could be mounted in the base of a car seat, without expensive redesign of the seat itself. Due to the low cost of the design, unlike the

existing anti-whiplash seat designs, this device could be implemented not only in new car models, but also in updated versions of existing car models to help control whiplash injury on a wider scale.

The final model has also been used to investigate not only the sagittal plane whiplash scenario, but also the newly indicated scenario where at the time of impact the head is rotated to one side. The initial rotation of the head about a vertical axis leads to axial acceleration and lateral bending being included in the whiplash kinematics. The presented model is the first research tool capable of investigating this scenario, since other computational investigations, as well as experimental approaches, have concentrated on the sagittal plane whiplash scenario. The alar ligament, as well as the capsular ligaments of the C1-C2 level, have been shown as the main victims of this new scenario. Based on individual ligament loading, it has been shown that these two structures are under immediate threat of breaking as a result of initial vertical rotation of the head, confirming the recently published hypothesis.

It has to be mentioned that the same model has been used for both whiplash scenarios, making possible a direct comparison of the damage imposed by them on the human cervical spine. It makes the final model the most advanced, unique and versatile FE model to investigate whiplash injury created to date.

In the present form, the final model could be used by the motor industry to test the safety of existing car models as well as to develop new designs which would be "whiplash friendly". This trend of combining the biomechanical models of individual parts of the human body with dummy models seems to be the first step in developing a full biomechanical model of car occupants and, according to the motor industry, the aim is for biomechanical models to replace the existing dummy models eventually.

Even though the present model is the most advanced model available to study whiplash there are still several limitations to it. On the biomechanical modelling level, the main limitation is the simplified intervertebral disc model. In its present form, the model of the disc does represent quite well the kinematics of the human disc, but it is not possible to investigate the structural loading of the disc to predict

its failure. There is already a parallel PhD project in the Biomechanics Research Group at The Nottingham Trent University concentrating on a new material law for the intervertebral disc model in the FE solver LS-DYNA. Therefore it is hoped that once the work is concluded the new intervertebral disc model will be implemented into the cervical spine model, giving the present model the capability of predicting disc failure in addition to its existing ligament loading capabilities.

The other limitation on the biomechanical level is the representation of the musculature of the cervical spine. So far only selected structures are represented in the model and only passive action of them is modelled. Since the present model is looking into the event only till 0.2 s, the active response of muscles is not expected. However, to be used in the future in full scale crash analysis, the present model will have to include the active phase of muscle response, since the simulation will not end at 0.2 s. At the same time, the full representation of muscles present in the human cervical spine will guarantee a proper response, not only up to the head -head restraint time of impact but also during the rebound phase.

On a general scale, the simple representation of the seating system has to be highlighted as a main limitation of the present study. Attempts to acquire a model of a current production seat have been made during this project, but without success. Therefore it is proposed for future work to create a full model of a production seat and include it in the whiplash simulation. At the present moment, due to the simple representation of the seating system, only the events up to the head impact are analysed. The inclusion of a fully deformable model of the seat will complete the whiplash injury picture, giving the opportunity to analyse even the seat rebound phase. Once the seat model is created and tested, it could be used as a base for new whiplash safety device designs in conjunction with the Bio-Hybrid Dummy model created in this study.

## REFERENCES

Adams M.A., 1998, "Biomechanics of the Cervical Spine" in *Whiplash Injuries: Current Concepts in Prevention, Diagnosis, and Treatment of the Cervical Whiplash Syndrome*, edited by Gunzburg R., Szpalski M., Lippincott-Raven Publishers, Philadelphia

Adobe Systems Incorporated, 1997, *Adobe Photoshop 4.0*, [www.adobe.com](http://www.adobe.com)

Alker G. J., Young S. O., Leslie E. V., 1978, "High cervical spine and craniocervical junction injuries in fatal traffic accidents", *J. Trauma*, Vol. 19, pp. 768-771

Ansys, 1997, *Ansys 5.3*, [www.ansys.com](http://www.ansys.com)

Beier G., Schuck M., Schuller E., Spann W., 1980, "Determination of physical data of the head. I. Centre of gravity and moments of inertia of human heads." *Proc. of the IRCOBI Conference on the Biomechanics of Impacts*,

Benson B.R, Smith G.C., Kent R.W., 1996, "Effect of Seat Stiffness in Out-of-Position Occupant Response in rear-End Collisions", *Proc. of the 40<sup>th</sup> Stapp Car Crash Conference*,(962434)

Bostrom O., Svensson M.Y., Aldman B., Hansson H.A., Haland Y., Lovsund P., Seeman T., Suneson A., Saljo A., Ortengren T., 1996, "A New Neck Injury Criterion Candidate – Based on Injury Findings in the Cervical Spinal Ganglia After Experimental Neck Extension Trauma", *Proc. of the IRCOBI Conference on the Biomechanics of Impacts*, Dublin, Ireland, pp 123-136

Bostrom O., Krafft M., Aldman B., Eichberger A., Fredriksson R., Haland Y., Lovsund P., Steffan H., Svensson M., Tingvall C., 1997, "Prediction of Neck Injuries in Rear Impacts Based on Accident Data and Simulations", *Proc. of the IRCOBI Conference on the Biomechanics of Impacts*, Hannover, Germany, pp 251-264

Camacho D.L., Nightingale R.W., Robinette J.J., Vanguri S.K., Coates D.J., Myers B.S., 1997, "Experimental Flexibility Measurements for the Development of a computational Head-Neck Model Validated for Near-Vertex Head Impact", *Proc. of the 41<sup>st</sup> Stapp Car Crash Conference*, (973345), pp. 473-483

Camacho D.L., Nightingale R.W., Myers B.S., 1999, "Surface Friction in Near-Vertex Head and Neck Impact Increases Risk of Injury ", *J. Biomechanics*, Vol. 32, pp. 293-301

Croft A.C., 1997, "Biomechanics" in Whiplash Injuries – the Clinical Acceleration / Deceleration Syndrome, second edition, edited by Forman S.M., Croft A.C., J. B. Lippincott Comp., Philadelphia,

Crowe H.E., 1928, "Injuries to the cervical spine", *Presented at the Meeting of the Western Orthopedic Association*, San Francisco, USA

Dauvilliers F., Bendjellal F., Weiss M., Lavaste F., Tarriere C., 1994, "Development of a Finite Element Model of the Neck", *Proc. of the 38<sup>th</sup> Stapp Car Crash Conference*, (942210), pp. 77-91

Davidsson J., Svensson M.Y., Flogard A., Haland Y., Jakobsson L., Linder A., Lovsund P., Wiklund K., 1998a, "BioRID – A New Biofidelic Rear Impact Dummy", *Proc. of the IRCOBI Conference on the Biomechanics of Impacts*, Gothenburg, Sweden, pp 377-390

Davidsson J., Deutscher C., Hell W., Linder A., Lovsund P., Svensson M.Y., 1998b, "Human Volunteer Kinematics in Rear-End Sled Collisions", *Proc. of the IRCOBI Conference on the Biomechanics of Impacts*, Gothenburg, Sweden, pp 289-301

Davis D., Bohlman H.H., Walker A.E., Fisher R., Robinson R.A., 1971, "The pathological findings in fatal craniospinal injuries", *J. Neurosurg.*, Vol. 34 pp. 603-613

De Jager M., Sauren A., Thunnissen J., Wismans J., 1994, "A Three-Dimensional Head-Neck Model: Validation for Frontal and Lateral Impacts", *Proc. of the 38<sup>th</sup> Stapp Car Crash Conference*, (942211), pp. 93-109

De Jager M., Sauren A., Thunnissen J., Wismans J., 1996, "A Global and Detailed Mathematical Model for Head-Neck Dynamics", *Proc. of the 40<sup>th</sup> Stapp Car Crash Conference*, (962430), pp. 269-281

Deng Y.C., Goldsmith W., 1987, "Response of Human Head/ Neck/ Upper-Torso Replica to Dynamic Loading – II. Analytical/ Numerical Model", *J. Biomechanics*, Vol. 20 (5), pp. 487-497

Dr. Steffan Datentechnik Ges.m.b.H, 1996, CD-Crash Version 1.3, Ledergasse 34 Linz, Austria

Dvorak J., Panjabi M. M., 1987a, "Functional Anatomy of the Alar Ligaments", *Spine*. Vol. 12(2), pp. 183-189

Dvorak J., Hayek J., Zehnder R., 1987b, "CT – Functional Diagnostics of the Rotatory Instability of the Upper Cervical Spine. Part 2. An Evaluation on Healthy Adults and Patients with Suspected Instability", *Spine*. Vol. 12(8), pp. 726–731

Dvorak J., Schneider E., Salinger P., Rahn B., 1988, "Biomechanics of the Craniocervical Region: The Alar and Transverse Ligaments", *J. Orthopaedic Research Society*, Vol. 6, pp. 452-461

Eichberger A., Geigl B. C., Moser A., Fachbach B., Steffan H., Hell W., Langwieder K., 1996, "Comparison of Different Car Seats Regarding Head-Neck Kinematics of Volunteers During Rear End Impact", *Proc. of the IRCOBI Conference on the Biomechanics of Impacts*, Dublin, Ireland, pp 153-164

Eichberger A., Steffan H., Geigl B. C., Svensson M., Bostrom O., Leinzinger P.E., Darok M., 1998, "Evaluation of the Applicability of the Neck Injury Criterion (NIC) in Rear End Impact on the Basis of Human Subject Test ", *Proc. of the IRCOBI Conference on the Biomechanics of Impacts*, Gothenburg, Sweden, pp 321-333

Ewing C.L., Thomas D.J., 1973, "Torque versus Angular Displacement Response of Human Head to -G<sub>x</sub> Impact Acceleration." *Proc. of the 17<sup>th</sup> Stapp Car Crash Conference*, (730976),

- Forman S.M., Croft A.C., 1997, *Whiplash Injuries – the Clinical Acceleration / Deceleration Syndrome*, second edition, J. B. Lippincott Comp., Philadelphia
- Foster J.K., Kortge J.O., Wolanin M.J., 1977, “Hybrid III - A Biomechanically Based Crash Test Dummy”, *Proc. of the 21<sup>st</sup> Stapp Car Crash Conf.*, pp. 975-1013
- Geigl B. C., Steffan H., Leinzinger P., Roll, Muehlbauer M., Bauer G., 1994, “The Movement of Head and Cervical Spine During Rear End Impact”, *Proc. of the IRCOBI Conference on the Biomechanics of Impacts*, Lyon, France, pp 127-137
- Geigl B.C., Steffan H., Dippel C., Muser M. H., Walz F., Svensson M.Y., 1995, “Comparison of Head-Neck Kinematics during Rear End Impact between Standard Hybrid III, RID Neck, Volunteers and PMTO’s”, *Proc. of the IRCOBI Conference on the Biomechanics of Impacts*, Brunnen, Switzerland, pp 261-270
- Goel V.K., Winterbottom J.M., Schulte K.R., Chang H., Gilbertson L.G., Pudgil A.G., Gwon J.K., 1990, “Ligamentous Laxity Across C0-C1-C2 Complex Axial Torgue-Rotation Characteristics Until Failure”, *Spine*, Vol. 15(10), pp. 990-996
- Golinski W.Z., Gentle C.R., 1999, “Assessment of a Whiplash Prevention Device with a Dynamic Biomechanical Finite Element Model”, *Proc. of the 2<sup>nd</sup> European LS-DYNA Users Conference*, Gothenburg, Sweden
- Golinski W.Z., Gentle C.R., 2000, “Finite Element Modelling of Biomechanical Dummies – the Ultimate Tool in Anti-whiplash safety design?”, *Proc. of 6<sup>th</sup> International LS-DYNA Users Conference*, Dearborn, USA,
- Grauer J. N., Panjabi M. M., Cholewicki J., Nibu K., Dvorak J., 1997, “Whiplash Produces an S-Shaped Curvature of the Neck With Hyperextension at the Lower Levels”, *Spine*, Vol. 22, pp. 2489-2494
- Gray H., 1980, “Gray’s Anatomy”, 36<sup>th</sup> edition, Churchill Livingstone, Edinburgh,
- Griffith H. J., Olson P. N., Everson L. I., Winemiller M., 1995, “Hyperextension strain of “whiplash” to the cervical spine”, *Skeletal Radiology*, Vol. 24, pp. 263-266

Gunzburg R., Szpalski M., 1998, Whiplash Injuries: Current Concepts in Prevention, Diagnosis, and Treatment of the Cervical Whiplash Syndrome, Lippincott-Raven, Philadelphia, New York

Heitplatz F., Golinski W.Z., Gentle C.R., 1998, "Development of a Biomechanical FE-Model to Investigate "Whiplash".", *Proc. of the 1998 LS-DYNA Users Conference*, Williams Grand Prix Engineering, Grove, UK,

Insurance Institute for Highway Safety, 1999, "Status Report No5. Special issue: neck injuries in rear-end crashes", [www.hwysafety.org](http://www.hwysafety.org)

Kleinberger M., 1993, "Application of finite element techniques to the study of cervical spine mechanics", *Proc. of the 37<sup>th</sup> Stapp Car Crash Conference*, (933131), pp 261-272.

Koch M., Kullgren A., Lie A., Nygren A., Tingvall C., 1995, "Soft Tissue Injury of the Cervical Spine in Rear-end and Frontal Car Collisions", *Proc. of the IRCOBI Conference on the Biomechanics of Impacts*, Brunnen, Switzerland, pp 273-283

Krafft M., 1998, "A Comparison of Short- and Long- Term Consequences of AIS 1 Neck Injuries in Rear Impact", *Proc. of the IRCOBI Conference on the Biomechanics of Impacts*, Gothenburg, Sweden, pp 235-248

Kullmer G., Richard H.A., Weiser J., 1997, "Finite-element-analysis on the basis of computed tomography data", *Advances in Computational Engineering Science*, edited by Alturi S.N., Yagawa G., Tech. Science Press, Georgia, USA

Lin H. S. Liu Y. K. Adams K. H., 1978, "Mechanical Response of the Lumbar Intervertebral Joint under Physiological (Complex) Loading", *J of Bone And Joint Surgery*, Vol. 60(1), pp. 41-55

Liu Y.K, Murray J.D., 1966, "A theoretical study of the effect of impulse on the human torso", *Proc. of A.S.M.E. Symposium on Biomechanics*, pp. 167-186

LSTC, 1994, "LS-DYNA Keyword Examples Manual"

LSTC, 1997, LS-Dyna 940 PC Version, [www.lstc.com](http://www.lstc.com)

LSTC, 1999, LS-Dyna 940 Unix Version, [www.lstc.com](http://www.lstc.com)

Matsushita T., Sato T.B., Hirabayashi K., Fujimura S., Asazuma T., Takatori T., 1994, "X-Ray Study of the Human Neck Motion Due to Head Inertia Loading", *Proc. of the 38<sup>th</sup> Stapp Car Crash Conference*, 942208, pp 55-64.

McKenzie J.A., Williams J.F., 1971, "The Dynamic Behaviour of the Head and Cervical Spine During Whiplash", *J. Biomechanics*, Vol. 4, pp. 477-490

McNab I., McCulloch J., 1990, *Backache*, 2<sup>nd</sup> ed., Williams and Wilkins, Baltimore

Merrill T., Goldsmith W., Deng Y.C., 1984, "Three- Dimensional Response of a Lumped Parametric Head-Neck Model Due to Impact and Impulsive Loading", *J. Biomechanics*, Vol. 17(2), pp. 81-95

Meyer S., Weber M., Castro W., Schilgen M., Peuker C., 1998, "The Minimal Collision Velocity for Whiplash" in *Whiplash Injuries: Current Concepts in Prevention, Diagnosis, and Treatment of the Cervical Whiplash Syndrome*, edited by Gunzburg R., Szpalski M., Lippincott-Raven Publishers, Philadelphia

Muenker M., Langwieder K., Chen, Hell W., 1994, "HWS Beschleunigungsverletzungen, VdS ( Institution of German Car Insurers )", Munich

Myklebust J. B., Pintar F., Yoganadan N., Cusick F., Maiman D., Mayers T. J., Sances A., 1988, "Tensile Strength of Spinal Ligaments", *Spine*, Vol. 13, pp. 526-531

National Library of Medicine, 1994,

[http://www.nlm.nih.gov/research/visible/visible\\_human.html](http://www.nlm.nih.gov/research/visible/visible_human.html)

Nightingale R.W., Camacho D.L., Armstrong A.J., Robinette J.J., Myers B.S., 2000, "Inertial Properties and Loading Rates Affect Buckling Modes and Injury Mechanism in the Cervical Spine", *J. Biomechanics* , Vol. 33, pp. 191-197

Nitsche S., Krabbel G., Appel H., Haug E., 1996, "Validation of a Finite-Element-Model of the Human Neck", *Proc. of the IRCOBI Conference on the Biomechanics of Impacts*, Dublin, Ireland, pp 107-122

- Olsson I., Bunketorp O., Carlsson G., Gustafsson C., Planath I., Norin H., Ysander L., 1990, "An In-depth Study of Neck Injuries in Rear-end Collisions", *Proc. of the IRCOBI Conference on the Biomechanics of Impacts*, Bron, Lyon, France, pp 269-282
- Ono K., Kaneoka K., Wittek A., Kajzer J., 1997a, "Cervical Injury Mechanism Based on the Analysis of Human Cervical Vertebral Motion and Head-Neck-Torso Kinematics During Low Speed Rear Impacts", *Proc. of the 41<sup>st</sup> Stapp Car Crash Conference*, 973340, pp 339-356.
- Ono K., Kaneoka K., 1997b, "Motion Analysis of Human Cervical Vertebrae During Low Speed Rear Impact by the Simulated Sled ", *Proc. of the IRCOBI Conference on the Biomechanics of Impacts*, Hannover, Germany, pp 223-237
- Ono K., Kaneoka K., Inami S., 1998, "Influence of Seat Properties on Human Cervical Vertebral Motion and Head/Neck/Torso Kinematics During Rear-end Impacts", *Proc. of the IRCOBI Conference on the Biomechanics of Impacts*, Gothenburg, Sweden, pp 303-318
- Ortengren T., Hansson H.A., Lovsund P., Svensson M.Y., Suneson A., Saljo A., 1996, "Membrane Leakage in Spinal Ganglia Nerve Cells Induced by Experimental Whiplash Extension Motion: A Study in Pigs ", *J. Neurotrauma*, Vol. 13(3)
- Panjabi M.M., Dvorak J., Duranceau J., Yamamoto I., Gerber M., Rauschnig W., Bueff U., 1988, "Three-Dimensional Movements of the Upper Cervical Spine", *Spine*, Vol. 13(7), pp. 726-730
- Panjabi M.M., Oxland T.R., Parks E.H., 1991a, "Quantative Anatomy of Cervical Spine Ligaments. Part I. Upper Cervical Spine." *Journal of Spinal Disorders*, Vol 4, pp. 270-276.
- Panjabi M.M., Oxland T.R., Parks E.H., 1991b, "Quantative Anatomy of Cervical Spine Ligaments. Part II. Middle and Lower Cervical Spine." *Journal of Spinal Disorders*, Vol 4, pp. 277-285.

Panjabi M.M., Cholewicki J., Nibu K., Babat L.B., Dvorak J., 1998a, "Simulation of Whiplash Trauma Using Whole Cervical Spine Specimens", *Spine*, Vol. 23(1), pp. 17-24

Panjabi M.M., Cholewicki J., Nibu K., Grauer J., Vahldiek M., 1998b, "Capsular Ligament Stretches During In Vitro Whiplash Simulations", *Journal of Spinal Disorders*, Vol. 11(3), pp. 227-232

Panjabi M.M., Cholewicki J., Nibu K., Grauer J.N., Babat L.B., Dvorak J., 1998c, "Mechanism of Whiplash injury", *Clinical Biomechanics*, Vol. 13, pp. 239-249

Penning L., 1992a, "Acceleration injury of the cervical spine by hypertranslation of the head. Part I. Effect of normal translation of the head on cervical spine motion: a radiological study". *European Spine Journal*, Vol. 1, pp. 7-12

Penning L., 1992b, "Acceleration injury of the cervical spine by hypertranslation of the head. Part II. Effect of hypertranslation of the head on cervical spine motion: discussion of literature data". *European Spine Journal*, Vol. 1, pp. 13-19

Penning L., 1994, "Hypertranslation of the head backwards: part of the mechanism of cervical whiplash injury". *Orthopaede*, Vol. 23, pp. 268-274.

Przybylski G.J., Patel P.R., Carlin G.J., Woo S.L-Y., 1998, "Quantitative Anthropometry of the Subatlantal Cervical Longitudinal Ligaments.", *Spine*, Vol 23, pp. 893-898.

PTC, 1997, *Pro/Engineer 18*, [www.ptc.com](http://www.ptc.com)

Saito T., Yamamuro T., Shikata J., Oka M., Tsutsumi S., 1991, "Analysis and Prevention of Spinal Column Deformity Following Cervical Laminectomy, Pathogenetic Analysis of Post Laminectomy Deformities", *Spine*, Vol. 24, pp. 95-107

Saldinger P., Dvorak J., Rahn B.A., Perren S.M., 1990, "Histology of the Alar and Transverse Ligaments", *Spine*, Vol. 15(4), pp. 257-261

Severy P.M., Brink H.M., Baird J.D., 1968, Backrest and head restraint design for rear-end collision protection., *Presented at the Automobile Engineering Congress*, SAE 680079.

Shea M., Edwards W.T., White A.A., Hayes W.C., 1991, "Variations of the Stiffness and Strength Along the Human Cervical Spine", *J. Biomechanics* , Vol. 24(2), pp. 95-107.

Skovron M.L., 1998, "Epidemiology of Whiplash" in Whiplash Injuries: Current Concepts in Prevention, Diagnosis, and Treatment of the Cervical Whiplash Syndrome ,edited by Gunzburg R., Szpalski M., Lippincott-Raven Publishers, Philadelphia

Svensson M.Y., Lovsund P., 1992, "A Dummy for Rear – End Collisions – Development and Validation of a New Dummy – Neck", *Proc. of the IRCOBI Conference on the Biomechanics of Impacts*, Verona, Italy, pp 299-310

Svensson M.Y., Aldman B., Lovsund P., Hansson H.A., Seeman T., Suneson A., Ortengren T., 1993, "Pressure Effect in the Spinal Canal During Whiplash Extension Motion – A Possible Cause of Injury to the Cervical Spinal Ganglia ", *Proc. of the IRCOBI Conference on the Biomechanics of Impacts*, Eindhoven, The Netherlands, pp 189-200

Thunnissen J.G.M., Ratingen van M.R., Beusenbergh M.C., Janssen E.G., 1996, "A Dummy Neck for Low Severity Impacts", *Proc. Int. Conf on Enhanced Safety of Vehicles*, (96-S10-O-12)

Unterharnscheidt F., Sances A., Thomas D. J., Ewing C. L., Lanson S. J., 1986, "Pathological and neuropathological findings in rehsus monkeys subjected to -Gx and +Gx indirect impact acceleration", *Proc. of the Mechanisms of Head and Spine Trauma*, Goshen New York, pp 565-665.

Van der Horst M.J., Thunnissen J., Happee R., Van Haaster R.M.H.P., Wismans J.S.H.M, 1997, "The Influence of Muscle Activity on Head-Neck Response During Impact", *Proc. of the 41<sup>st</sup> Stapp Car Crash Conference*, (973346), pp. 487-507

VdS (Institution of German Car Insurers), 1994, "Vehicle Safety 90: Analysis of car Accidents", Munich,

Viewpoint Datashop, 1996, *Library CD-ROM 4.0*, [www.viewpoint.com](http://www.viewpoint.com)

Wheeler J.B., Smith T.A., Siegmund G.P., Brault J.R., King D.J., 1998, "Validation of the Neck Injury Criterion (NIC) Using Kinematic and Clinical Results from Human Subjects in Rear-End Collisions", *Proc. of the IRCOBI Conference on the Biomechanics of Impacts*, Gothenburg, Sweden, pp 335-348

White A. A., Panjabi M. M., 1990, "Clinical Biomechanics of the Spine", second edition, J. B. Lippincott Comp., Philadelphia, p 231

Wismans J., Van Oorschot E., Woltring H.J., 1986, "Omni-Directional Human Head-Neck Response", *Proc. of the 30<sup>th</sup> Stapp Car Crash Conference*, (861893)

Wismans J., Philipps M., Van Oorschot E., Kallieris D., Mattern R., 1987, "Comparison of Human Volunteer and Cadaver Head-Neck Response in Frontal Flexion", *Proc. of the 31<sup>st</sup> Stapp Car Crash Conference*, (872194)

Worth D. R., 1985, "Cervical Spine Kinematics", PhD Thesis, Flinders University of South Australia

Yamada H., 1970, "Strength of Biological Materials", The Williams & Wilkins Comp., Baltimore, p 93-95

Yang K.H., Zhu F., Luan F., Zhao L., Begeman P.C., 1998, "Development of a Finite Element Model of the Human Neck", *Proc. of the 42<sup>nd</sup> Stapp Car Crash Conference*, (983157), pp. 195-205

Yoganandan N., Pintar F., Kumaresan S., Elhagediab A., 1998, "Biomechanical Assessment of Human Cervical Spine Ligaments.", *Proc. of the 42<sup>nd</sup> Stapp Car Crash Conference*, (983159),

# **APPENDIX A**

## **Guidelines for Car Seat Design Based on FE Analysis of Whiplash Injuries**

(copy of the paper)

# GUIDELINES FOR CAR SEAT DESIGN BASED ON FE ANALYSIS OF WHIPLASH INJURIES

**F. Heitplatz, W. Z. Golinski and C. R. Gentle**

Department of Mechanical and Manufacturing Engineering  
The Nottingham Trent University, UK

## ABSTRACT

A 3 Dimensional FEA model of the human head-neck-torso motion complex has been developed in order to investigate the mechanism of injury in so called "whiplash" accident situations. The model was loaded over a range of moderate crash conditions similar to those found in volunteer experiments. After evaluation and validation of the model against these experimental results, the range of conditions was extended to consider higher impact speeds and larger initial gaps between the head and the head restraint. The results show an S-shape deformation of the cervical spine during the initial parts of a rear-end impact, leading to flexion of the upper spine and extension of the lower spine. Particular attention was paid to the strain/time relation of the alar ligament in order to assess the injury risk and further investigate the hypertension hypothesis. It was found that the strains in the alar ligament increase exponentially with impact speed and initial gap, reaching traumatic levels before the head hits the restraint if the initial gap is larger than 80 mm. On the basis of the results, a clear recommendation may be made for future designs of safer car seat head restraints.

## INTRODUCTION

Cervical "whiplash" is the most common injury sustained in car accidents. In 93.5% of all rear end collisions involving personal injuries, at least one of the passengers claimed a neck injury, even though 70.4% of these accidents occur with speed differences smaller than 15 kph (Institution of German car insurers, 1994). Other injuries are comparatively rare (Muenker et al., 1994) and therefore the incidence of whiplash injuries is significant from both the economical and the medical point of view. The Mechanism of Injury (MoI) is not certain but it is generally considered to involve hyperextension. The inertia of the head tends to maintain it in its original position while the remainder of the body is accelerated forward by the seat, but the forward pull applied through the neck to the base of the skull produces a moment about the head's centre of gravity which results in backwards rotation of the head; this causes excessive extension of the cervical spine (White and Panjabi, 1992). Despite the common occurrence of the injury little is known about the exact cause of patients' complaints. Various attempts have been made to quantify whiplash by means of radiology and, although none of these has proven to be conclusive, it can be stated that little or no bony damage is sustained, whereas ligamentous injury is common (Griffith et al., 1990).

More recently a different MoI has been proposed. Based on a review of the literature, Penning (1994) has developed the theory that in whiplash the primary MoI is not hyperflexion but hypertranslation of the head backwards. The head's inertia is taken to lead to a situation of high shear at the top of the neck, causing over-stretching of not only the ligaments but also the joint capsule between vertebrae. The familiar indications of whiplash injury, chronic disturbance of posture and equilibrium, are then explained by chronic ligamentous instability of the upper cervical spine. The theory is supported through experimental findings by Unterharnscheidt et al. (1986) who subjected rhesus monkeys with fixed trunk and free head to deadly positive and negative accelerations. Autopsy revealed that for both positive and negative acceleration a dislocation of the atlas with complete destruction of the transverse and alar ligament as well as the spinal cord was present. It was concluded from pictures of the experiments that the injury already occurred before the translation of the head was completed. Animal experiments are not fully comparable with the *in situ* situations found in humans but, due to the comparable anatomy of the upper cervical region of the rhesus monkey, a similar conclusion may well prove to be valid. Experiments like the one Unterharnscheidt describes are certainly not repeatable with humans. However, experiments with volunteers have been undertaken by Geigl et al. (1994), using low speed differences. No injuries have been reported, but the translation effect can clearly be seen on high-speed video film. Geigl conducted 37 experiments with volunteers and six with post mortal test objects (PMTO's) on a sled construction. For the volunteers the maximum impact speed was limited to 10.5 kph and the maximum deceleration recorded was 40 m/s<sup>2</sup>. With regard to the rotation of the head, the following characteristic movement was found for all tests; independent of the initial seating position, no head rotation could be seen during the first 60 to 100 ms following impact. Only after this period does the head start to rotate slowly backward at a time when the shoulders are already reflected forward.

To summarise these findings it seems that the MoI of whiplash cannot be fully explained as a hyperextension trauma and that a possible link between translation of the head, during the initial stages of impact, and strains in the ligaments situated in the C0-C2 complex exists. Therefore a close look into the biomechanics of these ligaments is necessary. The most extensive *in vitro* investigation into this complex is reported by Dvorak et al. (1988). Investigating the biomechanics of the craniocervical region, they suggest that the role of the alar ligaments, with respect to the stability of the C0-C2 joint and the implications for possible injury mechanisms during whiplash accidents, may have been long underestimated, especially when the transverse ligament remains intact.

It is the aim of this study to establish the validity of these findings using FEA, having first corroborated numerical and experimental results. A 3-Dimensional FEA model of the human head, neck and torso has been developed with a special focus being given to the C0-C2 complex, including the spinal ligaments. A series of simulated collisions has been undertaken, using variations in impact speed and head restraint configurations, to simulate the displacements experienced during rear end impacts, investigating the strain/time behaviour of the alar ligaments.

## **METHOD**

### **Model Geometry**

The presented study investigates posterior impact for an adult, sitting in a normal seating position. Symmetry conditions are assumed along the sagittal plane and, in order to reduce calculation times, the skull, the vertebra bodies, the nuchal ligament, the discs and the

torso are modelled as linear elastic shells with appropriate wall thickness. Particular attention is given to the vertebral facet joints as their shape is of importance for the motion characteristic of the spine. Therefore they are modelled as 3-D solids and sliding contacts are established between the interacting surfaces (see Figure 1b).

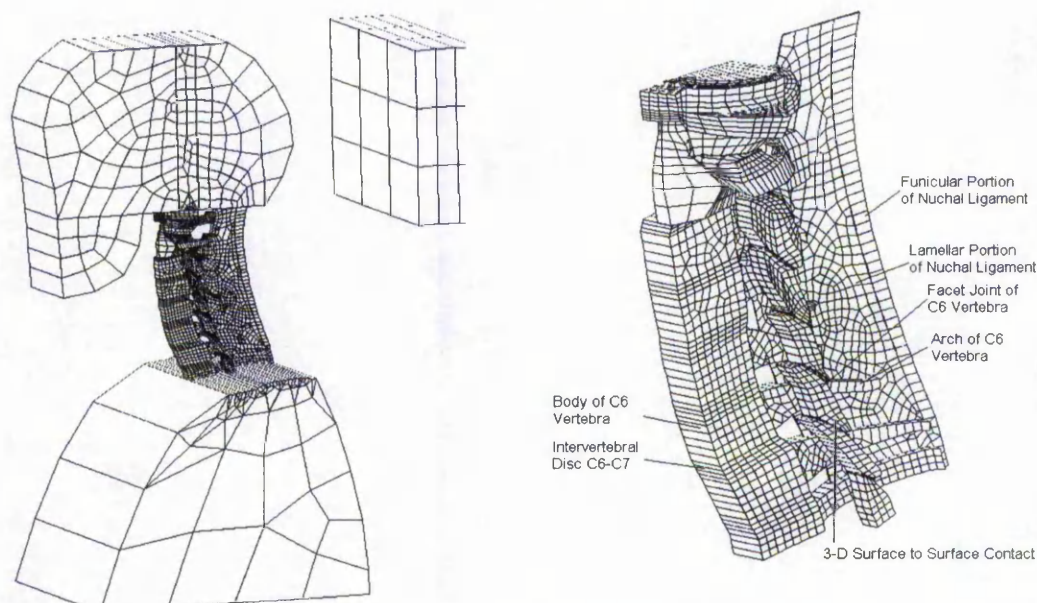


Figure 1a: ISO-View of the FEA Model. Figure 1b: ISO-View of the C0-T1 part of the FEA Model

Topological information relating to the size and shape of the skull and the human cervical vertebrae was extracted from full colour pictures obtained by the Visible Human Project (VHP) (National Library of Medicine, 1994). A parametric CAD model was created by interpreting the images of the male dataset. The topology was then simplified to accommodate meshing of the structure, with a mixed mesh keeping the number of degrees of freedom (DOF) as small as possible. Details of the model are given in Table 1. The main element types are 4-node shells and 8-node bricks. Special attention was given to the C0-C2 complex where a full 3-D topology was recreated. The alar and transverse ligaments were modelled as 3D solid structures (see Figure 2). The head restraint was modelled as a solid block with contact elements generated wherever it touched the posterior part of the skull (see Figure 1a). An algorithm was developed to modify easily the initial gap between the skull and the head restraint.

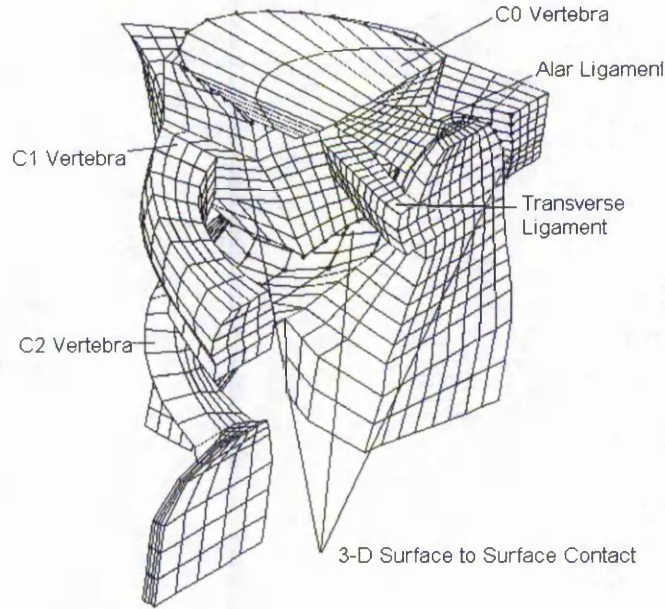


Figure 2: The C0-C2 Motion complex with ligamentous structure

| <i>Structure</i>                         | <i>Type of element</i>         | <i>Nr. of elements</i> |
|--|--------------------------------|------------------------|
| <i>Skull</i>                             | Elastic shell                  | 177                    |
| <i>Bony structure of C0-C2 complex</i>   | 3-D structural solid           | 1740                   |
| <i>Vertebrae C3-T1</i>                   | Elastic shell                  | 517                    |
| <i>Facet joints</i>                      | 3-D structural solid           | 363                    |
| <i>Discs</i>                             | Elastic shell                  | 176                    |
| <i>Alar ligament</i>                     | 3-D solid                      | 60                     |
| <i>Transverse ligament</i>               | 3-D solid                      | 66                     |
| <i>Nuchal ligament-Lamellar Portion</i>  | Elastic shell                  | 436                    |
|  | Gap                            | 16                     |
| <i>Nuchal ligament-Funicular Portion</i> | Elastic shell                  | 51                     |
| <i>Contact</i>                           | 3-D surface to surface contact | 2923                   |
| <i>Torso</i>                             | Elastic shell                  | 75                     |
| <i>Head restraint</i>                    | 3-D structural solid           | 27                     |
| <b>Total number of elements</b>          |                                | <b>6627</b>            |
| <b>Total number of nodes</b>             |                                | <b>5336</b>            |
| <b>Total number of DOF</b>               |                                | <b>12242</b>           |

Table 1: Summary of the FE Model Data

## Material Properties

All materials in the present investigation were defined as having linear elastic properties. The bony structures are seen as stiff compared to the spinal soft tissue. Material properties for the disc have been applied as found in the literature (Lin et al., 1978). The role of the nuchal ligament for the biomechanics of the neck region is generally unclear and no material properties could be found in the literature. Therefore their strength was estimated from data for the supraspinous ligament (Myklebust et al., 1988) of the lower spine. The topology of the transverse and alar ligaments and their ultimate strength has been previously reported by Dvorak et al. (1987 and 1988) and from these results a Young's modulus was calculated for both ligaments. Visual interpretation of the experimental video results reported by Geigl et al. (1996, CD-Crash Ver. 1.3) show a small deformation of the torso. Therefore a low Young's modulus was applied, allowing the model torso to deform in a similar fashion. Details of the material properties are summarised in Table 2 while masses are shown in Table 3.

| <i>Structure</i>                               | <i>Material Properties</i> |        |        |
|--|----------------------------|--------|--------|
| <i>Skull</i>                                   | E=1200                     | v=0.3  | t=75   |
| <i>Bony structure of C0-C2 complex</i>         | E=1200                     | v=0.3  |        |
| <i>Vertebrae C3-T1 body</i>                    | E=1200                     | v=0.3  | t=11.5 |
| <i>Vertebrae C3-T1 arch</i>                    | E=1200                     | v=0.3  | t=5    |
| <i>Discs</i>                                   | E=4.3                      | v=0.45 | t=11.5 |
| <i>Alar ligament</i>                           | E=42.23                    | v=0.3  |        |
| <i>Transverse ligament</i>                     | E=74.34                    | v=0.3  |        |
| <i>Nuchal ligament-Lamellar Portion</i>        | E=10                       | v=0.3  | t=0.25 |
| <i>Nuchal ligament-Funicular Portion</i>       | E=10                       | v=0.3  | t=0.5  |
| <i>Contact between vertebrae</i>               | k=120                      |        |        |
| <i>Contact between head and head restraint</i> | k=240                      |        |        |
| <i>Torso</i>                                   | E=0.5                      | v=0.3  | t=200  |
| <i>Head restraint</i>                          | E=15                       | v=0.3  |        |

Table 2: Summary of material properties: E = Young's Modulus (MPa); v = Poisson's Ratio; k = Contact Stiffness (MPa), t = Uniform Thickness of Shell Element (mm)

| <i>Part of the Model</i> | <i>Mass (kg) for half model</i> |
|--------------------------|---------------------------------|
| <i>Head</i>              | M=2.46                          |
| <i>Neck</i>              | M=1.21                          |
| <i>Torso</i>             | m=5.7                           |

Table 3: Summary of the masses of the different parts of the model. NB. all masses are applied for a half model because of the symmetry conditions.

## Loading Conditions

One of the aims of this investigation is to simulate real whiplash impacts as accurately as possible. Therefore, rather than apply unrealistic uniform accelerations to the finite element model, it was decided to recreate the experiments conducted by Geigl et al. (1996, CD-Crash Ver. 1.3) in order to validate the model. Geigl mounted car seats of different types on a sled construction and experimented with volunteers. The sled was accelerated backwards and then suddenly decelerated while recording the motion/acceleration/time history at the head and torso of the volunteer via accelerometers and a high speed camera. For the investigation here, one of the experiments (MERCEDES 200-300 W 124, 1987 [MB 190] test NR.2) was recreated using the original acceleration history of the torso as an input but leaving the motion of the head and cervical spine to be determined by the model.

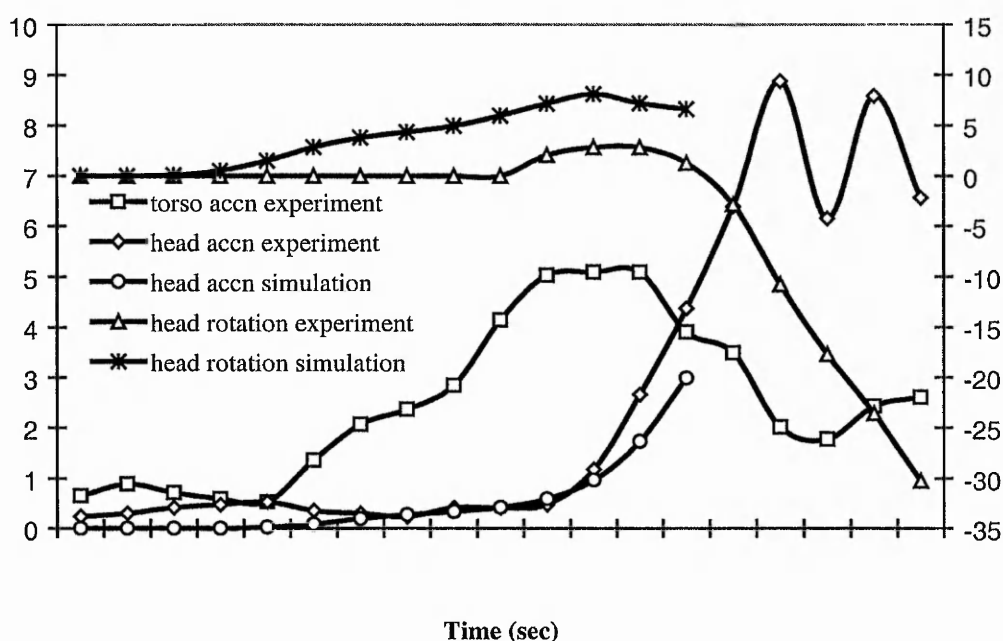


Figure 3: Acceleration and head rotation during a 10.5 kph impact, comparing the experimental data of Geigl et al. with the numerical prediction.

Two parameters were chosen to evaluate the model performance against the experiments: acceleration of the head and torso, and rotation of the head, as shown in Figure 3. It is noticeable that in the initial stages, 0.00-0.04 seconds, acceleration of the torso remains low; video data shows that the soft seatback construction allows the body to move into the seat. From 0.04-0.13 seconds the body accelerates strongly. At 0.13 sec, the relative speed of the torso to the car is zero and from now on the torso starts to move forwards inside the car due to the catapult effect of the seat-construction. It is noticeable that the head does not start to accelerate until much later, 0.10 seconds into the impact, and therefore relative translation movement between head and body occurs. The acceleration of the head is much greater, leading to high strains in the neck, which acts as a flexible coupling between the torso and the head. Figure 3 also shows the rotation of the head relative to the C3 vertebra adopting the convention of Geigl. It is noticeable that, for the experimental result, the head remains almost unrotated with respect to C3, indicating that the head is translating backward

into the head restraint rather than rotating. The numerical simulation for this investigation only analysed the event up to the point of impact between the head and the head restraint. The reason for this is that the study is mainly concerned with the injuries associated with hypertranslation of the head and this clearly occurs before the head reaches the restraint. The simulation therefore stops at 0.13 second, when impact is predicted. This has the advantage that there is no need to model the compression characteristics of the head restraint.

The model performance may be assessed as good, particularly in terms of the acceleration history for the head. However, the relative rotation between the head and the C3 vertebra is somewhat stronger in the simulation than in the experiment. This may be caused by the linear elastic material properties applied to the soft tissue, particularly the nuchal ligament, when the literature suggests that non-linear properties would be more appropriate. Following successful evaluation, nine simulations were conducted in total, with variations of initial speed between 10.5 and 21 kph and initial head/head restraint gap between 80 and 120 mm.

All calculations were conducted on a Digital™ A433 workstation using the full transient large deformation option of the ANSYS5.3™ FEA solver. The largest simulation, with an initial gap of 120 mm, involved 13 load steps with 10 sub-steps per load step, following a non-linear displacement curve as a boundary condition. Solution required a total of 233 computational iterations.

## RESULTS

Visual interpretation of the results shows the same S-shaped curvature of the neck as reported recently by Grauer et al. (1996) and also identified the same two main areas of traumatic strains. During impact there is hyperflexion of the C0-C2 Complex and hyperextension of the lower cervical spine.

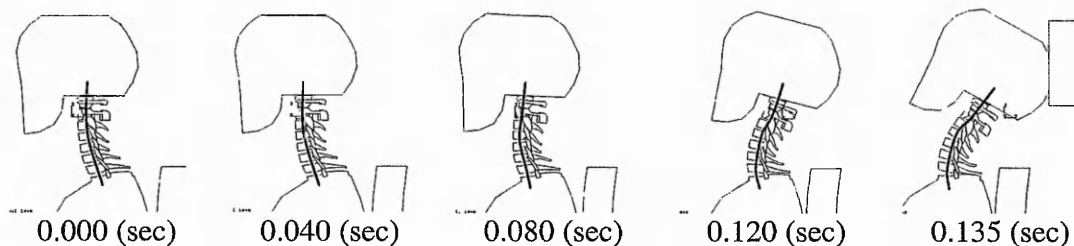


Figure 4: Deformation of the head/neck model during a 10.5 kph rear end impact with an initial gap between head and head restraint of 120 mm. Notice the initial translation of the head leading to flexion of the upper spine and extension of the lower spine.

The current FE model concentrates on the ligaments located in the C0-C2 complex and to evaluate the injury risk for the different load cases the time/strain history of the alar ligament was recorded for all load steps. The von Mises strains at the middle cross-section of the ligament were chosen to represent the ligament load since this avoids possible peak strains at the attachment points and takes torsional effects into account. The time/strain history was then compared with experimental data showing the maximum tensile load of the alar ligament at the point of rupture, as recorded by Dvorak et al. (1988). To allow direct comparison with the simulation results, the experimentally reported maximum tensile forces were divided by the Young's modulus and the cross-section area of the ligament, as used for the model, to give strains. Figure 5 shows the von Mises strain/time relation for the alar

ligament for all impact speeds. The average breaking strain and the standard deviation, as reported by Dvorak et al., are also shown.

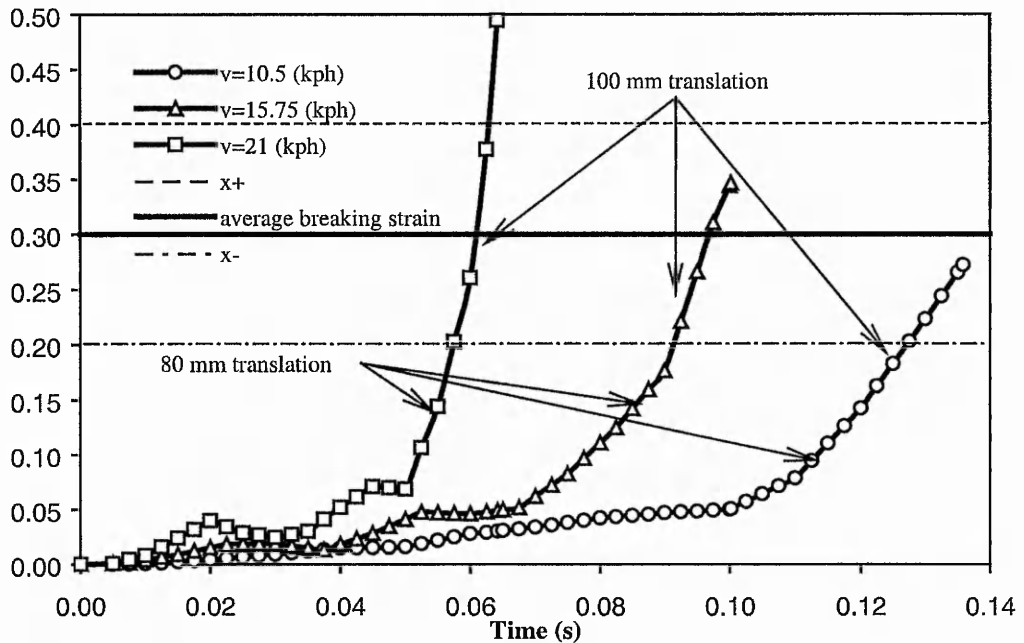


Figure 5 Von Mises strain of the alar ligament for an impact simulation with an initial head/head restraint gap of 120 mm. Strains are recorded up to the point of impact with the head restraint

The ligament strains increase exponentially for increasing speed and head restraint gap. There is a strong increase in strain when the neck forms the characteristic S-shaped deformation., a situation which is reached much faster for simulations with high speed. However, by noting the indicated translations of the head relative to the torso, it will be seen that a low initial gap of less than 80 mm would successfully prevent this MoI, even if the acceleration of the torso is high due to large speed differences.

## CONCLUSION

This study has shown that the motion of the head-neck-torso complex in whiplash situations can be simulated successfully using current computational methods. Evaluation of the present model has shown it to be successful in terms of predicting the rotation displacement and acceleration history of the head in comparison to experimental data. The results conform to previous studies of the MoI. In the early stages of a rear end impact, the head translates backward relative to the torso with little or no rotation. This forces the neck into a S-shape, leading to flexion of the upper cervical spine and extension of the lower cervical spine. Depending on how soon this movement is stopped, both effects can be traumatic. This study reports for the first time the strain/time history for one of the main ligaments involved. Qualitative analysis of the data shows that there are two main factors which determine the injury risk: the initial speed difference and the initial gap between the head and the head restraint. While the speed is undoubtedly the main factor, it is beyond control. The second factor, however, concerning the position of the head restraint can be

seen as of more concern since it can be controlled by better design. The results here indicate that, even at high impact speeds the injury risk for the alar ligament can be relatively low if the gap between head and head-restraint is small so that the flexion of the C0-C2 complex does not reach traumatic levels. The present quantitative evidence that the alar ligament is hardly at risk if the gap is less than 80 mm must be treated with some suspicion since a ligament trauma does occur before the braking strain is reached. However, there are several limiting factors in the current model which have to be taken into account. For example, the model does not include any muscular structure, even though this must play a supporting role. Furthermore, not all the ligament structures of the upper cervical spine are modelled here and so it would be reasonable to expect *in situ* strains of the real alar ligament to be somewhat smaller. Furthermore, the results of *in vitro* testing of human ligaments are themselves somewhat misleading due to the very nature of the tests and are generally thought to lead to lower strengths than would be found *in vivo*. Nevertheless, the very high strains predicted for high speed impacts with large initial gap do strongly suggest that injury will occur in this situation and it can be concluded that a seating position that leads to a horizontal gap between head and head restraint of much more than 80 mm may be seen as inappropriate; there is an apparent danger of trauma to the alar ligament occurring before the head reaches the head restraint. It is therefore recommended that this should be taken into account in the design of future car seats and that passengers should be advised as to correct adjustment of seating position and head restraint configuration in order to avoid a gap larger than 80 mm.

The present model has symmetry conditions applied to the sagittal plane and so investigation of axial rotation of the head is not possible. Since it has been suggested that the alar ligament is particularly at risk if the translational movement coincides with an axial rotation of the head, the present model will be extended to include a fully 3-dimensional head and neck structure. Furthermore non-linear material properties for the discs and the ligaments will be applied while spring damper elements will be introduced to simulate the muscular structure. The model will then be capable of more realistically simulating whiplash impacts that occur, in practice, from varying angles and with the occupants in varying starting positions.

## REFERENCES

Dr. Steffan Datentechnik Ges.m.b.H, 1996, CD-Crash Version 1.3,  
<http://fmechds01.tu-graz.ac.at/dsd/>, Ledergasse 34 Linz, Austria

Dvorak J., Panjabi M. M., 1987, "Functional Anatomy of the Alar Ligaments", *Spine*.  
Vol 12:183-189

Dvorak J., Schnieder E., Salinger P., Rahn B., 1988, "Biomechanics of the  
Craniocervical Region: The Alar and Transverse Ligaments", *J. Orthopedic Research  
Society*, Vol. 6:652-461

Geigl B. C., Steffan H., Leinzinger P., Roll, Muehlbauer M., Bauer G., 1994, "The  
movement of Head and Cervical Spine During Rear End Impact", *Proc. of the  
IRCOBI Conference on the Biomechanics of Impacts*, Lyon, France, pp 127-137

Girffith H. J., Olson P. N., Everson L. I., Winemiller M., 1995, "Hyperextension  
strain of "whiplash" to the cervical spine", *Skeletal Radiology*, Vol. 24:263-266

Grauer J. N., Panjabi M. M., Cholewicki J., Nibu K., Dvorak J., 1997, "Whiplash Produces an S-Shaped Curvature of the Neck With Hyperextension at the Lower Levels", *Spine*, Vol. 22:2489-2494

National Library of Medicine, 1994,  
[http://www.nlm.nih.gov/research/visible/visible\\_human.html](http://www.nlm.nih.gov/research/visible/visible_human.html)

Lin H. S. Liu Y. K. Adams K. H., 1978, "Mechanical Response of the Lumbar Intervertebral Joint under Physiological (Complex) Loading", *J of Bone And Joint Surgery*, Vol. 60;1:41-55

Muenker M., Langwieder K., Chen, Hell W., 1994, "HWS Beschleunigungsverletzungen, VdS (Institution of German car insurers)", Munich

Myklebust J. B., Pintar F., Yoganadan N., Cusick F., Maiman D., Mayers T. J., Sances A., 1988, "Tensile Strength of Spinal Ligaments", *Spine*, Vol. 13:526-531

Penning L., 1994, "Hypertranslation of the head backwards: part of the mechanism of cervical whiplash injury". *Orthopaede*, Vol. 23:268-274.

Unterharnscheidt F., Sances A., Thomas D. J., Ewing C. L., Lanson S. J., 1986, "Pathological and neuropathological findings in rehsus monkeys subjected to -Gx and +Gx indirect impact acceleration", *Proc. Of the Mechnaismus of head and spine trauma*, Goshen New York, pp 565-665.

VdS (Institution of German car insurers), 1994, "Vehicle Safety 90: Analysis of car Accidents", Munich,

White A. A., Panjabi M. M., 1990, "Clinical Biomechanics of the Spine", second edition, J. B. Lippincott Comp., Philadelphia, p 231

## **APPENDIX B**

### **Development of a Biomechanical FE Model to Investigate “Whiplash”**

(copy of paper)

## **DEVELOPMENT OF A BIOMECHANICAL FE-MODEL TO INVESTIGATE “WHIPLASH”**

**F. Heitplatz, W. Z. Golinski and C. R. Gentle**  
Department of Mechanical and Manufacturing Engineering  
The Nottingham Trent University, UK

### **ABSTRACT**

A 3 Dimensional dynamic FEA model of the human head-neck-torso motion complex has been developed in order to investigate the mechanism of injury in so called “whiplash” accident situations. The model was loaded over a range of moderate crash conditions similar to those found in volunteer experiments. After evaluation and validation of the model against these experimental results, the range of conditions was extended to consider higher impact speeds and larger initial gaps between the head and the head restraint. The results show an S-shape deformation of the cervical spine during the initial parts of a rearend impact, leading to flexion of the upper spine and extension of the lower spine. Particular attention was paid to the force/time relation of the spinal soft tissue in order to assess the injury risk and further investigate the hypertanslation hypothesis. It was found that the forces in the apical ligament increase exponentially with impact speed and initial gap, reaching traumatic levels before the head hits the restraint if the initial gap is larger than 50 mm. Based on the results, a clear recommendation may be made for future designs of safer car seat head restraints.

### **INTRODUCTION**

Cervical “whiplash” is the most common injury sustained in car accidents. In 93.5% of all rear end collisions involving personal injuries, at least one of the passengers claimed a neck injury, even though 70.4% of these accidents occur with speed differences smaller than 15 kph (Institution of German Car Insurers, 1994). Other injuries are comparatively rare (Muenker et al., 1994) and therefore the incidence of whiplash injuries is significant from both the economical and the medical point of view. Despite the common occurrence of the injury, little is known about the exact cause of patients’ complaints. The Mechanism of Injury (MoI) is not certain but it is generally considered to involve hyperextension (White and Panjabi, 1992). Various attempts have been made to quantify whiplash by means of radiology and, although none of these has proven to be conclusive, it can be stated that little or no bony damage is sustained, whereas ligamentous injury is common (Griffith et al., 1990).

More recently a new possible MoI has been proposed. Based on a review of the literature, Penning (1994) has developed the theory that in whiplash the primary MoI is not hyperflexion but hypertranslation of the head backwards. The head’s inertia is taken to lead

to a situation of high shear at the top of the neck, causing over-stretching of not only the ligaments but also the joint capsule between vertebrae. The familiar indications of whiplash injury, chronic disturbance of posture and equilibrium, are then explained by chronic ligamentous instability of the upper cervical spine. The theory is supported through experimental findings by Unterharnscheidt et al. (1986) who subjected rhesus monkeys with fixed trunk and free head to deadly positive and negative accelerations. Autopsy revealed that for both positive and negative acceleration a dislocation of the atlas with complete destruction of the transverse and alar ligament as well as the spinal cord was present. It was concluded from pictures of the experiments that the injury had already occurred before the translation of the head was completed. Animal experiments are not fully comparable with the *in situ* situations found in humans but, due to the comparable anatomy of the upper cervical region of the rhesus monkey, a similar conclusion may well prove to be valid. Experiments like the one Unterharnscheidt describes are certainly not repeatable with humans. However, experiments with volunteers have been undertaken by Geigl et al. (1994), using low speed differences. No injuries have been reported, but the translation effect can clearly be seen on high-speed video film. Geigl conducted 37 experiments with volunteers and six with post mortal test objects (PMTO's) on a sled construction. For the volunteers the maximum impact speed was limited to 10.5 kph and the maximum deceleration recorded was  $40 \text{ m/s}^2$ . With regard to the rotation of the head, the following characteristic movement was found for all tests; independent of the initial seating position, no head rotation could be seen during the first 60 to 100 ms following impact. Only after this period does the head start to rotate slowly backward at a time when the shoulders are already reflected forward.

It seems therefore that the MoI of whiplash cannot be fully explained as a hyperextension trauma and that a possible link between translation of the head, during the initial stages of impact, and strains in the ligaments situated in the C0-C2 complex exists. Therefore, a close look into the biomechanics of these ligaments is necessary. The most extensive *in vitro* investigation into this complex is reported by Dvorak et al. (1988). Investigating the biomechanics of the craniocervical region, they suggest that the role of the alar ligaments, with respect to the stability of the C0-C2 joint and the implications for possible injury mechanisms during whiplash accidents, may have been long underestimated, especially when the transverse ligament remains intact.

Experimental studies of the MoI of whiplash are limited by several factors. Volunteer testing is only possible for relatively low impact speeds in order to protect the test person. Furthermore, there are no means to measure the ligamental strain *in vivo*. Recently an extensive *in vitro* test series has been published by Grauer et al. (1997). Reporting the deformation motion characteristic of whole cervical spine specimens under whiplash loading. These tests have provided invaluable information into the complex. However, several problems remain. It has proved to be impossible to test specimens with the muscular structure in place. Furthermore, the head of the specimen had to be removed and was replaced by a steel surrogate head, therefore destroying vital ligaments in the C0-C2 complex. In light of these limitations, numerical simulation offers a cost effective and valuable alternative. The ability to easily modify loading and boundary conditions give the researcher the ability to quickly experiment with different head-restraint configurations giving a unique insight into the loads associated with the spinal soft tissue during the impact. There have been several FE-models of the cervical spine reported in the literature but there has been only one study of the full three-dimensional cervical spine as a FE-Model, which has been used to investigate the effects of whiplash (Kleinberger, 1993). Kleinberger developed a 3D FE-Model of the C0-T1 section of the spine with highly simplified topology; there are no topology differences between the vertebrae on different levels; linear material-

properties are applied to all regions; the muscular structure is not modelled. However, this model did show promising results in terms of the overall model displacement when subjected to dynamic loading and it therefore showed the potential of FE-modelling for investigating whiplash.

In previous work at Nottingham Trent University Heitplatz et al (1998) presented a simplified FE-model of the Head-Neck-Torso complex. The model was validated using loading conditions from Geigl's (1996) experiments on volunteers. A series of collisions was simulated using variations in impact speed and head restraint configurations and investigating the strain/time behaviour of the alar ligament. The presented results showed a risk of alar ligament injury when the initial gap between the head and the head restraint is larger than 80mm. This work, however, was conducted on a simplified model with the geometry focused only on the C0-C2 complex and using implicit solver technology (Ansys53). The limitations of the model, particularly with respect to the contact algorithm and the large strain behaviour under dynamic loading, soon became apparent, resulting in the development of a new model simulating the full 3D structure of the cervical spine using explicit solver technology (LS-Dyna).

## **METHOD**

### **Model Geometry**

The present study investigates posterior impact for an adult, sitting in a normal seating position. Symmetry conditions are assumed along the sagittal plane. Details of the model are given in Table 1. Topological information relating to the size and shape of the skull and the human cervical vertebrae was extracted from full colour pictures obtained by the Visible Human Project (National Library of Medicine, 1994). A 3-D parametric CAD model was created by interpreting the images of the male dataset. The FE-mesh was developed with respect to the hardware available. The number of elements was kept as small as feasible, still representing all major anatomical parts of the cervical spine. Therefore, the topology was simplified to accommodate 8-node brick meshing of the structure with special focus given to the joint surfaces in order to allow realistic motion characteristic, using surface to surface contact. The mesh structure and joint contact surfaces are illustrated in Figures 2 and 3.

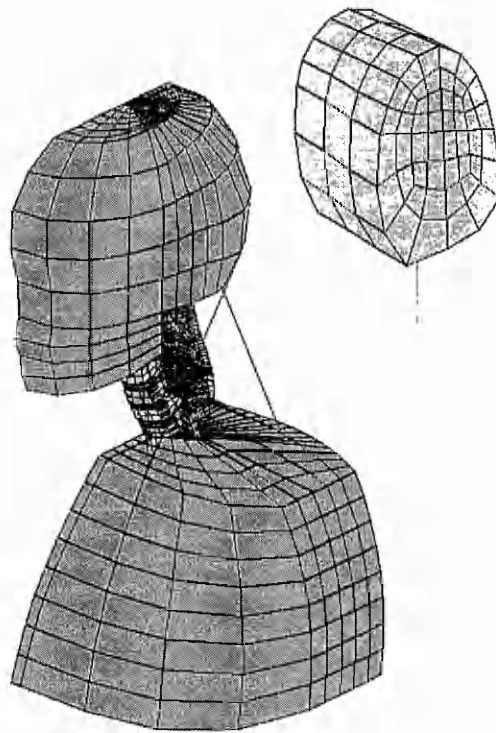


Figure 1: Isometric-View of the FEA Model

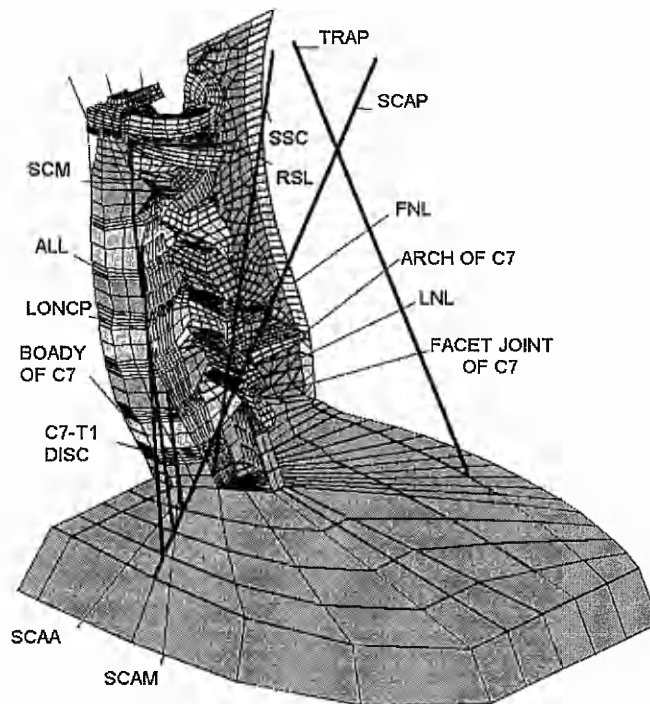


Figure 2 Isometric-View of the C1-T1 part of FEA Model. ALL: anterior longitudinal ligament; FNL: funicular portion of the nuchal ligament; LNL: lamellar portion of nuchal ligament; TRAP: trapezius; SSC: semispinalis capitis; LONCP: longus capitis; SCM: sternocleidomastoid; SCAA: scalenus anterior; SCAM: scalenus medius; SCAP: scalenus posterior; RSL: rectus capitis lateralis.

In order to achieve a realistic deformation pattern for the model, anatomically correct representation of the spinal soft tissue is essential. The model therefore incorporates intervertebral discs and a wide range of ligaments, particularly in the C0-C2 complex (Figure 3). The two strongest ligaments of the complex, alar and transverse, are modelled as 3-D structures using solid elements, whilst the remaining ligaments are modeled with non-linear springs. The tectorial membrane and the vertical portion of the cruciate ligament were combined into one structure due to their close anatomical relationship. A mixed structure of non-linear spring and shell elements is used to simulate the bio-mechanics of the ligamentum flavum and the nuchal ligament, with the latter has been divided into lamellar and funicular portion. Furthermore, the muscular structure of the neck is represented by nine non-linear springs, with the location of the attachments based on anatomical description (Gray, 1980). Figure 2 shows the C1-T1 spine unit with nomenclature of the muscular and ligamentous structure. The topology of the head restraint is a simplified representation of the Mercedes W124 headrest modeled as a combination of soft foam and steel tubing. Surface to surface contact has been established between the facet joints as well as the head and headrest, amounting to a total of 11 contact interfaces.

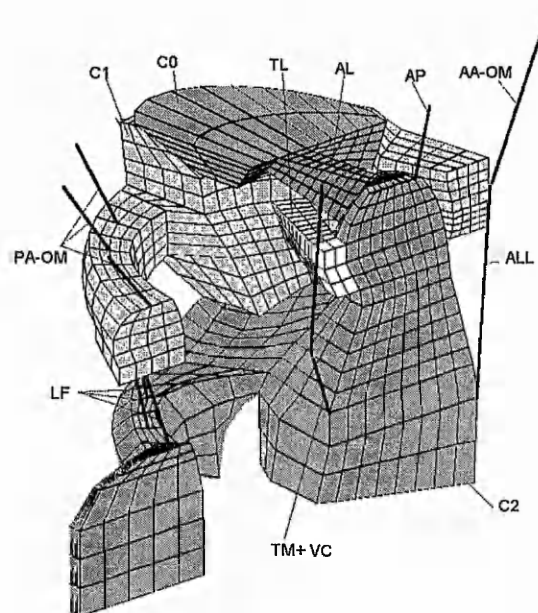


Figure 3: The C0-C2 motion complex with ligamentous structure. AL: alar ligament; TL: transvers ligament; AP: apical ligament; AA-OM: anterior atlanto-occipital membrane; ALL: anterior longitudinal ligament; TM+VC: tectorial membrane with vertical portion of cruciate ligament; LF: ligamentum flavum; PA-OM: posterior atlanto-occipital membrane

| <b>Structure</b>                         | <b>Type of element</b>      | <b>No. of elements/<br/>interfaces</b> |
|--|-----------------------------|--|
| <i>Skull</i>                             | *ELEMENT_SOLID              | 856                                    |
| <i>Cervical vertebrae</i>                | *ELEMENT_SOLID              | 2803                                   |
| <i>Discs</i>                             | *ELEMENT_SOLID              | 624                                    |
| <i>Alar ligament</i>                     | *ELEMENT_SOLID              | 60                                     |
| <i>Transverse ligament</i>               | *ELEMENT_SOLID              | 66                                     |
| <i>Nuchal ligament-Lamellar Portion</i>  | *ELEMENT_SHELL              | 421                                    |
| <i>Nuchal ligament-Funicular Portion</i> | *ELEMENT_SHELL              | 49                                     |
|  | *ELEMENT_DISCRETE           | 98                                     |
| <i>Other Ligaments</i>                   | *ELEMENT_DISCRETE           | 17                                     |
| <i>Muscles</i>                           | *ELEMENT_DISCRETE           | 9                                      |
| <i>Torso</i>                             | *ELEMENT_SOLID              | 1348                                   |
| <i>Head restraint</i>                    | *ELEMENT_SOLID              | 144                                    |
|  | *ELEMENT_BEAM               | 11                                     |
| <i>Contact</i>                           | *CONTACT_SURFACE_TO_SURFACE | 11                                     |
| <b>Total number of elements</b>          |                             | <b>6512</b>                            |
| <b>Total number of nodes</b>             |                             | <b>9076</b>                            |

Table 1: Summary of the FE Model Data

### **Material Properties**

Among the main obstacles to the development of biomechanical FE models are the highly non-linear material properties found in human tissue. In particular, modelling of intervertebral discs remains difficult due to their complex mechanical behaviour which is based on a proteoglycan membrane surrounding the soft tissue of the annulus fibrous and a water filled nucleus (Adams and Dolan, 1995). Complete modelling of the disc would require a large number of elements and exact topological representation of the discs. This was not feasible with respect to the hardware available. Therefore the disc is modelled with a Blatz-Ko rubber model using a shear modulus of 4 N/mm<sup>2</sup> which has been shown to lead to a realistic deformation stiffness for bending load cases, which are the main loads associated with the disc under rearend impact.

Alar and Transverse ligaments are also modelled using the Blatz-Ko hyperelastic material law, applying material properties as found in the literature (Dvorac et al., 1988). Due to their large extension the nuchal ligament has been modelled using 4 node Belytschko-Tsay shell elements which have been reinforced by tension-only beams in the funicular part of the ligament, using a positive offset in order to model the non-linear progressive stiffness which is characteristic for all ligamentous structures. The remaining ligaments are modelled using non-linear discrete tension-only elements. Force/deformation load curves have been developed using *in vitro* test data, which is readily available in the literature (Myklebust et al., 1988). The same technique has been applied to the muscular structure using *in vitro* test data of the sternocleidomastoid as a reference (Yamada, 1970). No active muscular response is expected, due to the short simulation period, which has been shown to be well below the human reaction time (Panjabi, 1998). The bony structure of the spine can be assumed stiff in

respect to the soft tissue. Furthermore, according to accident statistics (Institution of German Car Insurers, 1994) no damage to the bony structure is expected for the applied load cases. Therefore, all bony structures as well as the head and torso are modelled as rigid bodies, thereby reducing the calculation time. The acceleration/time profile of the head during rear-end impact is largely dependent on the stiffness and the energy absorbing characteristics of the head restraint. The present model uses the Blatz-Ko foam material law for the cushion material. However, further research in this area is necessary in order to achieve a more realistic energy conservation pattern. Table 2 shows a summary of all material properties used for the model.

| <b>Structure</b>                         | <b>Material formulation</b>   | <b>Material Properties</b> |           |
|--|-------------------------------|----------------------------|-----------|
| <i>Skull</i>                             | *MAT_RIGID                    | -                          | -         |
| <i>Cervical vertebrae</i>                | *MAT_RIGID                    | -                          | -         |
| <i>Discs</i>                             | *MAT_BLATZ-KO_RUBBER          | G=4                        |           |
| <i>Alar ligament</i>                     | *MAT_BLATZ-KO_RUBBER          | G=14.12                    |           |
| <i>Transverse ligament</i>               | *MAT_BLATZ-KO_RUBBER          | G=25.37                    |           |
| <i>Nuchal ligament-Lamellar Portion</i>  | *MAT_ELASTIC                  | E=4.42                     | $\nu=0.3$ |
| <i>Nuchal ligament-Funicular Portion</i> | *MAT_ELASTIC                  | E=4.42                     | $\nu=0.3$ |
|  | *MAT_CABEL_DISCRETE_BEAM      | E=5                        |           |
| <i>Other Ligaments</i>                   | *MAT_SPRING_NONLINEAR_ELASTIC | Loadcurve                  | -         |
| <i>Muscles</i>                           | *MAT_SPRING_NONLINEAR_ELASTIC | Loadcurve                  | -         |
| <i>Torso</i>                             | *MAT_RIGID                    | -                          | -         |
| <i>Head restraint Foam</i>               | *MAT_BLATZ-KO_FOAM            | G=1.5                      |           |
| <i>Head restraint Mounting</i>           | *MAT_ELASTIC                  | E=210000                   | $\nu=0.3$ |

Table 2: Summary of material properties: E = Young's Modulus (MPa);  $\nu$  = Poisson's Ratio; G = Shear Modulus (MPa), k=Elastic Stiffness (N/mm)

### **Loading Conditions**

One of the aims of this investigation is to simulate real whiplash impacts as accurately as possible. Therefore, rather than apply unrealistic uniform accelerations to the finite element model, it was decided to recreate the experiments conducted by Geigl et al. (1996, CD-Crash Ver. 1.3) in order to validate the model. Geigl mounted car seats of different types on a sled construction and experimented with volunteers. The sled was accelerated backwards and then suddenly decelerated while recording the motion/acceleration/time history at the head and torso of the volunteer via accelerometers and a high-speed camera. For the investigation here, one of the experiments (MERCEDES 200-300 W 124, 1987 [MB 190] test NR.2) was recreated using the original acceleration history of the torso as an input but leaving the motion of the head and cervical spine to be determined by the model (see Figure 4 and 5).

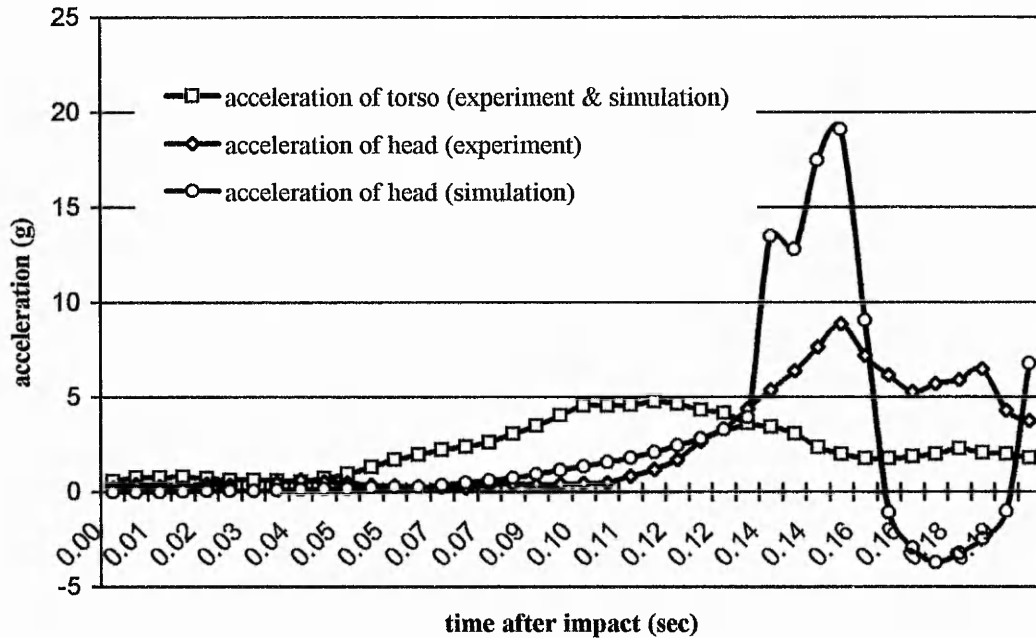


Figure 4: Acceleration of the head and torso during a 10.5 kph rear-end impact, comparing the experimental data of Geigl et al. with the numerical prediction.

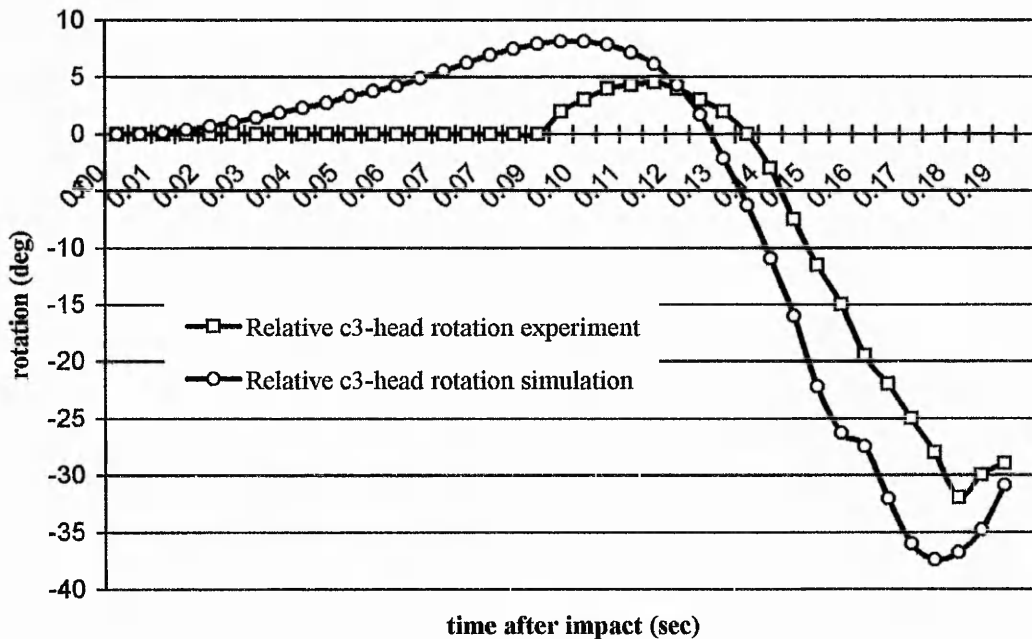


Figure 5: Relative rotation between head and C3 during a 10.5 kph rear-end impact, comparing the experimental data of Geigl et al. with the numerical prediction.

It is noticeable that in the initial stages, 0.00-0.04 seconds, acceleration of the torso remains low; video data shows that the soft seatback construction allows the body to move into the seat. From 0.04-0.13 seconds the body accelerates strongly. At 0.13 sec, the relative speed of

the torso to the car is zero and from now on the torso starts to move forwards inside the car due to the catapult effect of the seat-construction. It is noticeable that the head does not start to accelerate until much later, 0.10 seconds into the impact, and therefore relative translation movement between head and body occurs. The acceleration of the head is much greater, leading to high strains in the neck, which acts as a flexible coupling between the torso and the head.

Interpretation of the video data shows, that the car seatback is bent backwards due to the acceleration force of the body, thereby continually increasing the gap between head and head restraint from its starting value of 80mm. This effect can not be simulated with the present FE-Model. Therefore, the simulation was conducted, with a fixed horizontal gap of 110mm. This produced a more accurate acceleration profile in terms of the time/acceleration relationship than a simulation with an 80mm horizontal gap and general the argument is good qualitatively. However, the magnitude of the acceleration peak is a factor of two higher in the numerical simulation than in the experiment. It is apparent that the ability to absorb energy is higher for the experimental head restraint, leading to a longer impact period and a reduced rebound.

Figure 5 shows the rotation of the head relative to the C3 vertebra adopting the convention of Geigl. With respect to the relative head rotation, a much better qualitative match has been found between experiment and simulation, thereby showing that the model has reproduced natural motion behaviour under dynamic loading.

All calculations were conducted on a Digital™ A433 workstation using the LS-Dyna PC version 940.1a solver. All loads have been applied as a non-linear prescribed motion. The average time step was  $6.7E-7$  seconds, resulting in 11 hours calculation time for 0.190 seconds to termination.

## RESULTS

Following the successful evaluation of the model, several simulations have been conducted using twice the impact speed of the volunteer experiment. Visual interpretation of the results shows the same S-shaped curvature of the neck as reported recently by Grauer et al. (1997) who also identified the same two main areas of traumatic strains. During impact there is hyperflexion of the C0-C2 Complex and hyperextension of the lower cervical spine.

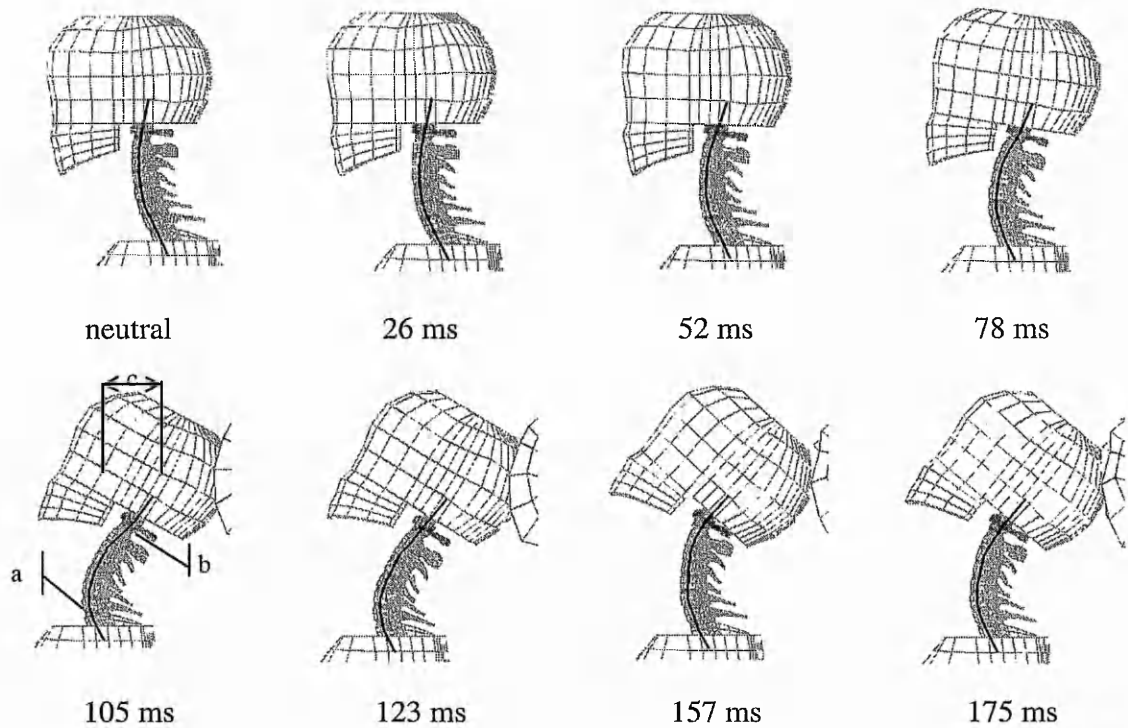


Figure 6: Deformation of the head/neck model during a 21 kph rear end impact with an initial gap between head and headrest of 80 mm. Notice the initial translation of the head c) leading to flexion of the upper spine b) and extension of the lower spine a).

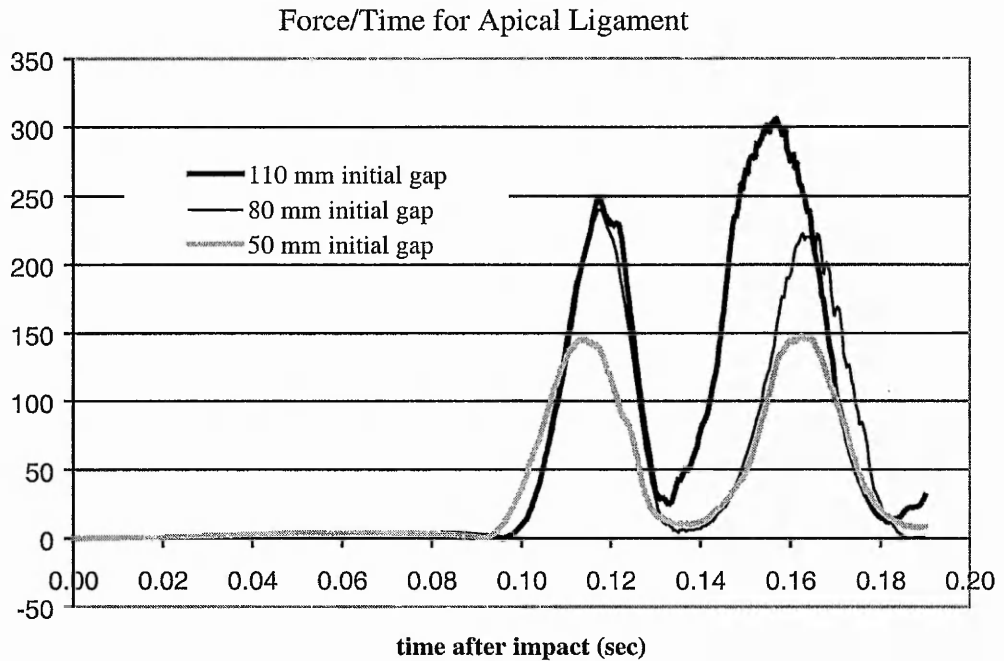


Figure 7 Force/time relationship of the apical ligament for a simulated 21kph impact and three different initial gaps between head and headrest

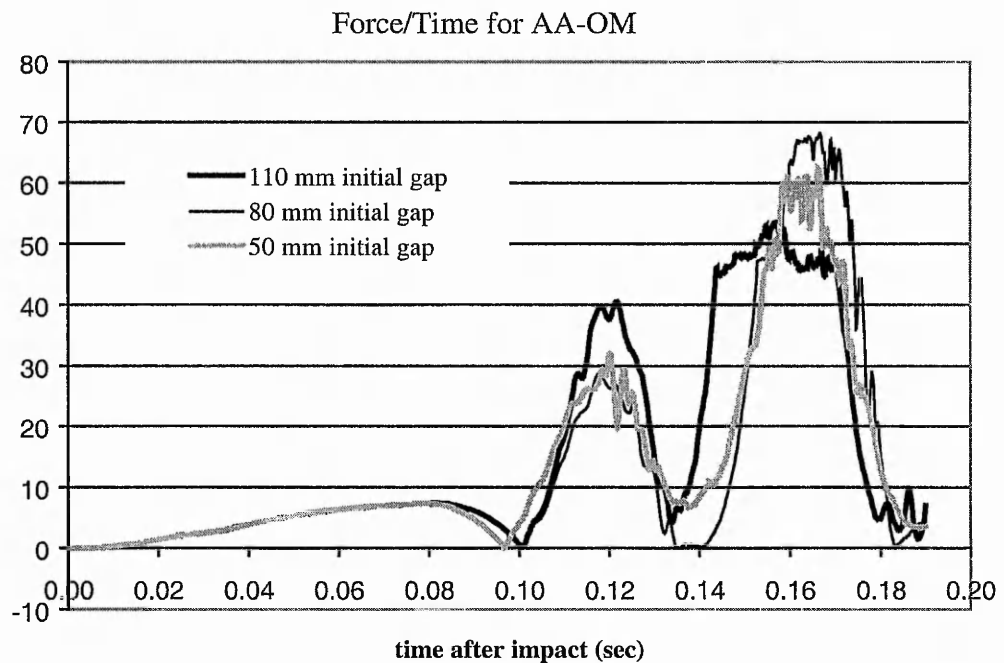


Figure 8 Force/time relationship of the anterior atlanto-occipital membrane for a simulated 21kph impact and three different initial gaps between head and headrest

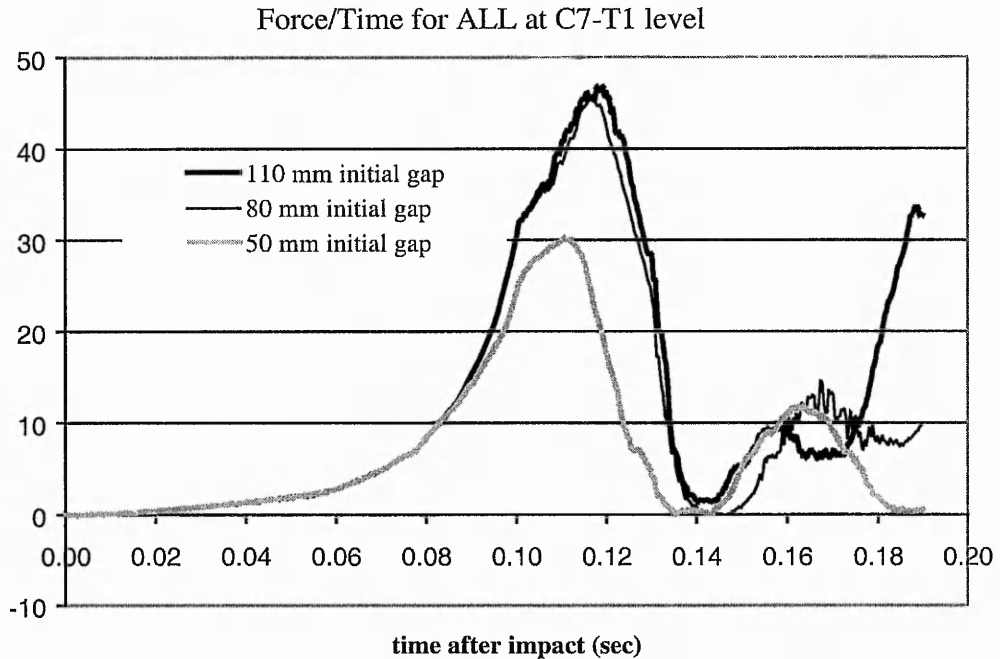


Figure 9 Force/time relationship of the anterior longitudinal ligament at C7-T1 level for a simulated 21kph impact and three different initial gaps between head and headrest

Qualitative interpretation of the ligament axial forces shows previously unreported high loads on the apical ligament situated within the C0-C2 complex. These are particularly high if the initial gap is large, reaching 310N. The average braking strain of the apical ligament is reported with 214N ( $\pm 115$ ) (Myklebust et al. 1988). The forces in the anterior atlanto-occipital membrane remain at a low level ( $< 70$ N) for all three load-cases. The average braking force of this structure is reported to be 281N ( $\pm 136$ ). There is a strong increase in strain for the discs of the lower cervical spine when the neck forms the characteristic S-shaped deformation. By noting the indicated translations of the head relative to the torso, it has been shown that maintaining a small initial head restraint gap of less than 50 mm would successfully prevent this MoI, even if the acceleration of the torso is high due to large speed differences.

## CONCLUSION

This study has shown that the dynamic motion of the head-neck-torso complex in whiplash situations can be simulated successfully using the LS-Dyna solver. Evaluation of the present model has shown it to be successful in terms of predicting the rotation displacement and acceleration history of the head in comparison to experimental data. The results conform to previous studies of the MoI. In the early stages of a rear end impact, the head translates backward relative to the torso with little or no rotation. This forces the neck into an S-shape, leading to flexion of the upper cervical spine and extension of the lower cervical spine. Depending on how soon this movement is stopped, both effects can be traumatic. This study reports for the first time the force/time history for several of the main ligaments involved.

Qualitative analysis of the data shows that there are two main factors which determine the injury risk: the initial speed difference and the initial gap between the head and the head

restraint. While the speed is undoubtedly the main factor, it is beyond the control of the car designer. However, the second factor, the position of the head restraint, can be seen as of more concern since it can be controlled through the car seat design features. The results shown here indicate that, even at relatively high impact speeds, the injury risk for the spinal soft tissue can be low if the gap between head and head restraint is small so that neither the flexion of the C0-C2 complex nor the extension of the lower cervical spine reaches traumatic levels. The present quantitative evidence that the spinal soft tissue is hardly at risk if the gap is less than 50 mm must be treated with some suspicion since some ligament trauma will occur before the breaking strain is reached.

With respect to the load on the intervertebral joints of the lower cervical spine during the extension phase, it has been noted that the load on the anterior longitudinal ligament does not necessarily reveal the full picture since rupture of the posterior annulus fibrosus may be the main concern in respect of spinal trauma. It is noticeable however, that the highest forces occur **before** the head impacts the head restraint when the initial gap is larger than 50mm. This is of particular concern since the interpretation of high-speed video data shows that the gap between head and head restraint increases dynamically during impact. The simulations show unusually high loads for the apical ligament. This has to be seen with some care since the present model does not include the C0-C1 joint capsules, which could play a supporting role. However, the very high loads suggest strongly that the apical ligament is at risk and therefore it could be a contributing factor of spinal instability of the craniocervical region, which previously has been overlooked.

There are several limiting factors in the current model which have to be taken into account. For example, the results of *in vitro* testing of human ligaments are somewhat misleading due to the very nature of the tests and are generally thought to lead to lower strengths than would be found *in vivo*. Furthermore, the applied material properties for the intervertebral disc are insufficient; although the LS-Dyna code is well equipped to simulate the material laws present in more technical applications it remains difficult to apply these to the biological materials. Further research in this area is indicated to improve the applicability of dynamic FEA to complex human soft tissue structures. Nevertheless, the very high forces predicted for high speed impacts with large initial gap do strongly suggest that injury will occur in this situation and it can be concluded that a seating position that leads to a horizontal gap between head and head restraint of much more than 50 mm may be seen as inappropriate; there is an apparent danger of trauma to the apical ligament and the intervertebral discs at the C7-T1 level occurring before the head reaches the head restraint. It is therefore recommended that this should be taken into account in the design of future car seats and that passengers should be advised as to correct adjustment of seating position and head restraint configuration in order to avoid a gap larger than 50 mm.

The present model has symmetry conditions applied to the sagittal plane and so investigation of axial rotation of the head is not possible. Since it has been suggested that the alar ligament is particularly at risk if the translational movement coincides with an axial rotation of the head, the present model will be extended to include a fully 3-dimensional head and neck structure as well as a simplified full body structure. The model will then be capable of more realistically simulating whiplash impacts that occur, in practice, from varying angles and with the occupants in varying starting positions.

## REFERENCES

- Adams M.A., Dolan P., "Recent advances in lumbar spinal mechanics and their clinical significance" *Clinical Biomechanics*, 1995, Vol. **10**(1):3-19
- Dr. Steffan Datentechnik Ges.m.b.H, 1996, CD-Crash Version 1.3,  
<http://fmechds01.tu-graz.ac.at/dsd/>, Ledergasse 34 Linz, Austria
- Dvorak J., Panjabi M. M., 1987, "Functional Anatomy of the Alar Ligaments", *Spine*. Vol. **12**:183-189
- Dvorak J., Schneider E., Salinger P., Rahn B., 1988, "Biomechanics of the Craniocervical Region: The Alar and Transverse Ligaments", *J. Orthopaedic Research Society*, Vol. **6**:652-461
- Geigl B. C., Steffan H., Leinzinger P., Roll, Muehlbauer M., Bauer G., 1994, "The Movement of Head and Cervical Spine During Rear End Impact", *Proc. of the IRCOBI Conference on the Biomechanics of Impacts*, Lyon, France, pp 127-137
- Grauer J. N., Panjabi M. M., Cholewicki J., Nibu K., Dvorak J., 1997, "Whiplash Produces an S-Shaped Curvature of the Neck With Hyperextension at the Lower Levels", *Spine*, Vol. **22**:2489-2494
- Gray H., 1980, "Gray's Anatomy", 36<sup>th</sup> edition, Churchill Livingstone, Edinburgh,
- Griffith H. J., Olson P. N., Everson L. I., Winemiller M., 1995, "Hyperextension strain of "whiplash" to the cervical spine", *Skeletal Radiology*, Vol. **24**:263-266
- Heitplatz F., Golinski W.Z., Gentle C.R., 1998, "Guidelines for Car Seat Design based on FE Analysis of Whiplash Injuries" *Proc. of Mechanics in Design (MID'98)*, Nottingham, UK, (in press)
- Kleinberger M., "Application of finite element techniques to the study of cervical spine mechanics", *Proc. of the 37th Stapp Car Crash Conference*, San Antonio, Texas, November 7-8, 1993, pp 261-272.
- Muenker M., Langwieder K., Chen, Hell W., 1994, "HWS Beschleunigungsverletzungen, VdS ( Institution of German Car Insurers )", Munich
- Myklebust J. B., Pintar F., Yoganadan N., Cusick F., Maiman D., Mayers T. J., Sances A., 1988, "Tensile Strength of Spinal Ligaments", *Spine*, Vol. **13**:526-531
- National Library of Medicine, 1994,  
[http://www.nlm.nih.gov/research/visible/visible\\_human.html](http://www.nlm.nih.gov/research/visible/visible_human.html)
- Panjabi M.M., et al., "Simulation of Whiplash Trauma Using Whole Cervical Specimens", *Spine*, 1998, Vol. **23**(1):17-24
- Penning L., 1994, "Hypertranslation of the head backwards: part of the mechanism of cervical whiplash injury". *Orthopaede*, Vol. **23**:268-274.

Unterharnscheidt F., Sances A., Thomas D. J., Ewing C. L., Lanson S. J., 1986, "Pathological and neuropathological findings in rehsus monkeys subjected to -Gx and +Gx indirect impact acceleration", *Proc. of the Mechanisms of Head and Spine Trauma*, Goshen New York, pp 565-665.

VdS (Institution of German Car Insurers), 1994, "Vehicle Safety 90: Analysis of car Accidents", Munich,

White A. A., Panjabi M. M., 1990, "Clinical Biomechanics of the Spine", second edition, J. B. Lippincott Comp., Philadelphia, p 231

Yamada H.,1970, "Strength of Biological Materials", The Williams & Wilkins Comp., Baltimore, p 93-95

## **APPENDIX C**

# **Assesment of a Whiplash Prevention Device with a Dynamic Biomechanical Finite Element Model**

(copy of paper)

**ASSESSMENT OF A WHIPLASH PREVENTION DEVICE WITH A DYNAMIC  
BIOMECHANICAL FINITE ELEMENT MODEL**

**Waldemar GOLINSKI and Richard GENTLE**

Department of Mechanical and Manufacturing Engineering  
The Nottingham Trent University, UK

*Corresponding author:*

Mr. Waldemar Z. Golinski

The Nottingham Trent University  
Department of Mechanical and Manufacturing Engineering  
Burton Street  
Nottingham NG1 4BU; UK

Tel : +44 115 8484728  
Fax : +44 115 8484749

E-mail: [waldemar.golinski@ntu.ac.uk](mailto:waldemar.golinski@ntu.ac.uk)  
Internet: <http://www.domme.ntu.ac.uk/biomech>

*Keywords:*

***FEM, biomechanical, spine, model, whiplash, prevention***

## ABSTRACT

A full 3-dimensional dynamic finite element model of the head-neck complex has been constructed in order to investigate the mode of injury in "whiplash" situations, principally rear end impacts on cars. The geometry of the model is simplified wherever possible in order to reduce the computational requirements but it provides a particularly full representation of the facet joints and the ligaments in the cervical spine. Validation procedures against published real crash test data applied to simulated crashes on volunteers have shown that the model represents the linear and rotational motion of the head, neck and torso quite accurately. Furthermore the model has shown itself to be useful in analysing the loads on individual ligaments so that safe positions for a head restraint can be identified. The work described here reports an extension of the model to include a fuller representation of the interactions between the whole body and a typical car seat. The outcome is the basis of a useful tool for studying various modifications to the seat in terms of their effect on the loads on all the ligaments in the neck. To illustrate the utility of this tool, a simple collapsible spring is considered to be located as a link between the floor of the car and the seat, aligned along the main axis of the car; this is intended to absorb some of the energy in a rear end impact and hence act as an anti-whiplash device. Results for the rotation of the head relative to the cervical spine and for the linear acceleration of the head indicate a beneficial, but small, reduction in both these parameters as a direct consequence of installing the device. They seem to indicate that the device would offer little improvement, a conclusion which could have been produced equally well with a finite element model of a crash test dummy. However, results for the loads on individual ligaments indicate that there is a significant reduction which takes the levels down below the point of rupture for relative impact speeds of 10.5 kph. This kind of data can only be obtained with this kind of biomechanical model.

## INTRODUCTION

Cervical "whiplash" is the most common injury sustained in car accidents. In 93.5% of all rear end collisions involving personal injuries, at least one of the passengers claimed a neck injury, even though 70.4% of these accidents occur with speed differences smaller than 15 kph (Institution of German Car Insurers, 1994). Other injuries are comparatively rare (Muenker, 1994) and therefore the incidence of whiplash injuries is significant from both the economical and the medical point of view. Various attempts have been made to quantify whiplash by means of radiology and, although none of these has proven to be conclusive, it can be stated that little or no bony damage is sustained, whereas ligamentous injury is common (Griffith, 1995).

Experimental studies of the Mechanism of Injury (MoI) of whiplash are limited by several factors. Volunteer testing is only possible for relatively low impact speeds in order to protect the test person (Geigl, 1994), when the use of Post Mortal Test Objects is morally questionable. Furthermore, there are no means to measure the ligamentous strain *in vivo*. Recently an extensive *in vitro* test series has been published by Grauer (1997). This study used selected cervical spines to investigate the MoI, but for the requirements of the test the head had to be replaced by a surrogate metal plate, which led to the destruction of the ligamentous structure in the most critical C0-C2 complex. There was therefore a clear case for developing dynamic FE-Models to study the effects of whiplash on the ligaments of the cervical spine.

There have been several FE-models of the cervical spine reported in the literature but there have been only two studies of the full three-dimensional cervical spine as FE-Models, which have been used to investigate the effects of whiplash (Kleinberger, 1993; Heitplatz, 1998).

None of these models, however significant for explanation of the MoI, and the cause of pain, are suitable directly for reducing injury. Therefore this study, based on the validated

preliminary model of Heitplatz (1998) attempts to assess a simple anti-whiplash device using a hybrid model of the occupant body with a biomechanical head-neck complex, in order to demonstrate the usefulness of this approach in creating safer cars.

### MODEL GEOMETRY

This study concentrates on developing a whiplash protection device and needs to study the whole body and its interaction with the vehicle. Therefore, the preliminary model (Heitplatz, 1998) was extended to a whole 3-dimensional structure and implemented onto a simplified model of a vehicle occupant body (Figure 1).

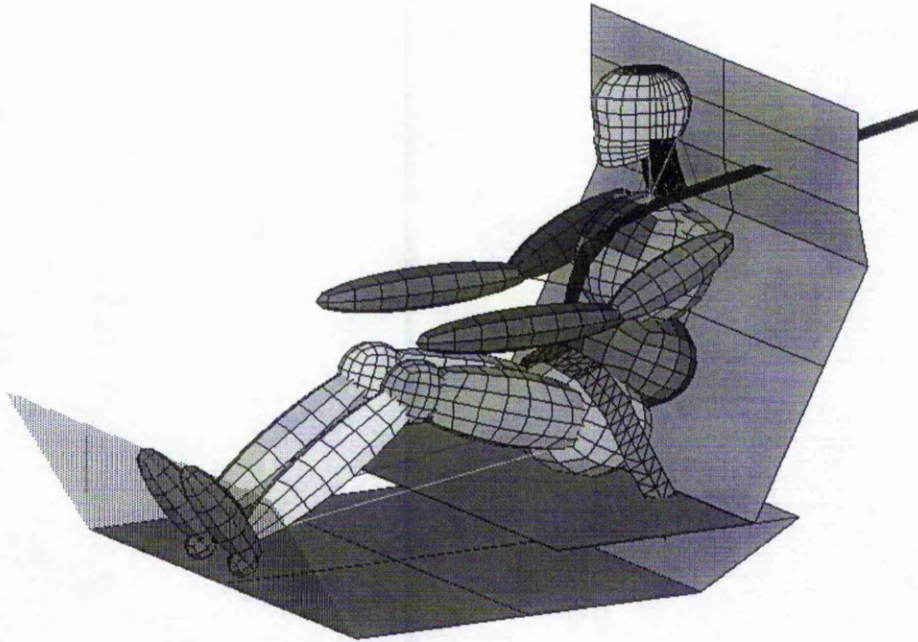


Figure 1: Isometric-View of the FEA Model

Symmetry conditions in the head-neck model were assumed along the sagittal plane. Details of the model are given in Table 1. Topological information relating to the size and shape of the skull and the human cervical vertebrae was extracted from full colour pictures obtained by the Visible Human Project (National Library of Medicine, 1994). A 3-D parametric CAD model was created by interpreting the images of the male dataset. The number of elements was kept as small as feasible, still representing all major anatomical parts of the cervical spine. Therefore, the topology was simplified to accommodate 8-node brick meshing of the structure with special focus given to the joint surfaces in order to allow realistic motion characteristics, using surface to surface contact. The full representation of ligament structures has been achieved by including the Joint Capsules and the Posterior Longitudinal Ligament. To implement non-linear material properties, all ligaments except the Nuchal Ligament, which is modelled with shell elements, are represented by non-linear spring elements. Furthermore, spring elements are used to model the nine muscles present in the model. The mesh of the model with the nomenclature of the ligamentous and muscular structures can be seen in Figure 2, with the focus given to the C0-C2 complex in Figure 3.

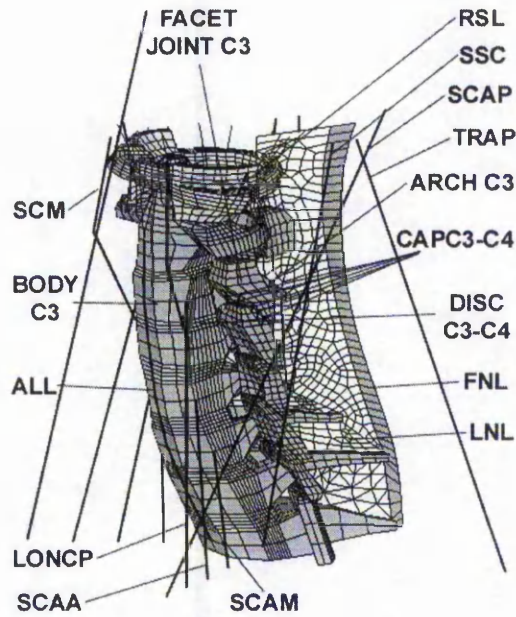


Figure 2 Isometric-View of the C1-T1 part of FEA Model. ALL: anterior longitudinal ligament; CAPC3-C4: joint capsules C3-C4; FNL: funicular portion of the nuchal ligament; LNL: lamellar portion of nuchal ligament; TRAP: trapezius; SSC: semispinalis capitis; LONCP: longus capitis; SCM: sternocleidomastoid; SCAA: scalenus anterior; SCAM: scalenus medius; SCAP: scalenus posterior; RSL: rectus capitis lateralis.

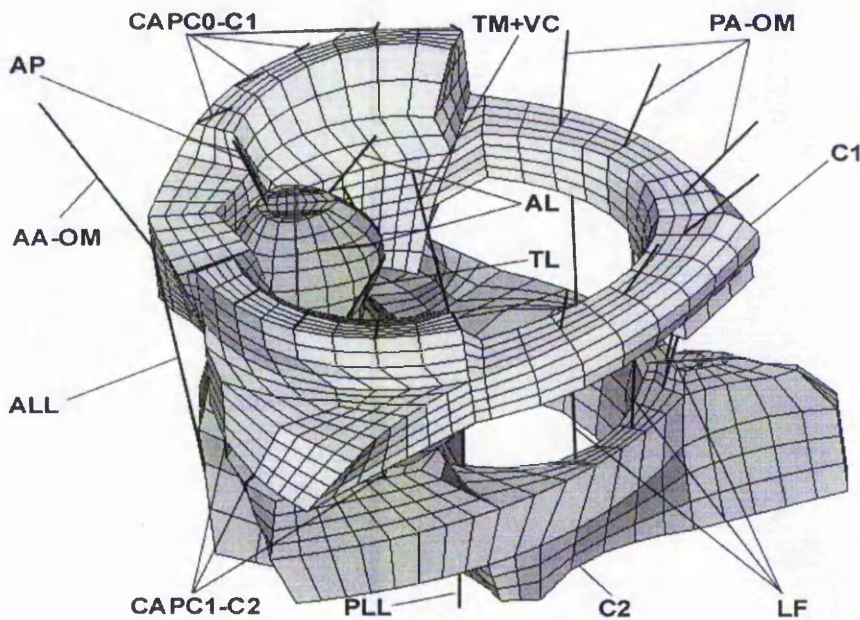


Figure 3: The C1-C2 motion complex with ligamentous structure. AL: alar ligament; TL: transvers ligament; AP: apical ligament; AA-OM: anterior atlanto-occipital membrane; ALL: anterior longitudinal ligament; PLL: posterior longitudinal ligament; TM+VC: tectorial membrane with vertical portion of cruciate ligament; LF: ligamentum flavum; PA-OM: posterior atlanto-occipital membrane; CAPC0-C1: joint capsules C0-C1; CAPC1-C2: joint capsules C1-C2

The dummy model used in this investigation consists of ellipsoidal rigid bodies connected through cylindrical joints, springs and dampers and includes a seating system consisting of seat and seat belts (LSTC, 1998).

Table 1: Summary of the FE Model Data

| <i>Structure</i>   | <i>Type of element</i> | <i>No. of elements</i>   |
|--|------------------------|--------------------------|
| <i>Skull</i>   | *ELEMENT_SOLID         | 1712                     |
| <i>Cervical vertebrae</i>                                  | *ELEMENT_SOLID         | 5926                     |
| <i>Discs</i>   | *ELEMENT_SOLID         | 1248                     |
| <i>Nuchal ligament</i>                                     | *ELEMENT_SHELL         | 940                      |
| <i>Other Ligaments</i>                                     | *ELEMENT_DISCRETE      | 124                      |
| <i>Muscles</i>   | *ELEMENT_DISCRETE      | 18                       |
| <b>Total number of elements<br/>(head-neck model only)</b> |                        | <b>11838<br/>(9984)</b>  |
| <b>Total number of nodes<br/>(head-neck model only)</b>    |                        | <b>15415<br/>(13671)</b> |

#### WHIPLASH PROTECTION DEVICE

The collapsing spring considered in this investigation as a simple whiplash prevention device could be mounted in existing seat designs, aligned along the main axis of the car. The physical design of the device can be seen in Figure 4. The proposed design consists of two shallow angled coned tubes on a double-ended cone. One of the tubes will be connected to the seat while the other will be mounted on the floor of the car. When the floor is loaded due to the accident, the conical tubes will be pushed onto the cone and will deform elastically with the properties of a linear spring. However, friction between the metal surfaces will prevent the device springing back and so the device is locked like a one-way spring. The collapsing spring was represented in the model by a pair of simple springs located on both sides of the seat (Figure 1).

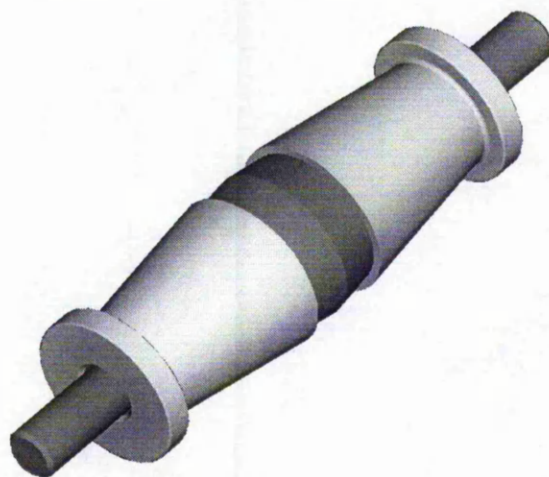


Figure 4 Whiplash protection device.

The material formulation for the device is based on LS-DYNA's "inelastic spring" classification, which gave the possibility of defining the element as a one way spring with a compression-only formulation. To achieve self-locking behaviour of the spring elements, the unloading stiffness was set on a very high level ( $1E +12$  N/m<sup>2</sup>) which successfully prevented the spring from unloading after the initial impact.

In this study the elements were set with a maximum loading force of 3500 N and initially two different lengths – 50 and 100mm. The length of the spring was based on the safety of back seat passengers. After investigating the average distance between front seats and back seats it was decided that a movement of the front seat of up to 100mm during the accident should not lead to serious injury of the back seat passengers since they would also move back on impact. However the 50mm deformable spring was considered to be a more likely option. The stiffness of the spring was estimated from test simulations of the full model with the initial maximum loading value of the spring calculated from Newton's Second Law on the basis of reducing the maximum acceleration of the head by 2g.

### MATERIAL PROPERTIES

The skull and vertebrae were assumed to be rigid since, according to the accident statistics (Institution of German Car Insurers, 1994), no damage to the bone structure is expected. All the ligaments, except the nuchal, were modelled as non-linear discrete tension-only elements. The force/deformation load curves were based on experimental results (Dvorak, 1988; Myklebust, 1988). The same technique was applied to the muscular structure using test data for the sternocleidomastoid as a reference (Yamada, 1970). The discs were modelled with a Blatz-Ko rubber model using a shear modulus of 4 MPa which has been shown to lead to a realistic deformation.

The dummy body parts are rigid bodies with discrete springs and dampers between them to provide relative stiffness and viscosity

Table 2 shows a summary of the material properties used for the model of the head-neck complex. For the properties of the body model refer to LSTC (1998).

Table 2: Summary of material properties of Head-neck complex.  
E = Young's Modulus (MPa);  $\nu$  = Poisson's Ratio; G =Shear Modulus (MPa)

| <i>Structure</i>          | <i>Material formulation</i>   | <i>Material Properties</i> |           |
|---------------------------|-------------------------------|----------------------------|-----------|
| <i>Skull</i>              | *MAT_RIGID                    | -                          | -         |
| <i>Cervical vertebrae</i> | *MAT_RIGID                    | -                          | -         |
| <i>Discs</i>              | *MAT_BLATZ-KO_RUBBER          | G=4                        |           |
| <i>Nuchal Ligament</i>    | *MAT_ELASTIC                  | E=4.42                     | $\nu=0.3$ |
| <i>Other Ligaments</i>    | *MAT_SPRING_NONLINEAR_ELASTIC | Loadcurve                  | -         |
| <i>Muscles</i>            | *MAT_SPRING_NONLINEAR_ELASTIC | Loadcurve                  | -         |

## LOADING CONDITIONS

The loading data for the present study were based on sled experiments conducted by Geigl (1996, CD-Crash Ver. 1.3). To evaluate the model, one of the experiments (MERCEDES 200-300 W 124, 1987 [MB 190] test NR.2) was reconstructed. The recorded test sled acceleration history was used to load the floor of the car, leaving the motion of the seating system with the occupant to be determined by the model.

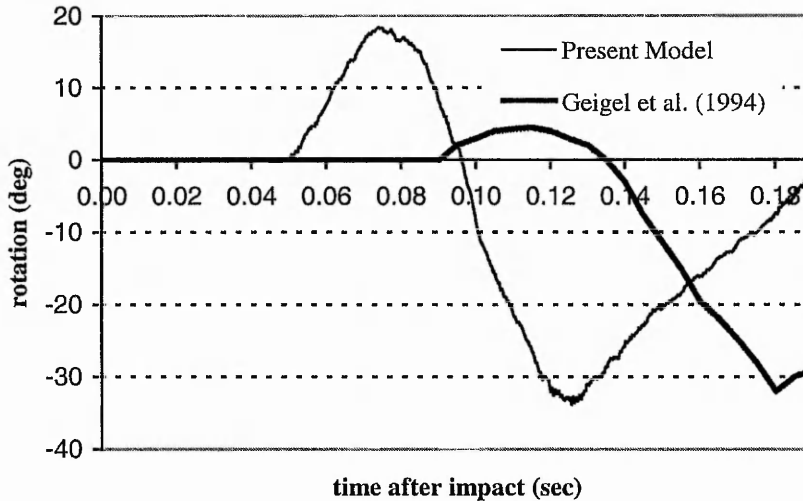


Figure 5: Relative rotation between head and C3 during a 10.5 kph rearend impact, comparing the experimental data of Geigl et al. with the numerical prediction.

A real seat back would deform backwards under the impact with the torso, extending the initial distance between the head and the head restraint and delaying a head response. The use of a symbolic seat system in the present model, which does not deform, resulted in moving the impact of the head to an earlier stage in the event (Figure 5). Therefore, in the model under investigation, the rotation of the head starts earlier than in the volunteer experiment. However the same general movement of the head can be clearly seen. Looking at the difference in the peak values of the rotation a few issues must be borne in mind. First of all the experimental results are based on a movie recorded during the experiments and the reference points for these results (external markers on the volunteer's head and torso) are clearly different from the internal ones used in the simulation. Secondly the simple model of the occupant body as well as the simple model of the seat environment used in the simulation did not satisfy energy conservation as well as the real deformations observed in the experiment. In that light, the performance of the model can be assessed as quite good.

## RESULTS

Following the evaluation of the model several simulations were conducted to establish the optimum properties of the one-way spring buffer device as well as the most representative gap between the head and the head restraint. Finally, it was decided to test the device using an 80mm gap between the head and the head restraint and springs of 50mm and 100mm length with linear characteristics and a maximum force of 3500N.

The use of this self-locking device reduced the acceleration of the head before impact with the head restraint by about 1.5g. Furthermore it reduced the peak rotation as well as the relative angular acceleration quite significantly (Figure 6).

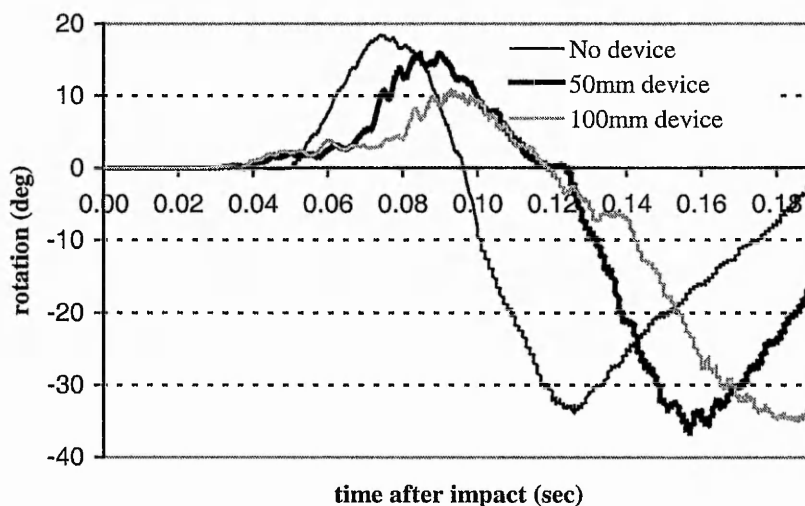


Figure 6: Head relative rotation for simulation with and without device.

The potential benefit of the device can be most clearly seen, however, on the individual ligaments' loading, particularly in the C0-C2 motion complex. The device reduced the maximum force in the apical ligament (Figure 7), enough to bring it under the average breaking force reported by Myklebust et al (1988). The reduction in loading can be seen as well in the ligamentum flavum (Figure 8). Unlikely the apical ligament, this was already under the average braking force, but now it is close to the lowest value reported for injury ever to occur.

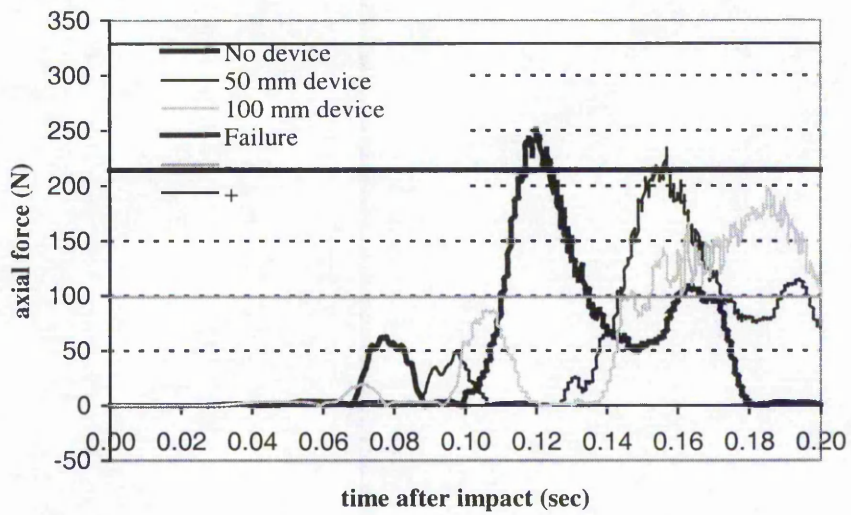


Figure 7 Force/time relationship of the apical ligament with and without the device.

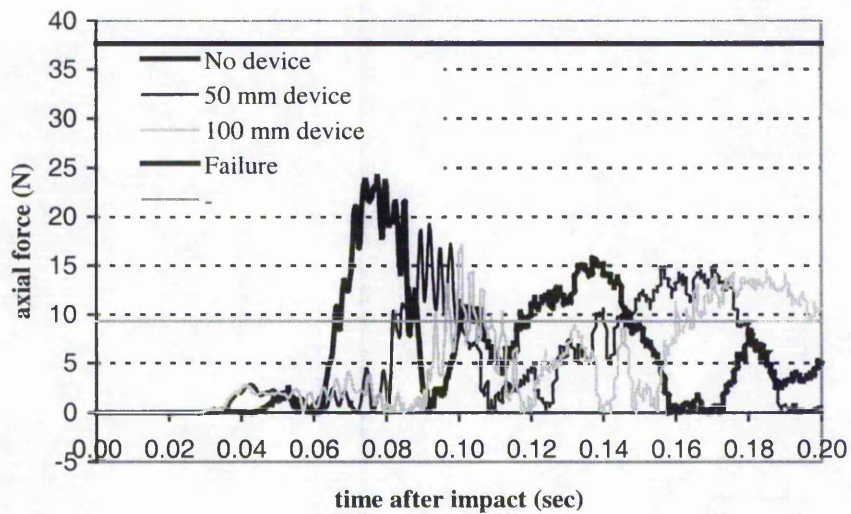


Figure 8 Force/time relationship of the ligamentum flavum with and without the device.

## CONCLUSION

The work presented describes a new approach to some aspects of car safety design based on biomechanical modelling of the human body. So far, motor industry designs have been based on real tests or Finite Element investigations based on test dummies. While dummies seem to be irreplaceable for real crash tests, there is potential in Finite Element investigations for a biomechanical approach to enhance the safety of car occupants. However there is still a long way to go to create a full biomechanical model of the human body. The approach presented in this study of combining biomechanical parts with dummy models can be seen as the first step in this process.

The results presented in this work, although preliminary, are a strong recommendation for the use of biomechanical modelling in car safety studies. While the information such as head rotation and acceleration can already be extracted from existing mechanical dummy models, this approach of using a hybrid model with a fully biomechanical head-neck complex is completely new and gives the first opportunity to investigate the loading in individual ligaments. This investigation shows the present limited model already to be a useful and original tool for studying various modifications to the seat in terms of their effect on the loads on all the ligaments of the neck.

The anti-whiplash device proposed in this investigation has been shown to be one valid possible approach to minimising the injury risk during whiplash accidents. The advantage of using a one-way spring lies in its low cost as well as its compatibility. In its proposed form, the device could be implemented not only in new car designs but also in existing car models without expensive major changes in the car construction. Therefore, although some whiplash prevention seat designs exist in a few new models of cars, the proposed design could solve the problem on a bigger scale by being suitable for all operating cars.

## REFERENCES

- Dr. Steffan Datentechnik Ges.m.b.H. (1996), CD-Crash Version 1.3, Ledergasse 34 Linz, Austria
- DVORAK, J. SCHNEIDER E. SALINGER P. and RAHN B. (1988). "Biomechanics of the Craniocervical Region: The Alar and Transverse Ligaments." J. Orthopaedic Research Society, Vol 12, pp. 652-461.
- GEIGL, B.C. STEFFAN, H. LEINZINGER, P. ROLL, MUEHLBAUER, M. and BAUER, G. (1994). "The Movement of Head and Cervical Spine During Rear End Impact." Proc. of the IRCOBI Conference on the Biomechanics of Impacts, Lyon, France, pp 127-137.
- GRAUER, J.N. PANJABI, M.M. CHOLEWICKI, J. NIBU, K. and DVORAK, J. (1997). "Whiplash Produces an S-Shaped Curvature of the Neck With Hyperextension at the Lower Levels." Spine, Vol 22, pp. 2489-2494.
- GRIFFITH, H.J. OLSON, P.N. EVERSON, L.I. and WINEMILLER, M. (1995). "Hyperextension strain of "whiplash" to the cervical spine." Skeletal Radiology, Vol 24, pp. 263-266.
- HEITPLATZ, F. GOLINSKI, W.Z. and GENTLE, C.R. (1998). "Development of a Biomechanical FE-Model to Investigate "Whiplash"." Proc. 1998 LS-DYNA Users Conference, Williams Grand Prix Engineering, Grove, UK, section 12
- KLEINBERGER, M. (1993). "Application of finite element techniques to the study of cervical spine mechanics." Proc. of the 37th Stapp Car Crash Conference, San Antonio, Texas, USA, pp 261-272.
- LSTC (1998). LS-DYNA Examples Manual
- MUENKER, M. LANGWIEDER, K. CHEN and HELL, W. (1994). "HWS Beschleunigungsverletzungen, VdS ( Institution of German Car Insurers ).", Munich
- MYKLEBUST, J.B. PINTAR, F. YOGANADAN, N. CUSICK, F. MAIMAN, D. MAYERS, T.J. and SANCES A. (1988). "Tensile Strength of Spinal Ligaments." Spine, Vol. 13, pp. 526-531.
- National Library of Medicine (1994)  
[http://www.nlm.nih.gov/research/visible/visible\\_human.html](http://www.nlm.nih.gov/research/visible/visible_human.html)
- VdS (Institution of German Car Insurers) (1994) "Vehicle Safety 90: Analysis of car Accidents", Munich,
- YAMADA, H. (1970) Strength of Biological Materials. The Williams & Wilkins Comp., Baltimore, pp 93-95

## **APPENDIX D**

# **Finite Element Modelling of Biomechanical Dummies – The Ultimate Toll in Anti-Whiplash Safety Design?**

(copy of paper)

**FINITE ELEMENT MODELLING OF BIOMECHANICAL DUMMIES -  
THE ULTIMATE TOOL IN ANTI-WHIPLASH SAFETY DESIGN?**

**Waldemar Z. GOLINSKI and Richard GENTLE**

Department of Mechanical and Manufacturing Engineering  
The Nottingham Trent University, UK

*Corresponding author:*

Mr. Waldemar Z. Golinski

The Nottingham Trent University  
Department of Mechanical and Manufacturing Engineering  
Burton Street  
Nottingham NG1 4BU; UK

Tel : +44 115 8484728

Fax : +44 115 8484749

E-mail: [waldemar.golinski@ntu.ac.uk](mailto:waldemar.golinski@ntu.ac.uk)

Internet: <http://www.domme.ntu.ac.uk/biomech>

*Keywords:*

*biomechanical, dummy, model, spine, prevention, whiplash*

## Abstract

Nowadays people purchasing a new car are no longer simply looking for attractive styling, good performance and an efficient, reliable engine; one of their main concerns is now also the safety of the car. During the last decade significant progress in improving car occupant safety has been made through the use of safety devices, such as airbags and advanced seat belts, as well as the construction of the car body itself. Much still needs to be done, however, to satisfy increasingly stringent legislation and public demand.

This work deals with the problem of whiplash injuries which traditionally, due to difficulties in diagnosis, have been very difficult to investigate let alone prevent. Nevertheless, some progress has recently been made in this field and we have previously presented a simplified dynamic FE model of the cervical spine which, using comparisons with the latest experimental work on fresh cadavers, allowed the mechanism of injury to be defined. Subsequently the spine model was used in conjunction with a simple occupant model to investigate the possibility of creating a design tool for anti-whiplash devices. This work, although only preliminary, indicated that the approach of grafting a fully biomechanical FE model of the cervical spine onto a conventional FE model of a crash test dummy could produce an unrivalled analysis of a whiplash injury situation.

In the present work a new, more advanced biomechanical FE model of the head-neck complex has been created and combined with the Hybrid III FE dummy model, which is the industry standard tool for occupant safety. The principal modifications are to the method of modelling soft tissues, and to the representation of the inertial properties of the head in order to achieve more realistic behaviour of the model.

## INTRODUCTION

Cervical "whiplash" is the most common injury sustained in car accidents. In 93.5% of all rear end collisions involving personal injuries, at least one of the passengers claimed a neck injury, even though 70.4% of these accidents occur with speed differences smaller than 15 kph (Institution of German Car Insurers, 1994). Other injuries are comparatively rare (Muenker, 1994) and therefore the incidence of whiplash injuries is significant from both the economical and the medical point of view

Experimental studies of the Mechanism of Injury (MoI) of whiplash are limited by several factors. Volunteer testing is only possible for relatively low impact speeds in order to protect the test person (Geigl, 1994), while the use of Post Mortal Test Objects is morally questionable. Furthermore, there are no means to measure the ligamental strain *in vivo*. Recently an extensive *in vitro* test series has been published by Grauer (1997). This study used selected cervical spines to investigate the MoI, but for the requirements of the test the head had to be replaced by a surrogate metal plate, which led to the destruction of the ligamentous structure in the most critical C0-C2 complex.

There have been several FE-models of the cervical spine reported in the literature (Kleinberger, 1993;Nitsche, 1996;Yang, 1998 ), mainly concentrating on explanation of the injury mechanism. The most common approach uses self-contained models of the cervical spine, sometimes not even including the head, not to mention any detailed representation of the vital C0-C1 complex. That kind of modelling, however significant for explanation of the MoI could not be used in the full scale accident simulations necessary for testing new designs, where interaction between the body of the occupant and the seating system is very important.

The automobile industry uses models of crash test dummies for computer simulations, but their biofidelity is questionable. Since biomechanical modelling of the whole occupant body is a very complicated task, the grafting of biomechanical models of critical parts onto more general models of occupants seems to be the only available approach right

now. The use of crash test dummy models seems to be the obvious choice for representing the human body in this kind of hybrid modelling since they are an industry standard for safety.

### MODEL GEOMETRY

The model used in the present investigation (Figure 1) consists of a biomechanical head-neck complex combined with the Hybrid III dummy model in a simplified vehicle seat environment.

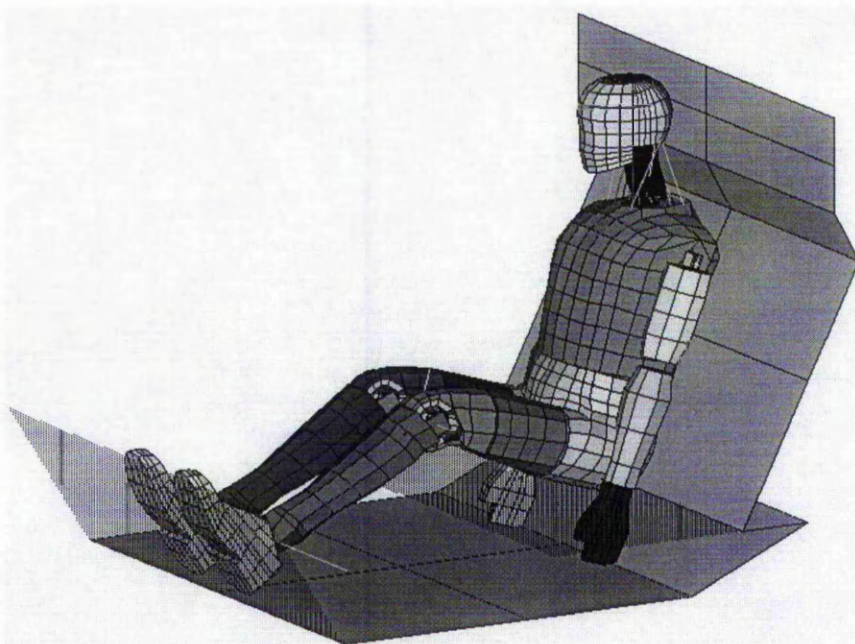


Figure 1: Isometric view of the FEA Model

The new head-neck model was developed using the preliminary model (Golinski, 1999; Heitplatz, 1998) as an overall geometrical reference. The bony structures are modelled using shell elements with the geometry modified to achieve better interaction with soft tissue. All the ligaments of the cervical spine are represented in the model using a mixed structure of shell and non-linear spring elements, except for the Nuchal Ligament, which is modelled with shell elements only. Due to this approach, interaction through the contact interfaces between ligaments and bones was made possible, preserving the non-linear properties of soft tissue. Spring elements are used to model the nine muscles present in the model. The intervertebral discs are represented using solid elements. Symmetry conditions in the head-neck model were assumed along the sagittal plane. The details of the head-neck model are given in Table 1, while the neck part of it can be seen in Figure 2.

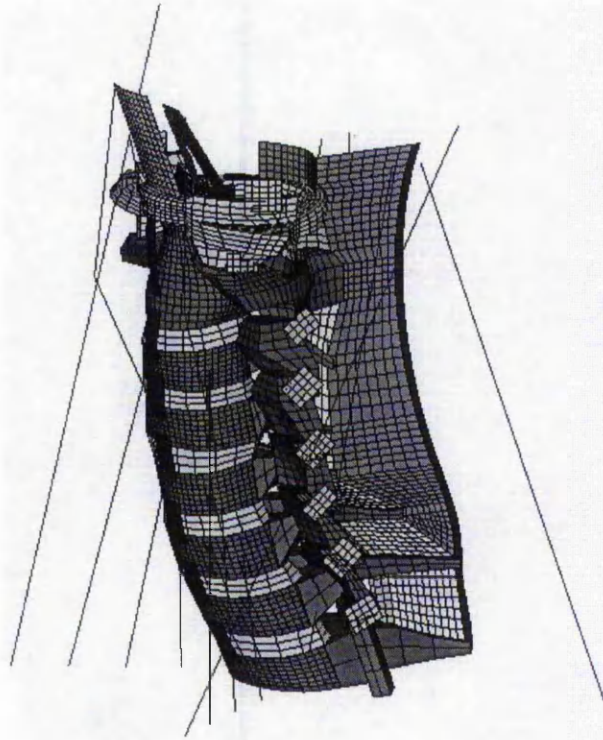


Figure 2 Isometric view of the C1-T1 part of the FEA Model.

The rigidised FE Hybrid III dummy model of a 50<sup>th</sup> percentile male, supplied with LS-DYNA (LSTC, 1998), has been used in this investigation as a representation of an industry standard for occupant safety engineering. The combined model of the Hybrid III dummy model with the biomechanical head-neck complex was placed in a simple model of a seat environment.

Table 1: Summary of the FE Model Data

| <i>Structure</i>   | <i>Type of element</i> | <i>No. of elements</i>   |
|--|------------------------|--------------------------|
| <i>Skull</i>   | *ELEMENT_SHELL         | 1124                     |
| <i>Cervical vertebrae</i>                                  | *ELEMENT_SHELL         | 8268                     |
| <i>Discs</i>   | *ELEMENT_SOLID         | 576                      |
| <i>Ligaments</i>   | *ELEMENT_SHELL         | 1984                     |
|  | *ELEMENT_DISCRETE      | 1891                     |
| <i>Muscles</i>   | *ELEMENT_DISCRETE      | 18                       |
| <b>Total number of elements<br/>(head-neck model only)</b> |                        | <b>17011<br/>(13861)</b> |
| <b>Total number of nodes<br/>(head-neck model only)</b>    |                        | <b>18872<br/>(13305)</b> |

## MODEL PROPERTIES

The skull and vertebrae were assumed rigid since, according to the accident statistics (Institution of German Car Insurers, 1994), no damage to the bone structure is expected. All the ligaments, except the Nuchal Ligament, were modelled as mixed structures of non-linear discrete tension-only elements and elastic shells. The force/deformation load curves for discrete elements were based on experimental results (Dvorak, 1988; Myklebust, 1988). The shell element stiffness properties were calculated from 1% of the breaking force and the corresponding deflection. The geometrical properties of the ligaments were based on available experimental results (Yoganandan, 1998; Dvorak, 1988; Panjabi, 1991; Przybylski 1998), while properties of the muscular structure were established from test data for the sternocleidomastoid muscles (Yamada, 1970). The discs were modelled with a Blatz-Ko rubber model using a shear modulus of 4 MPa which has been shown to lead to a realistic deformation.

The inertia properties of the head-neck model were implemented using LS-Dyna's PART\_INERTIA card.

The head mass and inertia characteristics were taken from a study by Dauvilliers (1994):  
 $M = 4.615 \text{ kg}$ ;  $I_{xx} = 0.0159 \text{ kgm}^2$ ;  $I_{yy} = 0.024 \text{ kgm}^2$ ;  $I_{zz} = 0.0221 \text{ kgm}^2$

The position of the head centre of gravity was based on the results of Ewing (1973) and Beier (1980).

The vertebrae inertia properties were taken from the preliminary model (Golinski 1999, Heitplatz 1998).

Table 2 shows a summary of the material properties used for the model of the head-neck complex. For the properties of the body model refer to LSTC (1998).

Table 2: Summary of material properties of the head-neck complex.  
 $E$  = Young's Modulus (MPa);  $\nu$  = Poisson's Ratio;  $G$  = Shear Modulus (MPa);  
 LCM = Tearing Force of Ligament

| <i>Structure</i>          | <i>Material formulation</i>   | <i>Material Properties</i> |           |
|---------------------------|-------------------------------|----------------------------|-----------|
| <i>Skull</i>              | *MAT_RIGID                    | -                          | -         |
| <i>Cervical vertebrae</i> | *MAT_RIGID                    | -                          | -         |
| <i>Discs</i>              | *MAT_BLATZ-KO_RUBBER          | $G=4$                      |           |
| <i>Nuchal Ligament</i>    | *MAT_ELASTIC                  | $E=4.42$                   | $\nu=0.3$ |
| <i>Other Ligaments</i>    | *MAT_SPRING_NONLINEAR_ELASTIC | Loadcurve                  | -         |
|                           | *MAT_ELASTIC                  | $E \sim 1\% \text{LCM}$    | $\nu=0.3$ |
| <i>Muscles</i>            | *MAT_SPRING_NONLINEAR_ELASTIC | Loadcurve                  | -         |

## LOADING CONDITIONS

The loading data for the present study were based on sled experiments conducted by Geigl (1996, CD-Crash Ver. 1.3). To evaluate the model, one of the experiments (MERCEDES 200-300 W 124, 1987 [MB 190] test NR.2) was reconstructed. The recorded test sled acceleration history was used to load the floor of the car, leaving the motion of the seating system with the occupant to be determined by the model.

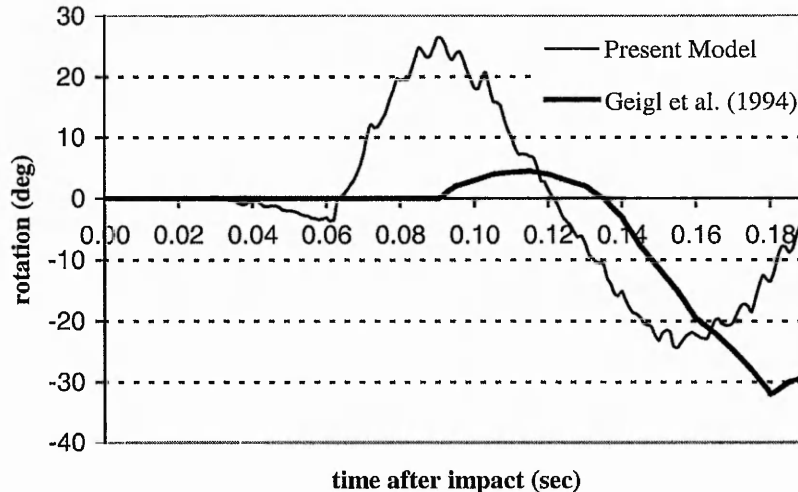


Figure 3: Relative rotation between head and C3 during a 10.5 kph rear end impact, comparing the experimental data of Geigl et al. with the numerical prediction.

A real seat back would deform backwards under the impact with the torso, extending the initial distance between the head and the head restraint delaying the head response and reducing much of the impact. The use of a symbolic seat system in the present model, which does not deform, resulted in moving the impact of the head to an earlier stage in the event and making it more severe (Figure 3). Therefore, in the model under investigation, the rotation of the head starts earlier than in the volunteer experiment. However the same general movement of the head can be clearly seen. Looking at the difference in the peak values of the rotation a few issues must be borne in mind. First of all the experimental results are based on a movie recorded during the experiments and the reference points for these results (external markers on the volunteer's head and torso) are clearly different from the internal ones used in the simulation. Secondly the simple model of the occupant body as well as the simple model of the seat environment used in the simulation did not satisfy energy conservation as well as the real deformations observed in the experiment. In that light, the performance of the model can be assessed as quite good.

## RESULTS

Since the hybrid model uses the dummy body, the first natural comparison is done against the behaviour of the dummy. On Figure 5 the relative rotation of the head to the base of the neck has been shown. As can be seen the dummy neck does not even closely resemble the behaviour of the biomechanical neck, which has been validated against experimental data from test with volunteers. Note that due to the dummy neck being a vertical "tube" the head rest for the dummy simulation had to be moved backwards by 52mm to achieve the same initial 80mm gap between the head and the head restraint.

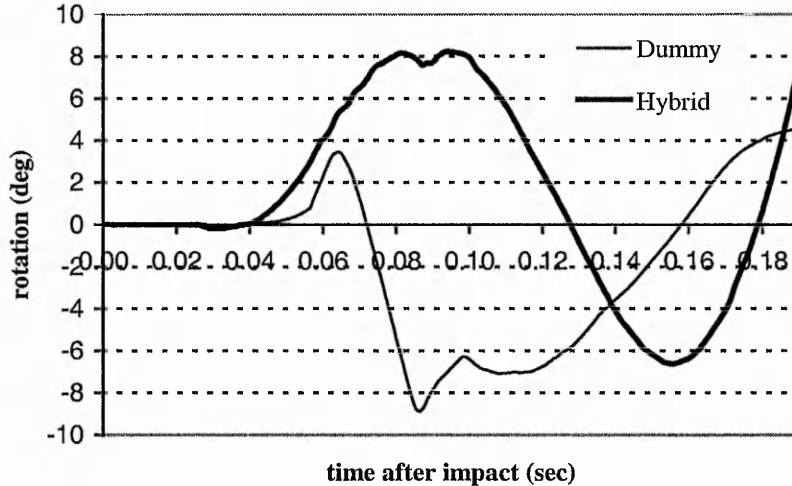


Figure 4: Head rotation relative to the base of the neck.

This result alone is a good recommendation for using the hybrid model for safety design. The dummy on its own is not capable of representing the behaviour of the neck in rear accidents situations, and will give misleading results to designers.

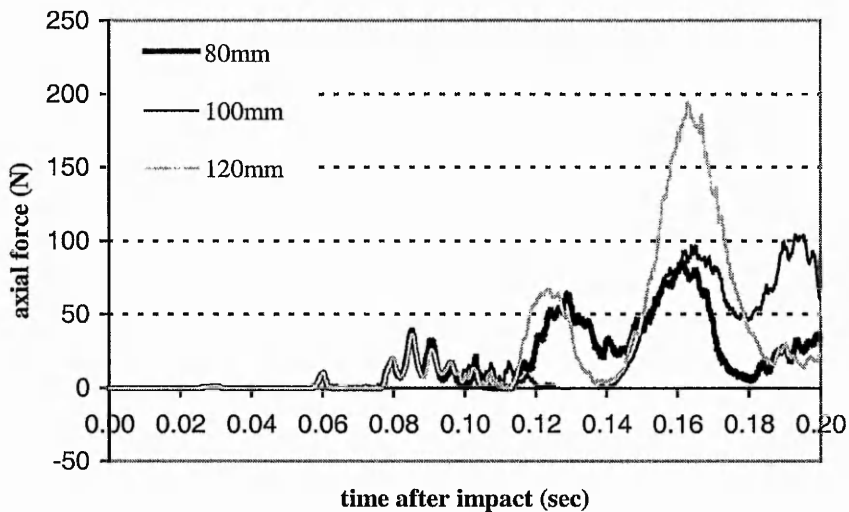


Figure 5 Force/time relationship of the apical ligament.

To show the most important characteristic of the biomechanical neck model, some more solutions with different initial gaps have been calculated. The biomechanical modelling advantage over the common dummy models can be clearly see on the two following examples of loading on individual ligaments shown in Figures 5 and 6. For example the loading of the Apical ligament increases with the remoteness of the head restraint, implying the need to keep the head restraint as close as possible to the head.

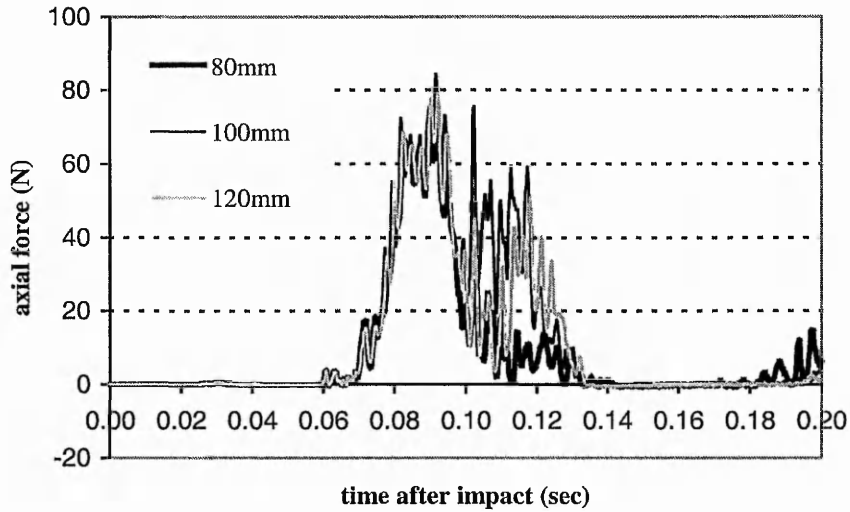


Figure 6 Force/time relationship of the ligamentum flavum.

This kind of data, which can be very valuable for safety design, is not available using crash test dummy models. Based on the results from individual ligaments, present seat designs can be assessed and new anti-whiplash designs can be developed.

## CONCLUSION

The work presented describes a new approach to some aspects of car safety design based on biomechanical modelling of the human body. So far, motor industry designs have been based on real tests or Finite Element investigations based on test dummies. While dummies seem to be irreplaceable for real crash tests, there is potential in Finite Element investigations for a biomechanical approach to enhance the safety of car occupants. However there is still a long way to go to create a full biomechanical model of the human body. The approach presented in this study of combining biomechanical parts with dummy models can be seen as the first step in this process.

The results presented in this work, although preliminary, are a strong recommendation for the use of biomechanical modelling in car safety studies. While information such as head rotation and acceleration can already be extracted from existing mechanical dummy models, this approach of using a hybrid model with a fully biomechanical head-neck complex is completely new and gives the first opportunity to investigate the loading in individual ligaments.

During the investigation the lack of a deformable seat model has been the biggest obstacle to showing the full capabilities of the present model. In future investigations it will be necessary, therefore, to include a more accurate generic model of a deformable seat in order to use the hybrid dummy model for the project's overall aim of developing an anti-whiplash device.

## REFERENCES

- BEIER, G. SCHUCK, M. SCHULLER, E. and SPANN, W. (1980). "Determination of physical data of the head. I. Centre of gravity and moments of inertia of human heads." Proc. International IRCOBI Conference.
- Dr. Steffan Datentechnik Ges.m.b.H. (1996), CD-Crash Version 1.3, Ledergasse 34 Linz, Austria
- DAUVILLIERS, F. BENDJELLAL, F. WEISS, M. LAVASTE, F. and TARRIERE, C. (1994). "Development of a Finite Element Model of the Neck." Proc. of the 38th Stapp Car Crash Conference, 942210.
- DVORAK, J. SCHNEIDER E. SALINGER P. and RAHN B. (1988). "Biomechanics of the Craniocervical Region: The Alar and Transverse Ligaments." J. Orthopaedic Research Society, Vol 12, pp. 652-461.
- EWING, C.L. and THOMAS, D.J. (1973). "Torque versus Angular Displacement Response of Human Head to -Gx Impact Acceleration." Proc. of the 17th Stapp Car Crash Conference. 730976
- GEIGL, B.C. STEFFAN, H. LEINZINGER, P. ROLL, MUEHLBAUER, M. and BAUER, G. (1994). "The Movement of Head and Cervical Spine During Rear End Impact." Proc. of the IRCOBI Conference on the Biomechanics of Impacts, Lyon, France, pp 127-137.
- GRAUER, J.N. PANJABI, M.M. CHOLEWICKI, J. NIBU, K. and DVORAK, J. (1997). "Whiplash Produces an S-Shaped Curvature of the Neck With Hyperextension at the Lower Levels." Spine, Vol 22, pp. 2489-2494.
- GOLINSKI, W.Z. and GENTLE, C.R. (1999). "Assessment of a Whiplash Prevention Device with a Dynamic Biomechanical Finite Element Model" Proc. 2<sup>nd</sup> European LS-DYNA Users Conference, Gothenburg, Sweden.
- GRIFFITH, H.J. OLSON, P.N. EVERSON, L.I. and WINEMILLER, M. (1995). "Hyperextension strain of "whiplash" to the cervical spine." Skeletal Radiology, Vol 24, pp. 263-266.
- HEITPLATZ, F. GOLINSKI, W.Z. and GENTLE, C.R. (1998). "Development of a Biomechanical FE-Model to Investigate "Whiplash"." Proc. 1998 LS-DYNA Users Conference, Williams Grand Prix Engineering, Grove, UK, section 12
- KLEINBERGER, M. (1993). "Application of finite element techniques to the study of cervical spine mechanics." Proc. of the 37th Stapp Car Crash Conference, San Antonio, Texas, USA, pp 261-272.
- LSTC (1998). LS-DYNA Examples Manual
- MYKLEBUST, J.B. PINTAR, F. YOGANADAN, N. CUSICK, F. MAIMAN, D. MAYERS, T.J. and SANCES A. (1988). "Tensile Strength of Spinal Ligaments." Spine, Vol. 13, pp. 526-531.
- NITSCHKE, S. KRABELL, G. APPEL, H. and HAUG, E. (1996). "Validation of a finite-element-model of the human neck." Proc. of the IRCOBI Conference on the Biomechanics of Impacts, Dublin, Ireland, pp 107-122.

- PANJABI, M.M. OXLAND, T.R. and PARKS, E.H. (1991). "Quantative Anatomy of Cervical Spine Ligaments. Part I. Upper Cervical Spine." *Journal of Spinal Disorders*, Vol 4, pp. 270-276.
- PANJABI, M.M. OXLAND, T.R. and PARKS, E.H. (1991). "Quantative Anatomy of Cervical Spine Ligaments. Part II. Middle and Lower Cervical Spine." *Journal of Spinal Disorders*, Vol 4, pp. 277-285.
- PRZYBYLSKI, G.J. PATEL, P.R. CARLIN, G.J. and WOO, S.L-Y. (1998). "Quantitative Anthropometry of the Subatlantal Cervical Longitudinal Ligaments." *Spine*, Vol 23, pp. 893-898.
- VdS (Institution of German Car Insurers) (1994) "Vehicle Safety 90: Analysis of car Accidents", Munich,
- YAMADA, H. (1970) *Strength of Biological Materials*. The Williams & Wilkins Comp., Baltimore, pp 93-95
- YANG, K.H. ZHU, F. LUAN, F. ZHAO, L. and BEGEMAN, P.C. (1998). "Development of a Finite Element Model of Human Neck." *Proc. of the 42nd Stapp Car Crash Conference*, 983157.
- YOGANANDAN, N. PINTAR, F. KUMARESAN, S. and ELHAGEDIAB, A. (1998). "Biomechanical Assessment of Human Cervical Spine Ligaments." *Proc. of the 42nd Stapp Car Crash Conference*, 983159.

## **APPENDIX E**

# **An Investigation of Whiplash Using Finite Element Modelling of Biomechanical Dummies**

(copy of paper)

# AN INVESTIGATION OF WHIPLASH USING FINITE ELEMENT MODELLING OF BIOMECHANICAL DUMMIES

W Z Golinski and C R Gentle

Department of Mechanical and Manufacturing Engineering, The Nottingham Trent University,  
Burton Street, Nottingham NG1 4BU

## Abstract

During the last decade significant progress in improving car occupant safety has been made through the use of safety devices, such as airbags and advanced seat belts, as well as the construction of the car body itself. Much still needs to be done, however, to satisfy increasingly stringent legislation and public demand. This work deals with the problem of whiplash injuries which traditionally, due to difficulties in diagnosis, have been very difficult to investigate let alone prevent. A new advanced biomechanical FE model of the head-neck complex has been created, and combined with the Hybrid III FE dummy model, which is the industry standard tool for occupant safety. The final model has been used to assess a simple anti-whiplash device. The analysis not only shows the efficacy of this device as an affordable modification to existing car designs but also demonstrates the implementation possibilities of combined biomechanical/dummy modelling in vehicle safety design.

## INTRODUCTION

Cervical "whiplash" is the most common injury sustained in car accidents. In 93.5% of all rear end collisions involving personal injuries, at least one of the passengers claimed a neck injury, even though 70.4% of these accidents occur with speed differences smaller than 15 kph [1]. Other injuries are comparatively rare [2] and therefore the incidence of whiplash injuries is significant from both the economical and the medical point of view

Experimental studies of the Mechanism of Injury (MoI) of whiplash are limited by several factors. Volunteer testing is only possible for relatively low impact speeds in order to protect the test person [3], while the use of Post Mortal Test Objects is morally questionable. Furthermore, there are no means to measure the ligamental strain *in vivo*. Recently an extensive *in vitro* test series has been published by Grauer [4]. This study used selected excised cervical spines to investigate the MoI, but for the requirements of the test the head had to be replaced by a surrogate metal plate, which led to the destruction of the ligamentous structure in the most critical C0-C2 complex.

There have been several FE-models of the cervical spine reported in the literature [5-7]. The most common approach uses self-contained models of the cervical spine, sometimes not even including the head, not to mention any detailed representation of the vital C0-C1 complex. That kind of modelling, however significant for explanation of the MoI, could not be used in the full scale accident simulations necessary for testing new designs, where interaction between the body of the occupant and the seating system is very important.

The automobile industry uses models of crash test dummies for computer simulations, but their biofidelity is questionable. Since biomechanical modelling of the whole occupant body is a very complicated task, the grafting of biomechanical models of critical parts onto more general models of occupants seems to be the only available approach right now. The use of crash test dummy models seems to be the obvious choice for representing the human body in this kind of hybrid modelling since they are an industry standard for safety.

## MODEL GEOMETRY

The model used in the present investigation (Figure 1) consists of a biomechanical head-neck complex combined with the Hybrid III dummy model in a simplified vehicle seat environment.

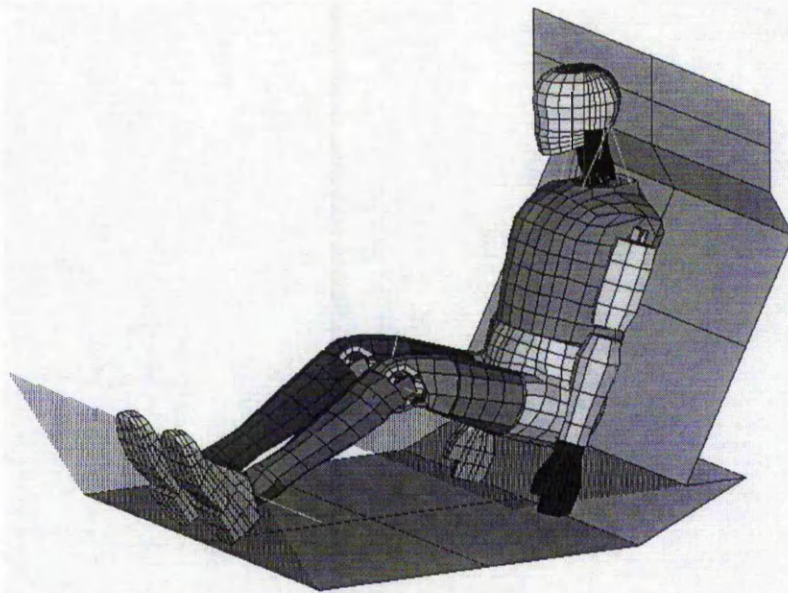


Figure 1: Isometric view of the FEA Model

The new head-neck model was developed using the preliminary model [8,9] as an overall geometrical reference. The bony structures are modelled using shell elements with the geometry modified to achieve better interaction with soft tissue. All the ligaments of the cervical spine are represented in the model using a mixed structure of shell and non-linear spring elements, except for the Nuchal Ligament, which is modelled with shell elements only. Due to this approach, interaction through the contact interfaces between ligaments and bones was made possible, preserving the non-linear properties of soft tissue. Spring elements are used to model the nine muscles present in the model. The intervertebral discs are represented using solid elements. Symmetry conditions in the head-neck model were assumed along the sagittal plane. Details of the model are given in the preliminary paper by Golinski et al [10], while the neck part of it can be seen in Figure 2.

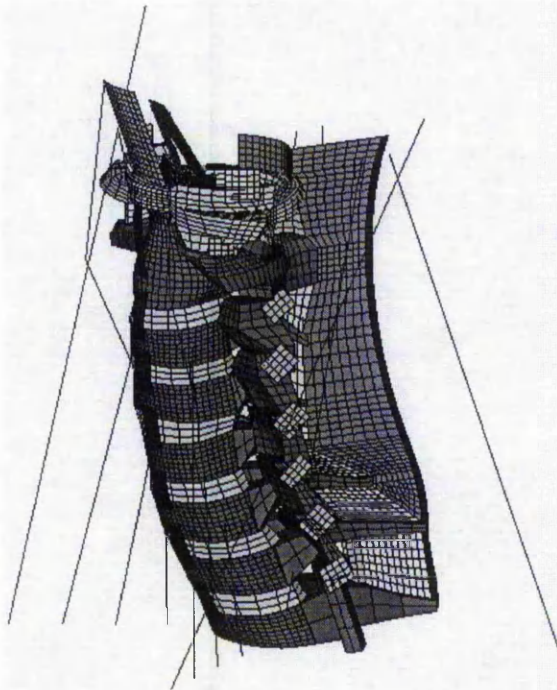


Figure 2 Isometric view of the C1-T1 part of the FEA Model.

The rigidised FE Hybrid III dummy model of a 50<sup>th</sup> percentile male, supplied with LS-DYNA [11], has been used in this investigation as a representation of an industry standard for occupant safety engineering. The combined model of the Hybrid III dummy model with the biomechanical head-neck complex was placed in a simple model of a seat environment.

## WHIPLASH PROTECTION DEVICE

The collapsing spring considered in this investigation as a simple whiplash prevention device could be mounted in existing seat designs, aligned along the main axis of the car. The physical design of the device can be seen in Figure 3. The proposed design consists of two shallow angle coned tubes on a double-ended cone. One of the tubes will be connected to the seat while the other will be mounted on the floor of the car. When the floor is loaded due to the accident, the conical tubes will be pushed onto the cone and will deform elastically with the properties of a linear spring. However, friction between the metal surfaces will prevent the device springing back and so the device is locked like a one-way spring. The collapsing spring was represented in the model by a pair of simple springs located on both sides of the seat (Figure 1).

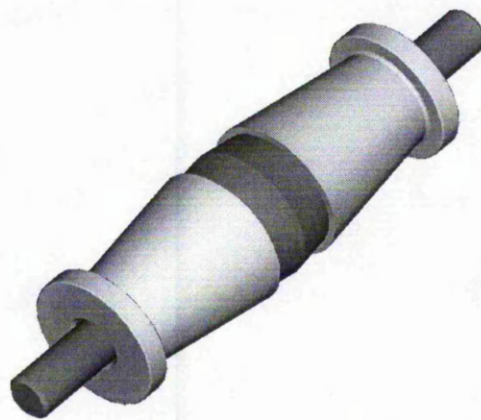


Figure 3 Whiplash protection device.

The material formulation for the device is based on LS-DYNA's "inelastic spring" classification, which gave the possibility of defining the element as a one way linear elastic spring with a compression-only formulation. To achieve self-locking behaviour of the spring elements, the unloading stiffness was set on a very high level (1E +8 N/mm) which successfully prevented the spring from unloading after the initial impact.

In this study the elements were set with a maximum loading force of 3500 N and initially two different lengths – 50 and 100mm. The length of the spring was based on the safety of back seat passengers. After investigating the average distance between front seats and back seats it was decided that a backward movement of the front seat of up to 100mm during the accident should not lead to serious injury of the back seat passengers since they would also move back on impact. However the 50mm deformable spring was considered to be a preferred option. The stiffness of the spring was estimated from test simulations of the full model with the initial maximum loading value of the spring calculated from Newton's Second Law on the basis of reducing the maximum acceleration of the head by 2g.

## MODEL PROPERTIES

The skull and vertebrae were assumed rigid since, according to the accident statistics [1], no damage to the bone structure is expected. All the ligaments, except the Nuchal Ligament, were modelled as mixed structures of non-linear discrete tension-only elements and elastic shells. The force/deformation load curves for discrete elements were based on experimental results [12,13]. The shell element stiffness properties were calculated from 1% of the breaking force and the corresponding deflection. The geometrical properties of the ligaments were based on available experimental results [12,14-17],

while properties of the muscular structure were established from test data for the sternocleidomastoid muscles [18]. The discs were modelled with a Blatz-Ko rubber model using a shear modulus of 4 MPa which has been shown to lead to a realistic deformation.

The head mass and inertia characteristics were taken from a study by Dauvilliers [19]:

$$M = 4.615 \text{ kg}; I_{xx} = 0.0159 \text{ kgm}^2; I_{yy} = 0.024 \text{ kgm}^2; I_{zz} = 0.0221 \text{ kgm}^2$$

The position of the head centre of gravity was based on the results of Ewing [20] and Beier [21].

The vertebrae inertia properties were taken from the preliminary model [8,9].

Table 1 shows a summary of the material properties used for the model of the head-neck complex. For the properties of the body model refer to LSTC [11].

Table 1: Summary of material properties of the head-neck complex. E = Young's Modulus (MPa);  $\nu$  = Poisson's Ratio; G = Shear Modulus (MPa); LCM = Tearing Force of Ligament

| Structure          | Material formulation | Material Properties |           |
|--------------------|----------------------|---------------------|-----------|
| Skull              | rigid                | -                   | -         |
| Cervical vertebrae | rigid                | -                   | -         |
| Discs              | blatz-ko rubber      | G=4                 |           |
| Nuchal Ligament    | elastic              | E=4.42              | $\nu=0.3$ |
| Other Ligaments    | nonlinear elastic    | Loadcurve           | -         |
|                    | elastic              | E from 1%LCM        | $\nu=0.3$ |
| Muscles            | nonlinear elastic    | Loadcurve           | -         |

## LOADING CONDITIONS

The loading data for the present study were based on sled experiments conducted by Geigl [22]. To evaluate the model, one of the experiments (MERCEDES 200-300 W 124, 1987 [MB 190] test NR.2) was reconstructed. The recorded test sled acceleration history was used to load the floor of the car, leaving the motion of the seating system with the occupant to be determined by the model.

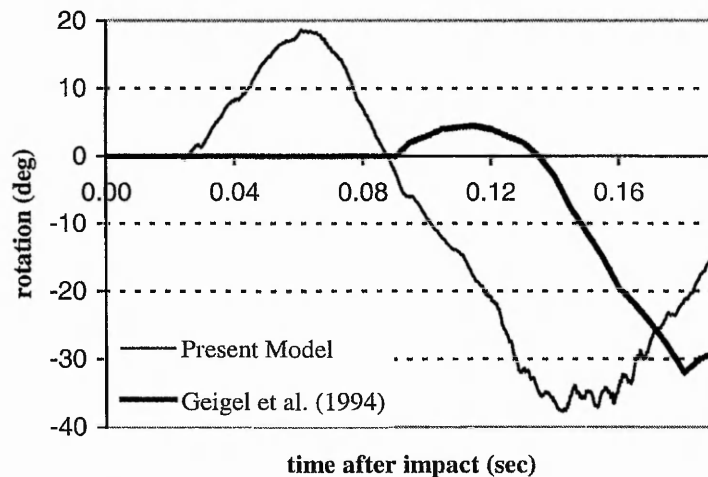


Figure 4: Relative rotation between head and C3 during a 10.5 kph rear end impact, comparing the experimental data of Geigel et al. with the numerical prediction.

A real seat back would deform backwards under the impact with the torso, extending the initial distance between the head and the head restraint, delaying the head response and reducing much of the impact. The use of a symbolic seat system in the present model, which does not deform, resulted in moving the impact of the head to an earlier stage in the event and making it more severe (Figure 4). Therefore, in the model under investigation, the rotation of the head starts earlier than in the volunteer experiment. However the same general movement of the head can be clearly seen. Looking at the

difference in the peak values of the rotation a few issues must be borne in mind. First of all the experimental results are based on a movie recorded during the experiments and the reference points for these results (external markers on the volunteer's head and torso) are clearly different from the internal ones used in the simulation. Secondly the simple model of the occupant body as well as the simple model of the seat environment used in the simulation did not satisfy energy conservation as well as the real deformations observed in the experiment. In that light, the performance of the model can be assessed as quite good, in spite of the obvious discrepancies in Figure 4.

## RESULTS

Following the evaluation of the model several simulations were conducted, using this some crash conditions, to establish the optimum properties of the one-way spring buffer device as well as the most representative gap between the head and the head restraint. Finally, it was decided to test the device using an 80mm gap between the head and the head restraint and springs of 50mm and 100mm length with linear characteristics and a maximum force of 3500N.

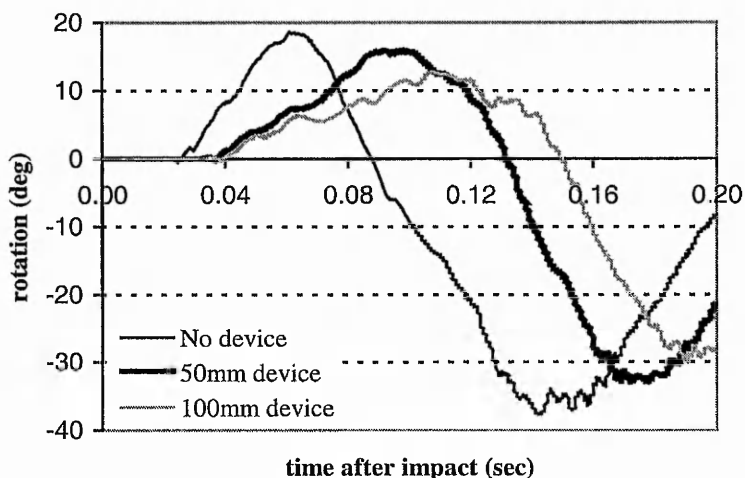


Figure 5: Relative rotation between head and C3.

It was found that the anti-whiplash device significantly reduced the relative rotation between the head and C3 which produces hyperflexion in the C0-C2 complex and is thought to lead to whiplash injuries. As shown in Figure 5, the rotation also takes place over a longer time and so the angular accelerations are doubly reduced.

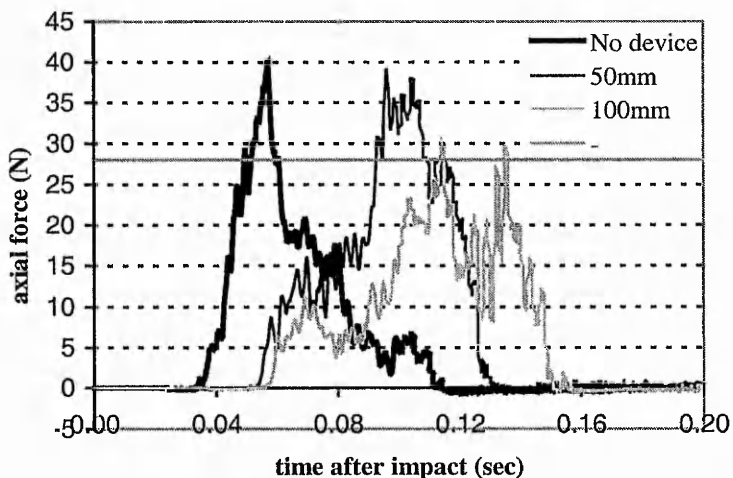


Figure 6 Force/time relationship of the ligamentum flavum with and without the device.

The potential benefit of the device can be most clearly seen, however, on the individual ligaments' loading, particularly in the C0-C2 motion complex. The 100 mm device reduced the maximum force in the ligamentum flavum (Figure 6), enough to bring it under the lowest breaking force of 28N reported by Myklebust et al [13]. The reduction in loading can be seen as well in the posterior atlanto – occipital membrane (Figure 7). Unlike the ligamentum flavum, this already experienced less than the lowest breaking force, but it has to be seen in the context of the loading being deduced from tests on volunteers, implying they are harmless to test subjects.

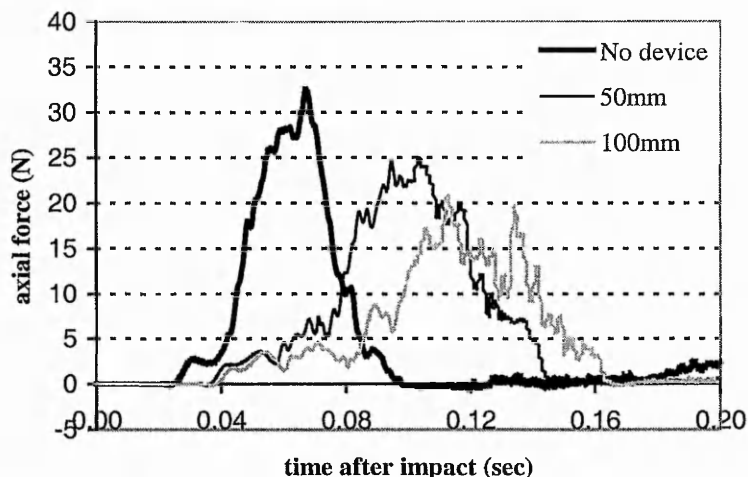


Figure 7 Force/time relationship of the posterior atlanto – occipital membrane with and without the device.

This kind of ligament force data, which can be very valuable for safety design, is not available using crash test dummy models. Based on the results from individual ligaments, present seat designs can be assessed and new anti-whiplash designs can be developed.

## CONCLUSION

The work presented describes a new approach to some aspects of car safety design based on biomechanical modelling of the human body. So far, motor industry designs have been based on real tests, or Finite Element investigations, based on test dummies. While dummies seem to be irreplaceable for real crash tests, there is potential in Finite Element investigations for a biomechanical approach to enhance the safety of car occupants. However there is still a long way to go to create a full biomechanical model of the human body. The approach presented in this study of combining biomechanical parts with dummy models can be seen as the first step in this process.

The results presented in this work are strong recommendations for the use of biomechanical modelling in car safety studies. While information such as head rotation and acceleration can already be extracted from existing mechanical dummy models, this approach of using a hybrid model with a fully biomechanical head-neck complex is completely new and gives the first opportunity to investigate the loading in individual ligaments. This investigation shows the present model to be a useful and original tool for studying various modifications to the seat in terms of their effect on the loads on all the ligaments of the neck.

The anti-whiplash device proposed in this investigation has been shown to be one valid possible approach to minimising the injury risk during whiplash accidents. The advantage of using a one-way spring lies in its low cost as well as its adaptability. In its proposed form, the device could be implemented not only in new car designs but also in existing car models without expensive major changes in the car construction. Therefore, although some whiplash prevention seat designs exist in a few new models of cars, the proposed design could solve the problem on a bigger scale by being suitable for all operating cars.

## REFERENCES

- 1 VdS (Institution of German Car Insurers), *Vehicle Safety 90: Analysis of car Accidents*, Munich, 1994.
- 2 M Muenker, K Langwieder, Chen and W Hell, *HWS Beschleunigungsverletzungen*, VdS, Munich 1994.
- 3 B C Geigl, H Steffan, P Leinzinger, Roll, M Muehlbauer, and G Bauer, 'The Movement of Head and Cervical Spine During Rear End Impact', *The IRCOBI Conference on the Biomechanics of Impacts*, Lyon, France, 1994.
- 4 J N Grauer, M M Panjabi, J Cholewicki, K Nibu and J Dvorak, 'Whiplash Produces an S-Shaped Curvature of the Neck With Hyperextension at the Lower Levels', *Spine*, 1997 **22** 2489-2494.
- 5 M Kleinberger, 'Application of finite element techniques to the study of cervical spine mechanics', *37th Stapp Car Crash Conference*, San Antonio, Texas, USA, 1993
- 6 S Nitsche, G Krabbel, H Appel and E Haug, 'Validation of a finite-element-model of the human neck', *The IRCOBI Conference on the Biomechanics of Impacts*, Dublin, Ireland, 1996.
- 7 K H Yang, F Zhu, F Luan, L Zhao and P C Begeman, 'Development of a Finite Element Model of Human Neck', *42nd Stapp Car Crash Conference*, 1998.
- 8 W Z Golinski and C R Gentle, 'Assessment of a Whiplash Prevention Device with a Dynamic Biomechanical Finite Element Model', *2<sup>nd</sup> European LS-DYNA Users Conference*, Gothenburg, Sweden, 1999.
- 9 F Heitplatz, W Z Golinski and C R Gentle, 'Development of a Biomechanical FE-Model to Investigate "Whiplash"', *1998 LS-DYNA Users Conference*, Williams Grand Prix Engineering, Grove, UK, 1998.
- 10 W Z Golinski and C R Gentle, 'Finite Element Modelling of Biomechanical Dummies – the Ultimate Tool in Anti-whiplash safety design?', *6<sup>th</sup> International LS-DYNA Users Conference*, Dearborn, USA, 2000.
- 11 LSTC, [www.lstc.com](http://www.lstc.com)
- 12 J Dvorak, E Schneider, P Salinger and B Rahn, 'Biomechanics of the Craniocervical Region: The Alar and Transverse Ligaments', *J. Orthopaedic Research Society*, 1988 **12** 452-461.
- 13 J B Myklebust, F Pintar, N Yoganadan, F Cusick, D Maiman, T J Mayers and A Sances, 'Tensile Strength of Spinal Ligaments', *Spine*, 1988 **13** 526-531.
- 14 N Yoganandan, F Pintar, S Kumaresan and A Elhagediab, 'Biomechanical Assessment of Human Cervical Spine Ligaments', *42nd Stapp Car Crash Conference*, 1998.
- 15 M M Panjabi, T R Oxland and E H Parks, 'Quantative Anatomy of Cervical Spine Ligaments. Part I. Upper Cervical Spine', *Journal of Spinal Disorders*, 1991 **4** 270-276.
- 16 M M Panjabi, T R Oxland and E H Parks, 'Quantative Anatomy of Cervical Spine Ligaments. Part II. Middle and Lower Cervical Spine', *Journal of Spinal Disorders*, 1991 **4** 277-285.
- 17 G J Przybylski, P R Patel, G J Carlin and S L-Y Woo, 'Quantitative Anthropometry of the Subatlantal Cervical Longitudinal Ligaments', *Spine*, 1998 **23** 893-898.
- 18 H Yamada, *Strength of Biological Materials*, Baltimore, The Williams & Wilkins Comp, 1970
- 19 F Dauvilliers, F Bendjellal, M Weiss, F Lavaste and C Tarriere, 'Development of a Finite Element Model of the Neck', *38th Stapp Car Crash Conference*, 1994.
- 20 C L Ewing and D J Thomas, 'Torque versus Angular Displacement Response of Human Head to -G<sub>x</sub> Impact Acceleration', *17th Stapp Car Crash Conference*, 1973.
- 21 G Beier, M Schuck, E Schuller and W Spann, 'Determination of physical data of the head. I. Centre of gravity and moments of inertia of human heads', *International IRCOBI Conference*, 1980.
- 22 Dr. Steffan Datentechnik Ges.m.b.H, *CD-Crash Version 1.3*, Ledergasse 34 Linz, Austria, 1996.